Regulation of MicroRNA Expression in Prostate Cancer by Hypoxia

Charlotte Zoe Angel, BSc MRes

Faculty of Life and Health Sciences of Ulster University

Thesis submitted for the degree of PhD

July 2020

I confirm that the word count of this thesis is less than 100,000 words.

Contents

Acknowledgements

First, thank-you to my primary supervisor, Dr Declan McKenna. I am extremely lucky to have had you as a supervisor. Thank-you for being so patient, encouraging, logical, practical, approachable, and passionate about the project, and for all of the time and feedback that you have given me which has helped me to improve. Working in your group has been a brilliant experience, I have learned a great deal from you and it has been a lot of fun. I hope that someday I can be half the scientist and teacher that you are.

Prof Colum Walsh, thank-you for being a brilliant second supervisor - I sincerely appreciate all the advice you have given me. You are such an inspiring scientist and I have really benefited from working so closely with your group. I have also enjoyed all our random chats in the tearoom, and thank-you for including me in your group outings.

Big love to the other members of the wider Genomic Medicine Research Group, both past and present, who have helped me. Thank-you so much, Dr Séodhna Lynch, Dr Heather Nesbitt, Dr Rachelle Irwin, Niall McElhatton, Dr Sarah-Jayne Mackin, Dr Caroline Conway, Catherine McBride, Catherine Scullion, Christopher McNally, Sara-Jayne Thursby, Mirka Ondicova, Dr Katie Christie, Gareth Pollin, Sophia Amenyah, and Dr Karen Lester. All of you have been generous with your time and advice and I appreciate every one of you. There isn't space to give everyone the individual thanks they deserve but I hope you each know what you mean to me. A special shout-out to my long-time office buddy Catherine, an amazing scientist and a lovely friend.

Many thanks to all the technical and other staff at BMSRI who do a fantastic job of supporting our research and making the institute a great place to work.

I also want to thank the amazing staff at the gym. Going to the circuits classes has been a real highlight of my time here, because of the kind and fun community of people who work there and attend the classes.

Thanks to my parents – Sarah Angel and Tony Paxton - for being the most awesome parents in the world and for teaching me that nothing is impossible except skiing through a revolving door. Thank-you to my fabulous grandmothers – Marion Paxton and the late Do Angel – and the rest of my family for supporting me and for putting up with me.

I also want to thank my lovely boyfriend of the last four years, Sean Maguire. I don't know what I would do without you.

Thank-you to my friends Meghann, Clare, Hannah, Emma, Kaye, and others for visiting me and generally being amazing friends. I love you all to bits. To Clare and Hannah in particular, thank-you for being such a great support over the last few months - I really appreciate it.

Finally, I would like to thank sincerely my thesis assessors for reviewing my work.

Index of abbreviations

PCa	Prostate Cancer
PSA	Prostate Specific Antigen
BPH	Benign Prostatic Hyperplasia
CpG	Cytosine-Guanine (dinucleotide sequence)
DNMT	DNA Methyltransferase
RP	Radical Prostatectomy
AR	Androgen Receptor
LBD	Ligand-binding domain
DBD	DNA-binding domain
NTD	N-terminal domain
ADT	Androgen Deprivation Therapy
CSC	Cancer Stem Cell
CRPC	Castration Resistant Prostate Cancer
mCRPC	Metastatic Castration Resistant Prostate Cancer
HIF	Hypoxia Inducible Factor
MiRNA	Micro RNA
AGO	Argonaute
DE	Differentially Expressed
DM	Differentially Methylated
Aza-dc	5-aza-2'-deoxycytidine
WHO	World Health Organization
IARC	WHO International Agency for Research in Cancer
TCGA	The Cancer Genome Atlas
FDR	False Discovery Rate
IPA	Ingenuity Pathway Analysis
NCAM	Neural Cell Adhesion Molecule
RHOB	Rho-B

Abstract

Background: Hypoxia (a pathologically low oxygen level) is a well-established driver of aggressive behaviour in prostate cancer (PCa), the second most common cancer in men worldwide. MicroRNAs (microRNAs) are short non-coding RNA molecules that are essential for many cell processes by regulating gene expression post-transcriptionally. In prostate cancer, several microRNAs are abnormally expressed but the relationship between microRNAs and the hypoxic response has not been extensively studied. The primary objective of this thesis was to investigate the expression and functional role of microRNAs in response to hypoxia in prostate cancer.

Methods: Three laboratory models of hypoxia were utilised: (i) *in vitro* PCa cell line culture at 0.1% oxygen, (ii) 3D cell spheroid culture, and (iii) an *in vivo* murine tumour xenograft experiment. MicroRNA expression was monitored by RT-qPCR to establish a list of hypoxia-responsive microRNAs. The effect on mRNA targets was determined by RT-qPCR, western blot and luciferase assay following transient transfection to over-express the microRNAs. For miRNAs that were upregulated by hypoxia in all three models, functional bioassays were used to examine the effect on PCa cell proliferation, migration and invasion. Regulation of miRNA expression by DNA methylation was explored by pyrosequencing. The laboratory work was complemented by *in silico* and next-generation sequencing (NGS) analyses of data collected from human prostate tumours, including prostate cancer datasets archived in The Cancer Genome Atlas (TCGA) repository. Bioinformatics analyses was also utilised in collaborative work investigating the impact of androgen receptor variants (ARV) on gene expression. Finally, a systematic review and meta-analysis on the role of appetite-regulating hormones in prostate cancer development was performed.

Results: The hypoxic models generated novel data demonstrating that miR-210, miR-21 and miR-196a were upregulated by hypoxia. In the case of miR-210 and miR-21, functional assays showed they could contribute to tumour progression by regulation of an adhesion protein (NCAM) and by increasing clonogenicity and migration, respectively. *In silico* TCGA analyses revealed that the expression of both microRNAs correlated significantly with markers of hypoxia and tumour aggressiveness in clinical samples, providing strong evidence for their role in prostate tumour progression. NGS data analyses and methylation analysis generated results to show how bioinformatics can identify key networks of cellular signalling associated with hypoxia and epigenetic regulation of microRNA expression. Collaborative bioinformatics analyses also utilised NGS data to demonstrate how ARV can contribute to prostate cancer progression. The systematic review revealed that obesity related hormones may also be important in prostate cancer development.

Conclusions: This thesis provides evidence that microRNAs play a crucial role in the progression of prostate cancer through hypoxia-related mechanisms. The data presented builds upon previous research of

microRNA function in prostate cancer by presenting novel results linking individual microRNAs with hypoxia-associated tumour progression. Increasing our understanding of the functionality of specific microRNAs in prostate cancer will be crucial in developing this exciting field of research so that it can inform precision medicine and improve patient outcome. This work provides evidence that microRNA profiling has great potential for improving diagnostic, prognostic, and therapeutic approaches in this disease.

Chapter 1: General Introduction

1.1 Prostate cancer

1.1. I. Structure and function of the prostate

The prostate is a small gland of the male reproductive system of most mammals, which is located under the bladder and wraps partially around the urethra. In humans, the prostate is about the size of a walnut and consists of three anatomical zones: the peripheral zone, the central zone, and the transition zone. The peripheral zone is the largest (accounting for around 65% of the prostate) followed by the central zone (around 25%) and the transitional zone (5-10%) (McNeal, 1981). The prostate is an exocrine gland, its secretions mix with fluid from the seminal vesicles and sperm from the testes, and it contributes 30-35% of the fluid in ejaculate. The prostate is highly muscular and its contractions propel the ejaculate. Like other glands, histologically it contains pouches (acini) of secretory cells (Figure 1). These secretory cells are also known as luminal cells, since they are the innermost cells within the lumen of the acini, and they are enveloped within a basal cell layer and basal lamina, which together comprises the basement membrane. The acini are embedded within layers of smooth muscle. Histologically, the three zones appear very similar but have distinct enzymatic and receptor profiles, for instance the androgen receptor is enriched in the peripheral zone and most prostate tumours arise from this zone (Al Kadhi *et al.*, 2017).

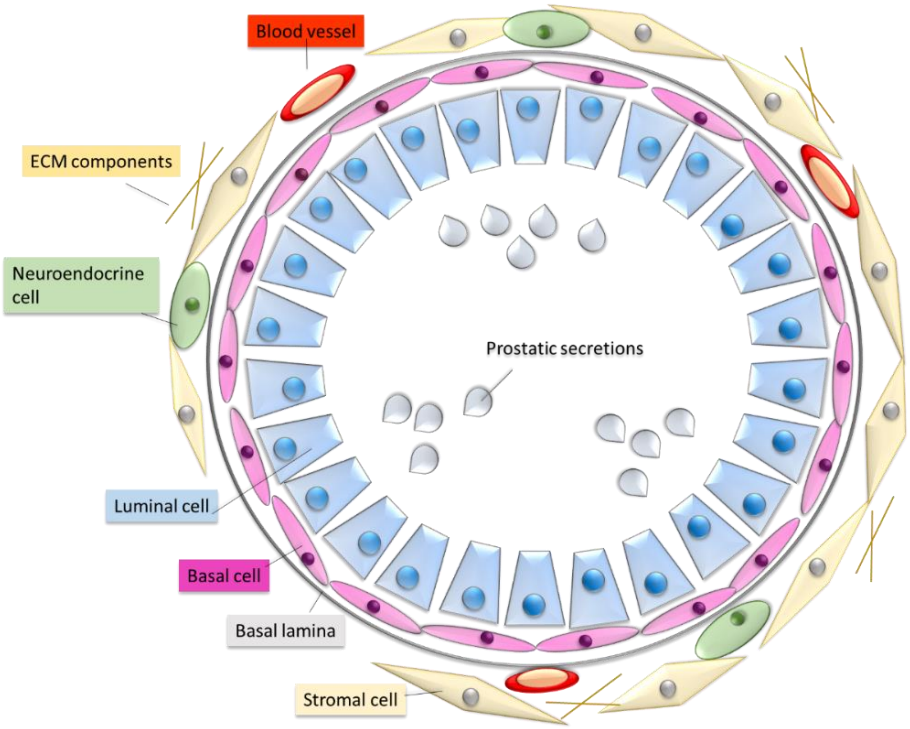

Figure 1. Diagram of a prostatic acinar. Luminal cells secrete seminal fluid into the lumen, encapsulated by a layer of basal cells and the basal lamina membrane, nested within the stromal network and components of the extracellular matrix (such as laminin and collagen).

The prostate is not a vital organ but has an essential function in reproduction. Prostatic secretions are critical for effective fertilisation, as they contain prostate specific antigen (PSA) which counteracts clotting factors from the seminal fluid, allowing the sperm to migrate up the uterus from the cervix. Prostatic secretions are also alkaline, which buffers and protects sperm in the acidic environment of the vagina. The prostate also acts as a filter, removing toxins from the seminal fluids to protect sperm and promote effective impregnation (Verze, Cai and Lorenzetti, 2016). Moreover, the prostate produces an essential enzyme, 5-alpha-reductase, which converts testosterone to dihydrotestosterone (DHT) (Randall, 1994). Testosterone and DHT are androgens (sex hormones produced by the gonads and adrenal glands) that stimulate the androgen receptor (AR), although DHT is over ten times more potent an agonist. The AR is widely expressed across the body and androgens regulate a myriad of body functions including cognition, mood, bone and muscle function, libido, and puberty. With ageing, the accumulation of toxins in the prostate, due to its filter function, affects production of 5-alpha-reductase which is evident by a decline in libido and also increases the risk of prostate cancer (PCa) (Bain & Bain, 2007). There are two sphincter muscles in the urethra, at the base of the prostate (external lower sphincter) and at the intersection with the bladder (internal upper sphincter), which act as valves and allow the flow of either ejaculate or urine. Abnormalities in prostate function, such as hyperplasia, cancer, prostate enlargement, or surgeries, can damage the sphincters resulting in loss of integrity of the sphincter muscles and causing urinary incontinence or retrograde ejaculation (ejaculatory fluid entering the bladder) (Mobley, Feibus and Baum, 2015).

1.1. II. Carcinogenesis

Carcinogenesis refers to the transformation of a healthy cell into a cancer cell *via* mutations that affect specific processes, giving rise to cells with specific features or “hallmarks”, and causing the cell to become deregulated and proliferate uncontrollably within its tissue. The hallmarks of cancer are: 1) Genome instability and mutation (ineffective repair pathways causing an accumulation of unrepaired damage). 2) Sustained proliferative signalling in the absence of growth factors. 3) Evasion of growth suppressors. 4) Suppression of cell death pathways. 5) Replicative immortality (due to a constitutively active telomerase). 6) Angiogenesis (beckoning of blood vessels). 7) Capacity for invasion, extravasation and metastasis. 8) Reprogramming of cellular energetics (abnormal metabolism). 9) Tumour-promoting inflammation. 10) Subversion of immune surveillance (hiding from immune cells) (Hanahan and Weinberg, 2011).

A healthy cell transforms into a cancer cell by relatively simultaneous mutations occurring in these key pathways (driver mutations). Due to the combination of genome instability, an accumulation of DNA-damaging agents such as toxic by-products of metabolism, and the inhibition of cell death, the transformed cell continues to acquire mutations, resulting in increasingly malignant phenotypes. Therefore, as tumours grow the cancer cells often become more aggressive as they acquire additional mutations, and tumour aggressiveness can sometimes be a function of time. However, the rate of progression is highly dynamic

and depends on the types of initial mutations (for instance, determining the propensity for metastasis) as well as the individual environment of the tumour. As an illustration of this phenomenon, in most cases PCa is indolent (slow growing), although a small subset will rapidly grow and metastasise. Increased understanding of the genetics of PCa is necessary to understand why some tumours turn out to be more dangerous than others (Shao *et al.*, 2009).

1.1. III. Epidemiology and risk factors

Despite being indolent in the majority of diagnoses, PCa is now the second most common cancer in men worldwide. The high prevalence of total disease makes PCa the fifth-leading cause of male cancer deaths worldwide (Ferlay *et al.*, 2015). Moreover, the global incidence of PCa is predicted to increase to 1.7 million new cases and 499,000 new deaths by 2030, due to population increase and ageing alone, without considering the increase in risk-associated lifestyle factors and behaviours (Ferlay *et al.*, 2010). Interestingly, the incidence across populations varies hugely, up to 30-fold across certain registries. The highest observed incidence is in USA Blacks, followed by France, then Australia. The striking differences in incidence are partly due to genetic susceptibility, for example, there is a particularly high incidence in some populations of African descent, although critical individual germline mutations have not been identified. Populations with the highest mortality are Trinidad and Tobago (44 deaths per 100,000 people per year), followed by USA Blacks (25 deaths per 100,000), Cuba (23.5 deaths per 100,000), and South Africa (22.4 deaths per 100,000). Asia has the lowest rates of incidence and mortality in the world (Torre *et al.*, 2015). In the UK, over 11,000 men died from PCa in 2016 (Cancer Research UK, 2019). The differences in incidence and mortality rates also reflect differences in diagnostic practices, genetic and lifestyle differences, and most importantly the differences in the treatment options available. Therefore, improvements in PCa treatments and prevention strategies could negate the natural increase in incidence due to population growth and ageing.

There are several confirmed risk factors for PCa: older age (above 60 years) (Glass, Cary and Cooperberg, 2013), black race/ethnicity (Thompson *et al.*, 2006), and a family history of PCa (Brawley, 2012). Although not considered confirmed risk factors by the World Health Organization (WHO), certain lifestyle factors may increase the risk of PCa, such as a high consumption of red meat and animal fats, obesity, and physical inactivity. Increasingly unhealthy “Western” lifestyles, ageing populations, and better treatments for major killers such as cardiovascular disease and breast cancer, is responsible for the increasing relative incidence in PCa (Torre *et al.*, 2015).

Chapter 6 is a Systematic Review and Meta-Analysis, which I wrote to address whether certain appetite-regulating (and obesity-related) hormones associate with the risk of PCa or the risk of an advanced or lethal form of the disease.

1.1. IV. Classification of prostate tumours

As previously mentioned, the majority of prostate tumours do not necessarily pose a threat to the patient's life (thus not considered "high-risk"). Yet, despite a vast number of published studies analysing the aetiology and treatment of PCa, there is not yet a consensus on what comprises a "high-risk" tumour. Accurate identification of high-risk tumours is paramount to ensure early intervention, and prevent over treatment of indolent tumours. The following sections discuss the various classification measures, to introduce the biochemical progression of PCa, to introduce diagnostic methods, and to highlight that new diagnostic tools are needed to supplement these approaches.

The most common means of tumour classification is to measure the physical extent of the tumour (tumour-node-metastasis (TNM) scale) or by histological examination alone (Gleason grading). Gleason grading scores the tumour as a sum of the two most common histological patterns, from 1 (well-differentiated cells) to 10 (de-differentiated cells with highly deteriorated tissue structure) (Figure 2). However, what is deemed a "high-risk" tumour varies considerably between these approaches, and despite extensive work to improve the stratification of PCa subtypes, significant heterogeneity in prognosis is observed within the "high-risk" groups (Chang *et al.*, 2014). This was demonstrated by a study that compared the different classification schemas, to prediction the 5-year relapse-free survival outcomes of a PCa cohort. The different classification schemas produced probabilities ranging from 49-80% (Yossepowitch *et al*, 2007).

Evidently, there is a need for more accurate diagnosis of the most aggressive cancer phenotypes. A new "grade group" system (which distinguishes between the two types of Gleason grade 7: 3+4 and 4+3) was designed to determine more accurately the patients prognosis, since 4+3 has been correlated with significantly poorer outcomes (Pierorazio *et al.*, 2013). Furthermore, Gleason grade is utilised when PCa has reached the stage where biopsy is required, so earlier biomarkers of PCa development would therefore be clinically valuable.

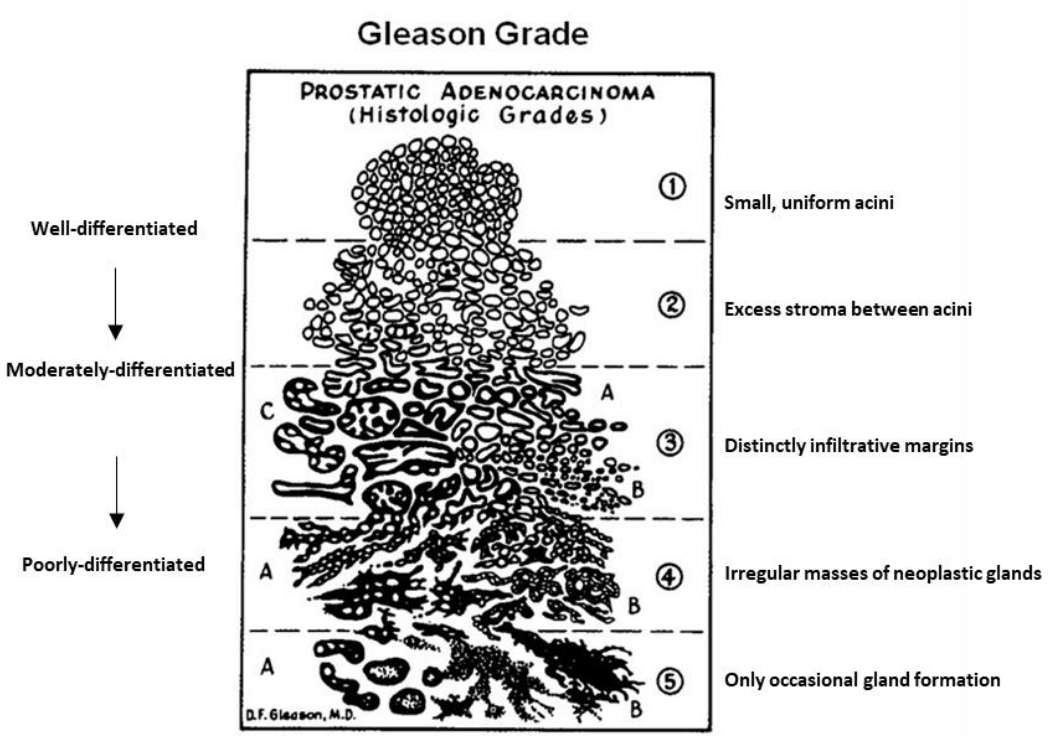

Figure 2. The original Gleason Grade diagram, drawn by Dr. Donald Gleason in 1966. Histological classification of cancer progression from well-differentiated to poorly-differentiated (grades 1-5), with details on histological appearance at each grade. From (American Urological Association, 2019), usage rights: non-commercial use. Adapted with text from (Chen and Zhou, 2016)

1.1. V. Screening and biomarkers

As with most cancers, early diagnosis greatly improves PCa prognosis. To improve early detection, PCa screening was widely employed in the late 1980s and 1990s in many high-income countries such as the USA, for men over the age of 60 years. This involved the routine measurement of serum levels of PSA, which serves as a marker of prostatic overgrowth (*i.e.*, cancer). PSA screening in the USA lead to a steep increase in the number of cases diagnosed, which then tailed off slightly as the bulk of cases had been diagnosed (Center *et al.*, 2012). However, the PSA test, while highly specific for prostate cells and indicative of prostate cell masses, is not specific to cancer cells. For instance, PSA levels are increased during the presence of benign prostatic hyperplasia (BPH, a non-cancerous type of cyst) and by low-risk tumours. A large proportion of the cases diagnosed by PSA screening in these populations turned out to be low-risk, indolent tumours. Considering the prostate is an inessential organ, arguably these tumours would be best left untreated unless noticeable symptoms develop that would indicate tumour progression to a high-risk state and puts the patient at risk of metastasis. PSA screening is thus associated with the over-diagnosis of indolent tumours, and a large study estimated that 23-42% of screening-detected PCa were indolent (Draisma *et al.*, 2009). These patients typically undergo a transurethral or transrectal biopsy, which has high risk of serious side effects: urinary incontinence, impotence, or sepsis. Furthermore, there are conflicting reports on the actual efficacy of PSA screening in terms of its effect on reducing PCa-specific

mortality. Initial evidence from the randomized Prostate, Lung, Colorectal, and Ovarian Cancer Screening Trial, which gathered mortality results after 13 years of follow-up, reported that screening was associated with reduced PCa-specific mortality (Andriole *et al.*, 2012). However, an analysis of eight European countries found no improvement in mortality rate associated with PSA screening (Schröder *et al.*, 2012). Based on this, PSA screening for PCa is now not in practice in any country in the world, at least for men with average risk. However, it is important to note that PSA testing remains the single best way to monitor biochemical recurrence following primary treatment for PCa. That is, its prostate cell specificity makes it ideal for monitoring tumour recurrence following surgical removal of the entire prostate.

A promising approach to improve the identification of "high-risk" tumours is the use of cellular markers measured at biopsy. A set of protein biomarkers that could predict "high-risk" patients' response to androgen deprivation therapy (ADT) were identified, including P16, Ki-67, MDM2, Cox-2, and PKA (Roach, Waldman and Pollack, 2009). Subsequently, a four-gene signature was identified that predicted biochemical recurrence and lethal metastasis, by expression of *PTEN*, *SMAD4*, *cyclin D1*, and *secreted phosphoprotein 1* (Roach, Waldman and Pollack, 2009). A panel of cell cycle markers was validated using advanced PCa specimens, as able to accurately predict post-RP outcomes. This panel included markers of proliferation and PI3K/PTEN signalling, as well as copy number variations, and the authors proposed it be used in addition to Gleason scoring to assess aggressiveness. Several gene expression panels measuring gene expression in biopsy cores by RT-qPCR have been marketed to indicate "high risk" tumour behaviour, such as the 46-gene panel Prolaris test and the 17-gene panel Oncotype DX test, by Myriad Genetics (Salt Lake City, Utah) and Genomic Health (Redwood City, California), respectively (Cooperberg *et al.*, 2013). One of the most promising new biomarkers of PCa is the prostate cancer gene 3 (PCA3), a long non-coding RNA. This reliably correlates with histopathological features such as tumour volume and positive surgical margins and can distinguish tumours of Gleason score 6 from ≥7, and stage pT0/2 from pT3/4. PCA3 is reliably cancer-specific, although it is not specific to prostate cells, and so could be biased by the presence of tumour cells from other tissues (whereas PSA is tissue-specific but not cancer-specific). PCA3 is detected from the urine and is thus non-invasive (Cooperberg *et al.*, 2013). Therefore, attention is increasingly focused on monitoring cellular features as well as global tumour parameters, and liquid biopsies are ideal since they do not require an invasive biopsy procedure.

In summary, despite advances in clinical classification and screening methods, many patients who present with a seemingly localised tumour still die each year from PCa, and arguably represent the true "high-risk" cases. Since the diagnostic procedures are unpleasant and risky, there is a clear need for biomarkers that can distinguish the high-risk tumours that will require treatment from those that do not require clinical intervention.

1.1. VI. Genomics and molecular subtypes

Compared to other cancers, PCa has a relatively low occurrence of germline mutations although notably, germline *BRCA2* mutation confers a 5-7 times increased risk of PCa and *BRCA1* mutation confers a 3.8 time risk in men younger than 65 years old (Attard *et al.*, 2016). There may also be an increased risk of PCa for men with defects in the DNA repair enzymes *CHEK2, NBS1, PALB2,* and *BRIP1*, although the associations are not strong (Attard *et al.*, 2016).

The most common genetic aberration in PCa is fusion of E26 transformation-specific (ETS) transcription family members (*ERG*, *FLI1* and *ETV1*) with the 5' region of androgen response genes. In particular, fusion of *TMPRSS2* and *ERG* genes which occurs in approximately 50% of PCa. ETS transcription factors regulate growth-related pathways such as the cell cycle, migration and differentiation. Therefore, deletions or translocations that place oncogenic *ERG* downstream of *TMPRSS2* causes *ERG* to become androgen responsive (Lara *et al.*, 2016). Aberrations in *PTEN* are also highly common and associate with poor prognosis; around 10% of PCa have mutations in *PTEN*, it is deleted in 10-70% of tumours removed by RP, and in over 50% of metastatic PCa (Roviello *et al.*, 2016). Genome-wide association studies (GWAS) of PCa have implicated numerous SNPs, such as 8q24, which affects the expression of c-Myc (Attard *et al.*, 2016).

Notably, two recent and very large sequencing studies have demonstrated molecular subtypes of localised and metastatic PCa. As part of The Cancer Genome Atlas (TCGA) database of cancer genomics, a cohort of 333 primary prostate carcinomas were analysed by RNA-seq, DNA-seq, methylation array, reverse phase protein lysate microarray (RPPA) as well as histopathological features. Tumour data was normalised to non-tumour tissue (from the same patient's organ) to determine differentially expressed genes and mutational and epigenetic events. In TCGA prostate adenocarcinoma (PRAD) cohort, 74% of the tumours sequenced could be categorised into seven subtypes, defined by specific gene fusions (ERG, ETV1 or ETV4, FLI1) or mutations (SPOP, FOXA1, IDH1). Twenty-five percent of the tumours had mutations in PI3K and MAPK signalling pathways, and DNA damage response genes were inactivated in 19% of the tumours. However, a limitation of this cohort is that all were localised tumours. A similar approach was subsequently employed to analyse 150 metastatic samples (Robinson *et al.*, 2015). Similarly, 40-60% of the tumours had abnormalities in the androgen receptor, ETS genes, TP53, and PTEN, with the latter two notably enriched compared to primary PCa. Again, BRCA1, BRCA2 and ATM (DNA-damage response mediators) were increased in this metastatic cohort compared to primary PCa. This study also revealed novel aberrations in PIK3CA/B, R-spondin, BRAF/RAF1, APC, b-catenin, and ZBTB16/PLZF. Opportunely, 89% of the tumours presented aberrations that are already clinically targetable, such as in the androgen receptor or other cancer-associated genes, and 8% of cases had actionable germline mutations (Robinson *et al.*, 2015). Recently, further analysis of 360 metastatic samples identified an immunogenic subtype characterised by loss of *CDK12* (due to biallelic inactivating mutations) meaning that they may be targetable by checkpoint blocking agents (Wu *et al.*, 2018).

1.1. VII. Epigenetics

1.1. VII. a) Epigenetic modifications

Epigenetics refers to heritable DNA modifications that do not involve changes to the sequence, such as the addition of chemical groups to DNA or to the histones that it envelopes, or changes in the configuration of secondary or tertiary DNA structure (nucleosomes and chromatin)(Figure 3). Epigenetic modification can be broadly categorised into: 1) DNA methylation, 2) ATP-dependent chromatin re-modelling, and 3) post-translational histone modifications (including the replacement of canonical histones, with variants that affect nucleosome-stability and higher-order chromatin structure and dynamics) (Portela and Esteller, 2010).

The most studied epigenetic modification is DNA methylation, which occurs on cytosines when adjacent to guanine (a "CpG" site). The fifth carbon is methylated by the action of a DNA methyltransferase (DNMT) enzyme using S-adenosyl-methionine (SAM) as the methyl-donor. DNA methylation induces transcriptional silencing *via* two mechanisms. Firstly, it repels transcriptional activators that cannot bind their target regions when methylated, and secondly it recruits transcriptional repressors that have affinity for methylated DNA (proteins with a Methylation-Binding Domain, MBD). MBD-containing proteins may have a positive or negative effect on transcription; they can have direct transcription activating or repressing effects, chromatic modifying effects such as influencing nucleosome structure or histone modification, or act as scaffolds to recruit other factors (Portela and Esteller, 2010).

1.1. VII. b) DNA methylation of CpG islands, promoters, and genes

There are clusters of CpG sites dotted across the genome, known as CpG islands (>200 base pair long sequences with over 50% GC content, and an observed/expected CpG ratio of >60%). CpG island methylation is essential for genomic imprinting, for example when hypermethylation of a gene on one allele may silence its expression while the other allele is hypomethylated to produce monoallelic expression, or when testis-specific genes are suppressed using DNA methylation in non-testis tissue. DNA methylation also regulates X chromosome inactivation in females, and often occurs at CpG islands within repetitive elements, such as those with repeated copies of retroviral elements or transposons, here it is essential for the repression of pro-viral DNA and intra-genomic parasites (Portela and Esteller, 2010). CpG islands not associated with imprinted genes are normally unmethyated and CpG island methylation is not generally utilised as a mechanism of somatic gene regulation. However, at non-CpG island regions, and particularly at promoter regions, methylation provides a rapid and reversible means of somatic gene regulation (Jones, 2012).

Generally, the methylation of promoters is associated with transcriptional repression. However, the effect of methylation of gene body regions is more complex. While transcription initiation is blocked by DNA methylation, elongation is not and may even be enhanced by it, and most studies have reported that gene

body methylation was associated with increased expression of the gene (Portela and Esteller, 2010)(Jones, 2012)(Irwin *et al*., 2016). However, inhibitory effects have also been observed, which could be because the gene body often contains functional elements that are stabilised by methylation, including alternative promoters, repetitive elements, enhancers, transcription factor binding sites, and intron-exon binding sites, which have an enrichment of nucleosomes (Yang *et al.*, 2014). Therefore, hypermethylation could be important to silence these elements to prevent intragenic transcription initiation, and it may regulate splicing. It also affects DNA architecture; a large bioinformatics study reported that reduced methylation at gene bodies increased chromatic accessibility and occupancy of the histone variant H2A.Z, and it induced changes in histone modifications (Yang *et al.*, 2014). H2A.Z is associated with both transcriptional activation and repression, and its occupancy in DNA has also been linked with poising genes for rapid induction. It also plays a role in recruiting the polycomb repressive complex 2, which catalyses di- and tri-methylation of histone 3 lysine 27 (H3K27), marks which have repressive effects on gene expression (Wang *et al.*, 2018).

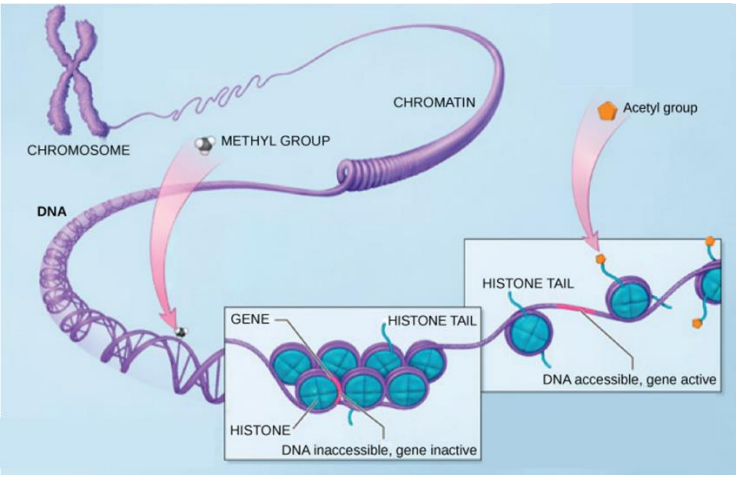

Figure 3. Epigenetic modifications influence the structure of chromatin. The double helix of DNA is coiled around histone proteins in nucleosomes (secondary structure) and further wound into a tertiary structure called chromatin. The addition of methyl groups influences the binding of transcription factors, whereas the addition of acetyl (or other) groups to histone tails increases the physical accessibility of the DNA. Image from Wikipedia commons free media repository (use rights: labelled for non-commercial use), modified by removing text.

1.1. VII. c) DNA methylation in cancer and prostate cancer

Changes in epigenetics are critical in mediating cell malignancy. Cancer cells commonly display a global reduction in DNA methylation, mainly attributed to changes at repetitive elements, which comprise just under 50% of the genome. This can lead to activation of these normally dormant regions, as well as destabilising the structure of chromatin and leading to genome and chromosome instability and thus increasing the rate of detrimental mutations and translocations. At the same time however, hypermethylation is observed at the promoters of tumour-suppressors (Pan *et al.*, 2018)(Ehrlich, 2002).

PCa is no exception and the promoter of numerous tumour-suppressors were hypermethylated and accordingly downregulated in PCa cell lines relative to non-cancer fibroblasts (*APC, MGMT, GPX3, TIMP2, GSTP1, PTGS2, DKK3, RASSF1* and *TNFRSF10D*) (Kamińska *et al.*, 2019). Treating cells with a demethylating agent (5-aza-2'-deoxycytidine) increased expression of several mesenchymal markers *in vitro* in PCa, including TWIST1, SNAI1, SNAI2, ZEB1 and CD146 (Dudzik *et al.*, 2019). Recently, a novel diagnostic panel was also validated which could accurately predict patient outcome after surgical removal of the prostate, which included three methylation markers (Strand *et al.*, 2019). Therefore, the importance of the epigenome as well as the mutational landscape in PCa development is emerging.

1.1 VII. Prostate cancer treatment

1.1. VII. Active surveillance, radiotherapy, and radical prostatectomy

As discussed in section *1.1. IV*, classification systems vary although PCa can be broadly categorised into clinical states: the localised tumour, the non-castrate rising PSA state, non-castrate metastatic state, and finally the castrate-resistant metastatic state (mCRPC), which for most men is lethal within two years (Figure 2). These states will define the clinical management decisions, and are based on an assessment of the risk that the tumour is expected to pose. The journal of the National Cancer Institute in the USA reported that 94% of newly diagnosed men had low-risk disease (stage T1 or T2). These tumours are considered as having favourable long-term oncologic outcomes (Shao *et al.*, 2009). A localised tumour that is deemed unthreatening is usually monitored over several years (by PSA level, imaging, or biopsies) and left untreated unless the tumour proves to be developing rapidly. This is known as "active surveillance" and effectively manages the majority of prostate tumours. If a localised tumour is diagnosed at a high TNM stage or Gleason grade, grows during active surveillance, becomes symptomatic, or if the patient prefers to intervene, the primary tumour will be treated by surgery, chemotherapy, or external beam radiotherapy (hereafter referred to as radiotherapy) (Keyes *et al.*, 2013).

Radiotherapy is administered at an optimal dose of 75Gy or above, often in parallel with chemotherapy (Roach, 2007). Brachytherapy, delivery of doses directly to the target area using a sealed radiation source, can be added to the treatment plan instead of a full course of radiotherapy, to improve outcomes and

reduce off-target damage (Keyes *et al.*, 2013). Unfortunately, radiotherapy is associated with a 50% increase in the risk of subsequent urological associated malignancies (Wallis *et al.*, 2016). Patients also typically develop digestive diseases and circulatory defects following radiotherapy, as well as an increased risk of cardiovascular disease (Baker, Moulder and Hopewell, 2011)(Shadad *et al.*, 2013).

Surgical removal of the tumour, or if large, the entire prostate (radical prostatectomy, RP) is performed *via* retropubic or perineal entry. RP usually includes removal of adjacent lymph nodes (extended pelvic lymph node dissection). There are numerous unpleasant side effects of RP, including urinary incontinence and increased frequency of urination, and erectile dysfunction (Frey, Sønksen and Fode, 2014).

Tumours that continue to grow despite primary treatment (locally advanced), or recur locally or systemically, can receive a different course of treatment (salvage treatment), for instance introducing radiotherapy after surgery. It has been estimated that approximately 15% of PCa diagnoses are high-risk and destined to progress to mCRPC, which is considered incurable although RP plus a combination of chemotherapies can delay tumour progression and prolong the patient's life (Bastian *et al.*, 2012)(Keyes *et al.*, 2013).

1.1. VII. Androgen deprivation (hormone) therapy

It has been known for over 200 years that the prostate depends on secretions from the testes. In 1786, the surgeon John Hunter noted while analysing cadaveric dissections, that: ''*The prostate and Cowper's glands, and those of the urethra, which in the perfect male are soft and bulky, with a secretion salt to the taste, in the castrated animal are small, flabby, tough and ligamentous, and have little secretion*'' (Zuckerman, 1936). In the 1940s, Huggins and Hodges confirmed that prostate cells are dependent on androgens secreted by the testes, and that PCa cells upregulate this pathway to proliferate irrespective of circulating levels of androgens (Huggins and Hodges, 1941). To this day, inhibition of the androgen receptor (AR) and its downstream signalling pathway remains the backbone of PCa therapy.

Upregulation of AR signalling ranges from overexpression of AR, production of intra-tumoural androgens, and mutations in AR that relax its ligand binding specificity or even abolish the requirement for a ligand. PCa patients typically receive a combination of treatments that inhibit circulating testicular androgens by physical or chemical castration (by luteinising hormone-releasing hormone (LHRH) analogue or antagonist which both reduce serum testosterone levels) plus an inhibitor of the AR, which together are known as combined androgen blockage or androgen deprivation therapy (ADT) (Heinlein and Chang, 2004)(Demir *et al.*, 2014). If a man present with a high-stage (locally advanced) tumour, the standard treatment is ADT plus RP or radiotherapy. At the discretion of the clinician, ADT can be short or long-term, or intermittent or continuous. A robust and continuous course may be necessary to abolish completely the tumour although this worsens side effects.

AR inhibitors have been the focus of PCa treatment and there are three generation of inhibitors that have been developed, mainly agents that compete with androgens for the ligand-binding domain. AR is a nuclear factor with a ligand-binding domain (LBD), DNA-binding domain (DBD), and N-terminal domain (NTD). In the basal state, the LBD binds the DBD, maintaining it in an inactive form until a ligand sequesters it (at which point AR dimerises, translocates to the nucleus, and binds DNA at androgen response elements (ARE)). To achieve combined androgen blockage, AR inhibitors are prescribed with abiraterone acetate, an inhibitor of the steroid biosynthesis enzyme CYP17A1 that was approved in 2011 and which inhibits intratumoural androgen synthesis (Denmeade and Isaacs, 2002).

Three generations of AR inhibitors have been developed; the first one and two target the LBD and some newer agents have additional affinity for the other domains. The first AR antagonist was flutamide, which was approved for medical use in 1983. An improved AR inhibitor, bicalutamide, was approved for use in 1995 and has been prescribed to millions of men with PCa worldwide. However, PCa was observed to quickly develop resistance to bicalutamide and there were concerns that it was exerting an agonist effect in some circumstances. A second generation antiandrogen, enzalutamide was developed (formerly MDV3100) and received FDA approval in 2012. Enzalutamide has superior affinity for the LBD, and additionally inhibits its nuclear translocation and DNA binding, blocks coactivator recruitment, and has no known agonist activity.

Despite the specificity of enzalutamide, as previously mentioned some PCa cells express splice variants of the AR that lack the ligand-binding domain and are thus constitutively active. Furthermore, the AR variants are insensitive to bicalutamide and enzalutamide which target the LBD. These pathological variants are observed in CRPC at a 20 fold higher level than hormone-sensitive PCa, associate with the ability of PCa to grow in the absence of androgens *in vitro* and *in vivo*, and are closely associated with poor prognosis in patients (Wadosky and Koochekpour, 2017). Chapter 6 reports a project by a research group in Strasbourg, on which I collaborated during a visit in 2018.

A third (next) generation anti-androgens is under development to target pathological AR variants and specifically focusing on agents that can bind the NTD. Since this region is highly disordered and does not have a “pocket”, it is notoriously difficult to design an agent that can bind it. However, a drug called EPI-001 (ralaniten) was developed which is a mixture of four stereoisomers, and can bind the activation region of the NTD (Brand *et al.*, 2015). EPI-001 inhibits nuclear translocation, prevents interactions with its cofactors, and blocks binding to the androgen response elements (ARE) of DNA. Thus, it functions by multiple mechanisms to efficiently prevent transcriptional activity and it is effective against all variants of AR. EP-001 had excellent effects on xenograft models and no known side effects on other pathways although in the end it was not marketed. Its successor, EPI-506 was then developed and is composed of a derivative of bisphenol A and a prodrug of ralaniten (EPI-002), which is one of the stereoisomers of EPI-001. EP-506 passed Phase I clinical trials although was halted due to side effects (Ito and Sadar, 2018).

Other next generation antiandrogens include galeterone, orteronel, and apalutamide. Galeterone is a tri-modal agent that inhibits CYP17A1, antagonises AR (*via* LBD), and promotes degradation of the AR protein (Alyamani *et al.*, 2017). Orteronel is an androgen biosynthesis inhibitor that antagonises CYP17A1. Apalutamide (ARN-509) is a LBD-binding AR antagonist which chemical similarity to enzalutamide but improved AR affinity and reduced distribution in the central nervous system and thus fewer off target effects. Apalutamide was approved for non-metastatic PCa in February 2018 (Al-Salama, 2018), although galeterone and orteronel were discontinued by manufacturer Takeda in 2018, since the results of their phase III trials showed that neither improved overall survival. Therefore, it is still only LBD-targeting AR inhibitors that are currently available to patients.

Due to the side effects of ADT, another subject of debate is the optimal treatment model. The use of intermittent versus continuous treatment was investigated to prevent ADT resistance, and to lessen toxic side-effects. One randomised control trial found that intermittent doses were as effective as continuous treatment to improve survival outcome, albeit with a short follow-up period (Crook *et al.*, 2012). However, a second study reported that intermittent ADT did not improve survival outcome in comparison to continuous dosing, although non-cancer related deaths were improved, indicating reduced toxicity (Hussain *et al.*, 2013). Long-term treatment with ADT appears to be superior to short-term dosing, long-term treatments were associated with improved disease-specific survival in three large randomised controlled trials, although differences were not highly significant and cannot be considered definitive (Bolla *et al.*, 2009)(Horwitz *et al.*, 2008). Therefore, while attempts have been made to reduce toxicities associated with ADT, including intermittent and shorter-duration dosing, these cannot be confirmed to be as effective as the standard 3-year continuous treatment. However, some physicians still consider the differences between treatment groups, which were modest at best, as negligible and they therefore do not recognise the benefit of ADT for longer than 6-months.

Furthermore, long-term systemic ADT has highly unfavourable side effects, including: decreased bone mineral density and weakening, dyslipidaemia, insomnia, muscle loss (and as a result of the associated increase in adiposity: insulin resistance and increased risk of diabetes), decreased libido and sexual dysfunction, hot flashes, anaemia, fatigue, and gynecomastia (growth of breast tissue) (Horwitz *et al.*, 2008). It may also be associated with an increased risk of cardiovascular disease although this is contested; a meta-analysis of observational studies found significant effect on combined risk (Bosco *et al.*, 2015) whereas a meta-analysis of RCTs found no association (Nguyen *et al.*, 2011). Inclusion of a GnRH (gonadotropin-releasing hormone) antagonist in the treatment plan may reduce the risk of cardiotoxic side effects (Hammerer and Manka, 2019).

Therefore, it is necessary to develop novel treatments for PCa that can be localised to the prostate and reduce the reliance on ADT.

1.1. VIII. Castration-resistant prostate cancer (CRPC)

On top of the unpleasant side effects, ADT is invariably associated with the emergence of resistance, after a latency period of approximately 2 years. PCa cells that have developed insensitivity to AR inhibition are known as androgen-independent, or castration-resistant PCa (CRPC) (Shen and Abate-Shen, 2010)(Cre*a et al*>, 2015). At this point, treatment typically consists of secondary anti-androgen treatment (*e.g*. enzalutamide following the failure of bicalutamide) combined with non-hormonal therapies (see section 1.1. IV). Over 90% of CRPC metastasise, normally to the bone, causing acute pain due to the associated skeletal compression and fractures. Currently, metastatic CRPC (mCRPC) has a median survival expectancy of 9-13 months (Kirby, Hirst and Crawford, 2011). Therefore, CRPC is considered incurable although treatments have prolonged patients' lives. This means that the vast majority of men who received hormone-therapy eventually died from their PCa.

1.1. IV. Non-hormone chemotherapies

To improve tumour reduction, ADT is normally combined with non-hormonal therapies. Several are generic anti-cancer agents that are approved for multiple cancer types, such as the taxanes docetaxel and cabazitaxel. Taxanes are a class of generic anti-cancer agents that target rapidly dividing cancer cells by binding intracellular microtubules to promote or inhibit the assembly of tubulin into microtubules, preventing mitosis and inducing apoptosis. Cabazitaxel is a newer agent with better efficacy and thus a lower occurrence of resistance and can provide a back-up if the patient does not respond to docetaxel. The alkylating agent carboplatin is also often prescribed and damages mitotic cells by crosslinking DNA (Quin*n et al*>, 2017).

Prednisone is a corticosteroid that acts as an immunosuppressant, and reduces the inflammation, oedema and pain associated with metastasis. Corticosteroids have been prescribed to patients with metastasis for over 30 years and prednisone is now commonly administered in combination with abiraterone and enzalutamide to patients with mCRPC (Fizazi *et al.*, 2017). It has the additional benefit of reducing mineralocorticoid excess due to abiraterone (Kato *et al.*, 2018). Everolimus is an analog of rapamycin and inhibits mTOR. Since PTEN was shown to regulate AR signalling, and the Akt/mTOR pathway becomes essential when PTEN is inactive or deleted, there is accumulating evidence that the addition of everolimus could reduce AR independence. Indeed, a Phase II result reported that everolimus improved the treatment of CRPC when in combination with bicalutamide (Chow *et al.*, 2016). In vitro and preclinical studies have also shown that the combination of EPI-002 with the mTOR inhibitor BEZ235 reduced the proliferation of enzalutamide resistant PCa cells, which are thought to be driven by AR-V7 signalling and the expression of AR-V7 target genes was also reduced (Kato *et al.*, 2016). Thus, increasing attention is being focused on achieving synthetic lethality by mTOR inhibition.

There are two non-hormonal options that were specifically developed for mCRPC: Sipuleucel-T and Radium-233. Sipuleucel-T is a form of immunotherapy, it is a personalised anti-cancer vaccine for mCRPC.

The patient's dendritic cells are isolated from the blood, exposed to a cancer antigen harvested from the tumour, and re-introduced by injection. The principle is to mount a systemic immune response, targeted to the patient's cancer cells. Sipuleucel-T was associated with a 4.1 month increase in median survival at phase III trial (Kantoff *et al*>, 2010). Currently, Sipuleucel-T for PCa is the only form of cancer immunotherapy that has ever demonstrated efficacy at Phase III. As a treatment for skeletal metastasis, radium-233 (alpharadin) was developed. Radium-233 has chemical similarity to calcium and is absorbed into the bones where it emits short-range alpha radiation, and acts as a targeted radiotherapy. Radium-233 increased overall survival by 2.8 months at phase III trial (Parker *et al.*, 2013).

Therefore, while advanced therapies have been developed that can statistically significantly increase a patient's survival; realistically the increases are modest (a few more months at most). Plus, the patient is likely to suffer from additional side effects which range from headaches, fatigue, and pain, to cardiovascular disease, infection, and respiratory disease which may themselves be fatal. More research is needed, particularly genetic-based investigations, to allow improvements in the current management of PCa, either by earlier detection or better understanding of the mechanisms of resistance to therapy and relapse.

Figure 4 illustrates the clinical stages of PCa with the appropriate treatment options.

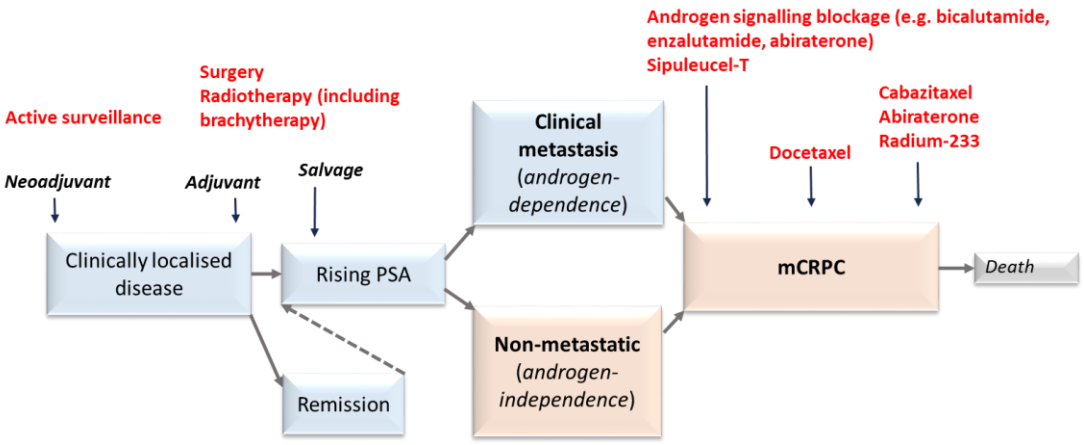

Figure 4. Clinical stages of prostate cancer ranging from indolent and/or localised to metastatic castration-resistant, with treatment options. Typical treatments for localised PCa at the neoadjuvant (initial) stage is active surveillance; end (adjuvant) and salvage (upon relapse) stages are surgery and radiotherapy, treatments for prostate cancer not responsive to primary therapy and progressing (either as androgen dependence (pink) or not (blue)) leading to progressive metastatic castration resistant prostate cancer include anti-androgen, taxane, radio-, or immuno-therapy.

1.1. VIII. Summary

The prognosis for men with PCa is heterogeneous; in the majority of cases the tumour follows an indolent course although in some cases the disease is aggressive and progresses to metastases and death. Therefore, the majority of tumours can be managed by "watchful waiting" although if locally advanced the patient may receive hormone-based therapy targeting the androgen receptor (AR). Androgens are growth factors that regulate prostate cell proliferation in both the physiological and cancer state. Androgens activate the AR and this signalling pathway becomes upregulated in PCa to permit excessive proliferation. Inhibition of the AR is the mainstay for PCa treatment, sometimes accompanied by traditional cytotoxic agents. However, although this is initially effective at abolishing the tumour, patients inevitably develop resistance and relapse with the incurable CRPC. It is imperative to understand why PCa relapses following ADT, for the development of new treatments that can supplement ADT in order to prevent drug resistance. To some extent, relapse is due to mutational events such as the upregulation of AR variants that are insensitive to LBD-targeting agents. Potentially, changes observed in the tumour microenvironment also contribute, to drive a selection of the most deadly cancer cells.

1.2 Hypoxia

Hypoxia refers to a reduced oxygen concentration, relative to the levels in other tissues in the body or relative to the tissue under healthy conditions. Mild hypoxia occurs in many tissues at physiological levels and can often be essential for its function. However, excessive or inappropriate hypoxia can become pathological and have deleterious consequences in the body (Taylor and Colgan, 2017).

1.2. I. Physiological hypoxic niches

Physiological hypoxia occurs naturally in many tissues due to their structure. For example, in the bone marrow, oxygen delivery is extremely low due to its impermeable structure and lack of vascularisation. Here, hypoxia is important to protect the haematopoietic stem cell populations from oxidative stress, to which stem cells are highly sensitive. In the kidney, a high metabolic activity produces hypoxia and this is important to regulate erythropoietin synthesis. Similarly, the cells of the germinal centres of secondary lymphoid tissues have a high metabolic activity and thus high oxygen demand, which produces a mild hypoxia that protects resident immune cells. Furthermore, germinal centres are the location where mature B cells proliferate, differentiate and obtain mutations in genes encoding antibodies (giving rise to B cell clones), and since this process is highly oxygen consuming, hypoxia increases further during clonal expansion and this favours B cell behaviour and phenotype. In the intestinal wall, the mucosal layer on the luminal face is relatively impermeable to oxygen, which creates a gradient between the anaerobic lumen and intestinal lamina propria (a highly vascularised connective layer beneath the intestinal epithelium). This helps to improve the barrier protection of the intestinal wall, and regulates the activity of immune

cells that are recruited to break down components of the intestinal microbiome and particles of digested food. The placenta becomes hypoxic as it grows, which is necessary to inhibit maternal immune cells and protect the semi-allogenic trophoblasts of the developing foetus (granting it immune privilege). Here, hypoxia has a dampening effect on the maternal T cells, as it induces expression of programmed cell death 1 ligand 1 (PDL1) which inactivates their cytotoxic activity and induces apoptosis (Taylor and Colgan, 2017).

1.2. II. Pathological hypoxia

Physiological hypoxia tends to be mild and relatively consistent; however, pathological hypoxia is severe and often chaotic and fluctuating. The causes of pathological hypoxia depend on the tissue and the outcomes are similarly varied and context-dependent. Pathological hypoxia may occur due to acute or chronic inflammation, reduced blood flow (including ischaemia), reduced vascularisation, increased oxygen consumption, thrombosis, infection, and tumorigenesis.

Importantly, due to extensive crosstalk between hypoxic signalling and inflammatory signalling, pathological hypoxia can cause immune cell dysfunction and further drive disease progression. Acute inflammation results in the accumulation of immune cells, mainly monocytes and neutrophils and extensive metabolic reprogramming which drastically increases oxygen consumption and is known as "inflammatory hypoxia". However, while in the intestinal mucosa this is beneficial, high numbers of activated neutrophils has been shown to be damaging to the lung epithelium and in this context a similar degree of hypoxia has pathological consequences. In chronically inflamed tissues, hypoxia is either pro- or anti-inflammatory depending on the context. For example, during irritable bowel syndrome the inflammation suppresses vasculature, increasing hypoxia (and ultimately leading to fibrosis), while in mucosal immune cells hypoxia increases their activity and survival. Many studies have now shown that the overall effect of pharmacological activation of hypoxic signalling is anti-inflammatory (Taylor and Colgan, 2017). Pathological hypoxia also occurs in tissues infected by pathogenic bacteria, due to the high rate of oxygen consumption by the bacteria, local inflammation, and the presence of impermeable biofilms. Here, hypoxia can have the dual effect of suppressing immune cell activity and promoting the virulence of the pathogen (Taylor and Colgan, 2017).

1.2. III. Tumour hypoxia

Hypoxia develops in solid tumours due to the deregulated proliferation of cancer cells away from their blood supply (from around 180µm) and the increasingly chaotic and leaky structure of tumour vasculature (Fraga *et al.*, 2015). In normal tissues the oxygen tension is between 40-60mmHg, however in solid tumours it drops as low as 10mmHg (McKeown, 2014).

Across all cancers, tumour hypoxia predicts poor patient outcome. Firstly, this is because hypoxia impedes treatments; poorly-vascularised regions have reduced delivery of chemotherapies and poorly-oxygenised regions are less sensitive to ionising radiation therapy (Saggar *et al.*, 2013)(Harrison *et al.*, 2002). Secondly,

hypoxia is a stress condition that induces profound changes at the cellular level that are associated with increased malignancy. There are four distinct types of tumour hypoxia which may exert different responses within the tumour: chronic hypoxia (diffusion-limited), acute/intermittent/cycling hypoxia (caused by temporary, local disturbances such as vascular collapse), anaemic hypoxia (due to reduced haemoglobin), and toxic hypoxia (inability of cells to utilise oxygen due to poisoning) (Bayer and Vaupel, 2012; Manoochehri Khoshinani, Afshar and Najafi, 2016).

1.2. IV. Hypoxia-inducible factor (HIF) signalling

The hypoxic response is governed by the hypoxia-inducible factor (HIF) transcription factors. Since hypoxia is involved in the pathogenesis of many diseases, the effects of HIF activation has been extensively studied in many tissues. The general HIF signaling pathway is outlined below.

HIF is a heterodimer composed of an alpha and beta subunit (also known as the aryl hydrocarbon receptor nuclear translocator (ARNT)). The alpha subunit (HIFα) has three isoforms (HIF-1/2/3) which have slightly different expression patterns and downstream targets. The alpha subunit is the rate-limiting subunit; both subunits are expressed constitutively although the alpha subunit is targeted for proteolytic degradation when cellular oxygen is sufficient. During normoxia, HIFα is hydroxylated at two proline residues (P402 and P564) by prolyl-hydroxylase domain-containing enzymes (PHDs) which allows it to bind the von Hippel-Lindau tumour suppressor protein (pVHL). pVHL mediates an interaction with the Elongin B/C-Cul2 ubiquitin ligase complex, which ubiquitylates them and targets them for proteasomal degradation. Additionally, factor inhibiting HIF (FIH) hydroxylates an asparagine residue on HIFα, which prevents interaction with its coactivator p300 (p300/CBP). PHD and FIH require oxygen as cofactor and therefore, during hypoxia HIFα is not hydroxylated and degraded, but interacts with p300 and translocates to the nucleus where it functions as a transcription factor and binding at androgen response elements of DNA (ARE). PHDs are also regulated negatively (*e.g*. by succinate, fumarate, reactive oxygen species (ROS) and nitric oxide (NO)) and positively (*e.g*. by ferrous iron (Fe^{2}+), 2-oxoglutarate (2-OG), and cysteine), allowing integration of other cellular stress response pathways (Figure 5).

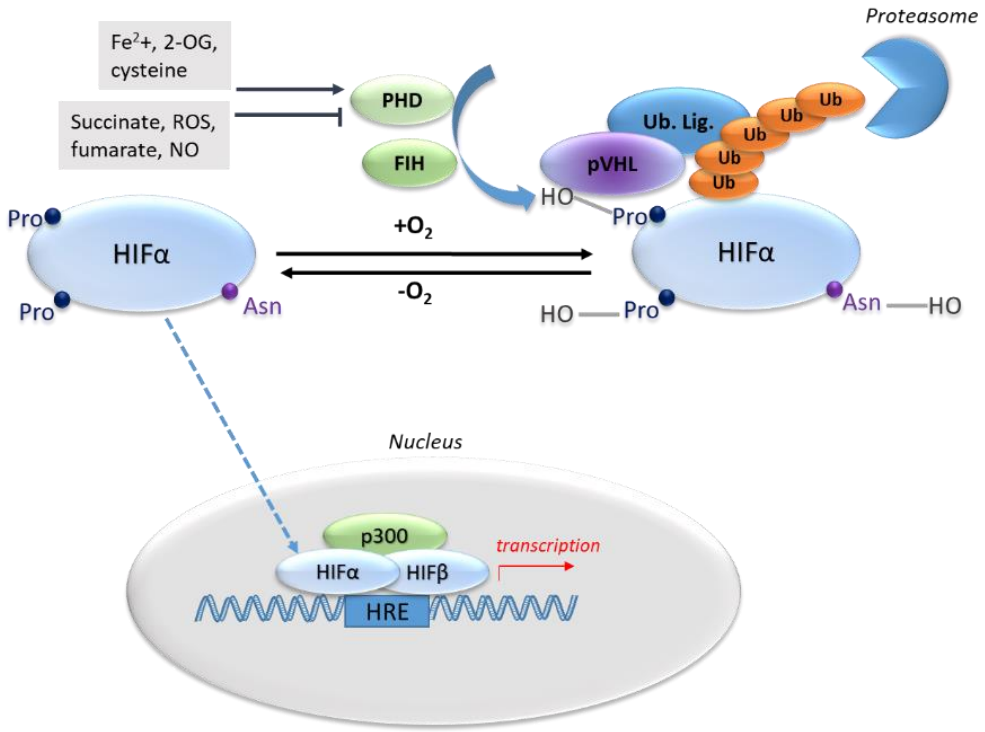

Figure 5. Oxygen-dependent regulation of HIFα. Inspired by a figure from (Araos, Sleeman and Garvalov, 2018a). Oxygen-dependent PHD and FIH hydroxylate HIFα on proline and asparagine, pVHL binds the hydroxylated residues and recruits an ubiquitin ligase (Ub. Lig.) that ubiquitylates HIFα, targeting it for degradation by the proteasome. In the absence of oxygen, PHD and FIH are inactive and HIFα translocates to the nucleus and transcribes genes with a HIF response element (HRE) in the promoter. PHD is positively regulated by Fe^{2}+, 2-OG, and cysteine; and negatively by succinate, ROS, fumarate, and NO.

Therefore, HIF is an essential component of the response to cellular stress and bioenergetics, and furthermore numerous growth factor signalling pathways affect HIF. For instance, platelet-derived growth factor (PDGF), insulin-like growth factor, insulin, and heregulin all upregulate HIFα transcription or translation. Phosphorylation of HIFα is also a vital means of regulating its activity, both positively and negatively. Ras-ERK (MAPK) signalling regulates HIF activity, by p42/p44 or p38 MAPK phosphorylation of HIFα or p300. Phosphorylation by glycogen synthase kinase 3β (GSK-3β) and polo-like kinase 3 (Plk3) reduce HIF transcription factor activity, while phosphorylation by the double strand break sensor ataxia-telangiectasia mutated (ATM) increases its activity. In cancer cells, activation of phosphatidylinositol 4,5-bisphosphate 3-kinase, Akt and mammalian target of rapamycin (PI3K/Akt/mTOR) regulated levels of HIFα at both the gene expression and protein level. Furthermore, HIFα is regulated post-translationally by modifications such as acetylation (for instance by p300/CBP-associated factor (PCAF)), which is associated with the transcription of specific target genes. HIF-α stability is additionally regulated by factors that mediate its ubiquitination or association with the proteasome. For example, E3 ubiquitin ligase hypoxia-associated factor (HAF) ubiquitylates HIF-1α regardless of oxygen levels, and translation initiation factor eIF3e promotes degradation of HIF2α. Receptor for activated C kinase 1 (RACK1) mediates the degradation of both HIF1α and HIF2α by recruiting Elongin C, however this can be inhibited by heat shock protein 90 (HSP90) which increases the stability of HIF during stress conditions such as acidosis. Basic helix-loop-helix family, member e41 (BHLHE41 or SHARP1) increases proteosomal degradation of HIF1/2α, and ubiquitin C-terminal hydrolase-L1 (UCHL1) stabilises HIF-1α by de-ubiquitination (Araos, Sleeman and Garvalov, 2018a).

Therefore, more than a guardian of oxygen homeostasis, HIF functions as a master integrator of oxygen levels, DNA damage and cellular stress, growth signalling, and metabolic status. Abnormal HIF signalling could thus have far-reaching consequences in terms of cell dynamics and behaviour.

1.2. V. Hypoxic Signalling and Cancer Progression

Considering that HIF is at the centre of the stress response network, it is unsurprising that hypoxia affects pathways that are involved in cancer, including angiogenesis, proliferation, metabolism, epithelial-mesenchymal-transition (EMT), and motility and metastasis.

Hypoxia facilitates angiogenesis by inducing expression of vascular-endothelial growth factor (VEGF) and SDF-1. It regulates the metabolic enzymes GLUT-1, GLUT-3 and glycolytic enzymes, and apoptosis *via* BNIP-3, p53, TGF-β and bFGF, as well as epithelial-mesenchymal-transition *via* E-cadherin, ZEB-1 and ZEB-2, TCF3, CXCR4, LOX, MMP-2, and MMP-9. A protein responsible for regulating intra- and extracellular pH, CAIX, is also a direct target of HIF. Moreover, hypoxia reduces proliferation, which protects the cell from traditional chemotherapies that target rapidly dividing cells. Furthermore, the hypoxic microenvironment intrinsically

selects for apoptosis-resistant cancer cells and may directly suppress apoptosis to permit proliferation despite an accumulation of mutations. This leads to clonal evolution and increasingly abnormal phenotypes (Harris, 2002)(Jang *et al.*, 2010).

Figure 6 illustrates how the activation of different cancer-associated pathways by hypoxia produces a cell that is stem-like, resistant to chemo- and radiotherapy, capable of metastasis, and stimulates an increased blood supply for nutrients, and through which it can escape from the primary tumour and enter the bloodstream to spread to distant sites. Regulation of these pathways by HIF is discussed below.

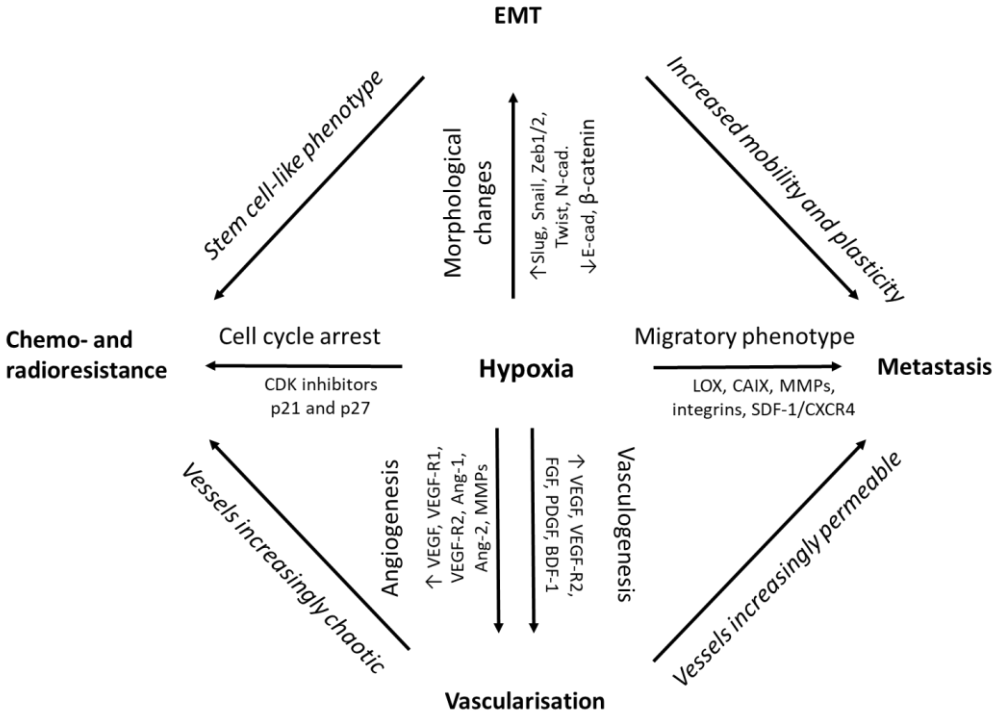

Figure 6. Schematic overview of the links between hypoxia and the cancer-associated pathways. Inspired by a figure from (Muz *et al.*, 2015). Hypoxia increases tumour vascularisation *via* upregulation of vascular-endothelial growth factor (VEGF) and its receptor 2 (VEGF-R2), fibroblast growth factor (FGF), platelet-derived growth factor (PDGF), bromodomain-containing factor 1 (BDF-1), angiopoietin 1 and 2 (ANG-1/2), and matrix metalloproteinases (MMPs). Migration is facilitated by upregulation of lectin-like oxidized low-density lipoprotein receptor-1 (LOX-1), carbonic anhydrase IX (CAIX), MMPs, integrins, stromal cell-derived factor 1 (SDF1), and C-X-C motif chemokine receptor 4 (CXCR4). The cell cycle is blocked by upregulation of cyclin dependent kinase (CDK) inhibitors p21 and p27. Cell morphology is altered to facilitate EMT by changes in the expression of slug, snail, twist, Zeb1/2, N-cadherin, E-cadherin, and β-catenin.

1.1. V. a) Epithelial-Mesenchymal-Transition

Epithelial-mesenchymal-transition (EMT) is a dynamic morphogenic program that is important during development, in which cells exhibit profound plasticity, and de-differentiate and acquire mesenchymal features. Crucially, they lose polarity and intercellular adhesion, and demonstrate increased motility, migration and invasive capabilities. This process is utilised by cancer cells and is key to metastatic spread. HIF can upregulate the expression of the transcription factors that drive EMT and have established oncogenic potential: Snail, Slug, ZEB1/2, and Twist (Puisieux, Brabletz and Caramel, 2014). By inactivating PHD3, stabilisation of HIF-1α and HIF-2α caused upregulation of TGFα/SMAD/EGFR signalling and lead to EMT and metastasis, in lung cancer cells. Furthermore, hypoxia has been shown to increase EMT through activation of Notch, Hedgehog, integrin-linked kinase, and NF-κB signalling (Araos, Sleeman and Garvalov, 2018a). Importantly, during hypoxia cancer cells may be encouraged to enter EMT as a result of changes in neighbouring, non-cancer cells. Hypoxia increased the secretion of IL-1β by infiltrating macrophages, which then upregulated HIF-1α in proximal, but normoxic, hepatocellular carcinoma cells (Zhang *et al.*, 2018). Furthermore, hepatocellular carcinoma cells increased expression and secretion of high mobility group box 1 (HMGB1) in response to hypoxia, and this induced macrophages to infiltrate and produce IL-6. The IL-6 secreted by macrophages in turn increased EMT in the hepatocellular carcinoma cells. This was confirmed by silencing of HMGB1, which inhibited macrophage infiltration, EMT, and metastasis in tumour xenografts (Jiang *et al.*, 2018).

1.2. V. b) Extracellular Matrix Remodelling

The extracellular matrix (ECM) refers to the network of macromolecules that provide structural and biochemical support to cells, including collagens, glycoproteins, and enzymes. Alterations in the ECM as well as the basement membrane facilitate cancer cell motility and extravasation. Hypoxia and HIFs upregulate many enzymes that can play a role in remodelling of the ECM, such as matrix metalloproteinases (MMPs), lysyl oxidases (LOX), procollagen lysyl hydroxylases (PLODs), collagen prolyl-4-hydroxylases (P4Hs), and cathepsins. Collagens vastly increase in the ECM during cancer, affecting cancer cell polarity, migration, and motility. Moreover, hypoxia is associated with fibrosis in tumours, as well as immune reactivity, which is an independent predictor of patient relapse and disease-free survival. The properties of the ECM determine the type and effect of cancer-associated fibrosis (Gilkes, Semenza and Wirtz, 2014). Hypoxia also downregulates tissue inhibitor of metalloproteinases 2 (TIMP2)(Rankin and Giaccia, 2016). In fact, P4HA1/2 and PLOD1/2 were essential for hypoxic-mediated metastasis of orthotopic breast cancer xenografts (Gilkes *et al.*, 2013).

The stroma refers to cells that provide a connective and supportive network, that do not have the specific function of the organ, in this case as glandular cells. The main cell type is fibroblasts, and these play a crucial role in tumour development. Cancer cells interact with neighbouring fibroblasts, which then become reprogrammed (known as cancer-associated fibroblasts, CAFs). Interestingly, hypoxic tumour cells secrete

soluble factors that can recruit fibroblasts and facilitate their conversion into CAFs. The microenvironment similarly promotes unwanted behaviours in the CAFs themselves, the upregulation of HIF in CAFs increased growth and metastasis of breast cancer xenografts. Research into the effect of hypoxia on CAFs is currently emerging and has shown that HIF1α causes the upregulation of ECM modellers P4HA1/2 and PLOD2. Moreover, culturing breast cancer cells in the ECM derived from hypoxic fibroblasts increased the cancer cells' migration (Gilkes, Semenza and Wirtz, 2014). However, another study reported conversely that hypoxia negatively regulated CAFs, CAFs were deactivated and unable to remodel the ECM when cultured in hypoxic conditions, and knocking down PHD2 activity in CAFs co-transplanted with breast cancer cells, was associated with reduced metastasis. Overall, this highlights that the effect of hypoxia depends on the type of CAF and type of tumour, and may also depend on the degree or duration of hypoxia as methods were highly varied in these studies, from the overexpression of HIF to hypoxic culture at various O2 concentrations (Araos, Sleeman and Garvalov, 2018a).

Notably, inhibition of angiogenesis as a treatment strategy has been associated with subsequent hypoxia, with detrimental effects on the ECM including increased collagen, hyaluronic acid, and sulphated glycosaminoglycans, and these were specifically correlated with increased metastasis in murine models of colorectal and pancreatic cancer (Aguilera *et al.*, 2014; Rahbari *et al.*, 2016). Finally, it is important to mention that the interaction between the cancer cell and ECM is dynamic and bi-directional. Biglycan in the ECM acted on gastric endothelial cells to increase HIF1α expression *via* NF-κB to increase migration and invasion, and extracellular matrix protein 1 (ECM1) increased HIF1α *via* integrin β4, FAK and SOX2 signalling to affect glucose metabolism and metastasis (Hu *et al.*, 2016; Gan *et al.*, 2018).

Therefore, both the ECM and neighbouring fibroblasts are highly sensitive and responsive to hypoxia, and this is pivotal in creating a microenvironment that is further conducive to tumour progression.

1.2. V c) Immune suppression

One hurdle that all cancers must overcome in order to progress is to escape destruction by the immune system. HIF-1α-dependent signalling contributes to this in several ways. Cancerous cells are normally detected by CD8+ cytotoxic T lymphocytes (CTLs) and natural killer cells, which attempt to eradicate the cancer cell by secreting cytotoxic granules towards the cell membrane. These granules contain granzymes, which activate both caspase-dependent and independent apoptosis (Lieberman, 2003). HIF signalling directly counteracts this by inhibiting apoptosis (Greijer and van der Wall, 2004), and inducing autophagy and STAT3 signalling which confers additional resistance to CTL-mediated lysis (Noman *et al.*, 2011)(Noman *et al.*, 2009). Expression of miRNA miR-210 during hypoxia was shown to encourage escape from CTL-mediated cytotoxicity, in melanoma and non-small cell lung carcinoma (Noman *et al.*, 2012). In a hepatocellular carcinoma cell line, hypoxia promoted an immunosuppressive phenotype. These results suggest that HIF inhibition would be a useful addition to a treatment strategy to counteract immune suppression. Unfortunately, HIF1α was essential for effective CD8+ CTL immune infiltration of the tumour

and cytotoxicity in a mouse model of melanoma and lung carcinoma, suggesting that HIF inhibition would prevent immune destruction (Palazon *et al.*, 2017). Immune checkpoint inhibitors, agents that block the receptors on cancer cells that repress immune recognition, such as CTLA-4-, PD-1-, and PD-L1 inhibitors, have shown marked success in tumours such as melanoma and lung cancer, but no success in cancers such as PCa due to the hypoxic microenvironment. Murine models have indicated that CTLs are rarely able to infiltrate hypoxic areas, and those that do, struggle to survive the hostile environment of low pH, low levels of glucose, amino acids and other nutrients, and the high concentrations of inhibitory ligands such as PD-L1 and inhibitory cytokines such as TGF-β, and extracellular adenosine (Chouaib *et al.*, 2017). However, use of a hypoxia-activated prodrug (TH-302/evofosfamide) was able to disrupt hypoxia and eradicated over 80% of PCa tumours in a transgenic adenocarcinoma of the mouse prostate (TRAMP) model, when in combination with immune checkpoint inhibitors (Jayaprakash *et al.*, 2018). This reinforces the importance of targeting hypoxia in effective chemo- and immunotherapies.

Thus, while reduction in hypoxia has been shown to increase the efficacy of therapies, HIF is unlikely to provide a robust therapeutic target due to its promiscuous role and complicated interaction with immune cells. Successful approaches have utilised hypoxia-activated pro-drugs, and better characterisation of the critical downstream mediators of HIF activity in this context should be explored, with the view to clinical applications.

1.2. V. d) Stemness

A hypoxic microenvironment is conducive to cells with a stem-like phenotype and this has huge implications for the development and treatment of cancer. Until recently, there were two schools of thought to explain the heterogeneous nature of tumours and the process of metastasis: the classic stochastic model (also known as the clonal evolution model) and the more recent hierarchical model (also known as the cancer stem cell (CSC) model). The stochastic model argues that tumour cells acquire a specific set of somatic mutations to obtain metastatic capability, and by this logic all cells in the tumour possess the potential to drive cancer progression. The hierarchical model makes a distinction between cells with a unique potential to generate malignant colonies and drive cancer progression and metastasis (tumour-initiating cells), and those that have differentiated from them and are cancerous but do not have sufficient pluripotency to increase malignancy. This is also known as the CSC model as these tumour-initiating cells share physiological similarity to stem cells and may in fact be transformed stem cells. Traditionally, the stochastic model proposed that normal somatic cells accumulate mutations in at least five pathways for the cell to possess all the hallmarks of cancer and that these mutations occur randomly due to stresses and ageing. Several observations contradict this model. Firstly, certain cancers have high incidence in early life and would unlikely have developed due to an accumulation of random mutations. Secondly, since differentiated cells have a finite lifespan, in order to accumulate mutations in the vital pathways a mutation causing unrestrained proliferation would need to occur very early to allow the

additional necessary mutations time to occur. The stochastic model also implies that each cell in a tumour is highly malignant and has equal tumour-initiating potential. However, *in vivo* studies have shown that implantation of at least 10,000 cancer cells are needed to reliably initiate tumours (in immunocompromised mice) which would indicate that relatively few have the appropriate tumour-initiating capabilities. Hence the hierarchical hypothesis was proposed in which CSCs are responsible for tumour initiation, maintenance, and the development of more malignant clones that underlie metastatic spread (Wang *et al.*, 2015). To support this, in numerous tumour types a specific subpopulation of cells have been isolated that have properties similar to stem cells, such as self-renewal, and that differentiate into tumour cells. These subpopulations have been confirmed as the drivers of metastatic spread in several tumour types (Schöning, Monteiro and Gu, 2017). However, currently the two models are not considered to be mutually exclusive, as it is unknown if the CSCs are indeed resident stem cells that have become transformed, or are somatic cells that have dedifferentiated during transformation.

Hypoxia increases the stemness of cancer cells, most evidently through the activation of NOTCH signalling (Marignol *et al.*, 2013). Furthermore, HIF-1α and HIF-2α regulate multiple stem cell marker genes and reduce proliferation. EMT is closely linked with acquisition of the CSC phenotype in several tumour types. Hypoxia also appears to play a vital role in CSC maintenance, and it is associated with CSC enrichment. This is because CSCs are known to prefer low oxygen environments since they are highly sensitive to ROS and may actively seek out a hypoxic niche. Two breast cancer studies showed that HIF-1α and HIF-2α regulated RNA demethylase ALKBH5, leading to increased Nanog expression and stability as well as significant enrichment of CSCs (C. Zhang *et al.*, 2016), and HIF1/2α also induced serine synthesis which was associated with CSC function and metastasis to the lungs (Samanta *et al.*, 2016). Intriguingly, hypoxia can also induce changes in CAFs that regulate CSCs; CAF-secreted TGF-β2 increased hedgehog signalling in CSCs and promoted chemoresistance in a colorectal cancer model (Tang *et al.*, 2018). These results highlight the detrimental effect of a hypoxic microenvironment, considering its effect on CAFs and CSCs.

1.2. V. e) Metastasis

Increased expression of either HIF-1/2α was correlated with metastasis in patients with follicular thyroid cancer (Klaus *et al.*, 2018), gastric carcinoma (Tong *et al.*, 2015), gastrointestinal stromal tumour (Chen *et al.*, 2005), osteosarcoma (El Naggar *et al.*, 2012), cervical squamous cell carcinoma (Ishikawa *et al.*, 2004). In vitro studies showed that hypoxia increased the metastatic potential of cancer cells and may also directly modulate stromal cells, although this area is poorly understood and requires further investigation (Araos, Sleeman and Garvalov, 2018b).

Metastasis is a multi-step process based on dynamic interactions between cancer cells and their microenvironment, resulting in escape from the stroma and finally colonisation of a distant site. In order to disseminate, cells acquire motility and invasiveness, usually by reverting to a mesenchymal phenotype *via* EMT. HIF signalling directly increases the migratory and invasive potential of cancer cells by activation

of: receptor tyrosine kinases AXL and c-MET, the Rab11/αvβ3 integrin/focal adhesion kinase (FAK)/PI3K pathway, and miRNAs miR-210, miR-224 and miR-191 (Araos, Sleeman and Garvalov, 2018b). As mentioned in section XX, HIF signalling drives angiogenesis by upregulation of vascular endothelial growth factor (VEGF) and angiopoietin, which encourage the development of blood vessels that are typically weaker and more permeable than in healthy tissue, and are more susceptible to invasion by tumour cells. Overexpression of tissue remodellers such as MMPs by the cancer cells further promotes entry to the blood vessels (intravasation). However, of those cells, very few can survive the shear stress of the blood flow. A seminal *in vivo* study of neuroblastoma reported that hypoxic culture increased the ability of cells to intravade, colonise distant sites (extravasation), and proliferate there. This reveals that hypoxia is capable of profoundly reprogramming cancer cells, to confer increased ability to survive and drive metastasis and to the extent that they maintain their reprogrammed state even after colonisation (Herrmann *et al.*, 2015). It is also important to note that the primary site of PCa metastasis is the bone (Hiraga, 2019), a naturally hypoxic region, and it could be that the PCa cells most prone to metastasis are also most resilient within hypoxic environments. Therefore, hypoxic signalling can promote all stages of metastasis and permanently reprogram cancer cells.

1.2. VI. Cancer cell metabolism and hypoxia

1.2. VI. a) The Warburg effect

Hypoxia also has a role in regulating global metabolism and determining how the cell produces and stores energy, which has implications for cancer cell behaviour. The metabolic pathway glycolysis is an important energy provider for the cell. It consumes two molecules of ATP for the initial phosphorylation and yields four molecules of ATP. However, since the net gain of energy from the alternative pathway oxidative phosphorylation (OXPHOS) is between 30 and 36 ATPs, OXPHOS is normally the primary source of energy. However, since oxygen is required as cofactor for OXPHOS, glycolysis is an essential resource for the cell during anaerobic conditions. Furthermore, since the rate of ATP production by OXPHOS pathway saturates rapidly at high levels of substrate or limited oxygen supply, upregulating the glycolysis pathways can be used to steady the rate of ATP production (Potter, Newport and Morten, 2016).

In the 1920s, biochemist Otto Warburg proposed that glycolysis was upregulated in cancer cells, even while oxygen levels were sufficient for OXPHOS, and he attributed this to impaired mitochondrial function. Later experiments by Weinhouse *et al* ran isotope-tracing experiments to show that glucose could be oxidised to CO2 by cancer cells at a rate comparable with normal cells. This indicated that cancer cells sustain a high rate of both glycolysis and OXPHOS, in contrast to normal cells (Otto, 2016). Indeed, one of the hallmarks of cancer is “Deregulating cellular energetics”. Cancer cells may upregulate glycolysis in order to boost the metabolic pathways that require glycolysis: the pentose phosphate pathway (for protein glycosylation); glycogenesis (for the storage of glucose); the serine biosynthesis pathway (which produces amino acids

and is followed by the one-carbon metabolism pathway that produces NADPH and is required for glutathione and purine biosynthesis), as well as for the methionine cycle (for methylation). Thus, upregulation of glycolysis allows cancer cells to increase the production of amino acids, nucleotides, and fatty acids and thus increase the production of proteins, nucleic acids, and membranes to support rapid growth. Cancer cells may exploit these regulatory pathways to fuel proliferation and to adapt to changing microenvironments.

1.2. VI. b) Hypoxia and the Pasteur Effect

The Pasteur Effect refers to the reflection of oxygen availability on metabolism, such that high levels of oxygen promote OXPHOS and inhibit glycolysis and *vice versa*. In fact, oxygen consumption can be used a measure of the rate of OXPHOS. This phenomenon has huge implications for cancer biology, in that hypoxic tumours would be expected to favour glycolysis. A review in 2004 by Zu and Guppy discussed how the perception that cancer cells invariably utilise aerobic glycolysis (a "Warburg effect") may be a misconception, they report many instances in which this assumption confounded research, and influenced strategies for the diagnosis, monitoring, and treatment of tumours. For example, the diagnostic method fludeoxyglucose-positron emission tomography (F DG–PET) technique measures glucose uptake to differentiate cancerous from normal tissue. Zu and Guppy argued that although FDG–PET may be reliable, the glucose absorbed is likely converted into lipids rather than used for glycolysis. They also reported that at the time of publication, over half of the studies that they had reviewed had not accurately measured the energy budget of the cells (*i.e*. measured oxygen consumption as well as lactate production) to determine the contributions of OXPHOS and glycolysis. A hypoxic condition could bias this as lactate is being released although oxygen consumption not increased. Interestingly, those studies that had correctly measured the energy budget had actually reported lower proportions of ATP contributed by glycolysis than OXPHOS. Therefore, while some cancers may indeed display the Warburg effect, there is insufficient evidence to confirm that this is an inherent feature of cancer cells and it may have been vastly overestimated. In fact, in many cancers, OXPHOS is intact or even upregulated. Cancer cells may upregulate glycolysis not as an inherent feature but in response to hypoxia (Pasteur Effect), which would also explain the efficacy of the FDG–PET technique as hypoxic tumours tend to be most aggressive (Zu and Guppy, 2004). This highlights the prevalence of hypoxia in solid tumours and the importance of understanding its effects on cancer cells.

1.2. IV g) Cancer cell dormancy

Cancer patients often spontaneously develop metastatic disease after years or even decades in remission. This is due to cancer cell dormancy – a state of temporary quiescence followed by reactivation of growth signalling. There may also be subpopulations of "micrometastases", cells that are cycling but dying at a similar rate due to CTL cytotoxicity (immunogenic dormancy) or insufficient blood supply (angiogenic dormancy) (Aguirre-Ghiso, 2007). Even very small tumours have been associated with metastases, suggesting that metastases can occur early but the cells can lie dormant and undetected for long periods.

Hypoxia may be pivotal in the process of dormancy, which is characterised by quiescence (G0-G1 arrest), low metabolism, and expression of stem cell markers (Manjili, 2017). In support of this, a study using breast cancer cells demonstrated that exposing cells to cycling hypoxia, conferred resistance to subsequent chronic hypoxia by entering a state of dormancy. Autophagy was upregulated in the dormant cells and may be important in the process (Carcereri de Prati *et al.*, 2017). Suppression of Akt signalling was key in the establishment of dormancy following hypoxia in pancreatic cells (Endo *et al.*, 2014). Dormancy is associated with resistance to chemotherapy, as traditional cytotoxic agents target mitotic cells. In colorectal cancer cells, hypoxia elicited dormancy as well as chemo-resistance (Endo *et al.*, 2014).

As mentioned previously, hypoxia is capable of extensive transcriptional reprogramming and this may include establishment of dormancy-like features, maintained throughout metastatic spread. Metastatic disseminations from hypoxic tumours showed propensity for dormancy and chemoresistance, *via* expression of HIF1α and dormancy factors NR2F1 and p27 (Fluegen *et al.*, 2017). Therefore, a hypoxic primary tumour microenvironment is associated with dormant cancer cells that disseminate and evade therapy. However, hypoxia is also implemental in the reactivation of dormant disseminated tumour cells. In a study of breast cancer metastasis to bone, hypoxia in the bone was the trigger to suppress dormancy-regulating signalling (the leukaemia inhibitory factor (LIFR)/STAT3/SOCS3 pathway) in the colonising breast cancer cells, and reawaken proliferation (Johnson *et al.*, 2016). This study is critical in highlighting the multiple roles of hypoxia in promoting entry into dormancy and later exit. Moreover, it is likely that similar mechanisms occur in a PCa setting.

1.2. VII. Hypoxia in Prostate Cancer

Early studies of tumour oxygenation by probe measurements, showed that the majority of prostate tumours were hypoxic (Parker *et al.*, 2004) and hypoxia is now considered a common feature of prostate tumours (Marignol *et al.*, 2013). As noted in section *1.1. I*, the prostate acts as a filter for toxins and age is associated with the accumulation of toxins, and the onset of PCa. Hypoxia also increases in the prostate with age, due to an ageing cardiovascular system causing reduced blood flow, or poorer vascular integrity in the transitional zone; there may also be age-related tissue remodelling which has a high consumption of oxygen. This hypoxia may promote the expression of pro-survival genes and indeed, transcriptional analyses have shown hypoxia-associated gene signatures in the ageing prostate (Watso*n et al*>, 2009). This suggests that hypoxia may play a role in driving the initiation of PCa. Moreover, the expression of hypoxic markers correlate with PCa aggressiveness, resistance to therapy, and relapse (Vergis *et al.*, 2008)(Deep and Panigrahi, 2015).

As discussed in section *1.1. VIII*, PCa invariably develops resistance to ADT (leading to relapse) because the cancer cells adaptively switch to an androgen-independent pathway. Hypoxia may play a critical role in mediating the development of androgen independence, although this is a largely unexplored area.

Early mechanistic studies investigating AR signalling highlighted crosstalk between AR, HIF-1α and NOTCH pathways. First, two groups showed that hypoxia upregulates NOTCH ligands in PCa, and HIF-1α binds NOTCH response elements and induces expression of target genes (Belandia *et al.*, 2005)(Gustafsson *et al.*, 2005). Then, two studies using the PCa cell line LNCaP revealed that DHT could increase expression of HIF-1α target gene *GLUT-1*, and hypoxia increased expression of *PSA* (Horii *et al.*, 2007), and hypoxic conditions increased AR transcriptional activity (Park *et al.*, 2006).

Since then, other reports have specifically associated ADT and the occurrence of CRPC with hypoxia. An epidemiological analysis of men who had received HIF-1α inhibitors for PCa, revealed a significant reduction in their risk of developing CRPC (Ranasinghe *et al.*, 2014). Furthermore, a genetic polymorphism in the *HIF-1α* gene (HIF1A +1772 T-allele) was associated with an increased chance of developing resistance to ADT and metastasis (Fraga *et al.*, 2014). Another group showed that hypoxia induced the transcription factor *STAT5* expression and this was also a feature of both long-term ADT treated and CRPC xenografts (Røe *et al.*, 2013). Important insights have come from an approach using dynamic contrast enhanced magnetic resonance imaging, which revealed that ADT-treated xenografts had increased vascularisation (increased number of vessels, vessel density, and vessel area fraction) and increased hypoxia (shown by hypoxia staining). After approximately 6 months, the xenografts had become androgen-independent (CRPC) and displayed further increases in tumour vascularisation (Røe *et al.*, 2012). A recent study found that CRPC samples overexpressed the oncogene positive cofactor 4 (PC4) which promotes proliferation *via* c-myc/p21, and they showed that it also activates HIF-1α and b-catenin, corroborating the link between hypoxic signalling and androgen-independence (Luo *et al.*, 2019).

Research from our laboratory has demonstrated that treatment with bicalutamide *in vivo* (using an LNCaP xenograft model of PCa) significantly increased hypoxia and also triggered the upregulation of genes involved in EMT (Ming *et al*>, 2013)(Byrne *et al.*, 2016). In line with this hypothesis, use of the hypoxia-activated pro-drug OCT1002 in combination with bicalutamide inhibited hypoxia and metastatic spread, in a murine model of PCa (Nesbitt *et al.*, 2016). These *in vitro* and *in vivo* studies at Ulster provided consistent evidence that hypoxia is an important factor in selecting for cells with increased capacity for cancerous growth, although the mechanisms underpinning this remain to be elucidated.

A recent study corroborated further the link between ADT, hypoxia and CRPC. The group reported that chronic ADT during hypoxia produced androgen-independence in cell lines, which was dependent on the expression of glucose-6-phosphate isomerase (GPI). *GPI* expression was repressed by AR during hypoxia, but was increased by ADT. The researchers concluded that during hypoxia, GPI diverts glucose metabolism away from the AR-dependent pentose phosphate pathway (PPP) and into glycolysis. This could explain why their enzalutamide treatment was less effective during hypoxia, as GPI was de-repressed and facilitated the switch to glycolysis. They also showed that inhibiting GPI prevented resistance to enzalutamide during hypoxia *in vitro* and that it improved the efficacy of enzalutamide *in vivo* (Geng *et al.*, 2018).

Taken together, these findings demonstrate that ADT is associated with increased hypoxia, and that in turn hypoxia can modulate AR signalling. This emphasises the need to understand the precise genetic changes that occur following ADT and hypoxia in PCa cells, and implicates hypoxia as a modifiable facet of the microenvironment that if inhibited during adjuvant therapy may prevent relapse.

1.2. IX. Summary

Hypoxia is a physiological condition in many tissues, but when dysregulated it has deleterious effects, such as the increased malignancy observed in hypoxic tumours. Hypoxic signalling has been extensively characterised although some aspects remain poorly understood, such as its links with AR signalling that may underlie its role in the promotion of CRPC. And as the next section demonstrates, there is still much to be discovered about the genetic pathways affected by hypoxia.

1.3 MicroRNAs

1.3. I. Non coding RNAs

The bulk of genetics research has focused on analysing the expression patterns of coding genes (comprising 1.5% of the human genome), and until relatively recently, it was thought that non protein-coding regions were non-functional "junk" DNA. However, in the last 30 years, it has become apparent that some non protein-coding regions are also critical in maintaining healthy physiology. These regions may be transcribed into non-coding RNAs (ncRNA) that mainly function to regulate the synthesis of protein from mRNAs. NcRNAs include microRNAs (miRNAs), PIWI-interacting RNAs (piRNAs), transcribed ultra-conserved regions (T-UCRs), small nucleolar RNAs (snoRNAs), large intergenic non-coding RNAs (lincRNAs) and long non-coding RNAs (lncRNAs) (a heterogeneous group of long RNAs). Even transfer RNAs can be cleaved to produce bioactive RNAs (tiRNAs)(Esteller, 2011).

MicroRNAs are short in length (18-25 nucleotides) and are the most widely studied form of ncRNA. In 1993, Viktor Ambros' and Gary Ruvkun's research groups together discovered that the *lin-4* gene in *C. elegans* encoded a short RNA molecule that was not detectable as a protein sequence but was nevertheless essential for *C. elegans'* development. Shortly afterwards they discovered that it had antisense complementarity to the *lin-14* gene and thus discovered the phenomenon of RNA-induced interference (RNAi) (Bartel, 2004). Twenty-five years later, miRNAs are recognised as pivotal regulators of essential cell processes. Many are highly conserved across animals and plants. In mammals, there are around 300 conserved miRNA genes and a further 1000 loci that encode miRNA-like transcripts, although these are less conserved (Mendell and Olson, 2012). Approximately one third of miRNA genes are located within the intronic regions of protein coding genes ("miRtrons") and are co-expressed with them, often with related functions (Mendell and Olson, 2012). In terms of mRNA targets, David Bartel's group have shown that in

humans, over 45,000 miRNA binding sites within 3'UTRs were conserved, and that over 60% of protein-coding genes were regulated by miRNAs (Friedman *et al.*, 2009).

1.3. II. MicroRNA biogenesis, structure and regulation

The mature miRNA is a short RNA sequence (18-25 nucleotides long, and on average 22 nucleotides), which is the finished product of a two-step cleavage from a longer primary transcript, by two class III nuclear ribonucleases: Drosha and Dicer (Figure 7). The primary transcript (pri-miRNA) is mainly transcribed by RNA polymerase II (although some Pol I derived transcripts have been identified) and has the classic features of an mRNA: a 5' cap and poly(A)tail. A microprocessor complex, containing Drosha and the double-stranded RNA binding protein DGCR8 (homolog of *D. melanogaster* and *C. elegans'* Pasha), binds the pri-miRNA. Then, Drosha cleaves the pri-miRNA to release one or more 60-90 nucleotide sequences that form stem-loop structures (the pre-miRNA). Pre-miRNAs can also arise as splice products of pre-mRNAs. Next, the pre-miRNA is exported from the nucleus to the cytoplasm by the Exportin 5-RAN-GTP complex, and cleaved a second time by Dicer into a short duplex. The mature miRNA is loaded to a member of the Argonaute (AGO) family by Dicer and the TAR RNA-binding protein 2 (TRBP), to form the miRNA-induced silencing complex (miRISC). Loading of the miRNA onto AGO requires ATP and the activity of the chaperones Hsc70 and Hsp90. MiRNA loading onto RISC is highly regulated, as is the activity of the proteins of the miRISC (Bartel, 2009).

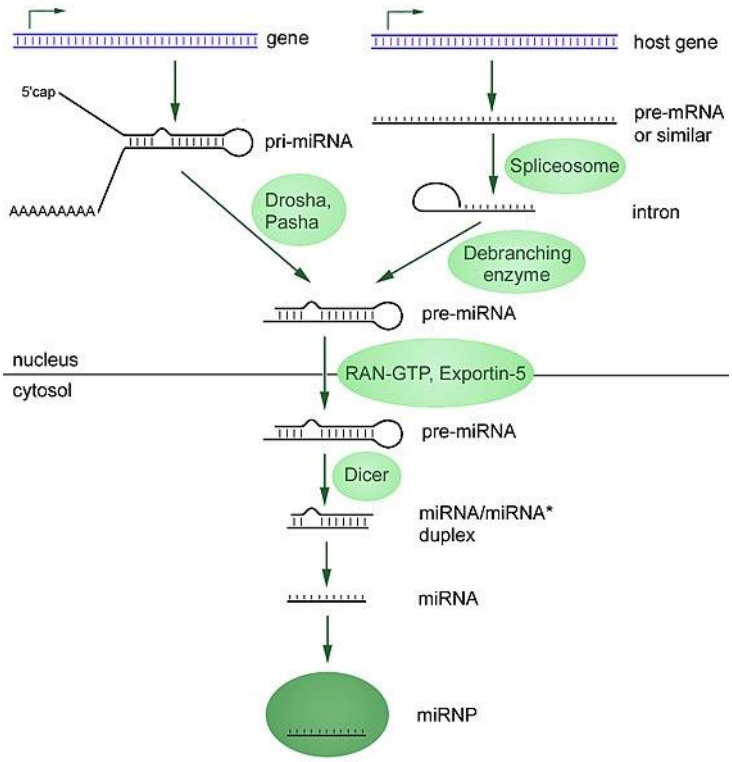

Figure 7. MicroRNA biogenesis. Image from Wikipedia, usage rights: labelled for reuse. Pre-miRNAs can arise as products of a pri-miRNA or as a splice product of a pre-mRNA. The pre-mRNA is exported from the nucleus by the exportin-RAN-GTP complex and cleaved by Dicer into the short duplex, one strand is retained and loaded onto miRNA ribonucleoprotein (miRNP/miRISC) complex.

One strand of the duplex is preferentially loaded onto RISC, which is determined by the thermodynamic stability of each sequence. AGO favours the strand with a thermodynamically less stable 5' end and it prefers U and A over G and C as the terminal 5' nucleotide. For some miRNAs (or in some specific tissue contexts), one "arm" of the pre-miR is associated with a drastically higher abundance of miRNAs, indicating that it is more biologically active and the opposing strand is degraded, and in some cases the more abundant strand switches (miRNA arm-switching). Traditionally, the less active strand was known as the "star" strand with an asterisk used to denote it (miRBase, 2019).

The sequence of the miRNA/siRNA guides AGO to mRNAs by base complementarity. In animals, miRNAs usually bind the 3' UTR of mRNA targets by their seed region (positions 2–8 of the mature miRNA, Figure 8) although recent reports have shown miRNAs capable of binding coding regions and the 5'UTR. Therefore, some miRNAs can target numerous mRNAs and act as master regulators of a process. On the other hand, an mRNA can be targeted by numerous miRNAs, and miRNAs can regulate their targets cooperatively. This produces highly complex networks of miRNA regulation and can orchestrate multiple cellular processes. Individual miRNAs have been shown to be essential for cellular functions such as differentiation, metabolism, apoptosis, and tissue development. MicroRNAs with important biological functions may be highly conserved; some miRNAs have an almost identical sequence across invertebrates and vertebrates (Esteller, 2011).

At the genomic level, over 40% of miRNAs are organised in clusters (within 10kb from one other, and on the same strand) which allows them to be regulated spatially and temporally and to act cooperatively (Altuvia *et al.*, 2005). For instance, the miR-17-92a cluster is a polycistronic transcription unit (C13orf25) giving rise to six miRNAs: miR-17, miR-18a, miR-19a, miR-19b, miR-20a, and miR-92a. MiRNAs may also have "family" members, which share a common ancestor and arose from duplication and mutational events. MiRNA families are often clustered, may have sequence similarity (particularly of the seed region) or similar secondary structure, and often target the same mRNAs providing redundancy. For example, the let-7 gene encodes a conserved miRNA family, including let-7b, let-7c and let-7d, which have various cell-specific influences but are all involved broadly in pathways associated with differentiation (Roush and Slack, 2008).

MicroRNA activity is regulated both transcriptionally and post-transcriptionally. The expression of pri-miRNA transcripts are controlled, as is the activity of splicing factors that may give rise to a pre-miRNA from an mRNA, and the activity of Drosha, Dicer, AGO and other enzymes involved in miRNA biogenesis and function. MicroRNAs may be actively degraded post-transcriptionally, and some have greater stability in tissues than others (Treiber, Treiber and Meister, 2012).

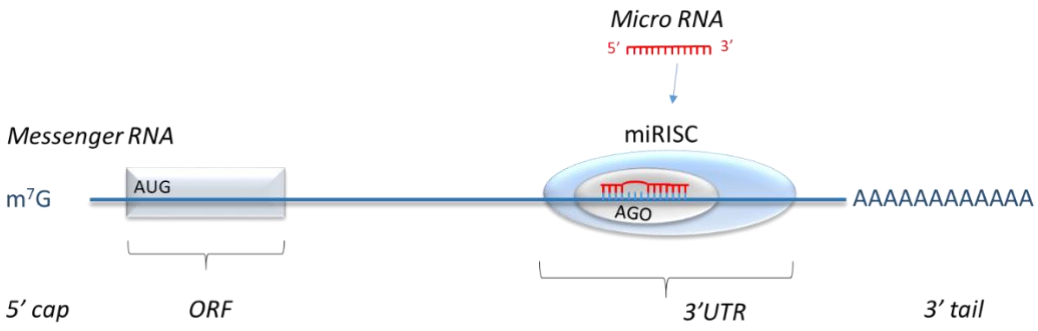

Figure 8. MicroRNA-messengerRNA interaction. MicroRNA bound to AGO-containing miRISC binds the 3'UTR of an mRNA by base-pairing of its seed region.

1.3. III. Mechanisms of microRNA-mediated gene silencing

The involvement of Dicer and the RISC complex is common to all forms of RNA-interference (RNAi), which includes siRNA gene knock down and is mechanistically similar to gene knock out by the CRISPR-Cas9 system. MicroRISC contains a mature miRNA and the RISC cofactors, including AGO that binds the mature miRNA and GW182 which is crucial for effective gene silencing. AGO has four variants, and is bilobal with four conserved domains: N-terminal, Piwi Argonaute Zwilli (PAZ), MID, and PIWI. AGO2 is unique in that it has slicer activity and can cleave perfectly matched targets, however, the other three variants can equally load miRNAs and guide the RISC complex. Interestingly, a Dicer independent miRNA biogenesis pathway was identified, using the slicer activity of AGO2 (Cifuentes *et al.*, 2010). The PAZ domain binds the 3' end of the miRNA, the PIWI domain is responsible for catalytic activity that allows the mRNA to be cleaved, and a hydrophilic pocket in the MID domain binds the 5' phosphate of the miRNA, and a rigid loop binds the 5' base (the nucleotide specificity loop). The 3' end is bound by the PAZ domain, although there is little or no specificity to the 3' base identity. Therefore, all the domains of AGO (including the linker domains) are in contact with the guide RNA, while specific pockets of the PAZ and MID domains bind its termini. The seed region (nucleotides 2-7) is held in an A-form helical loop by AGO by a series of salt bridges and hydrogen bonds with the phosphate backbone. Nucleotides 2-6 are exposed to the solvent, and form Watson-Crick base-pairing with target mRNAs. The remainder of the miRNA is wound through a hydrophobic channel between the two lobes (Schirle and MacRae, 2012).

MicroRISC binding causes translational repression, usually accompanied with mRNA decay. Messenger-RNA decay occurs by either whittling down of the poly(A) tail (de-association with the poly(A) binding protein removes its protection from degradation) or by immediate cleavage. Work from the Bartel group has recently shown that the initial length of the poly(A) tail determines the rate of mRNA degradation upon RNAi, with short-tailed mRNAs being more rapidly degraded. This staggers the rate at which mRNA targets are degraded upon miRNA overexpression. Mechanistically, translation repression is achieved in several ways: pre-initiation by interfering with eIF4E recognition of the cap (indeed, the MID domain of AGO has a structure similar to the cap-binding motif found in eIF4E), or by preventing recruitment of the 40S or 60S ribosomal subunit. Translation may be inhibited post-initiation by preventing ribosomal elongation. Alternatively, the miRISC causes mRNA decay through GW182 interacting with deadenylase complexes (CCR4–NOT and PAN2–PAN3), which deadenylate the poly(A) tail. Next, the 5' cap is removed by the DCP1–DCP2 complex. In the absence of the cap and poly(A) tail, an Xrn1 5'–3' exonuclease digests the mRNA. GW182 also binds poly(A) binding protein (PABP), which is known as a translation initiation factor by promoting mRNA circularisation. This indicates that GW182 may prevent translation initiation by competitively binding PABP and inhibiting the PABP-eIF4G association and mRNA circularisation, or by recruiting the deadenylation complexes to the cap. Therefore, the miRNA sequence determines which mRNAs are targeted, and the associated proteins determine the effect on the mRNA (Esteller, 2011).

1.3. IV. Functions of miRNAs in cell signalling pathways

MicroRNAs modulate cell signalling pathways through multiple mechanisms. The simplest is when a protein-coding gene regulates the expression of a miRNA, which then plays an integral part in the pathway. Secondly, a miRNA may be expressed constitutively and function to titrate the activity of an mRNA target that becomes induced. Here, the miRNA may play an important dampening or heightening effect on the target. Thirdly, miRNAs can facilitate both negative and positive feedback loops, by promoting or inhibiting the pathway through new targets, or by targeting their own transcriptional activators or repressors. Finally, miRNAs may simultaneously up- and down-regulate a pathway, producing a buffer effect and stabilising the signal. This is evident when the deletion and overexpression of a miRNA produces the same phenotype (Mendell and Olson, 2012). As well as intracellularly, miRNAs are essential mediators of paracrine signalling; they are detected in exosomes and may have important local and systemic effects. However, the levels of miRNAs found in circulating exosomes may be too low to exert significant biological effects on distant tissues, although this remains to be investigated (Mendell and Olson, 2012).

1.3. V. MicroRNAs and human disease

A single miRNA can play an enormous role in regulating the activity of a specific pathway and often functions to coordinate numerous pathways. Given their involvement in basic cell processes, the aberrant expression if miRNAs can result in developmental defects and disease. The abnormal expression of individual miRNAs is involved in the development of cancer, neurodegenerative and metabolic disorders, and viral infection (Eulalio, Huntzinger and Izaurralde, 2008). Here, dysregulation in miRNA expression can arise from mutational or epigenetic events at the pri-miRNA gene or promoter region, genomic relocations leading to amplifications or deletions, or in the expression (or activity) of transcription factors or enzymes involved in miRNA processing, such as the splicing factors (Eulalio, Huntzinger and Izaurralde, 2008).

1.3. VI. MicroRNAs in cancer

The link between miRNA dysregulation and cancer first arose as miRNAs were shown to be essential in key cancer-related pathways such as cell proliferation and apoptosis. Genome-wide association studies (GWAS) also indicated that specific miRNAs were lost in cancers. The first evidence of miRNA involvement in cancer was a study of chronic lymphocytic leukaemia (CLL), in which the authors reported frequent deletion of the miR-15a/16-1 and confirmed them as driver mutations of the disease (Calin *et al.*, 2002). Since then, the results of hundreds of sequencing-based studies have confirmed that tumours have highly abnormal miRNA expression patterns, and *in vitro* functional studies showed that miRNAs have oncogenic roles (*e.g.* miR-21, miR-155) and tumour-suppressive roles (*e.g*. miR-15∼16), while some are context-dependent (*e.g*. miR-29 and miR-146) (Kasinski and Slack, 2011). The miR-200 family have been extensively studied and are known to be involved in many tumour types, since they are key regulators of the ZEB family of transcription factors that induce EMT in numerous tumours including PCa (Chen *et al.*, 2014) (Abisoye-Ogunniyan *et al.*, 2018). Preclinical models have confirmed this: *in vivo* transgenic expression of the miR-17-92a cluster in

hematopoietic progenitor cells caused Myc-activated B-cell lymphomagenesis to progress rapidly *in vivo* (He *et al.*, 2005), while its deletion resulted in apoptosis in Myc-induced lymphoma cells *in vitro* (Mu *et al.*, 2009). Furthermore, delivery of certain tumour-suppressive miRNAs inhibited tumour growth, such as let-7, miR-34a, miR-26a, and miR-143/145 (Kota *et al.*, 2009; Pramanik *et al.*, 2011; Trang *et al.*, 2011).

1.3. VII. MicroRNAs and stress responses

Since GWAS studies showed that miRNAs were deleted in certain cancers, early studies focused on miRNA knock-out models to identify their function. However, most failed to identify precise roles as the mice appeared to develop normally. Moreover, miRNAs rarely played a vital role in the development of model organisms such as *C. elegans* and *D. melanogaster*. However, it was later observed that while deleting certain miRNAs often did not impact the development of a mammalian organ, it incapacitated its ability to respond to stress. For instance, mice with miR-208a$^{-/-}$ have normal cardiovascular development and function, but have impairments in cardiac remodelling and do not develop cardiac fibrosis following stresses (van Rooij *et al.*, 2007). Similarly, mice with homozygous knock-out of miR-375 develop normal pancreases but cannot induce pancreatic β-cell expansion after obesity-induced insulin resistance, leading to severe diabetes (Poy *et al.*, 2009). Intriguingly, miRNAs appear to be crucial in mediating the hypoxic response. One group knocked out Dicer in non-small cell lung carcinoma (NSCLC) cells and used them to establish a xenograft model; the resulting tumours were highly hypoxic but poorly vascularised, suggesting that miRNAs mediate angiogenesis (Chen *et al.*, 2014). Additionally, hypoxia is associated with a specific miRNA profile in many cancer types. In breast and lung cancer tumours, the miRNA miR-210 is highly upregulated by HIF-1α as one of the earliest effects of hypoxia. MiR-210 was also implicated in mitochondrial dysfunction following hypoxia (Chen *et al.*, 2014). MiRNAs are pivotal in inflammatory signalling, in particular, miR-155 and miR-342-5p. These miRNAs regulate intra- and intercellular inflammatory responses, and are thus involved in cancer progression (Chen *et al.*, 2014).

In support of their prominent role in stress responses and cancer cell maintenance, *in vitro* and *in vivo* studies have shown promising results in that miRNA-based therapies can damage cancer cells while healthy cells remain unaffected. This suggests that transformation renders the cell more sensitive to (or reliant) on changes in miRNA signalling. This may be because cancer essentially represents a state of chronic stress, with persistent DNA damage and sustained DNA-damage response, an accumulation of misfolded proteins and aggregates due to abnormal protein complexes, aneuploidy, and metabolic reprogramming that fuels increased growth but results in high levels of toxic intermediates such as ROS (Luo, Solimini and Elledge, 2009). Therefore, modulation of miRNAs may selectively affect diseased cells with minimal impact on healthy cells.

Alternatively, it has been suggested that miRNAs serve mainly to maintain cells in a differentiated state. This would also explain the abnormal miRNA expression patterns observed in cancer, and their importance in fully developed tissues rather than early development (Reid *et al.*, 2016).

1.3. VIII. MicroRNAs in prostate cancer

Individual miRNAs have been attributed oncogenic effects within the context of PCa. For example, miR-21 is a marker of cancer in many tumour types and increases with Gleason grade in a linear manner in PCa (Cannistraci *et al.*, 2014). Similarly, miR-221 and miR-222 are increased in PCa tissue and increase clonogenicity in vitro. Mechanistically, they may exert oncogenic effects by downregulating CDK inhibitor p27Kip1 and promoting cell cycle progression (le Sage et al. 2007; Galardi et al. 2007; Mercatelli et al. 2008). MiR-141 is overexpressed following castration and may play a role in androgen-independence (Zhang *et al.*, 2013); it was also increased in PCa patients' serum (Mitchell *et al.*, 2008). MiR-18a is highly upregulated in PCa and in advanced PCa as well as upregulation in the serum (Al-Kafaji, Al-Naieb and Bakhiet, 2016). Other miRNAs which are upregulated in PCa, and may have oncogenic effects, are miR-32 (regulator of PI3K) (Jalava *et al.*, 2012), the miR-106b/miR-25 cluster (regulator of CASP7) (Walter *et al.*, 2013), and miR-125b (Amir *et al.*, 2013).

Conversely, a number of miRNAs have been reported as downregulated in PCa, have been shown to regulate pathways involved in cancer progression, and thus may be tumour suppressors. For instance, miR-34 was reduced in PCa tissues and was confirmed to influence the cell cycle by targeting the cyclin-dependent kinases p16 and p27 (Lynch, McKenna, *et al.*, 2016). MiR-34 inhibits stemness by regulating the adhesion molecule CD44 (Liu *et al.*, 2011) and it is also downregulated by hypoxia, and derepresses *NOTCH1* and *JAG1* to facilitate EMT (Chen *et al.*, 2014). The miR-17-92a cluster appears to have tumour-suppressive effects in PCa, by inhibiting the cell cycle, EMT, and migration as well as improving sensitivity to bicalutamide (Ottman *et al.*, 2016). miR-30a was also proposed to be a tumour suppressor in CRPC, potentially by targeting cyclin E2 (L. Zhang *et al.*, 2016).

Interestingly, the role of epigenetics in regulating miRNA expression in PCa is emerging. For example, miR-4534 becomes expressed due to loss of hypermethylation of its promoter region and inhibits *PTEN* (Rea *et al.*, 2016), and the shared promoter region of miR-200c and miR-141 was methylated in inverse correlation with their expression level in PCa cell lines (Lynch, O'Neill, *et al.*, 2016).

1.3. IV. MicroRNAs as biomarkers and therapeutic targets

MicroRNAs are ideal candidates for biomarkers since their short size and association with the miRISC complex and/or exosomes renders them relatively stable compared to mRNAs and very suitable for testing in patient samples. They are abundant in tissues and bodily fluids (*e.g*. serum, urine, saliva) and readily quantified by polymerase chain reaction (PCR) experiments. Many miRNAs are detectable in systemic circulation and may be useful as biomarkers of a disease state or a response to treatment, and miRNAs profiling was capable of predicting cancer incidence or outcome in bladder cancer, gastro-oesophageal

cancer, pancreatic cancer, and lung cancer (Blick et al. 2015; Winther et al. 2016; Wu et al. 2016; Mace et al. 2013).

MicroRNAs are also attractive as therapeutic targets, as they can be mimicked or inhibited by synthetic oligonucleotides (Kreth, Hübner and Hinske, 2018). Firstly, this is useful because the oligo can regulate numerous signalling pathways at once, as opposed to the traditional "one target, one drug" approach. Targeting multiple pathways simultaneously improves the scope of the agent over different clones and reduces the chances of drug resistance developing (Reid *et al.*, 2016). Moreover, synthesising an oligo that is complementary to a miRNA is easy and cost-effective from a drug development perspective, compared with designing small molecules that fit a protein domain and have acceptable bioavailability, metabolic half-life, and minimal side effects. This means RNAi-based therapies may allow the targeting of previously "un-druggable" proteins.

The first miRNA-based therapy to enter clinical trials was MRX34, double-stranded synthetic version of miR-34a (23 nucleotides long) encapsulated in a ~110 nm liposomal nanoparticle, for the treatment of advanced solid tumours in the liver. MiR-23a is a master tumour-suppressor that regulates over 30 oncogenes. MRX34 was administered intravenously and permeated many organs including the spleen and bone marrow. It demonstrated significant anti-tumour activity and acceptable safety at Phase I although failed ta Phase II (Kreth, Hübner and Hinske, 2018). MiRNA "antagomiRs" and "sponges" exert the opposite effect to mimics. Unlike mimics they are single stranded, and can also be administered intravenously. AntagomiRs contain an antisense sequence and sponges are longer with multiple antisense seed sequences to "mop up" an excess of a miRNA. Recruitment is underway for Phase I trial for MRG-106, a miR-155 antagomiR to treat cutaneous T cell lymphoma. Currently the only miRNA-based therapy to have passed Phase II is an anti-miR-122 that treats hepatitis C virus infection, although many more are in development (Kreth, Hübner and Hinske, 2018). The main issues in RNAi based therapies are preventing off-target sequence binding, and facilitating the delivery and preservation of small RNA molecules (that eukaryotic cells have evolved to recognise as foreign genetic material). However, new delivery means are being developed, such as the GalNAc ligand which can be conjugated to siRNA and facilitates delivery in liver cells (Springer and Dowdy, 2018).

1.3. V. Summary

MicroRNAs are a species of non-coding RNA that were discovered 26 years ago and have since been shown to regulate literally all cellular pathways, and they are essential for rapid cellular adaptation to stress conditions. As a disease, cancer essentially comprises a state of chronic cellular stress and miRNAs are therefore of interest as novel cancer therapy targets. Indeed, the abnormal expression of individual or groups of miRNAs is observed in many cancers and modulating miRNA expression can reduce cancer

progression in preclinical models. Moreover, miRNAs make attractive candidates as biomarkers or treatment targets due to their physical stability in tissues and fluids, and they are simple to mimic or inhibit pharmaceutically, and a new generation of RNAi-based cancer therapies are entering the clinic. A role for miRNAs in the hypoxic response has been demonstrated in many tissues during both physiological and pathological conditions, although in the context of PCa progression it is relatively unexplored.

1.4. Overall summary and aims of the Project

1.4. I. Overall summary

Hypoxia following ADT may play a key role in facilitating cell survival and dormancy, and contribute to the observed relapse with CRPC. A clearer understanding of the effects of ADT and tumour hypoxia on biochemical progression is needed to reveal why AR inhibition ultimately fails. In particular, the role of miRNAs in the hypoxic response in PCa is understudied.

The overarching aim of this PhD project is to investigate the role of miRNAs in the hypoxic response in PCa, to explore how they may contribute to the development of CRPC in this context.

Figure 9 illustrates how the project has been designed to address this research question.

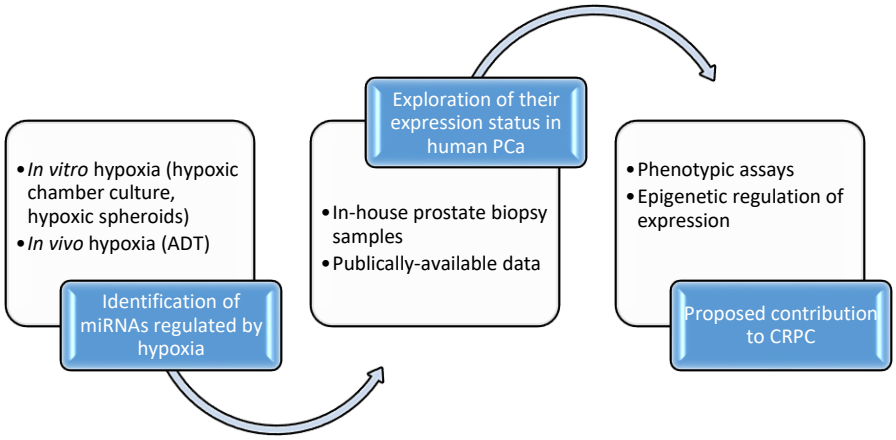

Figure 9. Outline of the PhD: identification of miRNAs involved in the hypoxic response in PCa. *In vitro* and *in vivo* models of PCa hypoxia were set up and used to identify hypoxia-regulated miRNAs. The clinical relevance of the hypoxia-associated miRNAs to human PCa was explored by measuring their expression in human prostate tumour samples (use of an in-house cohort and publically available datasets). To confirm oncogenic effects of the miRNAs, phenotypic assays were used and the regulation of the miRNAs' expression by epigenetics were explored in PCa cell lines.

1.4. II Project objectives

1. Produce a list of candidate miRNAs that are regulated by hypoxia or cancer in a variety of tissue contexts.
2. Develop models of tumour hypoxia in the laboratory and analyse expression of candidate miRNAs during hypoxia by RT-qPCR.
    I. PCa cell lines cultured in hypoxic gas chamber (2D cell layer).
    II. PCa cell lines cultured as spheroid "prostataspheres" (3D culture). Internal cells become hypoxic once a critical size is reached.
    III. Establish *in vivo* xenograft tumour model of prostate cancer. We expect that tumours become hypoxic with size increase, and hypoxia is accelerated by bicalutamide treatment.
3. Exploration of the clinical relevance of the hypoxia-associated miRNAs by measuring their expression in human PCa tissue relative to non-tumour tissue.
    I. Analysis of in-house cohort of prostate biopsy samples.
    II. Data mining of online repositories – to investigate expression of the miRNAs in sequenced prostate tumour samples, and for identification of key signalling pathways.
4. Analyse the functional role of the miRNAs in cancer progression by using phenotypic screening to examine the effect of miRNA inhibition/overexpression on markers of apoptosis, senescence or proliferation.
5. Investigate the regulation of miRNA expression by DNA methylation to explore how its expression may become deregulated during PCa.

1. 5. Bibliography

Abisoye-Ogunniyan, A. *et al.* (2018) 'Transcriptional repressor Kaiso promotes epithelial to mesenchymal transition and metastasis in prostate cancer through direct regulation of miR-200c', *Cancer Letters*, 431, pp. 1–10. doi: 10.1016/j.canlet.2018.04.044.

Aguilera, K. Y. *et al.* (2014) 'Collagen signaling enhances tumor progression after anti-VEGF therapy in a murine model of pancreatic ductal adenocarcinoma.', *Cancer research*. American Association for Cancer Research, 74(4), pp. 1032–44. doi: 10.1158/0008-5472.CAN-13-2800.

Aguirre-Ghiso, J. A. (2007) 'Models, mechanisms and clinical evidence for cancer dormancy', *Nature Reviews Cancer*. Nature Publishing Group, 7(11), pp. 834–846. doi: 10.1038/nrc2256.

Al-Kafaji, G., Al-Naieb, Z. T. and Bakhiet, M. (2016) 'Increased oncogenic microRNA-18a expression in the peripheral blood of patients with prostate cancer: A potential novel non-invasive biomarker.', *Oncology letters*. Spandidos Publications, 11(2), pp. 1201–1206. doi: 10.3892/ol.2015.4014.

Al-Salama, Z. T. (2018) 'Apalutamide: First Global Approval', *Drugs*, 78(6), pp. 699–705. doi: 10.1007/s40265-018-0900-z.

Altuvia, Y. *et al.* (2005) 'Clustering and conservation patterns of human microRNAs', *Nucleic Acids Research*. Oxford University Press, 33(8), pp. 2697–2706. doi: 10.1093/nar/gki567.

Alyamani, M. *et al.* (2017) 'Steroidogenic Metabolism of Galeterone Reveals a Diversity of Biochemical Activities', *Cell Chemical Biology*, 24(7), pp. 825-832.e6. doi: 10.1016/j.chembiol.2017.05.020.

American Urological Association (2019) *Prostatic Adenocarcinoma: Gleason Grading (Modified Grading by ISUP) - American Urological Association*. Available at: https://www.auanet.org/education/auauniversity/education-products-and-resources/pathology-for-urologists/prostate/adenocarcinoma/prostatic-adenocarcinoma-gleason-grading-(modified-grading-by-isup) (Accessed: 22 August 2019).

Amir, S. *et al.* (2013) 'Oncomir miR-125b Suppresses p14ARF to Modulate p53-Dependent and p53-Independent Apoptosis in Prostate Cancer', *PLoS ONE*. Edited by M. L. Anderson, 8(4), p. e61064. doi: 10.1371/journal.pone.0061064.

Andriole, G. L. *et al.* (2012) 'Prostate Cancer Screening in the Randomized Prostate, Lung, Colorectal, and Ovarian Cancer Screening Trial: Mortality Results after 13 Years of Follow-up', *JNCI Journal of the National Cancer Institute*, 104(2), pp. 125–132. doi: 10.1093/jnci/djr500.

Araos, J., Sleeman, J. P. and Garvalov, B. K. (2018a) 'The role of hypoxic signalling in metastasis: towards translating knowledge of basic biology into novel anti-tumour strategies', *Clinical & Experimental Metastasis*, 35(7), pp. 563–599. doi: 10.1007/s10585-018-9930-x.

Attard, G. *et al.* (2016) 'Prostate cancer', *The Lancet*. Elsevier, 387(10013), pp. 70–82. doi: 10.1016/S0140-6736(14)61947-4.

Bain, J. and Bain Mount Sinai Hospital, J. (2007) *The many faces of testosterone*, *Clinical Interventions in Aging*.

Baker, J. E., Moulder, J. E. and Hopewell, J. W. (2011) 'Radiation as a risk factor for cardiovascular disease.', *Antioxidants & redox signaling*. Mary Ann Liebert, Inc., 15(7), pp. 1945–56. doi: 10.1089/ars.2010.3742.

Bartel, D. P. (2004) *Review MicroRNAs: Genomics, Biogenesis, Mechanism, and Function ulation of hematopoietic lineage differentiation in mam-mals (Chen et al., 2004), and control of leaf and flower development in plants (Aukerman and Sakai, 2003*, *Cell*.

Bartel, D. P. (2009) 'MicroRNAs: Target Recognition and Regulatory Functions', *Cell*, 136(2), pp. 215–233. doi: 10.1016/j.cell.2009.01.002.

Bastian, P. J. *et al.* (2012) 'High-Risk Prostate Cancer: From Definition to Contemporary Management', *European Urology*, 61(6), pp. 1096–1106. doi: 10.1016/j.eururo.2012.02.031.

Bayer, C. and Vaupel, P. (2012) 'Acute versus chronic hypoxia in tumors', *Strahlentherapie und Onkologie*. Springer-Verlag, 188(7), pp. 616–627. doi: 10.1007/s00066-012-0085-4.

Belandia, B. *et al.* (2005) 'Hey1, a mediator of notch signaling, is an androgen receptor corepressor.', *Molecular and cellular biology*. American Society for Microbiology (ASM), 25(4), pp. 1425–36. doi: 10.1128/MCB.25.4.1425-1436.2005.

Blick, C. *et al.* (2015) 'Identification of a hypoxia-regulated miRNA signature in bladder cancer and a role for miR-145 in hypoxia-dependent apoptosis', *British Journal of Cancer*, 113(4), pp. 634–644. doi: 10.1038/bjc.2015.203.

Bolla, M. *et al.* (2009) 'Duration of Androgen Suppression in the Treatment of Prostate Cancer', *New England Journal of Medicine*, 360(24), pp. 2516–2527. doi: 10.1056/NEJMoa0810095.

Bosco, C. *et al.* (2015) 'Quantifying Observational Evidence for Risk of Fatal and Nonfatal Cardiovascular

Disease Following Androgen Deprivation Therapy for Prostate Cancer: A Meta-analysis', *European Urology*, 68(3), pp. 386–396. doi: 10.1016/j.eururo.2014.11.039.
Brand, L. J. *et al.* (2015) 'EPI-001 is a selective peroxisome proliferator-activated receptor-gamma modulator with inhibitory effects on androgen receptor expression and activity in prostate cancer', *Oncotarget*. Impact Journals, 6(6), pp. 3811–3824. doi: 10.18632/oncotarget.2924.
Brawley, O. (2012) 'Prostate cancer epidemiology in the United States', *World journal of urology*.
Byrne, N. M. *et al.* (2016) 'Androgen deprivation in LNCaP prostate tumour xenografts induces vascular changes and hypoxic stress, resulting in promotion of epithelial-to-mesenchymal transition', *British Journal of Cancer*, 114(6), pp. 659–668. doi: 10.1038/bjc.2016.29.
Calin, G. A. *et al.* (2002) 'Nonlinear partial differential equations and applications: Frequent deletions and down-regulation of micro- RNA genes miR15 and miR16 at 13q14 in chronic lymphocytic leukemia', *Proceedings of the National Academy of Sciences*, 99(24), pp. 15524–15529. doi: 10.1073/pnas.242606799.
Cannistraci, A. *et al.* (2014) 'MicroRNA as new tools for prostate cancer risk assessment and therapeutic intervention: results from clinical data set and patients' samples.', *BioMed research international*. Hindawi, 2014, p. 146170. doi: 10.1155/2014/146170.
Carcereri de Prati, A. *et al.* (2017) 'Metastatic Breast Cancer Cells Enter Into Dormant State and Express Cancer Stem Cells Phenotype Under Chronic Hypoxia', *Journal of Cellular Biochemistry*. Wiley-Blackwell, 118(10), pp. 3237–3248. doi: 10.1002/jcb.25972.
Center, M. M. *et al.* (2012) 'International Variation in Prostate Cancer Incidence and Mortality Rates', *European Urology*, 61(6), pp. 1079–1092. doi: 10.1016/j.eururo.2012.02.054.
Chang, A. J. *et al.* (2014) 'High-risk prostate cancer—classification and therapy', *Nature Reviews Clinical Oncology*, 11(6), pp. 308–323. doi: 10.1038/nrclinonc.2014.68.
Chen, N. and Zhou, Q. (2016) 'The evolving Gleason grading system.', *Chinese journal of cancer research = Chung-kuo yen cheng yen chiu*. Beijing Institute for Cancer Research, 28(1), pp. 58–64. doi: 10.3978/j.issn.1000-9604.2016.02.04.
Chen, S. *et al.* (2014) 'Global microRNA depletion suppresses tumor angiogenesis.', *Genes & development*. Cold Spring Harbor Laboratory Press, 28(10), pp. 1054–67. doi: 10.1101/gad.239681.114.
Chen, W.-T. *et al.* (2005) 'Hypoxia-inducible factor-1alpha is associated with risk of aggressive behavior and tumor angiogenesis in gastrointestinal stromal tumor.', *Japanese journal of clinical oncology*, 35(4), pp. 207–13. doi: 10.1093/jjco/hyi067.
Chouaib, S. *et al.* (2017) 'Hypoxic stress: obstacles and opportunities for innovative immunotherapy of cancer', *Oncogene*, 36(4), pp. 439–445. doi: 10.1038/onc.2016.225.
Chow, H. *et al.* (2016) 'A phase 2 clinical trial of everolimus plus bicalutamide for castration-resistant prostate cancer', *Cancer*, 122(12), pp. 1897–1904. doi: 10.1002/cncr.29927.
Cifuentes, D. *et al.* (2010) 'A novel miRNA processing pathway independent of Dicer requires Argonaute2 catalytic activity.', *Science (New York, N.Y.)*. American Association for the Advancement of Science, 328(5986), pp. 1694–8. doi: 10.1126/science.1190809.
Cooperberg, M. R. *et al.* (2013) 'Validation of a Cell-Cycle Progression Gene Panel to Improve Risk Stratification in a Contemporary Prostatectomy Cohort', *Journal of Clinical Oncology*, 31(11), pp. 1428–1434. doi: 10.1200/JCO.2012.46.4396.
Crea, F. *et al.* (2015) 'The epigenetic/noncoding origin of tumor dormancy.', *Trends in molecular medicine*, 21(4), pp. 206–11. doi: 10.1016/j.molmed.2015.02.005.
Crook, J. M. *et al.* (2012) 'Intermittent Androgen Suppression for Rising PSA Level after Radiotherapy', *New England Journal of Medicine*, 367(10), pp. 895–903. doi: 10.1056/NEJMoa1201546.
Deep, G. and Panigrahi, G. K. (2015) 'Hypoxia-Induced Signaling Promotes Prostate Cancer Progression: Exosomes Role as Messenger of Hypoxic Response in Tumor Microenvironment.', *Critical reviews in oncogenesis*. NIH Public Access, 20(5–6), pp. 419–34. doi: 10.1615/CritRevOncog.v20.i5-6.130.
Demir, A. *et al.* (2014) 'The course of metastatic prostate cancer under treatment', *SpringerPlus*. Springer, 3(1), p. 725. doi: 10.1186/2193-1801-3-725.
Denmeade, S. R. and Isaacs, J. T. (2002) 'A history of prostate cancer treatment.', *Nature reviews. Cancer*. NIH Public Access, 2(5), pp. 389–96. doi: 10.1038/nrc801.
Draisma, G. *et al.* (2009) 'Lead Time and Overdiagnosis in Prostate-Specific Antigen Screening: Importance of Methods and Context', *JNCI Journal of the National Cancer Institute*, 101(6), pp. 374–383. doi: 10.1093/jnci/djp001.
Dudzik, P. *et al.* (2019) 'The Epigenetic Modifier 5-Aza-2-deoxycytidine Triggers the Expression of CD146 Gene in Prostate Cancer Cells', *Anticancer Research*, 39(5), pp. 2395–2403. doi: 10.21873/anticanres.13357.

Ehrlich, M. (2002) 'DNA methylation in cancer: too much, but also too little', *Oncogene*. Nature Publishing Group, 21(35), pp. 5400–5413. doi: 10.1038/sj.onc.1205651.
Endo, H. *et al.* (2014) 'Dormancy of Cancer Cells with Suppression of AKT Activity Contributes to Survival in Chronic Hypoxia', *PLoS ONE*. Edited by P. K. Singh. Public Library of Science, 9(6), p. e98858. doi: 10.1371/journal.pone.0098858.
Esteller, M. (2011) 'Non-coding RNAs in human disease', *Nature Reviews Genetics*. Nature Publishing Group, 12(12), pp. 861–874. doi: 10.1038/nrg3074.
Eulalio, A., Huntzinger, E. and Izaurralde, E. (2008) 'Getting to the root of miRNA-mediated gene silencing.', *Cell*. Elsevier, 132(1), pp. 9–14. doi: 10.1016/j.cell.2007.12.024.
Ferlay, J. *et al.* (2010) 'Estimates of worldwide burden of cancer in 2008: GLOBOCAN 2008', *International Journal of Cancer*, 127(12), pp. 2893–2917. doi: 10.1002/ijc.25516.
Ferlay, J. *et al.* (2015) 'Cancer incidence and mortality worldwide: Sources, methods and major patterns in GLOBOCAN 2012', *International Journal of Cancer*, 136(5), pp. E359–E386. doi: 10.1002/ijc.29210.
Fizazi, K. *et al.* (2017) 'Abiraterone plus Prednisone in Metastatic, Castration-Sensitive Prostate Cancer', *New England Journal of Medicine*, 377(4), pp. 352–360. doi: 10.1056/NEJMoa1704174.
Fluegen, G. *et al.* (2017) 'Phenotypic heterogeneity of disseminated tumour cells is preset by primary tumour hypoxic microenvironments', *Nature Cell Biology*. Nature Publishing Group, 19(2), pp. 120–132. doi: 10.1038/ncb3465.
Fraga, A. *et al.* (2014) 'The HIF1A functional genetic polymorphism at locus +1772 associates with progression to metastatic prostate cancer and refractoriness to hormonal castration', *European Journal of Cancer*, 50(2), pp. 359–365. doi: 10.1016/j.ejca.2013.09.001.
Fraga, A. *et al.* (2015) 'Hypoxia and Prostate Cancer Aggressiveness: A Tale With Many Endings', *Clinical Genitourinary Cancer*, 13(4), pp. 295–301. doi: 10.1016/j.clgc.2015.03.006.
Frey, A. U., Sønksen, J. and Fode, M. (2014) 'Neglected Side Effects After Radical Prostatectomy: A Systematic Review', *The Journal of Sexual Medicine*, 11(2), pp. 374–385. doi: 10.1111/jsm.12403.
Friedman, R. C. *et al.* (2009) 'Most mammalian mRNAs are conserved targets of microRNAs.', *Genome research*. Cold Spring Harbor Laboratory Press, 19(1), pp. 92–105. doi: 10.1101/gr.082701.108.
Galardi, S. *et al.* (2007) 'miR-221 and miR-222 Expression Affects the Proliferation Potential of Human Prostate Carcinoma Cell Lines by Targeting p27 ^{Kip1}', *Journal of Biological Chemistry*, 282(32), pp. 23716–23724. doi: 10.1074/jbc.M701805200.
Gan, L. *et al.* (2018) 'Extracellular matrix protein 1 promotes cell metastasis and glucose metabolism by inducing integrin β4/FAK/SOX2/HIF-1α signaling pathway in gastric cancer', *Oncogene*. Nature Publishing Group, 37(6), pp. 744–755. doi: 10.1038/onc.2017.363.
Geng, H. *et al.* (2018) 'Interplay between hypoxia and androgen controls a metabolic switch conferring resistance to androgen/AR-targeted therapy', *Nature Communications*. Nature Publishing Group, 9(1), p. 4972. doi: 10.1038/s41467-018-07411-7.
Gilkes, D. M. *et al.* (2013) 'Collagen prolyl hydroxylases are essential for breast cancer metastasis.', *Cancer research*. American Association for Cancer Research, 73(11), pp. 3285–96. doi: 10.1158/0008-5472.CAN-12-3963.
Gilkes, D. M., Semenza, G. L. and Wirtz, D. (2014) 'Hypoxia and the extracellular matrix: drivers of tumour metastasis', *Nature Reviews Cancer*. Nature Publishing Group, 14(6), pp. 430–439. doi: 10.1038/nrc3726.
Glass, A. S., Cary, K. C. and Cooperberg, M. R. (2013) 'Risk-Based Prostate Cancer Screening: Who and How?', *Current Urology Reports*. Current Science Inc., 14(3), pp. 192–198. doi: 10.1007/s11934-013-0319-8.
Greijer, A. E. and van der Wall, E. (2004) 'The role of hypoxia inducible factor 1 (HIF-1) in hypoxia induced apoptosis', *Journal of Clinical Pathology*, 57(10), pp. 1009–1014. doi: 10.1136/jcp.2003.015032.
Gustafsson, M. V. *et al.* (2005) 'Hypoxia Requires Notch Signaling to Maintain the Undifferentiated Cell State', *Developmental Cell*, 9(5), pp. 617–628. doi: 10.1016/j.devcel.2005.09.010.
Hammerer, P. and Manka, L. (2019) 'Einsatz von Docetaxel oder Abirateron in Kombination mit einer Androgendeprivationstherapie beim metastasierten hormonnaiven Prostatakarzinom', *Der Urologe*. doi: 10.1007/s00120-019-0953-y.
Hanahan, D. and Weinberg, R. A. (2011) 'Hallmarks of cancer: the next generation.', *Cell*. Elsevier, 144(5), pp. 646–74. doi: 10.1016/j.cell.2011.02.013.
Harris, A. L. (2002) 'Hypoxia — a key regulatory factor in tumour growth', *Nature Reviews Cancer*. Nature Publishing Group, 2(1), pp. 38–47. doi: 10.1038/nrc704.
Harrison, L. B. *et al.* (2002) 'Impact of tumor hypoxia and anemia on radiation therapy outcomes.', *The oncologist*. United States, 7(6), pp. 492–508.

He, L. *et al.* (2005) 'A microRNA polycistron as a potential human oncogene', *Nature*. Nature Publishing Group, 435(7043), pp. 828–833. doi: 10.1038/nature03552.
Heinlein, C. A. and Chang, C. (2004) 'Androgen Receptor in Prostate Cancer', *Endocrine Reviews*, 25(2), pp. 276–308. doi: 10.1210/er.2002-0032.
Herrmann, A. *et al.* (2015) 'Cellular memory of hypoxia elicits neuroblastoma metastasis and enables invasion by non-aggressive neighbouring cells', *Oncogenesis*. Nature Publishing Group, 4(2), pp. e138–e138. doi: 10.1038/oncsis.2014.52.
Hiraga, T. (2019) 'Bone metastasis: Interaction between cancer cells and bone microenvironment', *Journal of Oral Biosciences*. Elsevier. doi: 10.1016/J.JOB.2019.02.002.
Horii, K. *et al.* (2007) 'Androgen-Dependent Gene Expression of Prostate-Specific Antigen Is Enhanced Synergistically by Hypoxia in Human Prostate Cancer Cells', *Molecular Cancer Research*. American Association for Cancer Research, 5(4), pp. 383–391. doi: 10.1158/1541-7786.MCR-06-0226.
Horwitz, E. M. *et al.* (2008) 'Ten-Year Follow-Up of Radiation Therapy Oncology Group Protocol 92-02: A Phase III Trial of the Duration of Elective Androgen Deprivation in Locally Advanced Prostate Cancer', *Journal of Clinical Oncology*, 26(15), pp. 2497–2504. doi: 10.1200/JCO.2007.14.9021.
Hu, L. *et al.* (2016) 'Biglycan stimulates VEGF expression in endothelial cells by activating the TLR signaling pathway', *Molecular Oncology*. John Wiley & Sons, Ltd, 10(9), pp. 1473–1484. doi: 10.1016/j.molonc.2016.08.002.
Huggins, C. and Hodges, C. V (1941) *Studies on Prostatic Cancer I. The Effect of Castration, of Estrogen and of Androgen Injection on Serum Phosphatases in Metastatic Carcinoma of the Prostate**.
Hussain, M. *et al.* (2013) 'Intermittent versus Continuous Androgen Deprivation in Prostate Cancer', *New England Journal of Medicine*, 368(14), pp. 1314–1325. doi: 10.1056/NEJMoa1212299.
Ishikawa, H. *et al.* (2004) 'Expression of hypoxic-inducible factor 1alpha predicts metastasis-free survival after radiation therapy alone in stage IIIB cervical squamous cell carcinoma.', *International journal of radiation oncology, biology, physics*, 60(2), pp. 513–21. doi: 10.1016/j.ijrobp.2004.03.025.
Ito, Y. and Sadar, M. D. (2018) 'Enzalutamide and blocking androgen receptor in advanced prostate cancer: lessons learnt from the history of drug development of antiandrogens', *Research and Reports in Urology*, Volume 10, pp. 23–32. doi: 10.2147/RRU.S157116.
Jalava, S. E. *et al.* (2012) 'Androgen-regulated miR-32 targets BTG2 and is overexpressed in castration-resistant prostate cancer', *Oncogene*, 31(41), pp. 4460–4471. doi: 10.1038/onc.2011.624.
Jang, G.-Y. *et al.* (2010) 'Transglutaminase 2 suppresses apoptosis by modulating caspase 3 and NF-κB activity in hypoxic tumor cells', *Oncogene*, 29(3), pp. 356–367. doi: 10.1038/onc.2009.342.
Jayaprakash, P. *et al.* (2018) 'Targeted hypoxia reduction restores T cell infiltration and sensitizes prostate cancer to immunotherapy', *Journal of Clinical Investigation*, 128(11), pp. 5137–5149. doi: 10.1172/JCI96268.
Jiang, J. *et al.* (2018) 'Hypoxia-induced HMGB1 expression of HCC promotes tumor invasiveness and metastasis via regulating macrophage-derived IL-6', *Experimental Cell Research*. Academic Press, 367(1), pp. 81–88. doi: 10.1016/J.YEXCR.2018.03.025.
Johnson, R. W. *et al.* (2016) 'Induction of LIFR confers a dormancy phenotype in breast cancer cells disseminated to the bone marrow', *Nature Cell Biology*. Nature Publishing Group, 18(10), pp. 1078–1089. doi: 10.1038/ncb3408.
Jones, P. A. (2012) 'Functions of DNA methylation: islands, start sites, gene bodies and beyond', *Nature Reviews Genetics*. Nature Publishing Group, 13(7), pp. 484–492. doi: 10.1038/nrg3230.
Al Kadhi, O. *et al.* (2017) 'Increased transcriptional and metabolic capacity for lipid metabolism in the peripheral zone of the prostate may underpin its increased susceptibility to cancer.', *Oncotarget*. Impact Journals, LLC, 8(49), pp. 84902–84916. doi: 10.18632/oncotarget.17926.
Kamińska, K. *et al.* (2019) 'Differential gene methylation patterns in cancerous and non-cancerous cells', *Oncology Reports*, 42(1), pp. 43–54. doi: 10.3892/or.2019.7159.
Kantoff, P. W. *et al.* (2010) 'Sipuleucel-T Immunotherapy for Castration-Resistant Prostate Cancer', *New England Journal of Medicine*. Massachusetts Medical Society , 363(5), pp. 411–422. doi: 10.1056/NEJMoa1001294.
Kasinski, A. L. and Slack, F. J. (2011) 'MicroRNAs en route to the clinic: progress in validating and targeting microRNAs for cancer therapy', *Nature Reviews Cancer*. Nature Publishing Group, 11(12), pp. 849–864. doi: 10.1038/nrc3166.
Kato, M. *et al.* (2016) 'Cotargeting Androgen Receptor Splice Variants and mTOR Signaling Pathway for the Treatment of Castration-Resistant Prostate Cancer', *Clinical Cancer Research*, 22(11), pp. 2744–2754. doi: 10.1158/1078-0432.CCR-15-2119.

Kato, T. *et al.* (2018) 'PSA response following the "steroid switch" in patients with castration-resistant prostate cancer treated with abiraterone: A case report', *Oncology Letters*. Spandidos Publications, 16(4), pp. 5383–5388. doi: 10.3892/ol.2018.9321.
Keyes, M. *et al.* (2013) 'Treatment options for localized prostate cancer', *Canadian Family Physician*. College of Family Physicians of Canada, 59(12), p. 1269.
Kirby, M., Hirst, C. and Crawford, E. D. (2011) 'Characterising the castration-resistant prostate cancer population: a systematic review', *International Journal of Clinical Practice*, 65(11), pp. 1180–1192. doi: 10.1111/j.1742-1241.2011.02799.x.
Klaus, A. *et al.* (2018) 'Expression of Hypoxia-Associated Protein HIF-1α in Follicular Thyroid Cancer is Associated with Distant Metastasis.', *Pathology oncology research : POR*, 24(2), pp. 289–296. doi: 10.1007/s12253-017-0232-4.
Kota, J. *et al.* (2009) 'Therapeutic microRNA Delivery Suppresses Tumorigenesis in a Murine Liver Cancer Model', *Cell*, 137(6), pp. 1005–1017. doi: 10.1016/j.cell.2009.04.021.
Kreth, S., Hübner, M. and Hinske, L. C. (2018) 'MicroRNAs as Clinical Biomarkers and Therapeutic Tools in Perioperative Medicine', *Anesthesia & Analgesia*, 126(2), pp. 670–681. doi: 10.1213/ANE.0000000000002444.
Lara, P. *et al.* (2016) 'TMPRSS-ERG fusion in men with prostate cancer (PCa) and non-prostate malignancies: Defining a role for comprehensive genomic profiling (CGP) to guide clinical care.', *Journal of Clinical Oncology*. American Society of Clinical Oncology, 34(15_suppl), pp. 5037–5037. doi: 10.1200/JCO.2016.34.15_suppl.5037.
Lieberman, J. (2003) 'The ABCs of granule-mediated cytotoxicity: new weapons in the arsenal', *Nature Reviews Immunology*, 3(5), pp. 361–370. doi: 10.1038/nri1083.
Liu, C. *et al.* (2011) 'The microRNA miR-34a inhibits prostate cancer stem cells and metastasis by directly repressing CD44', *Nature Medicine*, 17(2), pp. 211–215. doi: 10.1038/nm.2284.
Luo, J., Solimini, N. L. and Elledge, S. J. (2009) 'Principles of Cancer Therapy: Oncogene and Non-oncogene Addiction', *Cell*, 136(5), pp. 823–837. doi: 10.1016/j.cell.2009.02.024.
Luo, P. *et al.* (2019) 'The human positive cofactor 4 promotes androgen-independent prostate cancer development and progression through HIF-1α/β-catenin pathway.', *American journal of cancer research*, 9(4), pp. 682–698.
Lynch, S. M., McKenna, M. M., *et al.* (2016) 'miR-24 regulates CDKN1B/p27 expression in prostate cancer', *The Prostate*, 76(7), pp. 637–648. doi: 10.1002/pros.23156.
Lynch, S. M., O'Neill, K. M., *et al.* (2016) 'Regulation of miR-200c and miR-141 by Methylation in Prostate Cancer', *The Prostate*, 76(13), pp. 1146–1159. doi: 10.1002/pros.23201.
Mace, T. A. *et al.* (2013) 'Hypoxia induces the overexpression of microRNA-21 in pancreatic cancer cells', *Journal of Surgical Research*, 184(2), pp. 855–860. doi: 10.1016/j.jss.2013.04.061.
Manjili, M. H. (2017) 'Tumor Dormancy and Relapse: From a Natural Byproduct of Evolution to a Disease State.', *Cancer research*. American Association for Cancer Research, 77(10), pp. 2564–2569. doi: 10.1158/0008-5472.CAN-17-0068.
Manoochehri Khoshinani, H., Afshar, S. and Najafi, R. (2016) 'Hypoxia: A Double-Edged Sword in Cancer Therapy', *Cancer Investigation*, 34(10), pp. 536–545. doi: 10.1080/07357907.2016.1245317.
Marignol, L. *et al.* (2013) 'Hypoxia, notch signalling, and prostate cancer.', *Nature reviews. Urology*. NIH Public Access, 10(7), pp. 405–13. doi: 10.1038/nrurol.2013.110.
McKeown, S. R. (2014) 'Defining normoxia, physoxia and hypoxia in tumours-implications for treatment response.', *The British journal of radiology*. England, 87(1035), p. 20130676. doi: 10.1259/bjr.20130676.
McNeal, J. E. (1981) 'The zonal anatomy of the prostate.', *The Prostate*, 2(1), pp. 35–49.
Mendell, J. T. and Olson, E. N. (2012) 'MicroRNAs in Stress Signaling and Human Disease', *Cell*, 148(6), pp. 1172–1187. doi: 10.1016/j.cell.2012.02.005.
Mercatelli, N. *et al.* (2008) 'The Inhibition of the Highly Expressed Mir-221 and Mir-222 Impairs the Growth of Prostate Carcinoma Xenografts in Mice', *PLoS ONE*. Edited by M. V. Blagosklonny, 3(12), p. e4029. doi: 10.1371/journal.pone.0004029.
Ming, L. *et al.* (2013) 'Androgen deprivation results in time-dependent hypoxia in LNCaP prostate tumours: Informed scheduling of the bioreductive drug AQ4N improves treatment response', *International Journal of Cancer*, 132(6), pp. 1323–1332. doi: 10.1002/ijc.27796.
Mitchell, P. S. *et al.* (2008) 'Circulating microRNAs as stable blood-based markers for cancer detection', *Proceedings of the National Academy of Sciences*, 105(30), pp. 10513–10518. doi: 10.1073/pnas.0804549105.

Mobley, D., Feibus, A. and Baum, N. (2015) 'Benign prostatic hyperplasia and urinary symptoms: Evaluation and treatment', *Postgraduate Medicine*, 127(3), pp. 301–307. doi: 10.1080/00325481.2015.1018799.
Mu, P. *et al.* (2009) 'Genetic dissection of the miR-17 92 cluster of microRNAs in Myc-induced B-cell lymphomas', *Genes & Development*, 23(24), pp. 2806–2811. doi: 10.1101/gad.1872909.
Muz, B. *et al.* (2015) 'The role of hypoxia in cancer progression, angiogenesis, metastasis, and resistance to therapy.', *Hypoxia (Auckland, N.Z.)*. Dove Press, 3, pp. 83–92. doi: 10.2147/HP.S93413.
El Naggar, A. *et al.* (2012) 'Expression and stability of hypoxia inducible factor 1α in osteosarcoma', *Pediatric Blood & Cancer*, 59(7), pp. 1215–1222. doi: 10.1002/pbc.24191.
Nesbitt, H. *et al.* (2016) 'Targeting Hypoxic Prostate Tumors Using the Novel Hypoxia-Activated Prodrug OCT1002 Inhibits Expression of Genes Associated with Malignant Progression.', *Clinical cancer research : an official journal of the American Association for Cancer Research*. United States. doi: 10.1158/1078-0432.CCR-16-1361.
Nguyen, P. L. *et al.* (2011) 'Association of Androgen Deprivation Therapy With Cardiovascular Death in Patients With Prostate Cancer', *JAMA*, 306(21), pp. 2359–66. doi: 10.1001/jama.2011.1745.
Noman, M. Z. *et al.* (2009) 'The cooperative induction of hypoxia-inducible factor-1 alpha and STAT3 during hypoxia induced an impairment of tumor susceptibility to CTL-mediated cell lysis.', *Journal of immunology (Baltimore, Md. : 1950)*. American Association of Immunologists, 182(6), pp. 3510–21. doi: 10.4049/jimmunol.0800854.
Noman, M. Z. *et al.* (2011) 'Blocking hypoxia-induced autophagy in tumors restores cytotoxic T-cell activity and promotes regression.', *Cancer research*, 71(18), pp. 5976–86. doi: 10.1158/0008-5472.CAN-11-1094.
Noman, M. Z. *et al.* (2012) 'Hypoxia-inducible miR-210 regulates the susceptibility of tumor cells to lysis by cytotoxic T cells.', *Cancer research*. American Association for Cancer Research, 72(18), pp. 4629–41. doi: 10.1158/0008-5472.CAN-12-1383.
Ottman, R. *et al.* (2016) 'The other face of miR-17-92a cluster, exhibiting tumor suppressor effects in prostate cancer', *Oncotarget*, 7(45), pp. 73739–73753. doi: 10.18632/oncotarget.12061.
Otto, A. M. (2016) 'Warburg effect(s)-a biographical sketch of Otto Warburg and his impacts on tumor metabolism.', *Cancer & metabolism*. BioMed Central, 4, p. 5. doi: 10.1186/s40170-016-0145-9.
Palazon, A. *et al.* (2017) 'An HIF-1α/VEGF-A Axis in Cytotoxic T Cells Regulates Tumor Progression', *Cancer Cell*. Cell Press, 32(5), pp. 669-683.e5. doi: 10.1016/J.CCELL.2017.10.003.
Pan, Y. *et al.* (2018) 'DNA methylation profiles in cancer diagnosis and therapeutics', *Clinical and Experimental Medicine*, 18(1), pp. 1–14. doi: 10.1007/s10238-017-0467-0.
Park, S.-Y. *et al.* (2006) 'Hypoxia Increases Androgen Receptor Activity in Prostate Cancer Cells', *Cancer Research*. American Association for Cancer Research, 66(10), pp. 5121–5129. doi: 10.1158/0008-5472.CAN-05-1341.
Parker, C. *et al.* (2004) 'Polarographic electrode study of tumor oxygenation in clinically localized prostate cancer.', *International journal of radiation oncology, biology, physics*, 58(3), pp. 750–7. doi: 10.1016/S0360-3016(03)01621-3.
Parker, C. *et al.* (2013) 'Alpha Emitter Radium-223 and Survival in Metastatic Prostate Cancer', *New England Journal of Medicine*. Massachusetts Medical Society, 369(3), pp. 213–223. doi: 10.1056/NEJMoa1213755.
Pierorazio, P. M. *et al.* (2013) 'Prognostic Gleason grade grouping: data based on the modified Gleason scoring system', *BJU International*, 111(5), pp. 753–760. doi: 10.1111/j.1464-410X.2012.11611.x.
Portela, A. and Esteller, M. (2010) 'Epigenetic modifications and human disease', *Nature Biotechnology*, 28(10), pp. 1057–1068. doi: 10.1038/nbt.1685.
Potter, M., Newport, E. and Morten, K. J. (2016) 'The Warburg effect: 80 years on.', *Biochemical Society transactions*. Portland Press Ltd, 44(5), pp. 1499–1505. doi: 10.1042/BST20160094.
Poy, M. N. *et al.* (2009) 'miR-375 maintains normal pancreatic - and -cell mass', *Proceedings of the National Academy of Sciences*, 106(14), pp. 5813–5818. doi: 10.1073/pnas.0810550106.
Pramanik, D. *et al.* (2011) 'Restitution of Tumor Suppressor MicroRNAs Using a Systemic Nanovector Inhibits Pancreatic Cancer Growth in Mice', *Molecular Cancer Therapeutics*, 10(8), pp. 1470–1480. doi: 10.1158/1535-7163.MCT-11-0152.
Puisieux, A., Brabletz, T. and Caramel, J. (2014) 'Oncogenic roles of EMT-inducing transcription factors', *Nature Cell Biology*. Nature Publishing Group, 16(6), pp. 488–494. doi: 10.1038/ncb2976.
Quinn, D. I. *et al.* (2017) 'The evolution of chemotherapy for the treatment of prostate cancer', *Annals of Oncology*. Narnia, 28(11), pp. 2658–2669. doi: 10.1093/annonc/mdx348.
Rahbari, N. N. *et al.* (2016) 'Anti-VEGF therapy induces ECM remodeling and mechanical barriers to therapy in colorectal cancer liver metastases.', *Science translational medicine*. American Association for the

Advancement of Science, 8(360), p. 360ra135. doi: 10.1126/scitranslmed.aaf5219.
Ranasinghe, W. K. B. *et al.* (2014) 'The effects of nonspecific HIF1 *α* inhibitors on development of castrate resistance and metastases in prostate cancer', *Cancer Medicine*, 3(2), pp. 245–251. doi: 10.1002/cam4.189.
Randall, V. A. (1994) 'Role of 5 alpha-reductase in health and disease.', *Bailliere's clinical endocrinology and metabolism*, 8(2), pp. 405–31.
Rankin, E. B. and Giaccia, A. J. (2016) 'Hypoxic control of metastasis.', *Science (New York, N.Y.)*. American Association for the Advancement of Science, 352(6282), pp. 175–80. doi: 10.1126/science.aaf4405.
Rea, D. *et al.* (2016) 'Mouse Models in Prostate Cancer Translational Research: From Xenograft to PDX', *BioMed Research International*. Hindawi, 2016, pp. 1–11. doi: 10.1155/2016/9750795.
Reid, G. *et al.* (2016) 'Clinical development of TargomiRs, a miRNA mimic-based treatment for patients with recurrent thoracic cancer', *Epigenomics*. Future Medicine Ltd London, UK , 8(8), pp. 1079–1085. doi: 10.2217/epi-2016-0035.
Roach, M. (2007) 'Dose Escalated External Beam Radiotherapy versus Neoadjuvant Androgen Deprivation Therapy and Conventional Dose External Beam Radiotherapy for Clinically Localized Prostate Cancer: Do we Need Both?', *Strahlentherapie und Onkologie*, 183(S2), pp. 26–28. doi: 10.1007/s00066-007-2011-8.
Roach, M., Waldman, F. and Pollack, A. (2009) 'Predictive models in external beam radiotherapy for clinically localized prostate cancer', *Cancer*. John Wiley & Sons, Ltd, 115(S13), pp. 3112–3120. doi: 10.1002/cncr.24348.
Robinson, D. *et al.* (2015) 'Integrative Clinical Genomics of Advanced Prostate Cancer', *Cell*, 161(5), pp. 1215–1228. doi: 10.1016/j.cell.2015.05.001.
Røe, K. *et al.* (2012) 'Vascular responses to radiotherapy and androgen-deprivation therapy in experimental prostate cancer.', *Radiation oncology (London, England)*. BioMed Central, 7, p. 75. doi: 10.1186/1748-717X-7-75.
Røe, K. *et al.* (2013) 'Hypoxic Tumor Kinase Signaling Mediated by STAT5A in Development of Castration-Resistant Prostate Cancer', *PLoS ONE*. Edited by J.-M. A. Lobaccaro, 8(5), p. e63723. doi: 10.1371/journal.pone.0063723.
van Rooij, E. *et al.* (2007) 'Control of Stress-Dependent Cardiac Growth and Gene Expression by a MicroRNA', *Science*, 316(5824), pp. 575–579. doi: 10.1126/science.1139089.
Roush, S. and Slack, F. J. (2008) 'The let-7 family of microRNAs', *Trends in Cell Biology*, 18(10), pp. 505–516. doi: 10.1016/j.tcb.2008.07.007.
Roviello, G. *et al.* (2016) 'Is it time for everolimus-based combination in castration-resistant prostate cancer?', *Future Oncol*, (16), pp. 1849–1852. doi: 10.2217/fon-2016-0136.
le Sage, C. *et al.* (2007) 'Regulation of the p27Kip1 tumor suppressor by miR-221 and miR-222 promotes cancer cell proliferation', *The EMBO Journal*, 26(15), pp. 3699–3708. doi: 10.1038/sj.emboj.7601790.
Saggar, J. K. *et al.* (2013) 'The Tumor Microenvironment and Strategies to Improve Drug Distribution', *Frontiers in Oncology*, 3, p. 154. doi: 10.3389/fonc.2013.00154.
Samanta, D. *et al.* (2016) 'PHGDH Expression Is Required for Mitochondrial Redox Homeostasis, Breast Cancer Stem Cell Maintenance, and Lung Metastasis.', *Cancer research*. American Association for Cancer Research, 76(15), pp. 4430–42. doi: 10.1158/0008-5472.CAN-16-0530.
Schirle, N. T. and MacRae, I. J. (2012) 'Structure and Mechanism of Argonaute Proteins', *The Enzymes*. Academic Press, 32, pp. 83–100. doi: 10.1016/B978-0-12-404741-9.00004-0.
Schöning, J. P., Monteiro, M. and Gu, W. (2017) 'Drug resistance and cancer stem cells: the shared but distinct roles of hypoxia-inducible factors HIF1α and HIF2α', *Clinical and Experimental Pharmacology and Physiology*, 44(2), pp. 153–161. doi: 10.1111/1440-1681.12693.
Schröder, F. H. *et al.* (2012) 'Prostate-Cancer Mortality at 11 Years of Follow-up', *New England Journal of Medicine*, 366(11), pp. 981–990. doi: 10.1056/NEJMoa1113135.
Shadad, A. K. *et al.* (2013) 'Gastrointestinal radiation injury: symptoms, risk factors and mechanisms.', *World journal of gastroenterology*. Baishideng Publishing Group Inc, 19(2), pp. 185–98. doi: 10.3748/wjg.v19.i2.185.
Shao, Y.-H. *et al.* (2009) 'Contemporary risk profile of prostate cancer in the United States.', *Journal of the National Cancer Institute*. Oxford University Press, 101(18), pp. 1280–3. doi: 10.1093/jnci/djp262.
Shen, M. M. and Abate-Shen, C. (2010) 'Molecular genetics of prostate cancer: new prospects for old challenges.', *Genes & development*. United States, 24(18), pp. 1967–2000. doi: 10.1101/gad.1965810.
Springer, A. D. and Dowdy, S. F. (2018) 'GalNAc-siRNA Conjugates: Leading the Way for Delivery of RNAi Therapeutics', *Nucleic Acid Therapeutics*, 28(3), pp. 109–118. doi: 10.1089/nat.2018.0736.

Strand, S. H. *et al.* (2019) 'A novel combined miRNA and methylation marker panel (miMe) for prediction of prostate cancer outcome after radical prostatectomy', *International Journal of Cancer*, p. ijc.32427. doi: 10.1002/ijc.32427.

Tang, Y.-A. *et al.* (2018) 'Hypoxic tumor microenvironment activates GLI2 via HIF-1α and TGF-β2 to promote chemoresistance in colorectal cancer.', *Proceedings of the National Academy of Sciences of the United States of America*. National Academy of Sciences, 115(26), pp. E5990–E5999. doi: 10.1073/pnas.1801348115.

Taylor, C. T. and Colgan, S. P. (2017) 'Regulation of immunity and inflammation by hypoxia in immunological niches', *Nature Reviews Immunology*, 17(12), pp. 774–785. doi: 10.1038/nri.2017.103.

Thompson, I. M. *et al.* (2006) 'Assessing Prostate Cancer Risk: Results from the Prostate Cancer Prevention Trial', *JNCI Journal of the National Cancer Institute*, 98(8), pp. 529–534. doi: 10.1093/jnci/djj131.

Tong, W.-W. *et al.* (2015) 'HIF2α is associated with poor prognosis and affects the expression levels of survivin and cyclin D1 in gastric carcinoma', *International Journal of Oncology*, 46(1), pp. 233–242. doi: 10.3892/ijo.2014.2719.

Torre, L. A. *et al.* (2015) 'Global Cancer Incidence and Mortality Rates and Trends-An Update'. doi: 10.1158/1055-9965.EPI-15-0578.

Trang, P. *et al.* (2011) 'Systemic Delivery of Tumor Suppressor microRNA Mimics Using a Neutral Lipid Emulsion Inhibits Lung Tumors in Mice', *Molecular Therapy*, 19(6), pp. 1116–1122. doi: 10.1038/mt.2011.48.

Treiber, T., Treiber, N. and Meister, G. (2012) 'Regulation of microRNA biogenesis and function', *Thrombosis and Haemostasis*, 107(04), pp. 605–610. doi: 10.1160/TH11-12-0836.

Vergis, R. *et al.* (2008) 'Intrinsic markers of tumour hypoxia and angiogenesis in localised prostate cancer and outcome of radical treatment: a retrospective analysis of two randomised radiotherapy trials and one surgical cohort study.', *The Lancet. Oncology*, 9(4), pp. 342–51. doi: 10.1016/S1470-2045(08)70076-7.

Verze, P., Cai, T. and Lorenzetti, S. (2016) 'The role of the prostate in male fertility, health and disease', *Nature Reviews Urology*, 13(7), pp. 379–386. doi: 10.1038/nrurol.2016.89.

Wadosky, K. M. and Koochekpour, S. (2017) 'Androgen receptor splice variants and prostate cancer: From bench to bedside.', *Oncotarget*. Impact Journals, LLC, 8(11), pp. 18550–18576. doi: 10.18632/oncotarget.14537.

Wallis, C. J. D. *et al.* (2016) 'Second malignancies after radiotherapy for prostate cancer: systematic review and meta-analysis.', *BMJ (Clinical research ed.)*. BMJ Publishing Group, 352, p. i851. doi: 10.1136/bmj.i851.

Walter, B. A. *et al.* (2013) 'Comprehensive microRNA Profiling of Prostate Cancer', *Journal of Cancer*, 4(5), pp. 350–357. doi: 10.7150/jca.6394.

Wang, T. *et al.* (2015) 'Cancer stem cell targeted therapy: progress amid controversies', *Oncotarget*, 6(42), pp. 44191–206. doi: 10.18632/oncotarget.6176.

Wang, Y. *et al.* (2018) 'Histone variants H2A.Z and H3.3 coordinately regulate PRC2-dependent H3K27me3 deposition and gene expression regulation in mES cells', *BMC Biology*. BioMed Central, 16(1), p. 107. doi: 10.1186/s12915-018-0568-6.

Watson, J. A. *et al.* (2009) 'Generation of an epigenetic signature by chronic hypoxia in prostate cells', *Human Molecular Genetics*. Narnia, 18(19), pp. 3594–3604. doi: 10.1093/hmg/ddp307.

Winther, M. *et al.* (2016) 'Hypoxia-regulated MicroRNAs in Gastroesophageal Cancer.', *Anticancer research*, 36(2), pp. 721–30.

Wu, D. *et al.* (2016) 'Hypoxia-induced microRNA-301b regulates apoptosis by targeting Bim in lung cancer', *Cell Proliferation*, 49(4), pp. 476–483. doi: 10.1111/cpr.12264.

Wu, Y.-M. *et al.* (2018) 'Inactivation of CDK12 Delineates a Distinct Immunogenic Class of Advanced Prostate Cancer', *Cell*. Cell Press, 173(7), pp. 1770-1782.e14. doi: 10.1016/J.CELL.2018.04.034.

Yang, X. *et al.* (2014) 'Gene body methylation can alter gene expression and is a therapeutic target in cancer.', *Cancer cell*. Elsevier, 26(4), pp. 577–90. doi: 10.1016/j.ccr.2014.07.028.

Yossepowitch, O. *et al.* (2007) 'Radical Prostatectomy for Clinically Localized, High Risk Prostate Cancer: Critical Analysis of Risk Assessment Methods', *The Journal of Urology*, 178(2), pp. 493–499. doi: 10.1016/j.juro.2007.03.105.

Zhang, C. *et al.* (2016) 'Hypoxia induces the breast cancer stem cell phenotype by HIF-dependent and ALKBH5-mediated m^6A-demethylation of NANOG mRNA.', *Proceedings of the National Academy of Sciences of the United States of America*. National Academy of Sciences, 113(14), pp. E2047-56. doi: 10.1073/pnas.1602883113.

Zhang, H.-L. *et al.* (2013) 'An elevated serum miR-141 level in patients with bone-metastatic prostate cancer is correlated with more bone lesions', *Asian Journal of Andrology*, 15(2), pp. 231–235. doi: 10.1038/aja.2012.116.

Zhang, Jingying *et al.* (2018) 'Hypoxia-inducible factor-1α/interleukin-1β signaling enhances hepatoma epithelial-mesenchymal transition through macrophages in a hypoxic-inflammatory microenvironment', *Hepatology*. Wiley-Blackwell, 67(5), pp. 1872–1889. doi: 10.1002/hep.29681.
Zhang, L. *et al.* (2016) 'miRNA-30a functions as a tumor suppressor by downregulating cyclin E2 expression in castration-resistant prostate cancer', *Molecular Medicine Reports*, 14(3), pp. 2077–2084. doi: 10.3892/mmr.2016.5469.
Zu, X. L. and Guppy, M. (2004) 'Cancer metabolism: facts, fantasy, and fiction', *Biochemical and Biophysical Research Communications*. Academic Press, 313(3), pp. 459–465. doi: 10.1016/J.BBRC.2003.11.136.
Zuckerman, S. (1936) *The endocrine control of the prostate*, *Proceedings of the Royal Society of Medicine*.

Chapter 2. Materials and Methods

2.1. In vitro experiments

2. 1. I. Tissue culture

2. 1. I. a) Monolayer cell culture. LNCaP, 22RV1, DU145, PC3 and RWPE1 were obtained from American Type Culture Collection (ATCC) and were cultured as a monolayer on sterile culture dishes. All were grown in Roswell park memorial institute (RPMI) 1640 medium supplemented with 20% foetal bovine serum (FBS) (GIBCO, Thermo Scientific) except RWPE1, which were cultured in Keratinocyte Serum-Free medium supplemented with 25mg Bovine Pituitary Extract and 2.5µg extracellular growth factor per 500mL (GIBCO, Thermo Scientific). Media was aliquotted in 20mL volumes in universals and the required amount was warmed in a water bath at 37°C prior to use. Cells were incubated in a humidified incubator at 37°C with 5% CO_2. Cells were grown to a maximum of 90% confluency before passaging and used in experiments within 10 passages after breaking out. To passage, cells were rinsed with sterile phosphate buffer saline (PBS, pH 7.4) and detached by incubation in 0.05% trypsin in PBS for 3-10 mins before centrifugation at 1200rpm for 3-5mins and resuspension in fresh media. Cells were frozen at low passage in 60% complete media with 20% foetal bovine serum (GIBCO, Invitrogen) and 20% sterile dimethyl sulfoxide (DMSO) and stored in liquid nitrogen. Cells were broken out by warming 1 or 2 cryovials until semi-thawed and dropping the ice cube into a small flask containing 10mL pre-warmed complete media and gently swirling, and the media was carefully changed after 6h, and again after 24h including a PBS rinse. For counting, cells were trypisined and re-suspended in fresh media, 1µL was counting using the average of the four quadrants of a haemocytometer after staining for viability with trypan blue dye (1:10 dilution of trypan : cell suspension). To determine the number of cells per mL from the number (#) per µL, the following formula was used: #/mL = #/µL * (1/0.1) * 0.9 * 1000. To determine the volume required to obtain a specified number of cells (e.g. 100,000), the desired cell number per mL was divided by the current number per mL.

Table 1. Epithelial prostate cell lines used for experimental work including transformed status, site of origin, AR status, and AR variant status.

Cell line	*Transformation status*	*Site of isolation*	*AR status*	*Endogenous AR variant expression*	*References*
RWPE1	Non-tumorigenic	Human prostate epithelial, immortalised by transfection with HPV-18	AR-dependent, wild-type AR	None	(Bello *et al*., 1997)
LNCaP	Tumorigenic	Metastatic human prostate cancer, derived from the left supraclavicular lymph node	AR-dependent. AR with mutation at position T877A in the ligand-binding domain. Receptor is thus promiscuous to progesterone, estradiol, and anti-androgens	ARV3	(Horoszewicz *et al*., 1983)(Gaupel *et al.*, 2013)
22Rv1	Tumorigenic	Human prostate carcinoma epithelial cell line. Derived from a xenograft that was serially propagated in mice after castration-induced regression and relapse of the parental, androgen-dependent CWR22 xenograft	AR detectable and DHT weakly stimulates growth, but cell line is AR-independent	ARV7, ARV12, ARV3, ARV4, ARV5, ARV1, ARV9, ARV2, ARV5/6, AR8, ARV13, ARV14	(Sramkoski *et al*., 1999)(Wadosky and Koochekpour, 2017)
PC3	Tumorigenic	Metastatic human prostate cancer, derived from the bone	AR detectable, cells AR-independent	ARV7	(Kaighn *et al*., 1979)(Alimirah *et al.*, 2006)(Xu and Qiu, 2016)
DU145	Tumorigenic	Metastatic human prostate cancer, derived from the brain	AR detectable but cell line is AR-independent	ARV7	(Stone *et al.*, 1978)(Alimirah *et al.*, 2006)(Xu and Qiu, 2016)

2.1.I.b. Hypoxia Incubator Chamber. For paired hypoxic and normoxic samples, cells were split into two flasks, allowed to reseed overnight and incubated within a hypoxia incubator chamber (Stemcell technologies) and standard incubator for timepoints of 24h, 48h and 72h. The hypoxic incubator was supplied with HEPA-filtered air at 0.1% oxygen. Cells to be cultured in hypoxia were seeded at 70% confluence to account for the slower growth and cells for normoxic culture were seeded at 30% confluence.

2.1.I.c. Aza-dc treatment. Fresh media containing 5μM 5-aza-2'-deoxycytidine (aza-dc) that had been solubilised in DMSO was applied to the cells following a PBS rinse. Cells were treated for 3 consecutive days, then if necessary grown for 24h and harvested for RNA and DNA extractions. To confirm the aza-dc treatment had worked, mRNA levels of *SYPC3* and *DAZL* were measured.

2.1.I.d. Prostatosphere cell culture. 6-well plates were double-coated with a polyhema acrylamide layer (1.2% poly(2-hydroxyethyl methacrylate) solubilised at 50°C overnight in 95% ethanol) which inhibited cell adhesion to the base of the plate. 10,000 cells were seeded and grew in clusters, the growth of which was measured by microscopy. To obtain sufficient cells for protein extraction, prostatospheres were cultured in a 10cm petri dish seeded with 30,000 cells. Media was replaced every 3 days, with half the volume of media being carefully aspirated and replaced without disturbing the prostatospheres.

2.1.I.e. Transient transfection of precursor miRNA molecules. Transfections were performed at a final concentration of 25nM. Cells were transfected when 30% confluent and typically seeded 16h before transfection into wells of a 6-well plate (at 80,000 cells per well for RWPE1, PC3, and 22RV1, and 100,000 cells per well for LNCaP). To transfect, OptiMem serum-reduced media was used for transfection (GIBCO, Invitrogen). Lipofectamine 2000 reagent (Thermo-Scientific) was complexed to RNA of interest (pre-miRs, Ambion, Thermo Fisher) by incubation at room temperature for 20 minutes. The pre-miR was solubilised in 50μL NF-H_2O to provide a stock of 100μM (stored at -20°C). For transfection of the pre-miR, 1μL of the 100μM stock was complexed with 3μL Lipofectamine (1μL RNA : 199μL OptiMem, mixed with 3μL Lipofectamine : 197μL OptiMem) mixed by pipetting and incubated at room temperature for 20 minutes. The seeded cells were rinsed with PBS and 1.6mL OptiMem was added. The Lipofectamine/RNA solution was gently added (400μL total) and mixed by swirling. Cells were incubated with the Lipofectamine-RNA solution for 4-6 hours, before it was replaced with the normal complete media. The effects of pre-miRs were gauged relative to the control scrambled sequence pre-miR, which does not target known human mRNAs (pre-miR-neg). Cells were harvested at 48-72h depending on confluency.

2.1.II. Luciferase reporter assay. Cells were co-transfected with the precursor pre-miR molecules as described (non-targeting negative control pre-miR-neg, and pre-miR of interest), with plasmids containing luciferase gene cloned downstream of a wild-type or mutated promoter sequence of the gene of interest such that if the miRNA binds the promoter sequence then the expression of luciferase will be silenced. The plasmids were a kind gift from by Dr Fabio Martelli upon request (I.R.C.C.S. Policlinico San Donato, Milan,

Italy). Cells were co-transfected with 100ng of vector/mutant plasmid plus the miRNA precursor at 25nM. 30ng Renilla luciferase vector was included in each well to control for transfection efficiency. The two nucleic acids were independently complexed to Lipofectamine before the solutions were mixed and applied to the cells. After 48 hours, cells were lysed in lysis buffer (Promega) and luciferase activity measured using the Dual-Glo® Luciferase Assay Kit (Promega) on a FluoStar Omega plate reader (BMG LabTech). Transfections were carried out in triplicate, measurements within experiments were performed in duplicate, and firefly luciferase readings were normalised against renilla luciferase readings before analysis.

2. 1. III. Phenotypic assays

2.1.III.a. Scratch wound assay. Once 80-90% confluent, the cell monolayer was "scratched" using a 20µL pipette tip in a cross (used to orient when imaging), and rinsed with PBS to remove detached cells. Cells were rinsed before imaging at the same points (around the cross) for 24h, 48h, 72h, and 96h (Nikon Eclipse TS100).

2.1.III.b. XTT cell proliferation assay. Cells seeded into a 96-well plate at 500-1,000 cells per well in eight technical replicates. Cells were counted and the cell number per mL was adjusted and added to a basin (cleaned with 70% IMS) and a multichannel pipette used to add 100µL of the suspension to each well using a multichannel pipette. For each time point, a different 96-well plate was used. 50µL XTT reagent (2,3-Bis-(2-Methoxy-4-Nitro-5-Sulfophenyl)-2H-Tetrazolium-5-Carboxanilide) (Roche) was added to wells and allowed to incubate at 37°C for 4-6 hours. The XTT reagent was made up of XTT labelling reagent and XTT electron coupling reagent (5mL : 100µL, respectively). After 16h, absorbance (optical density, O.D.) was measured using the FLUOstar Omega Spectrophotometer (BMG LabTech) at 495nm, normalised to the reading at 650nm.

2.1.III.c. Flow cytometry. Cells were harvested by trypsinisation and pelleting, the pellet was flicked to gently re-suspend and 1mL ice-cold PBS was added to rinse (this ice-cold PBS rinse was repeated twice). To fix the cells, the cell pellet was re-suspended by flicking it in 100µL PBS then the cells were vortexed on the lowest speed while 900µL 100% ethanol was slowly dripped in. Cells were rinsed again twice in ice-cold PBS, and then re-suspended in the staining solution. **Cell cycle analysis**. Staining solution contained: 0.1mg/mL RNAse A, 0.01mg/ml propidium iodide (PI), 0.1% Triton X, and 5mg/mL tri-sodium citrate. After 5 minutes at room temperature in the dark, the solutions were analysed on a two laser eight colour Gallios™ flow cytometer (Beckman Coulter). **Apoptosis analysis:** The Alexa Fluor® 488 Annexin V/Dead Cell Apoptosis Kit (Thermo Fisher Scientific) was used. Cells were harvested and rinsed twice in ice-cold PBS, and a master mix was prepared containing 1X Annexin Binding Buffer, Alexa Flour stain, and PI at 100µg/µL (according to the manufacturer's instructions). 600µL of master mix was added to the cells and left to incubate in the dark at room temperature for 15 minutes before being analysed.

2.1.III.d. Colony forming assay. Cells were seeded as 500 cells per well of a 6-well plate, and left for 7 days without changing the media. The cells were rinsed with ice-cold PBS and an ice-cold fixing solution was gently added (7 parts methanol : 1 part acetic acid) for 5 minutes. Cells were stained with 0.5% crystal violet solution (Sigma) in 25% methanol for 5 mins and rinsed with water. To quantify the crystal violet, cells were lysed in 1% SDS solution for 30mins at room temperature with rapid rocking. 100µL of the SDS solution was added in triplicate to wells of a 96 well plate and the O.D. was measured at 595nm.

2.1.III.e. Migration and invasion assay by Boyden chamber. For migration analysis, the cells' ability to cross a porous membrane was assessed. For invasion analysis, the cells' ability to invade and cross a matrigel-coated porous membrane was assessed. xCELLigence® CIM-16 plates were used and analysed using the RTCA DP Instrument (both ACEA Bio). The upper chambers were filled with 20µL media lacking FBS/growth factors and the lower chamber with complete media to act as chemoattractant. The lower chambers were slightly overfilled with 160µL media to produce a meniscus and ensure contact with the upper chamber. The upper and lower parts were fitted together and were left in the incubator for 1 hour for a growth factor gradient to form, and a background reading was taken on the instrument. Next, 100µL of cell solution (adjusted to contain 20,000 cells) was added to the upper chamber and cells were left to seed for 30 mins at room temperature (in the hood) before adding to the instrument and monitoring growth. For invasion analysis, matrigel (growth-factor reduced, Corning) was thawed overnight in a small ice bucket in the fridge, and diluted at 1.2mg/mL, 0.6mg/mL, and 0.3mg/mL, in media lacking growth factors or FBS. The porous membranes of the upper chamber was coated in Matrigel (20µL of Matrigel was used per well, 50µL was initially added to cover base, and 30µL removed by pipette) and allowed to polymerise in a 37°C incubator for 4 hours without touching the underside side of the membranes. Then cells were seeded as for the migration assay.

2. 1. IV. Gene expression analysis

2. 1. IV. a). RNA extraction. RNA was extracted from cell lines, tumours and spheroids using Tripure® reagent (Life Technologies), using approximately 500µL Tripure® per $5x10^5$ cells (500µL per well-of a 6-well plate, 1mL per small flask and 1.5mL per medium flask). The media was removed as much as possible and the dish was placed on ice, cold Tripure was added directly to the plate and swirled to cover the cells. The dish was then incubated at 4°C for 15 mins to lyse the cells. The Tripure was then transferred to a chilled Eppendorf after pipetting gently over the plate to collect all cells. It was kept on ice for the duration of the RNA extraction and mixed only by gentle inversion or pipetting, never vortexing. Tumour samples were homogenised by pipetting or very gentle mashing, using a very small amount of tissue (approximately $2mm^2$ per 1mL Tripure). Chloroform (100µL per 1mL Tripure) was added, the solution was mixed by gently inverting the tubes for 15 seconds and left on ice for 5mins, before centrifugation at 13,200rpm for 10mins in a centrifuge pre-cooled to 4°C. The colourless upper fraction (aqueous) was transferred to a clean chilled 1.5mL Eppendorf and ice-cold isopropanol was added (200µL per 1mL Tripure), the solution was mixed by

inverting the tube gently 5 times and incubated on ice for 10mins before centrifugation at 13,200rpm at 4°C for 12mins to pellet the precipitated RNA. The supernatant was removed without touching the pellet. The pellet rinsed with 75% ethanol to reduce the salt content, by carefully adding 1mL and inverting the tube before removing as much as possible, a short centrifuge was sometimes needed to re-fix the pellet to the tube. As much as possible, any residual ethanol was removed by pipetting (without touching it) and air drying for less than 3mins at room temperature by lying the tube sideways on a clean bench. The RNA pellet was solubilised using high-grade nuclease-free water (NF-H_2O), the water was dripped down the side of the Eppendorf onto the pellet and incubated on ice to dissolve the pellet (30-50µL water used depending on the size of the pellet). Serum miRNA was extracted using a column-based RNA isolation kit miRCURY™ RNA Isolation Kit - Biofluids according to the instructions (Exiqon), with the small RNA fraction isolated by two sequential elutions with NF-H_2O at the final stage. All RNA was stored at -80°C. RNA integrity was always confirmed by agarose gel electrophoresis and examination of the ribosomal RNA fragments.

2.1.IV.b. Quantification. A NanoDrop 1000 spectrophotometer (Thermo Scientific) was used to estimate nucleic acid concentration and purity, absorbance at 260nm indicated nucleic acid concentration. Pure preparation of RNA indicated by OD_{260}:OD_{280} ratio of 2.00, absorbance at 230nm indicated organic compound contamination, absorbance at 280nm indicated protein contamination. Serum miRNA was not quantified by spectrophotometry; 50µL serum was used for the RNA extraction kit (and 5µL of the eluted water was used in for production of micro-cDNA in total volume of 10µL as described below.

2.1.IV.c. cDNA and micro cDNA production. First strand Complementary DNA (cDNA) synthesis was performed by 2-step reverse transcription kit (Roche) using 1µg total RNA, first annealing oligo dTs to the polyA tails of mRNAs with a 5 min 65°C step. Next, a mastermix containing the DNA polymerase, dNTPs and buffer was added and a PCR cycle was completed according to the manufacturer's instructions. Complementary DNA to miRNAs (micro-cDNA) was amplified using 50ng total RNA, with the miRCURY LNA™ microRNA 1-step PCR system of buffer and reverse transcriptase (Exiqon). Serum RNA was not quantified, 5µL RNA was used for the micro-cDNA synthesis and the final micro-cDNA diluted 1:10 with NF-H_2O for RT-qPCR.

2.1.IV.d. Primer design. Primers specific to regions flanking genes of interest were designed using NCBI Primer-BLAST (https://www.ncbi.nlm.nih.gov/tools/primer-blast/) using the accession code provided by a search for the gene of interest using PubMed Gene database and selecting human mRNA. Alternatively primers were designed using Primer3Plus (http://www.bioinformatics.nl/cgi-bin/primer3plus/primer3plus.cgi) based on the UCSC hg.38 mRNA sequence and purchased from Invitrogen (primer sequences in Table 2).

2.1.IV.e. Reverse transcription quantitative polymerase chain reaction (RT-qPCR). Gene expression was quantified by real-time quantitative PCR (RT–qPCR) using a SYBR™ Green fluorometric-based detection

system (Roche). cDNA was diluted 1:5 with NF-H_2O with 4µL used in each reaction. Primers were re-suspended in NF-H_2O to produce a 100µM stock and further diluted to produce 20µM working solutions, and used at a final concentration of 0.2µM. A master mix for each gene of interest was prepared containing 200nM forward and reverse primers, 5µL SYBR green reagent 2X (Roche) and 0.75µL NF-H_2O. 6µL master mix was added to each well of a 96-well qPCR plate. Each reaction was prepared in triplicate. Genes of interest were normalised to the expression of a reference "housekeeping" gene (hypoxanthine phosphoribosyltransferase 1 (HPRT) or actin-β). qPCR was performed on a LC480 Lightcycler (Roche). Wells containing only master mix and water for each primer set (no cDNA) were used to confirm the absence of contamination.

2.1.IV.f. miRNA-qPCR. 5ng micro-cDNA was used per reaction, with the small non-coding nucleolar genes SNORD48 or U6 as a housekeeping gene for human tissue samples or miR-191 for serum samples. Micro cDNA was diluted 1:50 and 4µL used per reaction. miRCURY LNA SYBR® Green PCR Kits were used with 5µL SYBR reagent, 0.5µL primer (both Exiqon), and 0.5µL NF-H_2O. Primers were purchased from Exiqon (sequences patented).

2.1.IV.g. qPCR analysis. A melting point dissociation curve (Tm curve) was automatically calculated by the Lightcycler after every assay, and was examined to confirm the presence of a single PCR product (a single peak), indicating primer specificity to the region of interest and absence of contaminating DNA (evident as multiple peaks spaced apart far enough so as not to indicate a splice variant), and the lack of primer-dimer formation (evident as a second peak at half the temperature and height). Relative expression of the genes of interest were calculated, normalised to the expression level of the endogenous reference gene and relative to the expression level of the same gene in the control sample. The "Cycle Threshold" (CT) value stands for the fractional PCR cycle, at which the quantity of the amplified PCR product reaches a predetermined threshold. Relative expression was calculated using the comparative CT equation:

$\Delta CT = CT(\text{gene of interest}) - CT(\text{reference gene})$

$\Delta\Delta CT = \Delta CT(\text{test condition}) - \Delta CT(\text{control condition})$

$2^{-\Delta\Delta CT}$ = expression level of the gene of interest

The qPCR graphs present the combined results from three independent biological replicates (different culture day), with 3 technical replicates on each plate (additions of cDNA and master mix). Primers were confirmed to be efficient by amplification of decreasing concentrations of cDNA in triplicate (at least 5 10-fold dilutions) and by plotting the log dilution factor against the mean CT obtained, calculating the slope and the percentage efficiency as: E=(10^(-1/The Slope Value)-1)*100.

2. 1. V. Epigenetics – DNA methylation quantification

2. 1. V. a). DNA extraction and bisufite conversion. Pelleted cells were lysed in 500µL lysis buffer (50mM Tris pH8, 0.1M EDTA, 0.5% SDS) and proteinase K (0.2mg/mL) and incubated at 55^{O}C for 24h with rotation. 500µL of a phenol chloroform buffer (phenyl: chloroform: isoamyl, ratio 25:24:1) was added, the solution was vortexed and centrifuged at 13200rpm for 10mins at room temperature. The aqueous layer was collected and the phenol chloroform separation was repeated twice more. 1mL DNA precipitation solution (1M ammonium acetate in 90% ethanol) and 2µL carrier glycogen were added and left to precipitate overnight at -20 ^{O}c. Samples were centrifuged at 13200rpm for 10mins, the pellet was washed with 80% ethanol (residual ethanol was evaporated off the pellet at 65^{O}c) and re-suspended in 100µL NF-H_2O. 500ng DNA was used in the bisulfite conversion reaction using the Epitect Bisulfite Kit (QIAGEN), including DNA clean up, according to manufacturer's instructions and eluted in 40µL NF-H_2O.

2. 1. V. b). PCR and Pyrosequencing. The PCR reaction has the dual purpose of amplifying the region of interest for sequencing, and converting unmethylated cytosines to thymine (since the DNA polymerase base-pairs uracil with adenine and subsequently thymine). Since the key to a successful pyrosequencing reaction is an ample PCR product, the PCR reaction involves a high performance DNA polymerase and an increased number of cycles (45 rather than the standard 30) to amplify as much as possible. Therefore, DNA contamination is a prominent risk and all PCR reactions included negative controls containing all reagents except input DNA. Gel electrophoresis was used to confirm the PCR amplicons expected sizes and the absence of a product in the negative controls. The PCR product was then extracted by sepharose beads (*via* a biotin tag on one of the PCR primers) and sequenced, in a sequencing-by-synthesis method that involves light emission due to a chain reaction in which pyrophosphate is released (hence the name "pyrosequencing"). The output is a type of electropherogram called a "pyrogram" that includes the percentage methylation at each methylated CpG. This refers to the percentage of sequenced fragments with T instead of C and thus approximates the frequency of its methylated state (Delaney, Garg and Yung, 2015).

The region of interest was amplified by Pyro PCR kit (PyroMark, QIAGEN) using 2µL bisulfite converted DNA, 12.5µL master mix, 2.5µL coral, 1.5µL of each primer (at 10µM) and 5.5µL NF-H_2O. 5-10µL PCR product was used in the pyrosequencing reaction. A master mix was prepared allowing for each reaction: 2µL streptavidin sepharose beads and 40µL binding buffer (PyroMark, QIAGEN) adjusted to 23µL reaction total with NF-H_2O. The PCR products were annealed to the beads by their biotin tag by shaking at 1400rpm for 10 mins. The beads were bound to suction and filter based probes on the pyrosequencing apparatus tool and rinsed in 70% ethanol (5 secs), denaturation buffer (0.2M NaOH, 5 secs) and 1X wash buffer (10X QIAGEN, 10 secs) and released onto wells of a PyroMark Q24 plate (QIAGEN) containing 0.3µM sequencing primer in 25µL annealing buffer. The plate was heated to 80^{O}c for 2mins on a heatblock and cooled at room

temperature for 5 mins. Samples were run on a PyroMark Q24 Pyrosequencer (Qiagen) using assays specific to the region (designed on PyroMark software v2.0.6).

2. 1. V. c). Primer design. The genomic sequence was obtained from UCSC Hg.38 and its bisulfite-converted form was generated by MethPrimer (assuming all cytosines converted to uracil). The PCR and sequencing primers and pyrosequencing assay were designed with PyroMark Q24 software (QIAGEN). Primers were obtained from Metabion, one of the PCR primers was biotinylated and HPLC grade, and the primer for sequencing binds complementary to the biotinylated strand.

Table 2. Primer sequences for mRNAs and genes analysed.

Gene name	***Forward sequence***	***Reverse sequence***	***Amplicon length***
Actin	ACAGAGCCTCGCCTTTGCC	GATATCATCATCCATGGTGAGCTGG	70
HPRT	CCTGGCGTCGTGATTAGTGA	CGAGCAAGACGTTCAGTCCT	137
PTEN	ACCCACCACAGCTAGAACTT	GGGAATAGTTACTCCCTTTTTGTC	221
POUF5	GTCATGCTGGATGTCAGGGC	AGCTTGCTTTGAGGGTCCCA	262
NCAM1	GATGCGACCATCCACCTCAA	CCATCCAGAGTCTCTTGCTTCT	212
Pri-miR-210-3p	*biotin-*GGCCGAGGACCAGGGTGACAGTGC	ACCTCTAAAACCTAAAAAAAATACCT (Sequencing primer: CTAAAACCTAAAAAAAATACCTC)	215
Pri-miR-2-5p (assay 1)	*biotin-*TAAGTGAAAGGATATTGGAGAGAGAA	CCAAAAAAACCCAAACATTTCTAACC (Sequencing primer: CCCAAACATTTCTAACCT)	273
Pri-miR-2-5p (assay 2)	*biotin-*AGAATTGGGGTTAGATTTTAATAGGTTAG	TCCTCCCTCCATACTACTACATTATA (Sequencing primer: AAAATATCAAACAACCCAT)	109
RhoB	*CGACGTCATTCTCATGTGCT*	*CGAGGTAGTCGTAGGCTTGG*	242
Spry2	GAGTGTTCATCAGCGGGGAA	CACATCTGAACTCCGTGATCG	198
TGFBR3	*TGAGCAGGCTGAAGTGACTG*	*GGCACAGCCTGACAAAACAG*	207

2. 1. V. Protein analysis

2. 1. V. a). Protein extraction. Protein was extracted using 40-100µL of urea-containing lysis buffer (8M urea, pH 7.5 with 1% β-mercaptoethanol (Sigma) and Complete Mini® protease inhibitor (Roche)), depending on the size of the cell pellet. The solution was gently and briefly vortexed and incubated at room temperature for 30mins. After this point, proteins were always kept on ice. The solution was centrifuged at 13200rpm for 8min at 4°C to pellet debris, which if large may be further broken down by additional lysis buffer to release transmembrane proteins. The supernatant was transferred to a clean tube and stored at -80°C. Protein samples were aliquoted if repeated use was required to avoid repeated freeze/thaw cycles.

2. 1. V. b). Protein quantification. A standard curve was produced using bovine serum albumin (BSA) with distilled water. Bradford assay was used for quantification (DC™ Protein Assay, Bio-Rad Life Science Research). In an Eppendorf, 2µL of the protein lysate was mixed with 8µL water, and 50µL solution A' was added (1µL reagent S + 50µL reagent A) and then 400µL solution B. The tube was vortexed lightly and incubated at room temperature in the dark for 10mins. 150µL was added to clear 96-well plates in triplicate and the absorbance was read on a FLUOstar Omega Spectrophotometer (BMG LabTech) at 650nm.

2. 1. V. c). Sample preparation and migration. Westerns were performed using the Invitrogen NuPage® Novex® Gel System and reagents. For each sample, 20-80µg protein was mixed with 3.5µL SDS-containing sample buffer and 2.5µL reducing agent, with distilled water to a total volume of 20-25µL, and kept on ice. 8-12% NuPAGE precast gels were used with 1X Running buffer. Samples were heated to 70°C for 15 mins to denature proteins for accurate sizing. The samples were pipetted into the wells while still hot, run at 100V for 5 mins or until the protein cleared the stacking gel and then 120V for 90mins. Prestained protein ladder (Invitrogen) was used as size marker.

2. 1. V. d). Transfer, antibody binding, and detection. The gels were removed from the casing and sandwiched against a 0.2µm or 0.45µm pore PVDF membrane, with 2 sheets of filter paper and a sponge on either side. The sandwich was positioned with the membrane between the gel and the anode, in the transfer tank with 1X transfer buffer (NuPage®, Invitrogen) with 10% methanol (increased to 20% if transferring 2 gels) and an ice block at 30V for 2 hours. After transfer, the membrane was stained with Ponceau solution (Sigma) and distilled water to confirm equal loading and then rinsed again in water for 5mins to remove the Ponceau. The membrane was blocked in 5% milk solution (TBS (6.05 g Tris and 8.76 g NaCl adjusted to 7.6 with 1 M HCl) with 1% Tween-20 (TBST) and 5% milk powder) for 1 hour at room temperature with gentle rocking. The primary antibody (also in TBST with 5% milk) was incubated with the membrane overnight at 4^{O}c with gentle rocking. The membrane was rinsed three times for 5 mins in TBST and then the membrane was incubated with the secondary antibody for 1 hour at room temperature with gentle rocking and rinsed again as before. Chemiluminescent detection (Thermo Scientific) was performed

by adding equal parts of reagents A and B to the membrane and incubating in the dark for 1 min before exposure on a high resolution G-BOX imager for fluorescence and chemiluminescence (Syngene).

Table 3. Primary antibodies used for Western blot analysis with supplier and dilution.

Protein name	***Supplier and identifier***	***Dilution factor***	***Animal***
A-actin	Sigma ABT1487	1 : 10,000	Mouse
GAPDH	Santa Cruz Biosciences, sc-47724	1 : 200	Mouse
HIF-1α	Sigma	1 : 500	Rabbit
NCAM	Santa Cruz Biosciences, sc-7326	1 : 200	Mouse
RhoB	Santa Cruz Biosciences, sc-8048	1 : 200	Mouse
Spry2	Santa Cruz Biosciences, sc-100862	1 : 200	Mouse
TGFβRIII	Santa Cruz Biosciences, sc-74511	1 : 200	Mouse
FKHR (FOXO1)	Santa Cruz Biosciences, sc-374427	1 : 200	Mouse

2. 2. In vivo experiments

In vivo experiments were conducted as established by previous research in the group (Nesbitt *et al.*, 2016, 2017).

2. 2. I. Animal maintenance. Experiments were performed in accordance with the Animal (Scientific Procedures) Act 1986 and the UKCCCR guidelines for the welfare of animals in experimental Neoplasia (Workman *et al.*, 1988). Male nude mice weighing 25-30g (Envigo, Cambridgeshire, UK) were housed under standard laboratory conditions in a temperature controlled ($22^{O}C$; 50-55% humidity) specific pathogen-free environment with a 12-hour light/dark cycle. Food and water were supplied *ad libitum*. Procedures were performed under aseptic conditions. The work was approved by the ethical review committee of Ulster University and covered by establishment licence and project licence.

2. 2. II. Animal care. Mice were sacrificed if the tumour reached (1,500mm^3), the mouse lost >20% of its body weight within one week or showed other signs of pain or suffering, otherwise 28 days after treatment had commenced.

2. 2. III. Xenograft establishment. LNCaP-luc xenografts were established on 24 nude mice at 8-10 weeks old. Mice were briefly anaesthetised by inhalation of isofluorane, and the cells were implanted. 100µl of ice-cold matrigel containing 5 x 10^6 LNCaP cells was slowly injected under the skin of the dorsum with an ice-cold 21 gauge needle (Becton Dickinson, Oxford, UK) and allowed to harden as a lump. After approximately 1 week the matrigel had been degraded and after approximately 2 weeks small tumours became palpable, and dimensions were then measured using Vernier calipers, using the formula (height x height x width)/2.

2. 2. IV. Drug administration. When tumour volume reached between 150mm^3, mice were randomly assigned to treatment groups and dosing initiated. Bicalutamide (Sigma) was solubilised in DMSO and diluted in corn oil (Sigma) to be administered orally *via* gavage at 6mg/kg as a daily dose. Mice receiving no treatment were given the vehicle alone (0.1% DMSO in corn oil).

2. 2. V. Oxygen electrode measurement. Mice were anaesthetised (1 hypnorm : 1 hypnovel : 2 sterile PBS) *via* intraperitoneal injection. A fibre optic probe (OxyLite®) was inserted into the tumour through a 21-gauge needle. 30 readings were taken at two sites, allowing the probe to adjust (readings becoming consistent) before readings were recorded. The median reading of each site was used, then the mean of the two medians per tumour to give the mean reading per mouse per day.

2. 3. Patient samples

2. 3. I. Ex vivo prostate biopsy cohort. A previous collaboration was established with Altnagelvin hospital, Derry and a cohort of 25 prostatectomy samples had been obtained as previously published (Lynch *et al.*, 2016). The study design was a paired comparison of tumour with non-tumour tissue from the same patient. These were excised whole tumours following radical prostatectomy from men aged 41-66 (Table 3). All tumours were localised at the time of surgery and between Gleason grades 6-8. The tumours were paraformaldehyde-fixed, paraffin embedded (FFPE) and sectioned by a pathologist who confirmed that tumour sections were >60% tumour cells. Use of patient material and information was approved by ORECNNI (ref 10/NIR0213). Paraffin was removed by two stages of immersion in xylene and heating (65^{O}C, 3 mins), two rinsing stages using 500µL 100% ethanol and centrifugation (13,200rpm, 2mins), air drying (ambient, 15mins). RNA was extracted by RecoverAll Total Nucleic Acid Isolation Kit (Ambion) according to manufacturer's instructions.

Table 3. Anonymised patient and tumour characteristics for the 22 prostatectomy samples. TNM: Tumour Node Metastasis. PIN: Prostatic Intraepithelial Neoplasia.

Case	Age	PSA (ng/ml)	Gleason Score	TNM stage	High Grade PIN	Involves Capsule	Circumferential Margin Involved	Apical Margin Involved
1	65	10	3 + 3 = 6	pT2	Yes	Yes	No	Yes
2	57	4.5	3 + 3 = 6	pT2	Yes	No	No	No
3	66	9.2	3 + 3 = 6	pT2	Uncertain	No	No	No
4	61	7	4 + 3 = 7	pT2	Yes	Yes	No	No
5	52	Not Stated	3 + 3 = 6	pT2	Yes	Yes	No	Yes
6	60	7.34	3 + 4 = 7	pT2	Yes	No	No	No
7	62	10.9	3 + 4 = 7	pT2	Yes	No	No	Yes
8	50	13	3 + 5 = 8	pT3	Yes	No	No	Yes
9	67	5.7	4 + 4 = 8	pT2	Yes	No	No	No
10	60	Not Stated	3 + 3 = 6	pT2	No	No	No	No
11	53	8	2 + 3 = 5	pT2	Yes	Yes	No	No
12	57	6.4	3 + 3 = 6	pT2	Yes	No	Yes	Yes
13	41	3.9	3 + 3 = 6	pT2	Yes	Yes	Yes	No
14	64	9.2	3 + 3 = 6	pT2	Yes	Yes	Yes	Yes
15	62	8.3	3 + 3 = 6	pT2+	Yes	Yes	Yes	Yes
16	58	10	3 + 4 = 7	pT2	Yes	Yes	No	No
17	47	8	3 + 3 = 6	pT2	Yes	Yes	Yes	Yes
18	65	6	3 + 3 = 6	pT2	No	No	No	No
19	59	5.7	3 + 5 = 8	pT3a	Yes	Yes	No	No
20	62	17.7	3 + 5 = 8	pT2	Yes	Yes	No	No
21	58	4.5	3 + 3 = 6	pT2	Yes	No	No	No
22	62	7.2	3 + 3 = 6	pT2	Uncertain	Yes	Yes	Yes
23	60	Not stated	3 + 4 = 7	pT2	Yes	No	No	No
24	65	6	3 + 3 = 6	pT2	No	No	No	No
25	51	8	2 + 3 = 5	pT2	Yes	Yes	No	No

2. 4. Statistical Analysis and Bioinformatics

2. 4. I. Statistical analyses. Graphs and statistics were generated Graphpad PRISM v5. Data normality was assessed by Shapiro-Wilk test. Group means were compared to the baseline value (100) by one-way t-test (or non-parametric Mann Whitney test) and multiple groups' means were compared by two-way t-test or in the case of three or more groups by ANOVA when at least five replicates were used (or non-parametric Kruskal Wallis test). For multiple hypothesis correction, the adjusted p-value was calculated (Q value / False Discovery Rate (FDR)) which is defined as the minimum FDR at which the test can be called significant (Benjamini and Hochberg 1995). The mean + SEM is shown. P-values considered significant when *p<0.05, **p<0.01, ***p<0.001. When differences were non-significant, no asterisks are shown.

2. 4. II. Databases. To identify mRNA targets of the miRNAs, databases miRTarBase (http://mirtarbase.mbc.nctu.edu.tw) (Chou *et al.*, 2016), miRWalk 2.0 (http://zmf.umm.uni-heidelberg.de/apps/zmf/mirwalk2/index.html) (Dweep and Gretz, 2015) were searched to find consistently predicted targets. MEDLINE/PubMed was searched using search strategies containing (miRNA) or (gene of interest) AND (prostate cancer) OR (hypoxia) to identify relevant literature (https://www.ncbi.nlm.nih.gov/pubmed/).

Analysis of The Cancer Genome Atlas (TCGA) repository data was performed using the Regulome Explorer (http://explorer.cancerregulome.org/) and Firebrowse (http://firebrowse.org/) analysis tools. Regulome Explorer analysis was based on a single primary prostate cancer dataset (TCGA Research Network, 2015). Firebrowse analysis was based on larger cohort of prostate adenocarcinoma (PRAD) samples (Broad Institute TCGA Centre, 2016). To identify significant correlation between miRNA expression and predicted target expression, the All Pairs Statistical Associations function was used. All Pairs parameters as follows: Feature 1: micro RNA expression, Label: [miRNA of interest] with Feature 2: All Gene Expression, using the parameters p value (-log10) ≥ 2, Correlation Abs ≤ 0, # of samples ≥ 0, Max Results = 2000, Filter by = Association. Significant correlations between the miRNA, or target at Gene Expression/ Protein level, with a Clinical Feature were identified using the same parameters. CSV data was downloaded. To identify significant correlations between clinical features with miRNA expression, the supplementary table 1 of all results was screened. To access boxplots of miRNA expression levels in features of prostate cancer, the file 'Analysis Results (MD5 checksum)' was downloaded and the graphs screened for the miRNAs of interest.

Survival analysis was performed using KM Express (http://ec2-52-201-246-161.compute-1.amazonaws.com/kmexpress/index.php) (Chen et al, 2018), Human Protein Atlas (https://www.proteinatlas.org/) (Uhlen et al, 2015), and Kaplan Meier Plotter (KM Plotter) (http://kmplot.com/analysis/) (Nagy *et al.*, 2018) analysis tools.

2. 4. III. RnBeads workflow for analysis of methylation array data. RnBeads package version 0.99.19 was used for exploratory and differential analysis, according to the 2015 vignette (http://rnbeads.mpi-inf.mpg.de/data/RnBeads.pdf)(Müller, Assenov and Lutsik, 2015). Ghostscript v9.27 for Windows (32 bit) (Artifex Software) was installed from (http://ghostscript.com/download/gsdnld.html).

2. 4. IV. RNA-seq analysis for the prostatectomy cohort. Needle core biopsies were sent to BioSpyder Technologies (Carlsbad, CA) who performed the following procedures for RNA extraction and sequencing by miRNAseq and mRNAseq. *RNA extraction.* 1mm^3 of tissue per sample was added to 50µL of 1x lysis buffer, for eventual (ideal) concentration of 0.02 mm3 per µL. 20µL of mineral oil was overlaid over the mixture, and the tube was heated to 95°C for ten seconds to remove the paraffin, and the process was repeated with 20 µL of fresh oil to completely remove paraffin. 5µL of proteinase K solution (100µg) was added to each sample. Samples were incubated at 37°C for 30 minutes, and the proteinase was inactivated at 95°C for 15 minutes. *Hybridisation.* The binding mix for hybridization was as follows: 0.4 µL 5X Annealing Buffer, 0.6 µL water, 1 µL DOs (human surrogate 1.0), 2 µL digested sample. The temperature settings were: 80°C for 10 seconds, cooled down until 70°C at 0.1°C per second. The samples were left at 70°C for 10 min, and decreased by.5°C per 1 min until a final temperature of 45°C and then left at final temperature overnight. *Exonuclease reaction.* Per reaction the following was added: 2.4µL 10x Exo Buffer, 0.25µL Exonuclease I (at 200U/µL), 21.4µL water, then incubated for 1.5 hours at 37°C. *Ligation Mix.* Per reaction the following was added 2.4µL 10X Ligation Buffer, 1 µL5 U/µL T4 DNA Ligase, 20.6µL Water, Incubate at 37°C for 1 hour. The exonuclease was inactivated by incubating at 80°C for 30 minutes. *Amplification Mix.* 10µL of the ligation product was added to 10µL PCR mix for a total of 20µL final, Per reaction: 1µL 20 µM forward primer, 1µL 20 µM reverse primer, 8µL BioSpyder PCR pre-mix. 10µL sample was added and the cycles were as follows: 37°C, 2 min, 95°C, 2 min, 6 cycles of 95°C, 30sec; 54°C 30sec; 72°C 120 sec, 21 cycles of 95°C, 30sec; 72°C 120 sec, 72°C 60 sec, before cooling to 40°C. *Analysis.* Differential expression analysis was calculated using the DESeq2 method and verified by MA plot. Volcano plots were made using R version 3.4.4 and RStudio (RStudio, Inc., Boston, 2015) (for code see Appendix 1). Log2foldchange <0 was considered downregulated, >0 upregulated, and statistically significantly when the adjusted p value <0.1.

2. 4. V. Network and Pathway Analysis. Functional enrichment analysis and gene set analysis were performed using KEGG and DAVID Bioinformatics Resources 6.8 (Huang et al, 2009a; 2009b) (https://david.ncifcrf.gov/) . Pathway analysis was performed by DAVID Bioinformatics Resources 6.8 and QIAGEN Bioinformatics Ingenuity Pathway Analysis (IPA) software (https://www.qiagenbioinformatics.com/products/ingenuity-pathway-analysis/). For IPA core analyses the Ingenuity knowledge base (genes only) was accessed, including all node types, and all data sources. The confidence level accepted was: experimentally observed or predicted with high confidence. Species: all mammals (human, rat, mouse). All tissues and cell lines. All Mutations. Log2FoldChange cutoffs

(<0=downreg, >0=upreg), p value <0.05, adj p value <0.1. For miRNAseq data these parameter allowed 12 analysis ready molecules (10 up, 2 down). For pathway analysis of differentially methylated sites, the cutoffs were <-0.1 and >0.1, p value <0.05, and adj p value <0.1.

2. 4. VI. RNA-sequencing of AR variant expressing LNCaP. Log2(fold change) results were the mean ratio of three biological replicates. Library preparation and high-throughput sequencing had been performed on the Illumina Hiseq 4000 as Single-Read 50 base reads, by the GenomEast genomic platform (IGBMC, Illkirch, France). Reads were mapped onto hg38 assembly of human genome using Tophat v2.0.14 (Kim *et al.*, 2013) and bowtie2 v2.1.0 aligner (Langmead and Salzberg, 2012). Quantification of gene expression was performed using HTSeq v0.6.1 (Anders, Pyl and Huber, 2015) and gene annotations from Ensembl release 84. Read counts were normalized across libraries with the method proposed by Anders and Huber (Anders and Huber, 2010) and then normalized according to the gene length. Comparisons of interest were performed using the method proposed by Love et al (Love, Huber and Anders, 2014) implemented in the DESeq2 Bioconductor library (DESeq2 1.6.3) in order to obtain $\log_2$(fold change) and corresponding p-values. P-values were adjusted for multiple testing using Benjamini and Hochberg method (BENJAMINI *et al.*, 1995) (p-value / number of hypotheses). Genes were considered significantly differentially expressed when the FDR adjusted p-value <0.05 and log2(Fold Change) >1 or <-1.

2. 4. VII. Python for data analysis. Data analysis and graphs for the ARV collaboration were written in python (Oliphant, 2007) using the Jupyter Notebook 5.4.0 from the Anaconda Navigator, using the panda, numpy, matplotlib and bokeh packages. Results with adjusted p-value <0.05 were considered significant.

2. 4. VIII. Analysis of ChIP-seq data. Two chip-seq datasets were analysed via the Cistrome Data Base webpage (http://cistrome.org/db/#/), by searching for datsets in LNCaP using an AR antibody. The Cistrome Database datasets used were numbers 44330 (Ramos-Montoya *et al.*, 2014) and 71170 (McNair *et al.*, 2017). Datasets were visualised in UCSC (https://genome.ucsc.edu) using human Hg.19 with the track 'GH Reg Elems (DE), Enhancers and promoters from GeneHancer (Double Elite)' on pack visibility. No ChIP-seq datasets including AR variant analyses were available on Cistrome DB, therefore a study was chosen that had used ChIP-seq to compare AR-WT with AR variants (He *et al.*, 2018). Files were downloaded from NCBI Gene Expression Omnibus (GEO) at accession number GSE80743. In this study, 22RV1 cells had been transfected with non-target siRNA (designated as ARFL+/ARVs+), siRNA targeting ARV1/3/4/7 (designated as ARFL+/ARVs-), or siRNA targeting AR exon7 (designated as ARFL-/ARVs+) therefore GSM2734940_AR_siARV_rep1.bw was assumed to represent AR-FL binding and GSM2734942_AR_siARFL_rep1.bw to represent AR-V7 binding. The files were visualised using Integrative Genome Viewer (https://igv.org/app/) with the RefSeq genes track, gene regions were searched by entering the chromosomal location as provided by UCSC Hg.19.

2. 5. Bibliography

Alimirah, F. *et al.* (2006) 'DU-145 and PC-3 human prostate cancer cell lines express androgen receptor: Implications for the androgen receptor functions and regulation', *FEBS Letters*. John Wiley & Sons, Ltd, 580(9), pp. 2294–2300. doi: 10.1016/j.febslet.2006.03.041.

Anders, S. and Huber, W. (2010) 'Differential expression analysis for sequence count data', *Genome Biology*, 11(10).

Anders, S., Pyl, P. T. and Huber, W. (2015) 'HTSeq-A Python framework to work with high-throughput sequencing data', *Bioinformatics*, 31(2), pp. 166–169. doi: 10.1093/bioinformatics/btu638.

Bello, D. *et al.* (1997) 'Androgen responsive adult human prostatic epithelial cell lines immortalized by human papillomavirus 18', *Carcinogenesis*, 18(6), pp. 1215–1223. doi: 10.1093/carcin/18.6.1215.

Benjamini, Y. *et al.* (1995) 'Controlling the false discovery rate: a practical and powerful approach to multiple testing.' doi: 10.2307/2346101.

Chou, C.-H. *et al.* (2016) 'miRTarBase 2016: updates to the experimentally validated miRNA-target interactions database', *Nucleic Acids Research*, 44(D1), pp. D239–D247. doi: 10.1093/nar/gkv1258.

Dweep, H. and Gretz, N. (2015) 'miRWalk2.0: a comprehensive atlas of microRNA-target interactions', *Nature Methods*, 12(8), pp. 697–697. doi: 10.1038/nmeth.3485.

Gaupel, A.-C. *et al.* (2013) 'Xenograft, Transgenic, and Knockout Models of Prostate Cancer', *Animal Models for the Study of Human Disease*. Academic Press, pp. 973–995. doi: 10.1016/B978-0-12-415894-8.00039-7.

He, Y. *et al.* (2018) 'Androgen receptor splice variants bind to constitutively open chromatin and promote abiraterone-resistant growth of prostate cancer.', *Nucleic acids research*. Oxford University Press, 46(4), pp. 1895–1911. doi: 10.1093/nar/gkx1306.

Horoszewicz, J. S. *et al.* (1983) 'LNCaP model of human prostatic carcinoma.', *Cancer research*, 43(4), pp. 1809–18.

Kaighn, M. E. *et al.* (1979) 'Establishment and characterization of a human prostatic carcinoma cell line (PC-3).', *Investigative urology*, 17(1), pp. 16–23.

Kim, D. *et al.* (2013) 'TopHat2: accurate alignment of transcriptomes in the presence of insertions, deletions and gene fusions Daehwan', *Genome Biology*, 14. doi: 10.1101/000851.

Langmead, B. and Salzberg, S. L. (2012) 'Fast gapped-read alignment with Bowtie 2', *Nature Methods*, 9(4), pp. 357–359. doi: 10.1038/nmeth.1923.

Love, M. I., Huber, W. and Anders, S. (2014) 'Moderated estimation of fold change and dispersion for RNA-seq data with DESeq2', *Genome Biology*, 15(12), pp. 1–21. doi: 10.1186/s13059-014-0550-8.

Lynch, S. M. *et al.* (2016) 'Regulation of miR-200c and miR-141 by Methylation in Prostate Cancer', *The Prostate*, 76(13), pp. 1146–1159. doi: 10.1002/pros.23201.

McNair, C. *et al.* (2017) 'Cell cycle-coupled expansion of AR activity promotes cancer progression', *Oncogene*, 36(12), pp. 1655–1668. doi: 10.1038/onc.2016.334.

Mootha, V. K. *et al.* (2003) 'PGC-1 alpha-responsive genes involved in oxidative phosphorylation are coordinately downregulated in human diabetes PGC-1 α -responsive genes involved in oxidative phosphorylation are coordinately downregulated in human diabetes', *Nature genetics*, 34(3), pp. 267–273. doi: 10.1038/ng1180.

Müller, F., Assenov, Y. and Lutsik, P. (2015) *RnBeads-Comprehensive Analysis of DNA Methylation Data*.

Nagy, Á. *et al.* (2018) 'Validation of miRNA prognostic power in hepatocellular carcinoma using expression data of independent datasets', *Scientific Reports*, 8(1), p. 9227. doi: 10.1038/s41598-018-27521-y.

Nesbitt, H. *et al.* (2016) 'Targeting Hypoxic Prostate Tumors Using the Novel Hypoxia-Activated Prodrug OCT1002 Inhibits Expression of Genes Associated with Malignant Progression.', *Clinical cancer research : an official journal of the American Association for Cancer Research*. United States. doi: 10.1158/1078-0432.CCR-16-1361.

Nesbitt, H. *et al.* (2017) 'The unidirectional hypoxia-activated prodrug OCT1002 inhibits growth and vascular development in castrate-resistant prostate tumors', *The Prostate*, 77(15), pp. 1539–1547. doi: 10.1002/pros.23434.

Oliphant, T. E. (2007) 'Python for scientific computing', *Computinh in Science @ Engineering*, pp. 10–20.

Ramos-Montoya, A. *et al.* (2014) 'HES6 drives a critical AR transcriptional programme to induce castration-resistant prostate cancer through activation of an E2F1-mediated cell cycle network.', *EMBO molecular medicine*. Wiley-Blackwell, 6(5), pp. 651–61. doi: 10.1002/emmm.201303581.

RStudio, Inc., Boston, M. (2015) *RStudio Team*, *RStudio: Integrated Development for R.* Available at: https://www.rstudio.com/ (Accessed: 22 January 2019).

Sramkoski, R. M. *et al.* (1999) 'A new human prostate carcinoma cell line, 22Rv1', *In Vitro Cellular & Developmental Biology - Animal*, 35(7), pp. 403–409. doi: 10.1007/s11626-999-0115-4.

Stone, K. R. *et al.* (1978) 'Isolation of a human prostate carcinoma cell line (DU 145).', *International journal of cancer*, 21(3), pp. 274–81.

Subramanian, A. *et al.* (2005) 'Gene set enrichment analysis: A knowledge-based approach for interpreting genome-wide expression profiles', *Proceedings of the National Academy of Sciences*, 102(43), pp. 15545–15550. doi: 10.1073/pnas.0506580102.

Wadosky, K. M. and Koochekpour, S. (2017) 'Androgen receptor splice variants and prostate cancer: From bench to bedside', *Oncotarget*, 8(11), pp. 18550–18576. doi: 10.18632/oncotarget.14537.

Workman, P. *et al.* (1988) 'UKCCCR guidelines for the welfare of animals in experimental neoplasia.', *Laboratory animals*. England, 22(3), pp. 195–201.

Xu, J. and Qiu, Y. (2016) 'Role of androgen receptor splice variants in prostate cancer metastasis.', *Asian journal of urology*. Second Military Medical University, 3(4), pp. 177–184. doi: 10.1016/j.ajur.2016.08.003.

Chapter 3. Investigating the link between miR-210 and the hypoxic response in prostate cancer.

This work was submitted for publication to the Journal of Cellular Physiology in July 2019 and accepted in January 2020.

3. 1. Introduction

One miRNA that has been consistently implicated in the hypoxic response is hsa-miR-210-3p (miR-210). MiR-210 expression is consistently associated with hypoxia in many tissues under both physiological and pathological conditions (Bavelloni *et al.*, 2017). Perhaps best characterised is its role in maintaining cellular integrity following hypoxia in the cardiovascular system; diseases such as acute myocardial infarction, heart failure, atherosclerosis, and aortic stenosis are accompanied by acute ischaemia and are associated with overexpression of miR-210. Here, miR-210 may exert a protective effect on the cells by promoting survival and angiogenesis, and inhibiting apoptosis *via* the regulation of proapoptotic proteins E2F3, PDK1, and BNIP3 (Guan *et al.*, 2019). Furthermore, miR-210 was secreted by the exosomes of stem cells and exerted protective effects on cardiomyocytes and attenuated fibrosis (Moghaddam *et al.*, 2019). It was also reported to be a marker of pre-eclampsia, a disorder of the placenta that occurs during pregnancy due to poor trophoblast invasion and results in hypoxia, oxidative stress and inflammation (Gan *et al.*, 2017). These studies suggest that the expression of miR-210 has protective effects that buffer against the effects of acute hypoxia, and that it may have diagnostic value as a marker of hypoxia in different tissues. As well as promoting cell survival, miR-210 plays a key role in regulating mitochondrial metabolism. MiR-210 has a HIF-binding site in its promoter region and is a direct transcriptional target of HIF, making it one of the earliest responders to hypoxia (Bavelloni *et al.*, 2017). Early experiments using pulmonary arterial endothelial cells showed that miR-210 targets iron-sulfur cluster assembly proteins (ISCU1/2) and inhibits the activity of prototypical iron-sulfur proteins such as acontiase Complex I. More metabolic targets have since been identified including GPD1L, SDHD, COX10, and NDUFA4 and sequencing experiments have linked miR-210 overexpression to mitochondrial dysfunction (Qin, Furong and Baosheng, 2014). These studies highlight the influence of miR-210 over the balance between glycolysis and oxidative phosphorylation.

However, since miR-210 has cytoprotective and metabolic regulatory effects, prolonged expression could facilitate carcinogenesis or facilitate tumour progression. Indeed, miR-210 is commonly overexpressed in cancers, including breast, pancreatic, head and neck, renal, lung, oesophageal and ovarian cancers, although occasionally it is downregulated or deleted (Qin, Furong and Baosheng, 2014). In colorectal cancer (CRC), miR-210 expression correlates with advanced clinical stage, tumour size, lymph node metastasis, resistance to radiotherapy, and poor outcome (Bavelloni *et al.*, 2017). Furthermore, miR-210 containing exosomes from CRC cell line HCT-8 were mediators of cross talk between primary tumour cells and disseminated metastatic cells (Yang *et al*>, 2017). Similarly in gastric cancer, miR-210 may promote migration, invasion, and chemo-resistance (Yang *et al*>, 2017). In breast cancer, miR-210 was induced by hypoxia and was associated with increased cell proliferation, epithelial-mesenchymal-transition (EMT), migration and invasion, and self-renewal (Tang *et al.*, 2018) and has been used as a prognostic factor (Camps *et al.*, 2008; Madhavan *et al.*, 2012; Li *et al.*, 2013). In non-small cell lung cancer (NSCLC), it was a

diagnostic factor (Jiang *et al.*, 2018) and was further overexpressed in the late stages (Puisségur *et al.*, 2011). Furthermore, miR-210 was upregulated in both the tumour and urine of patients with clear cell renal carcinoma (Petrozza *et al*>, 2017). In neuroblastoma cells, miR-210 targeted *BCL2* meaning that it could regulate both apoptosis and autophagy (Chio *et al.*, 2013). Therefore, miR-210 likely plays a key role in the hypoxic response in many tissues and was overexpressed in many cancers, which could indicate either hypoxia or oncogenic effects. For example, it may confer a survival advantage by regulating proliferation and motility, and by inhibiting oxidative phosphorylation and contributing to a glycolytic phenotype.

However, although prostate tumours are particularly hypoxic, relatively few studies have investigated miR-210 in PCa. Numerous studies have demonstrated that the overexpression of miR-210 in primary tumours correlated with lymphogenic metastatic and bone metastatic PCa (Eminaga *et al*>, 2018)(Dai *et al.*, 2017)(Ren *et al.*, 2017). Likewise, the sera from patients with PCa contained higher levels of miR-210 (Qu and Huang, 2018)(Cheng *et al*>, 2013). However, these studies did not confirm the hypoxic status of these tissues, meaning that it is unclear whether miR-210 was acting as a result of hypoxia in vivo. *In vitro* work has shown that miR-210 targets key players in the NF-κB (Ren *et al.*, 2017) and TGF-β (Dai *et al.*, 2017) signalling pathways in PCa, while others have suggested miR-210 expression in stromal fibroblasts can contribute to prostate tumour progression through promotion of EMT (Taddei *et al.*, 2014)(Andersen *et al.*, 2016)(Taddei *et al.*, 2014). However, the link between hypoxia and miR-210 in PCa has not been confirmed in vitro or in vivo. The hypothesis of this chapter was that miR-210 would be induced by hypoxia in PCa and that its expression would have cancer-promoting effects.

3. 2. Results

3. 2. I. Hypoxia upregulates miR-210 in prostate cancer cells.

To explore the regulation of miR-210 by hypoxia, three models of PCa hypoxia were designed. The first model involved culturing LNCaP prostate cancer cells in hypoxic (0.1% O_2) conditions using a hypoxic chamber and measuring miR-210 expression by RT-qPCR relative to the normoxic condition (Methods section *2.1.I.b.* and *2.1.IV*). Hypoxia resulted in significant miR-210 upregulation compared to 20% O_2 by 24h (Figure 1A). The induction of hypoxia in these cells was confirmed by upregulation of hypoxic marker genes *PTEN* and *POU5F1* (Figure 1B) and HIF-1α protein (Figure 1C). MiR-210 was further increased by 48h, although a reduction in cell viability was observed after 72h at 0.1% oxygen, indicated by abnormal cell morphology and trypan blue staining, and therefore 24h was considered the optimal duration for hypoxic experiments. The induction of miR-210 in response to 24h hypoxic culture was also noted in 22Rv1 and PC3 prostate cancer cells, as well as non-transformed RWPE-1 epithelial prostate cells (Supplementary Figure 1).

As a second model of PCa hypoxia, LNCaP cells were cultured as spheroids by double-coating the base of the culture dish in poly(2-hydroxyethyl methacrylate) to prevent seeding (Figure 1D-E)(Methods section *2.1.I.d*.). Cell spheroids are globular clusters of cells and the centres were predicted to become hypoxic once it reached a certain size. This was designed to produce a more representative model of tumour hypoxia since the proportion of cells that become hypoxic are lower and a gradient of diffused oxygen and hypoxic cells develops from the core to the surface. The spheroids became hypoxic at approximately 50µm (Figure 1F) which correlated with a significant upregulation in miR-210 expression (Figure 1G). LNCaP proved a perfect cell line model for establishing spheroids since they aggregate naturally in culture. Preliminary experimentation with LNCaP, 22Rv1, PC3 and RWPE-1 to generate suitable spheroid cultures was conducted. Of these, LNCaP spheroids proved the most reproducible and was used in subsequent experiments for miR-210 analysis.

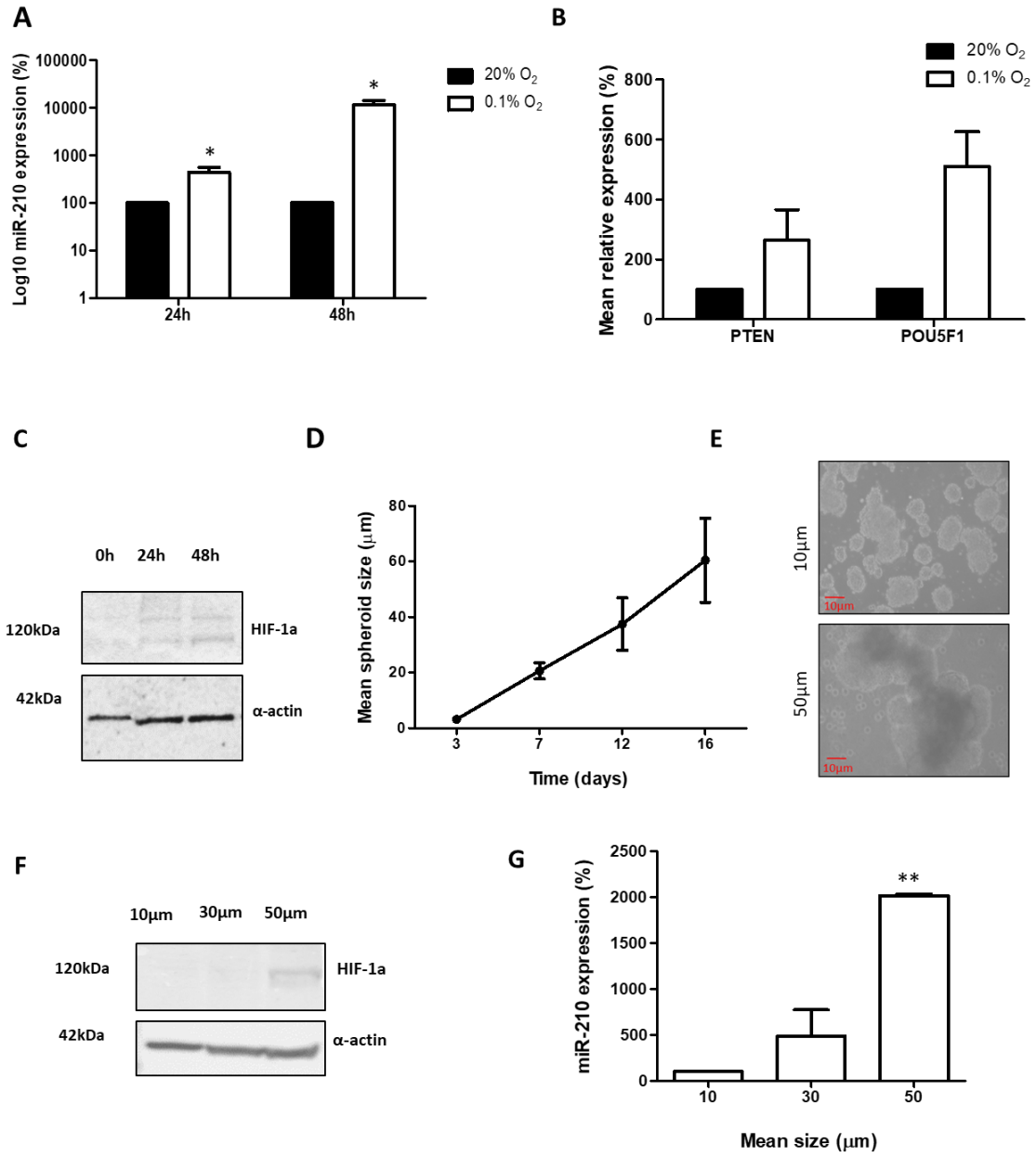

Figure 1. **Two *in vitro* models of hypoxia demonstrate miR-210 upregulation in LNCaP cells. A)** RT-qPCR result showing increased mean expression of miR-210 in three biological replicates following culture at 0.1% 0_2 (hypoxia) for 24h and 48h, relative to mean expression in paired flasks cultured at 20% 0_2 (normoxia). Mean + SEM of three biological replicates. **B)** Hypoxia successfully induced as indicated by RT-qPCR measurement of hypoxic response genes *PTEN* and *POUF51* after 24h hypoxia relative to normoxia (mean + SEM of three biological replicates), and **C)** Western blot analysis of HIF-1α following hypoxic culture for 0-48h. Representative image of two biological replicates. **D)** Spheroid size increase between day 3 and day 16 as measured by light microscope, mean + SEM of 10 spheroids at each time point shown. **E)** Light microscope images of the spheroids at mean 10µm and 50µm in size. **F)** Western blot analysis showing HIF-1α stabilisation in spheroids at 50µm. Representative image of two biological replicates. **G)** RT-qPCR analysis of miR-210 expression in spheroids showing significant upregulation at 50µm. Mean + SEM of three biological replicates (Student t-test p-values: *p<0.05, **p<0.01, ***p<0.001).

3. 2. II. In an in vivo model of prostate cancer, bicalutamide increases hypoxia and miR-210

Next, a murine LNCaP xenograft model was set up, which has previously been employed by the McKenna laboratory to study tumour hypoxia in response to bicalutamide treatment and is described in Methods section *2.2* (Nesbitt *et al.*, 2016)(Byrne *et al.*, 2016) (Figure 2A-C). Nude mice were chosen for the study, which have a mutation in the *FOXN1* gene resulting in an impaired thymus gland and greatly reduced number of T cells, and are thus incapable of mounting a rejection response (Szadvari, Krizanova and Babula, 2016). LNCaP cells were selected since they are AR-dependent and thus susceptible to AR inhibition. Briefly, ectopic implantation was performed, using $5X10^5$ LNCaP cells solubilised in 100µL ice-cold matrigel, under the skin of the dorsum. Once under the skin, the matrigel warms and polymerises, and acts as a solid matrix that remains for approximately 1 week, during which time the cancer cells may proliferate and form a tumour. At least four animals were used for each group at each time point. Once the tumour reached $150mm^3$, dosing was initiated; mice received either the AR-inhibitor bicalutamide or vehicle for 7 or 28 days. Tumour size was measured every 3 days (Figure 2D), and tumour oxygenation measured at day 7, day 14, and day 28 (Figure 2B and 2E) as well as tail vein bleeds for serum extraction, before culling and tumour excision at day 7 or day 28 (Figure 2C).

As expected, tumour growth was inhibited by bicalutamide treatment after 28 days, in comparison with vehicle treated tumours (Figure 2D). In accordance with previous research (Nesbitt *et al.*, 2016)(Byrne *et al.*, 2016), bicalutamide treatment induced tumour hypoxia after 7 days (Figure 2B), resulting in HIF-1α stabilisation (Figure 2E). In correlation, miR-210 expression was upregulated by day 7 and significantly so by day 28 (Figure 2C). There was also an induction of miR-210 expression in the sera of some bicalutamide-treated mice, although this varied across and was not statistically significant (Figure 2D).

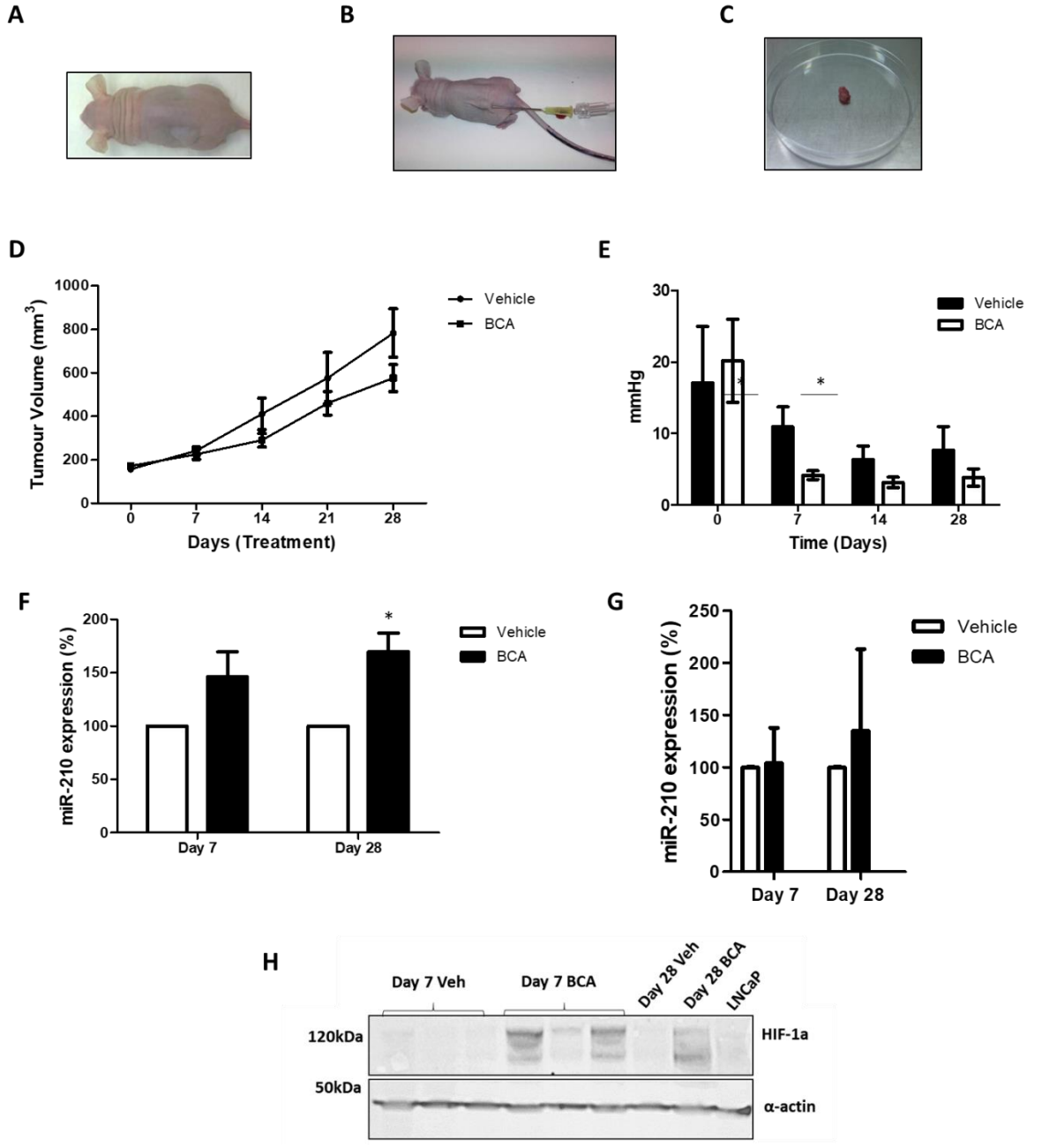

Figure 2. ***In vivo*** **model of hypoxia demonstrates miR-210 upregulation in LNCaP xenograft. A)** Photograph of LNCaP xenograft tumour on the dorsum of nude mouse at 150mm^3. **B)** Photograph of oxygen electrode measurement of partial oxygen tension (PO_2, in mmHg). **C)** Photograph of an excised tumour at day 7. **D)** Tumour growth curves in bicalutamide and vehicle treated mice at days 0, 7, 14, 21, and 28 showing reduced tumour size in bicalutamide-treated mice. Mean + SEM shown, data points represent measurements from at least four animals. **E)** Oxygen electrode readings showing significantly reduced PO_2 in tumours of bicalutamide-treated mice relative to vehicle treated mice at day 7. **F)** RT-qPCR analysis showing increased expression of miR-210 in bicalutamide-treated tumours at day 7 and day 28. **G)** RT-qPCR analysis of serum samples showing non-significantly increased levels of miR-210 in the serum of bicalutamide treated mice. **H)** Representative western blot image demonstrating stabilisation of HIF-1α in bicalutamide-treated tumours at day 7 and day 28 compared with vehicle-treated mice. One-way t-tests were used to compare condition means to the control (hypothetical value 100), two-way t-tests were used to compare two means, and p-values considered significant when *p<0.05, **p<0.01, ***p<0.001.

3. 2. III. MicroRNA-210 is associated with markers of prostate cancer progression.

Next, the clinical relevance of miR-210 expression was explored. A cohort of 19 prostatectomy samples were analysed, which had been acquired through a collaboration with Alnagelvin hospital in Derry, Northern Ireland. As described in Methods section *2.3*. these were whole tumours that had been excised from patients during surgery, and sectioned. A previous member of the lab (Dr Seodhna M. Lynch) had organised the collaboration and extracted RNA from the sections, the RNA from a tumour section was normalised to non-tumour section from the same prostate. These samples were analysed and miR-210 was successfully quantified in 17 of the paired samples (Figure 3A). The tumours did not uniformly have upregulated miR-210, which was not unexpected as previous work in our laboratory had noted a similar variation in expression of miR-24, miR-200c, and miR-141 in a related set of samples (Lynch *et al.*, 2016a; Lynch *et al.*, 2016b). This variation could be indicative of the relative hypoxic status across the tumours, which in turn may provide useful diagnostic or prognostic information, although protein levels of HIF-1α would need to be confirmed and unfortunately the sections were too small to obtain a protein sample. Due to the small size of the cohort, the tumours were grouped based on their Gleason grade group rather than Gleason score and interestingly, there was a mild trend of increasing miR-210 expression across the groups (Figure 3B). However, it was clear that a larger clinical dataset was needed to gain statistically significant results.

To explore a larger dataset, The Cancer Genome Atlas database was accessed. RNA-sequencing data from the Prostate Adenocarcinoma (PRAD) samples was downloaded, using the tools Regulome Explorer (http://explorer.cancerregulome.org/) and Firebrowse (http://firebrowse.org/). Regulome Explorer accesses a single primary prostate cancer dataset of 330 samples (hereafter referred to as Regulome Explorer dataset)) (TCGA Research Network, 2015). Firebrowse accesses a larger cohort of prostate adenocarcinoma (PRAD) samples, which is continually updated and currently has over 400 samples (hereafter referred to as PRAD dataset)(Broad Institute TCGA Centre (2016). The data consists of sequenced localised prostate tumour samples normalised against non-tumour tissue from the same patient. Analysis of this data using the Firebrowse tool revealed that miR-210 levels were significantly increased in correlation with Gleason score, lymph node metastasis, but not with TNM stage or PSA level (Figure 3C-D). Furthermore, analysis of the same data using the KM-Express informatics tool (https://omictools.com/km-express-tool) revealed that PCa patients with high miR-210 expression had significantly shorter time of disease-free progression than those with low expression (Figure 3E).

To further evidence that the increased expression of miR-210 is associated with hypoxia in clinical samples, expression of various hypoxia-related genes was examined using the Regulome Explorer tool. This showed that *EZH2*, another marker of prostate tumour hypoxia (Zhou *et al.*, 2018), has a strong positive correlation with miR-210 expression in these samples (Figure 3F). Finally, KEGG analysis and Gene Ontology mapping of validated miR-210 targets demonstrated that miR-210 is significantly associated with both PCa and

hypoxia-related cell processes, through its various target genes (Tables 1A-B). This *in silico* analysis corroborated the laboratory results in demonstrating that miR-210 is likely to be a key mediator of the hypoxic response in PCa.

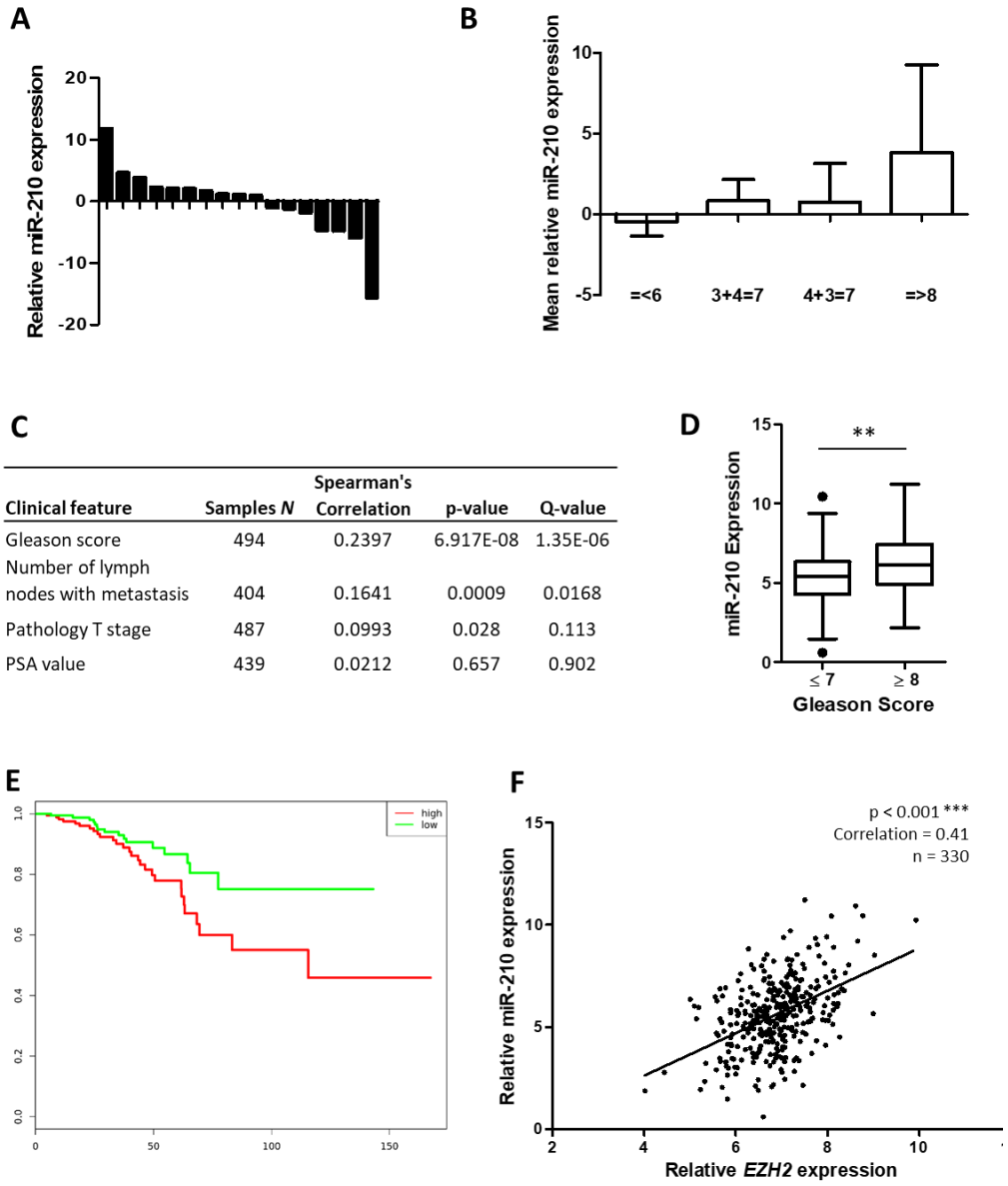

Clinical feature	Samples *N*	Spearman's Correlation	p-value	Q-value
Gleason score	494	0.2397	6.917E-08	1.35E-06
Number of lymph nodes with metastasis	404	0.1641	0.0009	0.0168
Pathology T stage	487	0.0993	0.028	0.113
PSA value	439	0.0212	0.657	0.902

Figure 3. MiR-210 correlates with prostate cancer aggressiveness in human prostate tumour samples. **A)** Cohort of 19 prostatectomy biopsies. RT-qPCR analysis shows miR-210 expression is can be both up-regulated and down-regulated in tumour tissue, which may reflect the relative hypoxic nature of the specimen. **B)** Grouping the prostate samples by Gleason grade group (≥6, 3+4=7, 4+3=7, 8) indicates that the mean relative expression of miR-210 is increased in tumours of higher grade group. Groups contained at least 2 samples. **C)** Analysis of data downloaded from The Cancer Genome Atlas prostate adenocarcinoma (PRAD) cohort using the Firebrowse tool. Mean relative miR-210 expression significantly correlated with tumours of higher Gleason score score (p=6.917E-08, adjusted p-value (Q)=1.35E-06) and with lymph node metastasis (p=0.0009338, adjusted p-value (Q)=0.0168), and correlated but not significantly with pathological T stage and PSA level. Analyses utilised Spearman's rank correlation, with p-values adjusted for multiple hypothesis testing. A p-value of < 0.05 and Q-value < 0.3 was deemed significant. **D)** Boxplot illustrating significantly increased mean relative miR-210 expression in tumours of Gleason score ≥8 compared with Gleason score ≤7 from Regulome Explorer data. **E)** Survival analysis of PRAD data using KM Express tool reveals miR-210 expression significantly increased in men with shorter progression-free survival (y-axis: miR-210 expression, x-axis: time (months), hazard ratio, 0.52, p=0.0375). **F)** In the Regulome Explorer data, relative miR-210 expression significantly correlated with relative *EZH2* expression, a marker of PCa progression.

Table 1. Analysis of the functions of predicted miR-210 target genes. A) KEGG pathway analysis shows highly significant association of miR-210 with cancer-related disease terms. **B)** Gene Ontology Mapping showing highly significant association of miR-210 with selected GO classifications related to hypoxia and oxidative stress. P-values generated by modified Fisher Exact test. Benjamini values represent corrected p-value for multiple hypothesis testing using the Benjamini-Hochberg method to minimise false discovery rate.

A

Disease Term	Gene Count	P-value	Benjamini
CANCER	38	0.0026	0.046
tobacco use disorder	33	0.023	0.91
breast cancer	11	0.0057	0.83
ovarian cancer	9	0.0069	0.76
prostate cancer	9	0.039	0.91
lung cancer	9	0.041	0.9
bladder Cancer	9	0.047	0.88

B

Gene Ontology Term	Gene Count	P-Value	Benjamini
cellular response to oxygen levels	8	0.000092	0.047
cellular response to oxidative stress	9	0.00022	0.048
cellular response to hypoxia	7	0.00035	0.049
cellular response to decreased oxygen levels	7	0.00047	0.054
response to oxidative stress	11	0.00049	0.05
response to oxygen levels	9	0.0018	0.11
response to hypoxia	8	0.0043	0.17
response to decreased oxygen levels	8	0.0051	0.19
regulation of oxidative stress-induced cell death	4	0.0063	0.21

3. 2. IV. Identification of a novel mRNA target of miR-210 in PCa

The previous figure illustrates how the function of miR-210 can be gauged by exploring the effects of the mRNAs that it binds and suppresses. Next, to probe the oncogenic effects of miR-210, a list of putative mRNA targets was compiled using the miRTarBase software tool (http://mirtarbase.mbc.nctu.edu.tw/php/index.php). Among these, neural cell adhesion molecule (*NCAM1*) was of particular interest as an adhesion molecule that could be a potential tumour-suppressor. The prostate cell lines in our laboratory were screened for expression of NCAM and interestingly it was only detected in the non-transformed cell line RWPE-1 (Figure 4B). Transient transfection was used to overexpress miR-210 in this cell line (Figure 4C) and levels of *NCAM1* were decreased as measured by RT-qPCR, although this was not significant, perhaps because the mRNA is incompletely degraded due to

imperfect binding of the seed region (Figure 4D). However, at the protein level there was a reduction in NCAM levels, suggesting miR-210 can indeed regulate levels of functional NCAM (Figure 4E).

Next, *NCAM1* was confirmed as a direct target of miR-210 by luciferase reporter assay, as outlined in Methods section *2.1.II.* (Figure 4F). Briefly, the luciferase activity of a reporter construct containing the wild-type *NCAM1* 3'UTR region (WT-3'UTR) was reduced when miR-210 was co-expressed in the same cells. However, when miR-210 was co-expressed with a reporter construct which had deleted residues in the miR-210 binding site of *NCAM1* 3'UTR (DEL-3'UTR), luciferase activity was intact, therefore indicating that *NCAM1* is a direct target of miR-210 in these cells. Hence, through this mechanism, the hypoxia-induced expression of miR-210 has the potential to impact upon cell adhesion processes and potentially with migration.

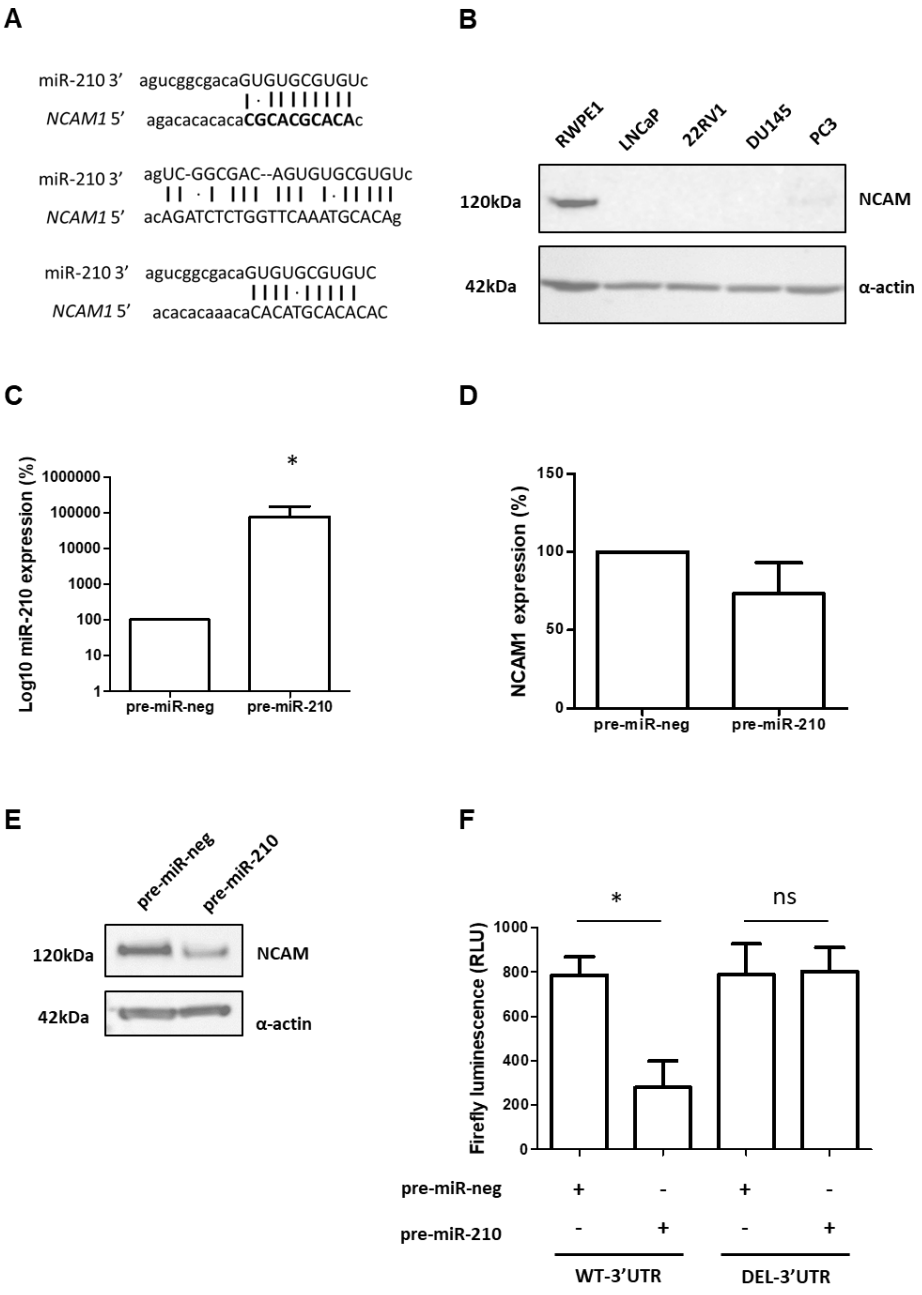

Figure 4. Neural cell adhesion molecule (NCAM) is a novel target of miR-210 in PCa. A) The seed region of miR-210 has three potential binding sites on the 3'UTR of NCAM, data from miRTarBase. **B)** Western blot analysis of NCAM in prostate cell lines reveals it is detectable in non-transformed RWPE-1 but not in the cancer cell lines LNCaP, 22RV1, or DU145, with small amount detected in PC3. **C)** Using RWPE-1, miR-210 was overexpressed artificially by transient transfection of precursor molecule (pre-miR-210) or the non-targeting negative control (pre-miR-neg). RT-qPCR analysis reveals successful transfection and overexpression of miR-210 in three biological replicates in RWPE-1. **D)** RT-qPCR analysis showing reduced NCAM levels in pre-miR-210 transfected cells relative to pre-miR-neg, in three biological replicates. **E)** Western blot showing reduced NCAM protein in pre-miR-210 transfected cells relative to pre-miR-neg, image representative of three biological replicates. **F)** Luciferase reporter assay showing that co-transfection of pre-miR-210, but not pre-miR-neg, silences expression of luciferase which has been cloned downstream of the intact but not deleted miR-210 binding region (top panel of A), mean of three biological replicates. One-way t-tests were used to compare condition means to the control (hypothetical value 100), two-way t-tests were used to compare two means, and p-values considered significant when *p<0.05, **p<0.01, ***p<0.001.

3. 2. V. MicroRNA-210 and NCAM expression is inversely correlated in prostate tissue

These experiments indicated that increased hypoxia in tumours induces miR-210 which in turn could decrease the levels of *NCAM1*. The Regulome Explorer and PRAD datasets were explored to investigate this relationship. Interestingly, there was a significant inverse correlation between miR-210 and *NCAM1* gene expression in the Regulome Explorer dataset (R=-0.34; -log10(p-value)=9.8; samples *n* = 330)(Figure 5A). Expression of *NCAM1* also showed a significant negative correlation with clinicopathological markers of prostate cancer progression in the Firebrowse dataset: Gleason score (R=-0.1282, adjusted p value (Q)=0.004215, samples *n*=497), and number of lymph nodes (R=-0.1282, adjusted p value (Q)=0.009714, samples *n*=406) (Figure 5B-C).

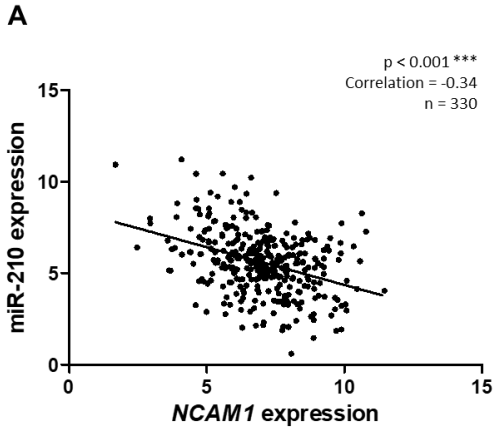

B

Clinical Feature	Samples *N*	Spearman's Correlation	p-value	Q-value
Gleason score	497	-0.1282	0.004215	0.0128
Number of lymph nodes with metastasis	406	-0.1282	0.009714	0.0531
Pathology T stage	490	-0.0414	0.3601	0.522
PSA value	440	-0.0211	0.6593	0.809

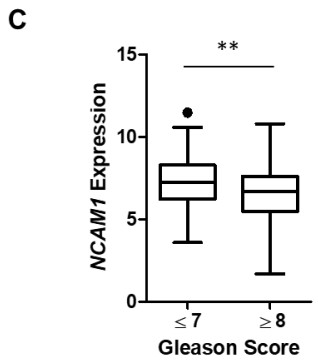

Figure 5. Evidence to support the regulation of NCAM by miR-210. A) Significant inverse association between gene expression levels of miR-210 and NCAM in sequencing data downloaded from Regulome Explorer. **B)** Significant correlation between *NCAM1* expression level and clinicopathological features of PCa as reported in Firebrowse data. **C)** Boxplot representation of the difference in mean *NCAM1* levels between patients with Gleason score ≤7 and ≥8 tumours, based on sequencing data downloaded from Regulome Explorer.

3. 2. VI. Phenotypic assays explore the effect of miR-210 overexpression on cell proliferation and migration

To assess the effect of miR-210 overexpression on cell behaviour *in vitro*, LNCaP, 22Rv1, PC3 and RWPE-1 cells were transfected pre-miR-210 or pre-miR-neg and phenotypic assays were used to examine the effect on cell behaviour. First, flow cytometry was employed to quantify the number of mitotic cells by propidium iodide staining, post-transfection with pre-miR-210, in the cell lines RWPE-1 and LNCaP (as described in Methods section *2.1.III.c.*). However, in both cell lines the cell cycle of pre-miR-210 transfected cells were equivalent to the control (Figure 6A-B).

Next, the transfected cells' ability to re-cover a scratch "wound" in the cell monolayer was monitored (Methods section *2.1.III.a.*). RWPE-1 cells were transfected and allowed to near confluence before a scratch in the cell layer was made using the tip of a pipette. The ability of the cells to cover the scratch was monitored for up to 96h. LNCaP were found to be unsuitable for this assay since they do not form a confluent monolayer but rather clusters across the plate and the scratches were inappropriate for measuring. There was no evident effect of miR-210 overexpression on the ability of RWPE-1 to cover over the scratch, and the speed at which pre-miR-210-transfected cells covered the scratch area was not significantly different from the negative control (Figure 6C-D). However, there was a striking difference in the morphology of the pre-miR-210 transfected cells. Numerous apoptotic cells can be observed, and the cells appeared slightly more fibroblastic, which was clear in all three technical replicates (1 representative image shown). The cells also did not become as confluent as the pre-miR-neg cells by the time of the scratch, indicating a slower growth rate in the first 24h post-transfection. Therefore, it may be that miR-210 exerts early effects on cell morphology and growth that cannot be captured by these assays.

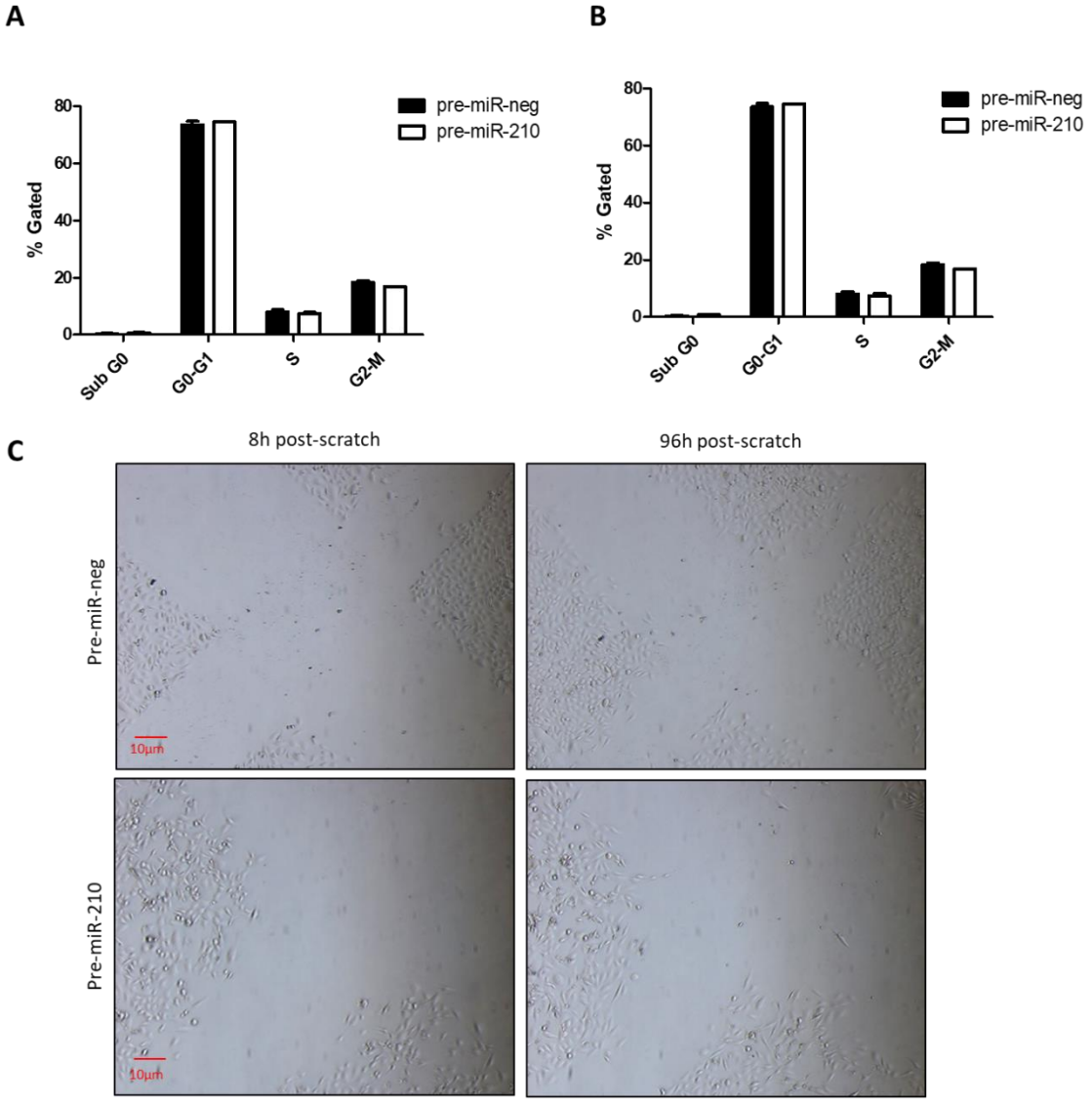

D

Replicate	Distance migrated	Time	Speed µm/h	Significance
Pre-miR-neg	20µm	88h	0.227	Two way t-test,
	35µm	88h	0.398	p=0.5993
	15µm	88h	0.170	
Pre-miR-210	20µm	88h	0.227	
	20µm	74h	0.270	
	10µm	40h	0.250	

Figure 6. Analysis of the cell cycle and scratch wound migration. A) Flow cytometry analysis of PI-stained RWPE-1, and **B)** LNCaP, showing no difference in the number of cells undergoing mitosis (G2/M) or growth arrest (G0) between pre-miR-210 and pre-miR-21 transfected cells, mean of two biological replicates shown. **C)** Scratch wound assay in RWPE-1 showing no evident difference in the rate of coverage between pre-miR-210 and pre-miR-neg transfected cells, although striking difference in cell morphology, representative image of 3 technical replicates. D) Two-way t-test used to compare mean speed of migration over 3 scratches (halted after 96h if scratch not already covered).

3. 2. Discussion

3. 2. I. Summary of findings

While extensive evidence has linked miR-210 expression with the hypoxic response in cancers such as breast cancer, there is little data available exploring its role in PCa, despite this being a tumour type with a high occurrence of hypoxia. This chapter presents novel data using three laboratory models of hypoxia, showing that hypoxia was consistently associated with miR-210 upregulation in a dose-dependent manner. That bicalutamide treatment was associated with increased hypoxia is in accordance with previous findings from our group, and this is the first study to show that miR-210 expression is expressed in correlation. Overall these experiments advocate miR-210 as a key mediator of the hypoxic response in PCa.

The analysis of 17 prostate tumour samples from a private in-house prostatectomy cohort as well as the independent TCGA datasets revealed that overexpression of miR-210 predicted Gleason grade and lymph node metastasis with strong statistical significance. This additionally associates miR-210 expression with tumour progression, and corroborates the deleterious effect of hypoxia in PCa. However, miR-210 expression was not consistently correlated with the incidence of cancer in our private cohort nor the TCGA repository, indicating that miR-210 could be a useful marker of hypoxia but not cancer incidence. This highlights the importance of measuring the hypoxic status of tumours when investigating miR-210 expression in cancers; numerous research groups have reported that miR-210 is overexpressed during cancer but it is unclear whether this reflects a driver mutation or is a result of hypoxia.

To understand better the functional role of miR-210, we explored the effect of miR-210 overexpression in several PCa cells lines and I show for the first time that miR-210 was capable of regulating neural cell adhesion molecule (NCAM) in PCa. I confirmed a binding site for miR-210 in its 3'UTR by luciferase reporter assay and *NCAM1* and miR-210 significantly inversely correlated in the TCGA cohort, which corroborates a regulatory relationship. NCAM is a large cell surface receptor from the immunoglobin superfamily. NCAM was chosen as a candidate target because it is involved in adhesion, cell: cell interactions and migration, and thus may be a tumour-suppressor. As the name suggests, the functions of NCAM have been mainly characterised in the context of neuroscience, it was highly expressed in neurons and glia, and during development it stimulated neurite outgrowth and dendritic branching and complexity (Sergaki and Ibáñez, 2017).

NCAM also has functions outside the CNS, although these have not been explored as extensively. It was detected on the surface of many haematopoieic cells (natural killer (NK) cells, gamma delta (γδ) T cells, activated CD8+ T cells, and plasmacytoid dendritic cells), where it is more frequently referred to as CD56. High levels of CD56 tend to indicate immune cell activation and cytotoxic capabilities, and NCAM was involved in immune surveillance and T cell expansion (Van Acker *et al*>, 2017). NK-derived exosomes contain NCAM, suggesting that it may be necessary for binding and to induce cell death in target cells (Van

Acker *et al.*, 2017). NCAM was detected in mesenchymal stromal cells of the bone marrow where it contributed to a favourable environment for haematopoietic stem cells (Prag *et al.*, 2002), and in some peripheral tissues such as skeletal myocytes where it facilitated the growth of neurons in muscles. The *NCAM1* gene was expressed by neuroendocrine cells (cells that respond to neurotransmitters and regulate endocrine secretions).

Three splice variants exist, giving rise to proteins of approximately 180 kDa, 140 kDa or 120 kDa and the downstream effects of its activation depend on the isoform present. Isoforms NCAM-180 and NCAM-140 are transmembrane proteins with long and short intracellular domains, respectively, whereas NCAM-120 lacks an intracellular domain and anchors extracellularly to the plasma membrane by a glycosylphosphatidylinositol. Interestingly, the NCAM isoforms have tissue- and temporal-specific differences in expression; typically, NCAM-140 and NCAM-180 predominate in embryonic tissues and NCAM-120 (which was detected in RWPE-1) predominates in adult tissues. Many neoplasms had detectable NCAM, including those of neuroendocrine origin (such as small cell lung carcinoma and pheochromocytoma), haematopoeic origin (myeloma, myeloid leukaemia, NK/T cell lymphomas), ovarian stromal tumours, tumours of brain (such as neuroblastoma and paraganglioma) pancreatic acinar cell carcinoma, nephroblastoma (Wilm's tumour), and Ewing's sarcomas of the bone (Van Acker *et al*>, 2017)(Prag *et al.*, 2002). Furthermore, NCAM staining could identify the origin of certain tumours, distinguishing between small cell and non-small cell lung carcinomas (Kontogianni *et al.*, 2005), and could differentiate subtypes of thyroid tumour (Golu *et al.*, 2017).

In some cancers NCAM-120 was replaced by NCAM-140 or NCAM-180 (Perl *et al*, 1999), which suggested that the cytoplasmic domain may have tumour-suppressive effects. The extracellular domain participates in both homophillic and heterophillic interactions (either on the same cell (*cis*) or an opposing cell (*trans*)). Notably, NCAM was a ligand for the fibroblast growth factor receptor (FGFR), such as on T cells (Kos and Chin, 2002)(Doherty and Walsh, 1996) and heterophillic *cis*-binding with FGFR was essential for FGF signalling in tumour-associated macrophages in oesophageal cancer (Takase *et al.*, 2016). The cytoplasmic domain of NCAM-140 activated the non-receptor tyrosine kinase $p59^{fyn}$ leading to sustained MAPK signalling in neurons (Beggs *et al.*, 1997)(Schmid *et al.*, 1999). However, NCAM-120 also activated intracellular signalling by interacting with other transmembrane proteins and creating functional membrane domains, and only NCAM-120 was able to *cis*-dimerise (Kulahin *et al.*, 2011). NCAM was considered a mesenchymal marker and in breast cancer cells, NCAM was upregulated by loss of E-cadherin during epithelial-mesenchymal-transition (Golu *et al.*, 2017) although this suggested an oncogenic association. Similarly, in melanoma NCAM-140 stimulated invasion by activating CAMP-dependent protein kinase and phosphatidylinositol 3-kinase pathways (Shi *et al.*, 2011). However, experiments using rat glioma cell lines showed that NCAM reduced motility *via* both the extracellular and cytoplasmic domains, activating $p59^{fyn}$ (intracellularly) and by binding a heparan sulfate proteoglycan (extracellularly) which

affected the cells' binding to the ECM (Prag *et al.*, 2002) and therefore may have tumour-suppressive associations in other cancer types. Moreover, in pancreatic and colorectal cancer, low levels of NCAM correlated with increased malignancy (Fogar *et al.*, 1997)(Roesler *et al.*, 1997) and in pancreatic β-cells, reduction of NCAM-120 was a rate-limiting step in metastatic dissemination (Perl *et al.*, 1999). In HuH28 cells (a liver carcinoma cell line), CD56 homophillic binding between CD56+ NK cells and the HuH28 cells inhibited NK-mediated cytosis, suggesting it was necessary for target recognition (Takasaki *et al.*, 2000).

Surprisingly, in PCa the role of NCAM has barely been investigated. The Protein Atlas Database reports that prostate tissue has low but detectable expression of *NCAM1* (Fagerberg *et al*., 2014), in accordance with my results. One subtype of prostate cancer (of neuroectoderm differentiation) stained positive for NCAM (Yamazaki *et al.*, 2012) but other than this study NCAM levels in PCa have not been studied. Here, I report for the first time that the cancer cell lines PC3, LNCaP and 22Rv1 do not express *NCAM* although it was detected in RWPE-1, suggesting that it may be present in the prostatic epithelium but is lost during carcinogenesis. Since miR-210 is expressed by many cell types and mediates cell: cell interactions, it could potentially downregulate targets such as NCAM in neighbouring cells producing a microenvironment conducive to tumour initiation and progression. This may allow PCa cells to evade CD56+ NK cells, FGFR+ T cells, or macrophages, to modulate immune subversion which is a critical step in tumorigenesis. Another hypothesis could be that the loss of homophillic NCAM binding between PCa cells increases their motility or de-differentiation, or affects their interaction with stromal cells. Therefore, by targeting NCAM it is likely that miR-210 can participate in the regulation of migration or cell : cell interactions in PCa. However, although there was an inverse association between miR-210 and *NCAM1* levels in the TCGA sequence data, this should be interpreted with caution as the sequencing was performed on whole tumour lysates, and we cannot rule out the possibility that this reflects a reduced number of infiltrating CD56+ immune cells, which was reported to occur during hypoxia (Jayaprakash *et al.*, 2018).

However, in these preliminary experiments, artificial overexpression of miR-210 in RWPE-1 did not increase the coverage of RWPE-1 cells over a scratch. This contrasts with the findings of another study which reported that miR-210 was capable of promoting migration, invasion and EMT in VCaP and C4-2B cells, although these authors utilised a boyden chamber assay method (Ren *et al*, 2017) which may be more sensitive, and perhaps these effects of miR-210 only occur in PCa cells. In hindsight I speculate that the scratch wound assay is generally insensitive to cell migration. Mainly, this is because the cells covering the scratch could simply be proliferating (aka, daughter cells of the cells from the leading edge). It seems unlikely that they would be migrating across the plate since there is no chemotaxic gradient as is used by the boyden chamber method. Furthermore, the creation of the scratch surely damages the cells at the leading edge, affecting their potential for migration/proliferation. Finally, in order to observe cells covering the scratch the cells must be almost confluent at the time of scratching. However, since they are transfected at approximately 30% confluency in order to grow and assume the effects of the transfection,

and this means that one must wait at least 4 days after transfection to create the scratch and another 4 days to monitor the scratch. This creates two issues: Firstly, the precursor molecules may be reduced in concentration by this point. Secondly, at the time of scratch the remainder of the plate is confluent meaning growth arrest and cell death are imminent (indeed many floating cells must be rinsed away before imaging) and apoptotic factors being released into the media may affect the behaviour of the cells at the leading edge.

Nevertheless, it was clear from the scratch wound images that cells with miR-210 overexpressed had striking changes in morphology, so it would be interesting to look for changes in the levels of epithelial/mesenchymal markers such as E-cadherin or N-cadherin, or apoptosis mediators in future studies. The flow cytometry experiments indicated no change in the cell cycle in pre-miR-210 transfected RWPE-1 nor LNCaP, however, I had observed during the hypoxic chamber experiments that hypoxic culture profoundly reduced LNCaP proliferation so perhaps a combination of HIF-1α induced factors are required to induce growth arrest and overexpression of miR-210 alone, while contributory, may be insufficient.

3. 2. II. Future directions

3. 2. II. a) Short-term

Since miRNAs are highly stable, it seems likely that high levels of miR-210 following hypoxia would persist long after re-oxygenation and degradation of HIF-1α (unless an active turnover process occurs as negative feedback). To explore this we could culture the cells at hypoxia for 24h and then return them to normoxic conditions and monitor the levels of miR-210 in the following hours or days and compare this with the stability of HIF-1α. This would have implications for the subsequent effect of acute hypoxia. Similarly, chronic hypoxia could be mimicked by culturing the cells at 0.5% oxygen for several days or weeks, to determine if miR-210 is involved in the chronic hypoxia response.

It is important to consider what exactly constitutes physiological oxygen levels (McKeown, 2014). Twenty percent is often used as the normoxic condition although in fact normoxic human tissues are between 3-5% O_2. It would be interesting to culture cells at 5% and use this as the normoxic conditions, to obtain a more realistic impression of miR-210 induction during tumour hypoxia. However, this would mean the cells were not paired samples from the same parental flask. It would also be interesting to investigate how rapidly miR-210 is upregulated, in hours rather than periods of 24h. However, the phenotypic assays that we use to investigate functionality commence 24h post-transfection so it seems logical to use a 24h time-point after commencing hypoxic culture. Similarly, future experiments could explore culturing cells at higher oxygen (*e.g*. 1% O_2) for longer time points to mimic chronic hypoxia.

Since miR-210 was induced by hypoxia and NCAM was reduced by miR-210 overexpression, it would be interesting to measure NCAM protein levels in RWPE-1 following hypoxia, to explore if it was reduced by hypoxia. However, the caveat of this experiment would be that 72h of culture is the standard length of

time between transfection with pre-miR-210 and cell harvesting, which is needed for protein turnover to observe clear differences between the conditions. My initial hypoxic experiments showed that cells were not viable after 72h at this oxygen level, and moreover they were inhibited from proliferating by hypoxia almost immediately. This means it is unlikely that NCAM levels would be noticeably reduced, however, we could experiment using chronic hypoxia (such as 1% O_2 for 72h) which may induce miR-210 and yet allow the cells to proliferate and survive longer periods.

As previously mentioned, we could quantify apoptosis signalling in RWPE-1 and LNCaP following 210 transfection by flow cytometry (quantifying Annexin V staining), by Tunel assay, or using Western blot to probe for cleaved caspase-3, as has been performed by other researchers (Bucur *et al.*, 2012). A suppressive effect of miR-210 on apoptosis would be interesting as it could indicate a mechanism through which hypoxia prevents ADT-induced apoptosis and facilitates survival.

3. 2. II. b) Medium-term

NCAM was detected at the protein level in non-transformed RWPE-1 but not in the cancer cell lines, which are cells harvested from metastatic sites and thus at the end stage of cancer development. It would be interesting to use immunohistochemistry to explore NCAM protein levels in human tumours compared with healthy prostate tissue of varying stages of progression, to determine if indeed it is lost during carcinogenesis. This would also allow us to see which cells NCAM is expressed in – epithelial cells or infiltrating immune cells. If there was an antibody available to detect NCAM by flow cytometry, we could use FACS to sort the cells expressing NCAM from fresh tumour lysate, and determine if they are epithelial cells or immune cells. We could also co-stain for NCAM plus in situ hybridisation of miR-210 on tissue sections to explore a potential inverse correlation, this would also confirm that miR-210 levels are stable in the cells and not being rapidly turned over which has been observed for some miRNAs (Guo *et al.*, 2015).

I consider the scratch wound assay insensitive to migration however it would be interesting to use a Boyden chamber method to explore migration and invasion potential of cells following overexpression of miR-210 (Falasca, Raimondi and Maffucci, 2011). Since the growth curves did not demonstrate an effect on proliferation, ki-67 staining could be used as a second indication (Scholzen and Gerdes, 2000).

I used an oxygen electrode probe to measure tumour hypoxia in the *in vivo* model, which was limited in that it only measures PO_2 at the region the probe enters and may not be representative of the total hypoxia of the tumour. There are numerous other ways to quantify hypoxia, such as staining with pimonidazole or PET imaging. Oxygen electrodes have long been considered the gold standard (Wals*h et al*>, 2014) but recent advances in technology mean that tumour hypoxia can be measured more accurately across the tumour by new devices based on PET imaging (Lopci *et al.*, 2014).

Interestingly, there is some evidence that miR-210 expression is regulated by DNA methylation of its promoter region. A study of schwannoma (tumour of the myelin sheath) found that the miR-210 promoter

region was hypermethylated in normoxia, and demethylated in hypoxia, and this demethylation was associated with enhanced proliferation, autophagy, and invasion (Wang *et al.*, 2017). Moreover, during helicobacter pylori infection increases DNA methylation of the miR-210 promoter which silences its expression and contributes to gastric disease (Kiga *et al.*, 2014). In neural progenitor cells, miR-210 expression was regulated by DNA methylation during both hypoxia and normoxia (Xiong *et al.*, 2012). Further methylation assays showed miR-210 expression correlated with DNA methylation during steroid-associated osteonecrosis of the femoral head (Yuan *et al.*, 2016). However, the regulation of miR-210 expression by DNA methylation has not been studied extensively and scarcely in the context of hypoxia.

3. 2. II. c) Long-term

Mass spectrometry could be used to quantify NCAM after transfection with pre-miR-210, since Western blot is not quantitative, and the mRNA level is not always an accurate representation of the efficacy of miRNA targeting. Alternatively, we could use immunohistochemistry (IHC) to probe for NCAM using a fluorescently labelled antibody, since it is a surface protein we may see a loss of extracellular NCAM after transfection or hypoxia without permeating the cells. If it was confirmed by IHC that NCAM is lost during prostate carcinogenesis, we could investigate if it has tumour suppressive function. To explore this, immunoprecipitation experiments could be used to pull it down and determine which proteins it is binding to in the basal state. Using fresh tissue samples may mean that we could determine if it was binding to receptors from other cell types such as immune or stromal cells. Mass spectrometry could be used to identify or quantify its binding partners. If there were potential binding partners in mind, Western blot could be used to detect them, or a yeast-two-hybrid assay (Maccarrone *et al.*, 2017)(Paiano *et al.*, 2019).

However, there is always the possibility that NCAM has no intrinsic tumour-suppressive effects and its loss during carcinogenesis is simple a result of the changing expression pattern of an upstream regulator or perhaps it is simply not required due to the changing behaviour of the cell. To test this, we could disrupt the function of NCAM and explore the effect in RWPE-1. NCAM-120 has no intracellular domain, and exerts its signalling effects by dimerising with other receptors; therefore siRNA could be used to silence expression or use point mutations by CRISPR-Cas9 to disrupt parts of the extracellular domain (Koch *et al.*, 2018).

If the previously mentioned FACS analysis showed that NCAM was expressed on tumour cells, we could purify the NCAM expressing cells from tumour lysates and sequence them, and compare them with cells not expressing NCAM and perform pathway analysis or functional enrichment to identify differential signalling. Similarly, transcriptomic effects of miR-210 could be explored by overexpression and RNA-seq.

Bicalutamide increased hypoxia and miR-210 expression, but the reason for this remains obscure. It would be interesting to use enzalutamide to determine if it similarly increases hypoxia. If so, it would be interesting to explore how AR inhibition increases hypoxia. Perhaps the loss of AR signalling, which is essentially a starvation of growth factors, induces a state of stress in the cell that somehow activates HIF-

1α as a means of slowing down cellular processes. Chromatin-immunoprecipitation (ChIP-seq) experiments (Chen, Bhadauria and Ma, 2018) could be useful to explore transcriptional targets of AR, perhaps focusing on HIF-1α regulators such as FIH or PHD.

Interrogation of publically available survival data using the KM plotter tool (http://kmplot.com/analysis/) revealed that when expression of miR-210 was dichotomised into "high" and "low", high expression was associated with reduced survival in several other cancer types: cervical squamous carcinoma, liver hepatocellular carcinoma, thyroid carcinoma, lung squamous cell carcinoma, pancreatic ductal adenocarcinoma, and sarcoma (Supplementary Figure 2)(data for PCa not provided)(Nagy *et al.*, 2018). The role of miR-210 and/or hypoxia in these cancer types could be a worthwhile avenue for further research.

3. 2. III. Summary

This is the first study to link miR-210 expression with hypoxia and bicalutamide treatment in PCa. We also suggest for the first time that NCAM, an important sensor and signal transducer, may be lost during PCa development and may be regulated by miR-210. Therefore, this study highlights a central role for miR-210 in the hypoxic response in PCa and its ability to modulate NCAM.

3. 3. Supplementary figures

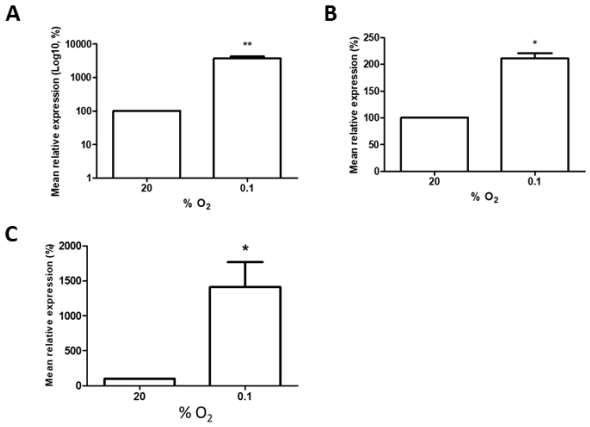

Supplementary Figure 1. MiR-210 expression in hypoxic 22Rv1, PC3 and RWPE1 cells. qRT-PCR analysis showed increased expression of miR-210 in 22Rv1, PC3 and RWPE1 cells exposed to hypoxia. **A)** 22Rv1 after 48h hypoxia**, B)** PC3 after 24h hypoxia, **C)** RWPE-1 after 48h hypoxia. Mean + SEM of three biological replicates shown (Student t-test p-values: *p<0.05, **p<0.01, ***p<0.001).

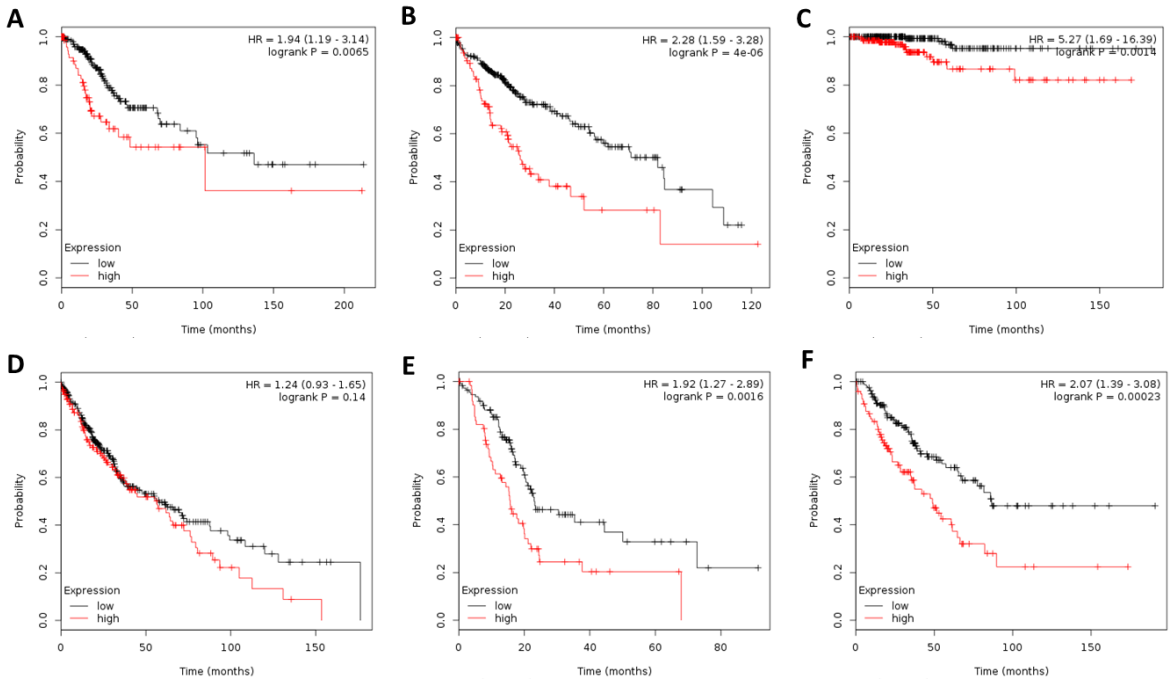

Supplementary Figure 2. High expression of miR-210 is associated with reduced survival. In **A)** Cervical squamous carcinoma, **B)** Liver hepatocellular carcinoma, **C)** Thyroid carcinoma, **D)** Lung squamous cell carcinoma, **E)** Pancreatic ductal adenocarcinoma, and **F)** sarcoma. Data for PCa not provided by this tool.

3. 4. Bibliography

Van Acker, H. H. *et al.* (2017) 'CD56 in the Immune System: More Than a Marker for Cytotoxicity?', *Frontiers in immunology*. Frontiers Media SA, 8, p. 892. doi: 10.3389/fimmu.2017.00892.

Andersen, S. *et al.* (2016) 'Fibroblast miR-210 overexpression is independently associated with clinical failure in Prostate Cancer – a multicenter (in situ hybridization) study', *Scientific Reports*. Nature Publishing Group, 6(1), p. 36573. doi: 10.1038/srep36573.

Bavelloni, A. *et al.* (2017) 'MiRNA-210: A Current Overview.', *Anticancer research*. International Institute of Anticancer Research, 37(12), pp. 6511–6521. doi: 10.21873/anticanres.12107.

Beggs, H. E. *et al.* (1997) 'NCAM140 interacts with the focal adhesion kinase p125(fak) and the SRC-related tyrosine kinase p59(fyn).', *The Journal of biological chemistry*, 272(13), pp. 8310–9.

Bucur, O. *et al.* (2012) 'Analysis of apoptosis methods recently used in Cancer Research and Cell Death & Disease publications.', *Cell death & disease*. Nature Publishing Group, 3(2), p. e263. doi: 10.1038/cddis.2012.2.

Byrne, N. M. *et al.* (2016) 'Androgen deprivation in LNCaP prostate tumour xenografts induces vascular changes and hypoxic stress, resulting in promotion of epithelial-to-mesenchymal transition', *British Journal of Cancer*, 114(6), pp. 659–668. doi: 10.1038/bjc.2016.29.

Camps, C. *et al.* (2008) 'hsa-miR-210 Is Induced by Hypoxia and Is an Independent Prognostic Factor in Breast Cancer', *Clinical Cancer Research*, 14(5), pp. 1340–1348. doi: 10.1158/1078-0432.CCR-07-1755.

Chen, X., Bhadauria, V. and Ma, B. (2018) 'ChIP-Seq: A Powerful Tool for Studying Protein-DNA Interactions in Plants', *Current Issues in Molecular Biology*, 27, pp. 171–180. doi: 10.21775/cimb.027.171.

Cheng, H. H. *et al.* (2013) 'Circulating microRNA Profiling Identifies a Subset of Metastatic Prostate Cancer Patients with Evidence of Cancer-Associated Hypoxia', *PLoS ONE*. Edited by R. Dahiya. Public Library of Science, 8(7), p. e69239. doi: 10.1371/journal.pone.0069239.

Chio, C.-C. *et al.* (2013) 'MicroRNA-210 targets antiapoptotic Bcl-2 expression and mediates hypoxia-induced apoptosis of neuroblastoma cells', *Archives of Toxicology*. Springer-Verlag, 87(3), pp. 459–468. doi: 10.1007/s00204-012-0965-5.

Dai, Y. *et al.* (2017) 'The TGF-β signalling negative regulator PICK1 represses prostate cancer metastasis to bone', *British Journal of Cancer*, 117(5), pp. 685–694. doi: 10.1038/bjc.2017.212.

Doherty, P. and Walsh, F. S. (1996) 'CAM-FGF Receptor Interactions: A Model for Axonal Growth', *Molecular and Cellular Neuroscience*. Academic Press, 8(2–3), pp. 99–111. doi: 10.1006/MCNE.1996.0049.

Eminaga, O. *et al.* (2018) 'The upregulation of hypoxia-related miRNA 210 in primary tumor of lymphogenic metastatic prostate cancer', *Epigenomics*. Future Medicine Ltd London, UK , 10(10), pp. 1347–1359. doi: 10.2217/epi-2017-0114.

Fagerberg, L. *et al.* (2014) 'Analysis of the Human Tissue-specific Expression by Genome-wide Integration of Transcriptomics and Antibody-based Proteomics', *Molecular & Cellular Proteomics*, 13(2), pp. 397–406. doi: 10.1074/mcp.M113.035600.

Falasca, M., Raimondi, C. and Maffucci, T. (2011) 'Boyden Chamber', in *Methods in molecular biology (Clifton, N.J.)*, pp. 87–95. doi: 10.1007/978-1-61779-207-6_7.

Fogar, P. *et al.* (1997) 'Neural cell adhesion molecule (N-CAM) in gastrointestinal neoplasias.', *Anticancer research*, 17(2B), pp. 1227–30.

Gan, L. *et al.* (2017) 'MiR-210 and miR-155 as potential diagnostic markers for pre-eclampsia pregnancies', *Medicine*. Wolters Kluwer Health, 96(28). doi: 10.1097/MD.0000000000007515.

Golu, I. *et al.* (2017) 'The absence of CD56 expression can differentiate papillary thyroid carcinoma from other thyroid lesions', *Indian Journal of Pathology and Microbiology*, 60(2), p. 161. doi: 10.4103/0377-4929.208378.

Guan, Y. *et al.* (2019) 'Effect of Hypoxia-Induced MicroRNA-210 Expression on Cardiovascular Disease and the Underlying Mechanism.', *Oxidative medicine and cellular longevity*. Hindawi Limited, 2019, p. 4727283. doi: 10.1155/2019/4727283.

Guo, Y. *et al.* (2015) 'Characterization of the mammalian miRNA turnover landscape.', *Nucleic acids research*. Oxford University Press, 43(4), pp. 2326–41. doi: 10.1093/nar/gkv057.

Jayaprakash, P. *et al.* (2018) 'Targeted hypoxia reduction restores T cell infiltration and sensitizes prostate cancer to immunotherapy', *Journal of Clinical Investigation*. doi: 10.1172/JCI96268.

Jiang, M. *et al.* (2018) 'Clinically Correlated MicroRNAs in the Diagnosis of Non-Small Cell Lung Cancer: A Systematic Review and Meta-Analysis.', *BioMed research international*. Hindawi Limited, 2018, p. 5930951. doi: 10.1155/2018/5930951.

Kiga, K. *et al.* (2014) 'Epigenetic silencing of miR-210 increases the proliferation of gastric epithelium during chronic Helicobacter pylori infection', *Nature Communications*, 5(1), p. 4497. doi: 10.1038/ncomms5497.

Koch, B. *et al.* (2018) 'Generation and validation of homozygous fluorescent knock-in cells using CRISPR–Cas9 genome editing', *Nature Protocols*. Nature Publishing Group, 13(6), pp. 1465–1487. doi: 10.1038/nprot.2018.042.

Kontogianni, K. *et al.* (2005) 'CD56: a useful tool for the diagnosis of small cell lung carcinomas on biopsies with extensive crush artefact.', *Journal of clinical pathology*. BMJ Publishing Group, 58(9), pp. 978–80. doi: 10.1136/jcp.2004.023044.

Kos, F. J. and Chin, C. S. (2002) 'Costimulation of T cell receptor-triggered IL-2 production by Jurkat T cells via fibroblast growth factor receptor 1 upon its engagement by CD56', *Immunology and Cell Biology*, 80(4), pp. 364–369. doi: 10.1046/j.1440-1711.2002.01098.x.

Kulahin, N. *et al.* (2011) 'Direct demonstration of NCAM cis-dimerization and inhibitory effect of palmitoylation using the BRET2 technique', *FEBS Letters*. No longer published by Elsevier, 585(1), pp. 58–64. doi: 10.1016/J.FEBSLET.2010.11.043.

Li, Y. *et al.* (2013) 'microRNA-210 as a prognostic factor in patients with breast cancer: Meta-analysis', *Cancer Biomarkers*, 13(6), pp. 471–481. doi: 10.3233/CBM-130385.

Lopci, E. *et al.* (2014) 'PET radiopharmaceuticals for imaging of tumor hypoxia: a review of the evidence.', *American journal of nuclear medicine and molecular imaging*. e-Century Publishing Corporation, 4(4), pp. 365–84.

Lynch, Seodhna M. *et al.* (2016) 'miR-24 regulates CDKN1B/p27 expression in prostate cancer', *The Prostate*, 76(7), pp. 637–648. doi: 10.1002/pros.23156.

Lynch, Seodhna M *et al.* (2016) 'Regulation of miR-200c and miR-141 by Methylation in Prostate Cancer.', *The Prostate*. United States, 76(13), pp. 1146–1159. doi: 10.1002/pros.23201.

Maccarrone, G. *et al.* (2017) 'Characterization of a Protein Interactome by Co-Immunoprecipitation and Shotgun Mass Spectrometry', in *Methods in molecular biology (Clifton, N.J.)*, pp. 223–234. doi: 10.1007/978-1-4939-6730-8_19.

Madhavan, D. *et al.* (2012) 'Circulating miRNAs as Surrogate Markers for Circulating Tumor Cells and Prognostic Markers in Metastatic Breast Cancer', *Clinical Cancer Research*, 18(21), pp. 5972–5982. doi: 10.1158/1078-0432.CCR-12-1407.

McKeown, S. R. (2014) 'Defining normoxia, physoxia and hypoxia in tumours - Implications for treatment response', *British Journal of Radiology*. British Institute of Radiology, p. 20130676. doi: 10.1259/bjr.20130676.

Moghaddam, A. S. *et al.* (2019) 'Cardioprotective microRNAs: Lessons from stem cell-derived exosomal microRNAs to treat cardiovascular disease', *Atherosclerosis*, 285, pp. 1–9. doi: 10.1016/j.atherosclerosis.2019.03.016.

Nagy, Á. *et al.* (2018) 'Validation of miRNA prognostic power in hepatocellular carcinoma using expression data of independent datasets', *Scientific Reports*, 8(1), p. 9227. doi: 10.1038/s41598-018-27521-y.

Nesbitt, H. *et al.* (2016) 'Targeting Hypoxic Prostate Tumors Using the Novel Hypoxia-Activated Prodrug OCT1002 Inhibits Expression of Genes Associated with Malignant Progression.', *Clinical cancer research : an official journal of the American Association for Cancer Research*. United States. doi: 10.1158/1078-0432.CCR-16-1361.

Paiano, A. *et al.* (2019) 'Yeast Two-Hybrid Assay to Identify Interacting Proteins', *Current Protocols in Protein Science*, 95(1), p. e70. doi: 10.1002/cpps.70.

Perl, A.-K. *et al.* (1999) 'Reduced expression of neural cell adhesion molecule induces metastatic dissemination of pancreatic β tumor cells', *Nature Medicine*. Nature Publishing Group, 5(3), pp. 286–291. doi: 10.1038/6502.

Petrozza, V. *et al.* (2017) 'Secreted miR-210-3p as non-invasive biomarker in clear cell renal cell carcinoma', *Oncotarget*, 8(41), pp. 69551–69558. doi: 10.18632/oncotarget.18449.

Prag, S. *et al.* (2002) 'NCAM regulates cell motility.', *Journal of cell science*, 115(Pt 2), pp. 283–92.

Puisségur, M.-P. *et al.* (2011) 'miR-210 is overexpressed in late stages of lung cancer and mediates mitochondrial alterations associated with modulation of HIF-1 activity.', *Cell death and differentiation*. Nature Publishing Group, 18(3), pp. 465–78. doi: 10.1038/cdd.2010.119.

Qin, Q., Furong, W. and Baosheng, L. (2014) 'Multiple functions of hypoxia-regulated miR-210 in cancer', *Journal of Experimental & Clinical Cancer Research*. BioMed Central, 33(1), p. 50. doi: 10.1186/1756-9966-33-50.

Qu, Y. and Huang, W. (2018) 'Effects of microRNA-210 on the diagnosis and treatment of prostate cancer', *Molecular Medicine Reports*, 18(2), pp. 1740–1744. doi: 10.3892/mmr.2018.9105.

Ren, D. *et al.* (2017) 'Oncogenic miR-210-3p promotes prostate cancer cell EMT and bone metastasis via NF-κB signaling pathway.', *Molecular cancer*. BioMed Central, 16(1), p. 117. doi: 10.1186/s12943-017-0688-6.

Roesler, J. *et al.* (1997) 'Tumor suppressor activity of neural cell adhesion molecule in colon carcinoma', *The American Journal of Surgery*. Elsevier, 174(3), pp. 251–257. doi: 10.1016/S0002-9610(97)00142-6.

Schmid, R. S. *et al.* (1999) 'NCAM stimulates the Ras-MAPK pathway and CREB phosphorylation in neuronal cells.', *Journal of neurobiology*, 38(4), pp. 542–58.

Scholzen, T. and Gerdes, J. (2000) 'The Ki-67 protein: From the known and the unknown', *Journal of Cellular Physiology*, 182(3), pp. 311–322. doi: 10.1002/(SICI)1097-4652(200003)182:3<311::AID-JCP1>3.0.CO;2-9.

Sergaki, M. C. and Ibáñez, C. F. (2017) 'GFRα1 Regulates Purkinje Cell Migration by Counteracting NCAM Function.', *Cell reports*. Elsevier, 18(2), pp. 367–379. doi: 10.1016/j.celrep.2016.12.039.

Shi, Y. *et al.* (2011) 'Neural cell adhesion molecule potentiates invasion and metastasis of melanoma cells through CAMP-dependent protein kinase and phosphatidylinositol 3-kinase pathways', *The International Journal of Biochemistry & Cell Biology*. Pergamon, 43(4), pp. 682–690. doi: 10.1016/J.BIOCEL.2011.01.016.

Szadvari, I., Krizanova, O. and Babula, P. (2016) 'Athymic Nude Mice as an Experimental Model for Cancer Treatment Cancer diseases and their treatment', *Physiol. Res*, 65, pp. 441–453.

Taddei, M. L. *et al.* (2014) 'Senescent stroma promotes prostate cancer progression: the role of miR-210.', *Molecular oncology*. Wiley-Blackwell, 8(8), pp. 1729–46. doi: 10.1016/j.molonc.2014.07.009.

Takasaki, S. *et al.* (2000) 'CD56 DIRECTLY INTERACTS IN THE PROCESS OF NCAM-POSITIVE TARGET CELL-KILLING BY NK CELLS', *Cell Biology International*, 24(2), pp. 101–108. doi: 10.1006/cbir.1999.0457.

Takase, N. *et al.* (2016) 'NCAM- and FGF-2-mediated FGFR1 signaling in the tumor microenvironment of esophageal cancer regulates the survival and migration of tumor-associated macrophages and cancer cells', *Cancer Letters*, 380(1), pp. 47–58. doi: 10.1016/j.canlet.2016.06.009.

Tang, T. *et al.* (2018) 'Up-regulation of miR-210 induced by a hypoxic microenvironment promotes breast cancer stem cells metastasis, proliferation, and self-renewal by targeting E-cadherin', *The FASEB Journal*, p. fj.201801013R. doi: 10.1096/fj.201801013R.

Walsh, J. C. *et al.* (2014) 'The clinical importance of assessing tumor hypoxia: relationship of tumor hypoxia to prognosis and therapeutic opportunities.', *Antioxidants & redox signaling*. Mary Ann Liebert, Inc., 21(10), pp. 1516–54. doi: 10.1089/ars.2013.5378.

Wang, Z. *et al.* (2017) 'Hypoxia-induced miR-210 promoter demethylation enhances proliferation, autophagy and angiogenesis of schwannoma cells', *Oncology Reports*, 37(5), pp. 3010–3018. doi: 10.3892/or.2017.5511.

Xiong, L. *et al.* (2012) 'DNA demethylation regulates the expression of miR-210 in neural progenitor cells subjected to hypoxia', *FEBS Journal*, 279(23), pp. 4318–4326. doi: 10.1111/febs.12021.

Yamazaki, H. *et al.* (2012) 'Prostatic stromal sarcoma with neuroectodermal differentiation', *Diagnostic Pathology*, 7(1), p. 173. doi: 10.1186/1746-1596-7-173.

Yang, X. *et al.* (2017) 'MiR-210-3p inhibits the tumor growth and metastasis of bladder cancer via targeting fibroblast growth factor receptor-like 1.', *American journal of cancer research*. e-Century Publishing Corporation, 7(8), pp. 1738–1753.

Yuan, H. *et al.* (2016) 'Involvement of MicroRNA-210 Demethylation in Steroid-associated Osteonecrosis of the Femoral Head', *Scientific Reports*, 6(1), p. 20046. doi: 10.1038/srep20046.

Zhou, H. *et al.* (2018) 'Attenuation of TGFBR2 expression and tumour progression in prostate cancer involve diverse hypoxia-regulated pathways', *Journal of Experimental & Clinical Cancer Research*, 37(1), p. 89. doi: 10.1186/s13046-018-0764-9.

Chapter 4. The Oncogenic MicroRNA-21 is Induced by Hypoxia in Prostate Cancer and Increases Prostate Cell Migration and Clonogenicity

4. 1. Introduction

Chapter 3 evaluated the relevance of hypoxia-associated miR-210 in PCa. Conversely, this chapter investigates hsa-miR-21-5p (miR-21), which has been attributed oncogenic effects in many cancer settings but scarcely investigated in PCa hypoxia.

MiR-21 expression correlates with cancer incidence in numerous tissue types including in the lung, colon, breast, pancreas and the stomach (Sha *et al*, 2015; Tao *et al*, 2015; Chen *et al*, 2016; Gao *et al*, 2016; He *et al*, 2016; Wu *et al*, 2016; Yan *et al*, 2016; Zheng *et al*, 2018). Furthermore, screenings of cancer patients consistently implicate miR-21 as a marker advanced forms of the tumour, in prostate, breast, pancreatic, and colon cancer (Anwar *et al*, 2019; Bahreyni *et al*, 2019a; Kurul *et al*, 2019; Vila-Navarro *et al*, 2019). Many *in vitro* studies have explored the phenotypic effects of miR-21 expression that may explain these associations, to the extent that reviews assessing its role in colorectal cancer, cervical cancer, and lung cancer have concluded that it has an oncogenic effect when overexpressed in cancer (Bahreyni *et al.*, 2019b)(Wang *et al.*, 2019)(Bica-Pop *et al.*, 2018). This places miR-21 as one of the most prominent "oncomiRs" in cancer research, and many studies have investigated it in the context of PCa. However, the majority of these studies were investigations into differentially expressed miRNAs in the tissue, blood, or urine of PCa patients compared to controls (or high-grade PCa compared with low-grade), concluding that miR-21 was a robust biomarker of disease status (Zhou and Zhu, 2019). The majority of PCa based studies did not investigate the functionality of miR-21, aside from validating its mRNA target interactions. These showed that many tumour suppressors were regulated by miR-21 either using qPCR or western blot approaches and in some instances by reporter assay. MiR-21 regulated Myristoylated Alanine-Rich protein Kinase C Substrate (MARCKS) which facilitates apoptosis and invasion (Li *et al.*, 2009a); Bone Morphogenetic Protein Receptor II (BMPRII) which may indicate a regulation of bone metastasis (Qin *et al.*, 2009); metalloproteinase (MMP) inhibitor RECK (Reis *et al.*, 2012)(Leite *et al.*, 2015); TGFβR2 the immune signalling mediator (S Mishra *et al.*, 2014); p57Kip2 which regulates the cell cycle (Sweta Mishra *et al.*, 2014); and RNA Binding Protein with Multiple Splicing (RBPMS), Regulator of Chromosome Condensation and POZ Domain Containing Protein 1 (RCBTB1), and Zinc Finger protein 608 (ZNF608) which were mediators of cisplatin resistance (Báez-Vega *et al.*, 2016), and programmed cell death 4 (PDCD4) and PTEN which are important tumour suppressors in PCa (Lu *et al.*, 2008)(Feng and Tsao, 2016).

A few studies have performed phenotypic assays to assess the effect of miR-21 overexpression or inhibition on cell functionality. One group transfected PC3 cells with inhibitors of miR-21-3p and miR-21-5p and observed reduction in colony formation in agar (Báez-Vega *et al*, 2016), another group similarly reported that the miR-21-5p inhibitor reduced the motility and increased sensitivity to apoptosis of DU145 and PC3, although proliferation was not affected (Li *et al.*, 2009b). In another small study, miR-21 transfection was associated with increased cell viability (Yang, Guo and Shao, 2017). Furthermore, in PCa cell lines miR-21 was upregulated by the androgen receptor and contributed to androgen-independence (Ribas *et al.*,

2009)(Guan *et al.*, 2019), it upregulated AKT, ERK and HIF-1a signalling (L.-Z. Liu *et al.*, 2011), and it was upregulated in docetaxel-resistance PCa cells (Shi *et al.*, 2010). However, another group treated PC3 and DU145 with miR-21 inhibitors and observed no effect on cell proliferation, radioresistance, nor an effect on PTEN and PDCD4; they concluded that miR-21 is not prominent in the carcinogensis of PCa (Folini *et al.*, 2010). Therefore, reports on its role in PCa have been mixed.

Interestingly, there is evidence from other tissue types that miR-21 is involved in the hypoxic response. The pri-miR-21 promoter has a HIF-binding site (Kulshreshtha *et al*., 2007) and early research demonstrated that its expression was deregulated in pulmonary arterial hypertension (caused by abnormal vasculature) following ischaemia and reperfusion injury (Xu *et al.*, 2014; Bienertova-Vasku, Novak and Vasku, 2015). This indicated that miR-21 responds to cellular oxygen levels and that it exerts control over vascularisation as well as inflammation. It was upregulated early in both the inflammatory and hypoxic responses and regulated a wide range of pathways to protect cell integrity and restore homeostasis during such fluctuations. For instance, it was upregulated by the drug gastrodin, thus revealing a mechanism through which gastrodin protects pulmonary tissue from hypoxic injury following myocardial infarction (Xing and Li, 2019). MiR-21 expression prevented hypoxia- and glucose deprivation-induced apoptosis in human neural stem cells by inhibiting JNK and p38 MAPK signalling (Chen *et al.*, 2019). Similarly, it mediated the protective effect of loperamide, a μ-opioid receptor agonist that protects against myocardial ischemia/reperfusion injury in cardiomyocytes (Shen *et al.*, 2019). Based on this it was proposed that miR-21 expression by cancer cells upon chemotherapy could promote survival and mediate chemoresistance and indeed, miR-21 expression has been associated with resistance to radiation therapy and cisplatin (Jiang *et al.*, 2016; Dong *et al.*, 2019).

However, in PCa an involvement of miR-21 in the hypoxic response has not been confirmed. One study investigated the effect of a curcumin-derived synthetic analogue called CDF on PCa cells, and measured the effect of CDF on attenuating the expression of hypoxia-associated genes. One of their initial assays included measuring the expression of miR-21 after culture at 1% oxygen although the duration of culture was not stated (Ba*o et al*., 2012). Therefore, the regulation of miR-21 by hypoxia in PCa warrants further investigation.

In summary, miR-21 has been studied in several cancers, and is generally accepted to have an oncogenic role, and it has been strongly promoted as a diagnostic marker in PCa although its effects in PCa cells are unclear. Furthermore, a link with PCa hypoxia remains understudied. Several mRNA targets of miR-21 have been identified in PCa although there is scope to discover further novel targets and/or mechanisms of action, particularly in relation to those that might be involved in the hypoxic response.

The hypothesis of this chapter was that miR-21 would be induced by hypoxia in PCa and would produce oncogenic effects when overexpressed in PCa cells.

4. 2. Results

4. 2. I MicroRNA-21 is regulated by hypoxia in vitro and in vivo

The three models of hypoxia were used: hypoxic chamber culture at 0.1% O_2 relative to 20% O_2, LNCaP spheroid culture, and bicalutamide-induced hypoxia in vivo (as described in chapter 3). MiR-21 was upregulated by hypoxia in a dose-dependent fashion in all three models, albeit not always significantly due to variation between replicates (Figure 1). As with miR-210, the *in vivo* analysis suggested miR-21 was most strongly upregulated by day 28 in the tumours of bicalutamide-treated mice relative to vehicle-treated mice. This suggested that hypoxia was further established by day 28 and that hypoxia-associated miRNAs accumulated by this time-point. Interestingly, we were able to detect miR-21 in the serum samples of the mice, even using such low volumes that none of the other miRNAs that were investigated could be detected including the housekeeping miR-191. This indicated that miR-21 is highly abundant in serum which lends further weight to the suggestions that is could be a useful diagnostic marker. Unlike miR-210, miR-21 was further upregulated between day 7 and day 28 in the serum suggesting it may be actively exported in correlation with hypoxia.

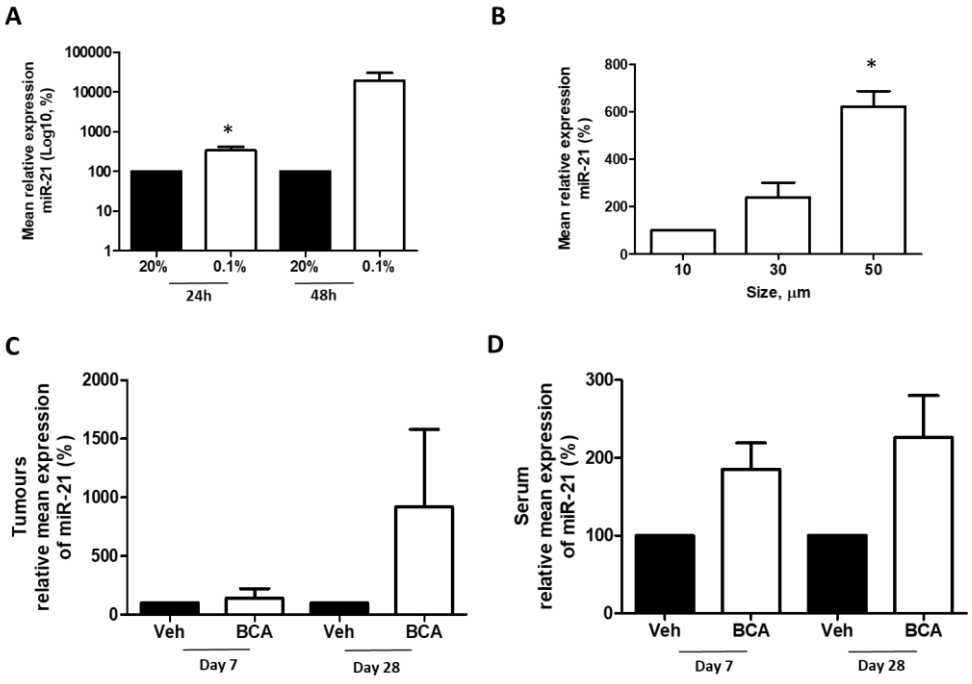

Figure 1. miR-21 is increased by hypoxia *in vitro* and *in vivo*. A) RT-qPCR analysis showing miR-21 expression increases in a dose-dependent fashion with hypoxia following hypoxic chamber culture of LNCaP. Mean + SEM of three biological replicates. **B)** RT-qPCR analysis showing miR-21 expression in LNCaP spheroids increased at 30µm and 50µm relative to 10µm. Mean + SEM of three biological replicates shown. **C)** RT-qPCR demonstrates increased expression of miR-21 in the tumours, and **D)** serum, of bicalutamide-treated mice relative to vehicle-treated mice at day 7 and day 28 of treatment. The mean + SEM is shown, groups contained at least 4 mice. One-way t-tests were used to compare condition means to the control (hypothetical value 100) and p-values considered significant when *p<0.05, **p<0.01, ***p<0.001.

4. 2. II MicroRNA-21 expression in 19 prostatectomy samples

Next, the clinical relevance of miR-21 expression was investigated by measuring its expression in our in-house bank of human prostatectomy samples, as described in Chapter 3. Since miR-210 is an established indicator of hypoxia, including in PCa as demonstrated in Chapter 3, we wanted to confirm that miR-21 expression correlated positively with miR-210 in both the in-house prostatectomy cohort and the TCGA prostate samples. MiR-21 expression significantly correlated with miR-210 expression which corroborated the regulation of miR-21 expression by hypoxia (Figure 2A). As was the case with miR-210, the prostatectomy samples did not display uniform upregulation of miR-21 relative to the paired non-tumour tissue, which would indicate upregulation in the cancer state (Figure 2B), however there was a mild trend of increasing miR-21 level in tumours of the higher Gleason grade group (Figure 2C).

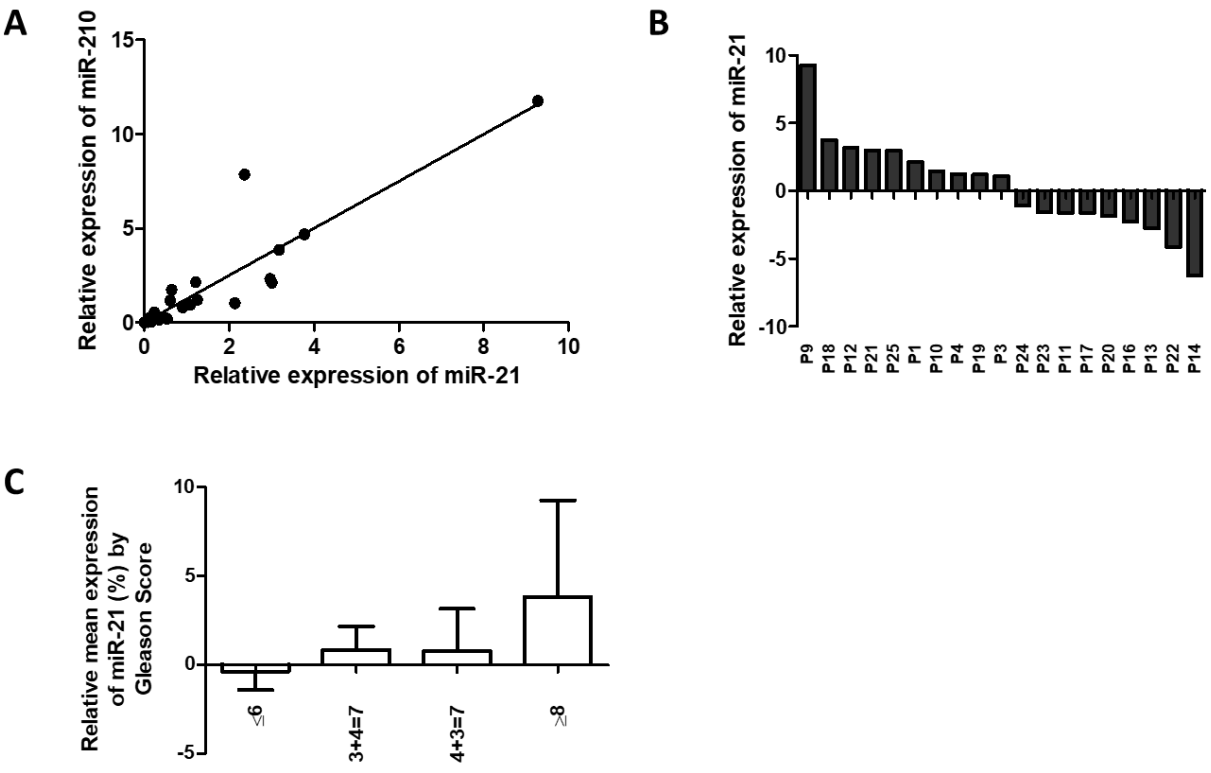

Figure 2. Expression of miR-21 correlates with hypoxic marker miR-210 and Gleason grade group in human prostatectomy samples (*n*=19). **A)** RT-qPCR analysis demonstrating significant correlation between miR-21 and miR-210 in prostatectomy samples (Pearson correlation, R=0.9006, p<0.001). **B)** RT-qPCR measurement of miR-21 levels across prostatectomy samples. **C)** RT-qPCR analysis revealed slight correlation (ns) between miR-21 expression level and Gleason grade group; groups contained at least 2 patient samples. P-values considered significant when *p<0.05, **p<0.01, ***p<0.001.

4. 2. III. MicroRNA-21 expression in the TCGA datasets

The Cancer Genome Atlas database was then analysed (n=330), using the Regulome Explorer tool (TCGA Research Network, 2015). In this data there was significant positive correlation between expression of miR-21 and miR-210 (Figure 3A). Furthermore, miR-21 expression was significantly increased in the highest Gleason grade tumours, it significantly correlated with an increased number of lymph nodes positive for PCa, and was significantly increased in the tumours that did not go into complete remission (suggesting an inherently more aggressive tumour or less susceptibility to treatment).

Analysis of the Firebrowse dataset Prostate Adenocarcinoma (PRAD) similarly revealed miR-21 expression significantly associated with Gleason score, number of positive lymph nodes, and pathological T stage (Figure 3C-F)(Broad Institute TCGA Centre, 2016). Since miR-21 was readily detected from extremely small amounts of tissues during the initial in vitro experiments, the expression levels of miR-21 and miR-210 in TCGA cohort were compared and indeed miR-21 was expressed at much higher levels, highlighting its potential value as a biomarker (Figure 3B).

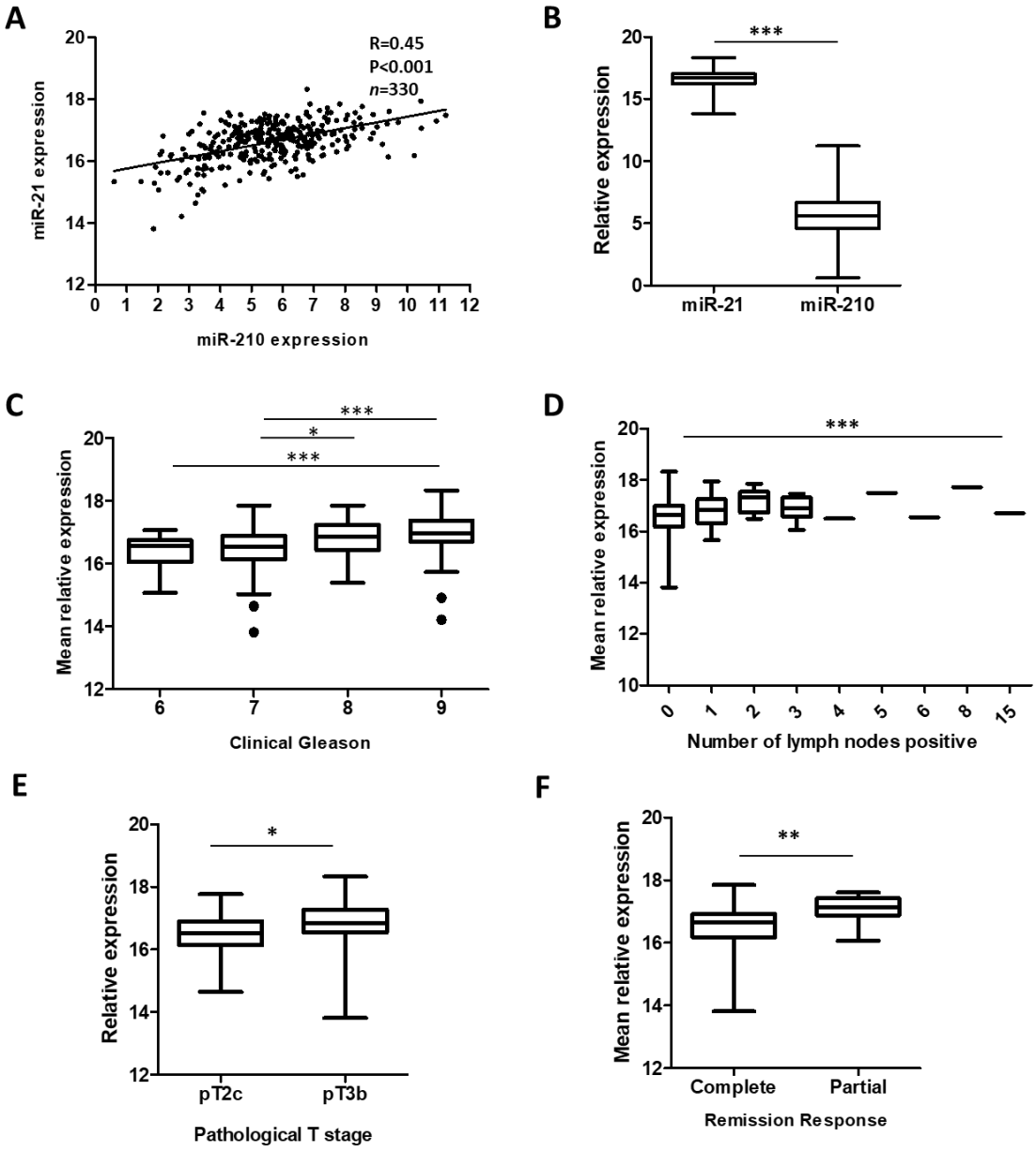

G

miR-21

CLINICAL FEATURE	No. of samples	Spearman's Correlation	p-value	Q-value
GLEASON SCORE	494	0.3534	5.61E-16	6.58E-14
NUMBER OF LYMPH NODES	404	0.2491	3.95E-07	9.25E-05
PATHOLOGY T STAGE	487	0.197	1.19E-05	0.000233
PSA VALUE	439	0.0634	0.1846	0.589

Figure 3. Expression of miR-21 correlated significantly with miR-210 and parameters of tumour aggressiveness in human prostate biopsy samples. Data from the from The Cancer Genome Atlas project was accessed using the Regulome Explorer tool (*n*=330) and the Firebrowse PRAD dataset (n=>400). Regulome Expolorer analysis reveals **A)** Significant correlation between expression of hypoxic miR-210 and miR-21 (Pearson correlation, p<0.001). **B)** MiR-21 levels significantly more abundant than miR-210 levels (Mann Whitney test p<0.0001). Significantly higher miR-21 expression positively associated with **C)** Gleason score (one way ANOVA, p<0.001), **D)** number of lymph nodes positive for PCa (one way ANOVA, p<0.001), **E)** pT3b tumours compared with pT2c, and **F)** in patients with partial remission compared with complete remission response (Mann Whitney test, p<0.001). **G)** In the Firebrowse PRAD dataset, miR-21 expression correlated with Gleason score, number of positive lymph nodes, and pathological T stage. P-values considered significant when *p<0.05, **p<0.01, ***p<0.001.

4. 2. V. Investigating the functionality of miR-21

These findings suggested that miR-21 appears to be a hypoxia-regulated miRNA that is overexpressed in aggressive PCa. To examine its oncogenic effects, transient transfection was used to overexpress miR-21 in cell lines and phenotypic assays were used to evaluate the resultant changes in cell behaviour. First, the basal expression of miR-21 in the prostate cell lines was compared to determine which cell lines would be suitable for overexpression. Interestingly, miR-21 was expressed at a lower level in the cancer cell lines relative to the non-cancer transformed RWPE-1 (Figure 4A), with the exception of DU145 in which expression was hugely upregulated (Figure 4B). This could suggest that in these cell lines miR-21 is not a constitutively overexpressed driver of the disease. Potentially however, its induction by hypoxia could promote cancer advancement. It was concluded that either LNCaP, PC3 or 22Rv1 could make suitable models for overexpressing miR-21 and exploring its effect on cancer cell function.

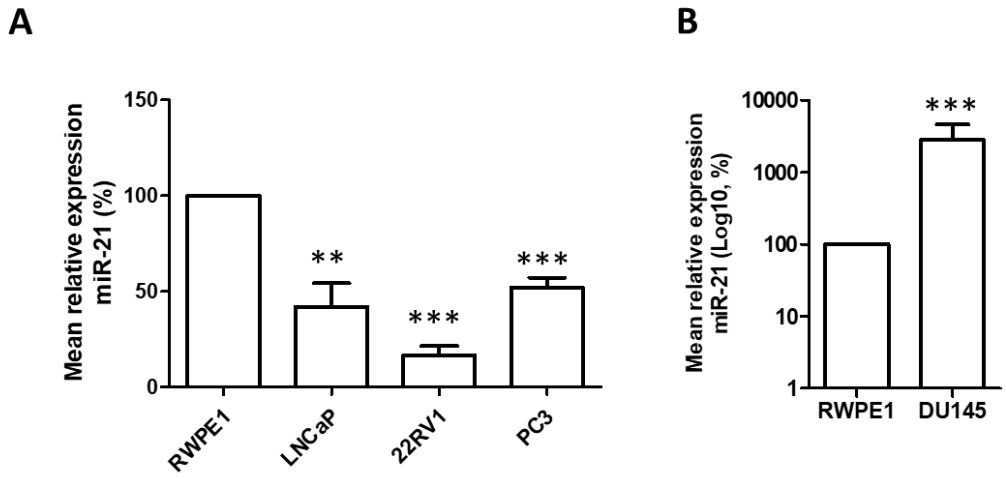

Figure 4. Establishing expression level of miR-21 in the prostate cell lines. Mean + SEM of three biological replicates shown. **A)** miR-21 levels are reduced in PCa cell lines compared with RWPE-1. **B)** Vastly increased expression level of miR-21 in DU145 compared with RWPE-1. One-way t-tests were used to compare condition means to the control (hypothetical value 100) and p-values considered significant when *p<0.05, **p<0.01, ***p<0.001.

4.2.V.a. The effect of miR-21 overexpression on proliferation

Since there were conflicting reports in the literature regarding the effect of miR-21 on PCa proliferation, XTT cell proliferation/viability assays were performed following transfection with pre-miR-21. The assay utilises the tetrazolium salt XTT, which is broken down to formazan indirectly due to the activity of mitochondrial enzymes. Formazan has a higher absorbance of light at wavelengths of around 495nm, and thus cell viability can be determined by comparing the absorbance across the transfection conditions. As described in Methods section *2.1.III.b.*, cells were transfected with either pre-miR-21 (two transfection replicates) or controls (untreated, lipofectamine alone "mock", or non-targeting pre-miR-neg). After 24h the transfected cells were trypsinised, counted and re-seeded at 500 cells per well of a 96-well plate, with a plate for each timepoint and 8 technical replicates per sample per plate. The results indicated that there was no consistent effect of miR-21 overexpression on the growth curves (Figure 5A-C).

A flow cytometry based analysis was then employed, which involved staining the transfected cells with propidium iodide (a nucleic acid stain) that allows quantification of genetic material and so estimation of cell cycle stage (see Methods section *2.1.III.c.*). Similarly, no difference was observed in the pre-miR-21 transfected cells compared to the controls (Figure 5D). This assay suggested that miR-21 overexpression did not influence cell proliferation.

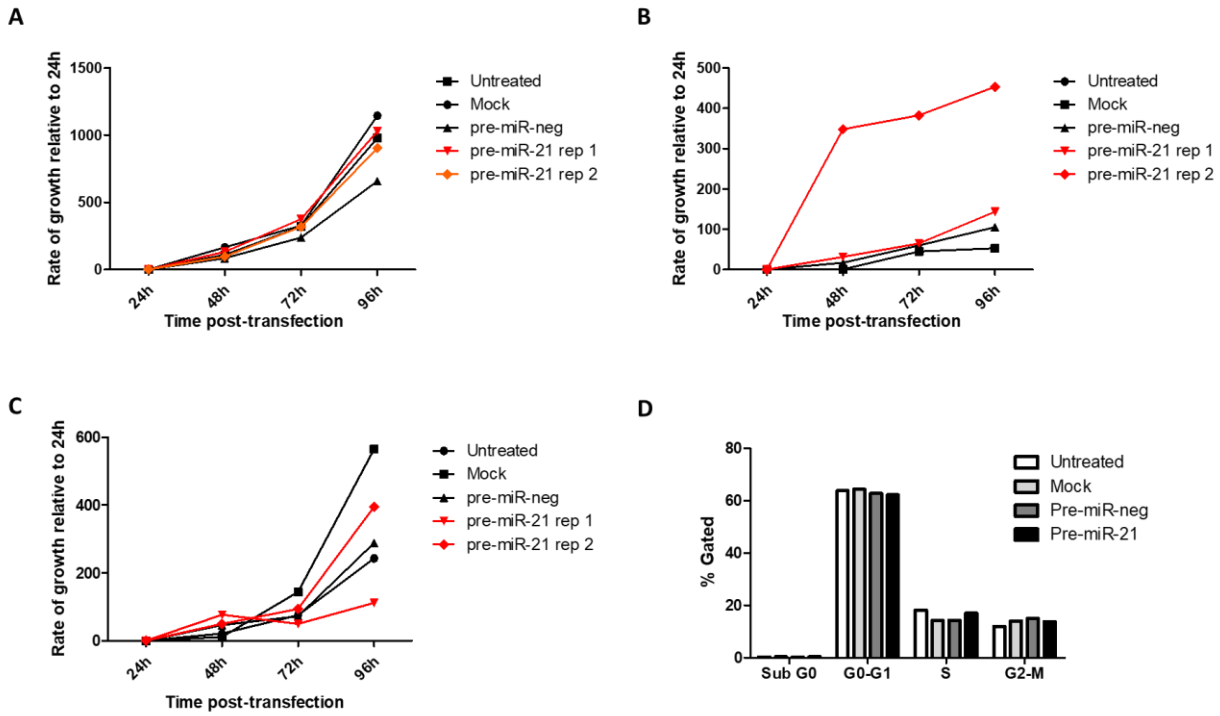

Figure 5. Investigation of the effect of miR-21 on cell proliferation. XTT assays of one biological replicate, two technical replicates of pre-miR-21 in **A)** RWPE-1, **B)** 22Rv1, and **C)** PC3, all showing no consistent influence of the transfection of pre-miR-21 on cell proliferation. Negative controls: untreated, lipofectamine alone (Mock), non-targeting and pre-miR-neg. **D)** Flow cytometry quantification of RWPE-1 cells showing no difference in the proportion of cells in each stage of the cell cycle following transfection with pre-miR-21 or controls. One biological replicate.

4.2.V.b. The effect of miR-21 overexpression on colony forming ability

As mentioned in the introduction (section *4.1*) previous research had suggested that miR-21 inhibitors reduced colony formation on agar (Báez-Vega *et al*., 2016). To complement this, the effect of miR-21 expression on the colony forming ability of RWPE-1, 22Rv1 and PC3 was assessed (described in Methods section *2.1.III.d.*). Briefly, the cells were transfected and 24h following transfection were counted and re-seeded at very low densities (optimised to be 750 or 1,000 cell per well of a 6-well plate). After 7 days, the cells were stained with crystal violet to evaluate cells' ability to survive at such low confluence. Interestingly, in all cell lines and at multiple seeding densities, transfection with pre-miR-21 increased the number of cell colonies that were present 1 week after seeding. The effect was most evident in RWPE-1 (Figure 6), to some extent in 22Rv1 (Figure 7) and least so in PC3 (Figure 8). The appearance of the colonies also differed, some colonies were larger following miR-21 overexpression indicating faster growth. The crystal violet was extracted using 1% SDS and quantified by measuring the absorbance at 595nm on a spectrophotometer; the rate of change in crystal violet concentration was determined in pre-miR-21 treated cells relative to pre-miR-neg treated cells in order to combine the results from all replicates (which had involved various seeding densities during optimisation). The crystal violet concentrations reflected the appearance of the plates.

Therefore, while an effect of miR-21 on proliferation was not isolated, it appeared to promote survival in multiple cell lines as assessed by the colony forming assay.

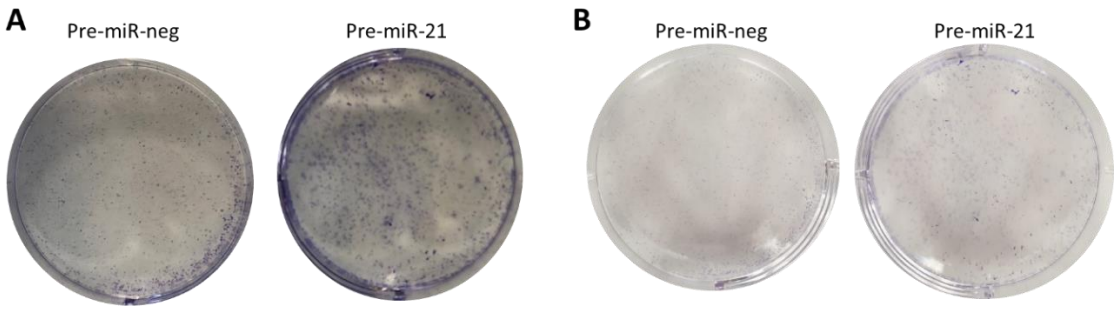

Figure 6. Colony forming assay in RWPE-1. Two biological replicates. **A)** 1,000 cells seeded. **B)** 750 cells seeded.

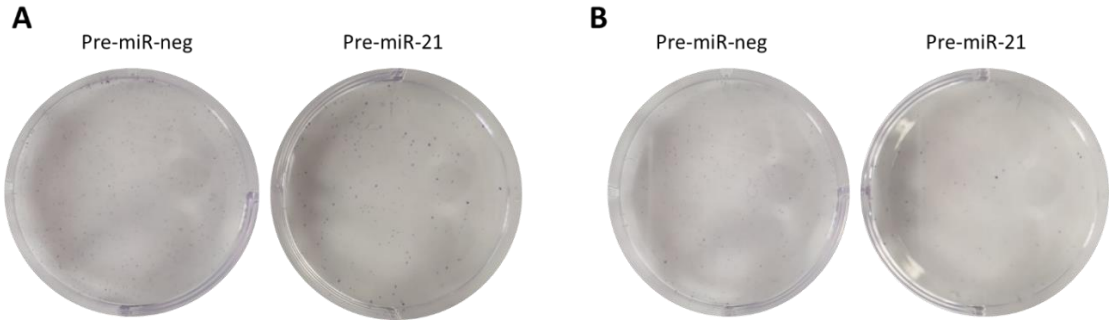

Figure 7. Colony forming assay in 22Rv1. One biological replicate. **A)** 1,000 cells seeded. **B)** 750 cells seeded.

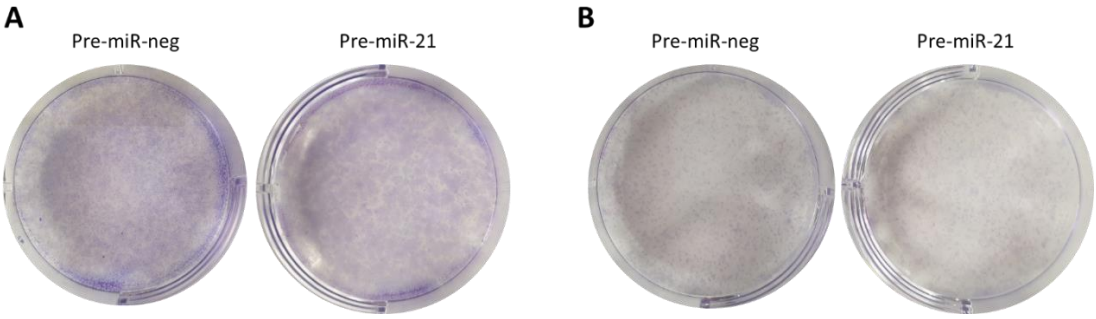

Figure 8. Colony forming assay in PC3. One biological replicate. **A)** 1,000 cells seeded. **B)** 750 cells seeded.

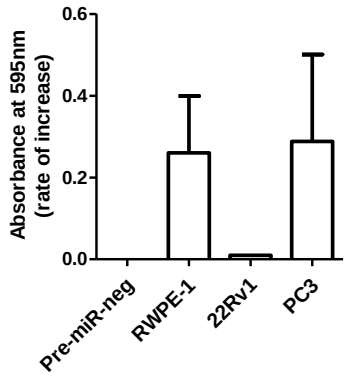

Figure 9. Rate of increase in the concentration of crystal violet in pre-miR-21 treated cells compared with pre-miR-neg treated cells. Crystal violet quantified using 1% SDS and absorbance at 595nm recorded using spectrophotometer. Rate calculated as (absorbance of condition – absorbance of control)/ absorbance of control.

4.2.V.c. The effect of miR-21 overexpression on migration

Another feature of cancer cells is increased motility and migration. To explore the effect of miR-21 on this process an electrode-monitored Boyden chamber assay was utilised (xCELLigence CIM16 system, ACEA bio). Since the greatest effect on colony forming assay was apparent in RWPE-1, this cell line was used. As described in Methods section *2.1.III.e.*,The cells were transfected, and after 24h were re-counted and seeded at 30,000 cells per well into the upper chamber in serum-free media, with complete media in the lower media. Three technical replicates were seeded per biological replicate, with serum-free lower chambers used to assess background migration in the absence of chemoattractant. Cell migration towards the serum-containing media was monitored (by electrical impedance as cells crossed the copper pore membrane dividing the chambers) for 120h post-transfection. Interestingly, the miR-21 overexpressing cells had increased ability to migrate across the membrane, the difference between cell migration of pre-miR-21 transfected cells and untreated cells was statistically significant although the difference between the pre-miR-21 and pre-miR-neg conditions did not reach significance (Figure 9).

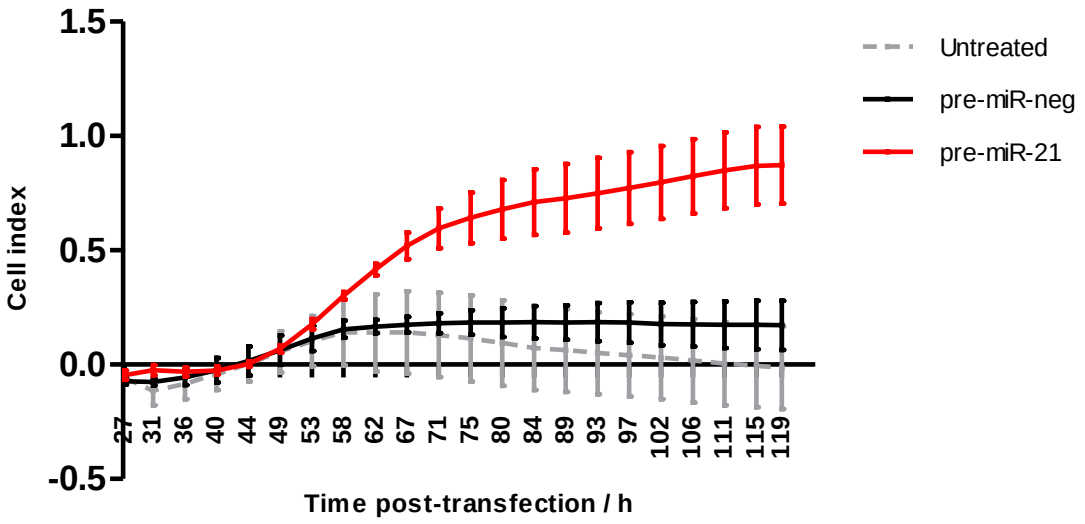

Figure 9. Boyden chamber based cell migration assay in RWPE-1. 30,000 cells untreated or transfected with pre-miR-neg or pre-miR-210 were seeded into the upper chamber, and the cell index that migrated across electrode monitored porous membrane towards serum-containing media was recorded. Significant difference between the migration curves of pre-miR-21 and untreated but not pre-miR-neg (one-way ANOVA, $p<0.001$). Mean + SEM of three biological replicates shown.

4. 2. VI. Identification of a novel target of miR-21 in prostate cancer

Next, a novel target of miR-21 in PCa was sought. Using miRTarBase, a list of potential miR-21 targets was collected. The candidate genes *TGFBR3*, *NTF3*, *SPRY2*, and *RHOB* were selected based on a literature review which found them all to have tumour-suppressive effects in PCa or another cancer, or evidence for involvement in the hypoxia response pathway.

RWPE-1 cells were transfected with pre-miR-21 or pre-miR-neg (in three biological replicates) and the mRNA levels of the candidate targets was measured. *PTEN* was selected as a positive control, as it is a known target of miR-21 in PCa (Feng and Tsao, 2016). The expression of several of the targets was unaffected by pre-miR-21 transfection, perhaps indicating that the mRNA was incompletely degraded following miR-21 binding, or that the interaction was not functional in this cell-line or perhaps that other interactions override this one such as transcriptional upregulation of the target in response to miR-21 due to an independent signalling axis. Intriguingly, levels of *TGFBR3* and *RHOB* were equivalent to PTEN in the miR-21 overexpressing cells (Figure 11A). As a second cell line, LNCaP cells were transfected and in this second cell line *RHOB* was also reduced (Figure 11B). The hypoxic murine tumour samples were then analysed, and in the bicalutamide-treated tumours *RHOB* expression was reduced slightly by day 7 and extensively by day 28, in inverse correlation with the expression of miR-21 (Figure 1E). To detect the protein level of RhoB by western blot following miR-21 overexpression, an antibody was ordered but it was not effective and the protein could not be visualised, even after the quantity was increased to 80µg and a non-denaturing lysis buffer was used, to determine if the antibody would bind better to the undenatured structure. Another antibody could be ordered from a different supplier to complete this experiment.

Corroborating a potential regulation of *RHOB* by miR-21, analysis of the TCGA data by Regulome Explorer revealed that the expression levels of *RHOB* and miR-21 were significantly inversely correlated, and *RHOB* levels were significantly reduced in tumours of Gleason score ≥8 compared with score ≤7, and with pathological T stage pT3b compared with pT2b. Of note, while miR-21 levels were significantly different between pT2c and pT3b, *RHOB* expression levels differed between pT3b and pT2b. This suggests that *RHOB* levels are independently associated with cancer progression independently of its inverse correlation with miR-21, and that it may have tumour suppressive effects in this dataset.

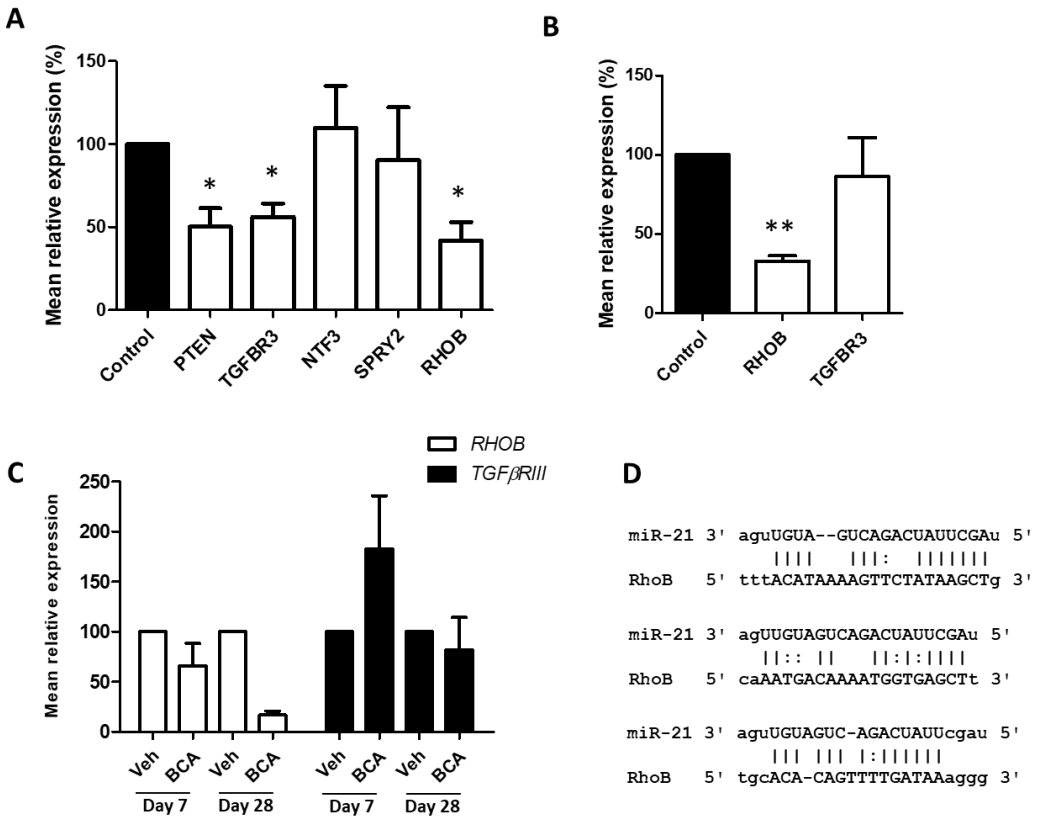

Figure 11. Identification of *RHOB* as a target of miR-21 in PCa. A) Mean + SEM relative expression of candidate targets of miR-21 following miR-21 overexpression in RWPE-1 cells, *PTEN* as positive control as a known target of miR-21. Mean + SEM of three biological replicates shown. **B)** RhoB is similarly reduced by miR-21 overexpression in LNCaP cells. **C)** *RHOB* is reduced in the tumours of bicalutamide-treated mice at day 7 and day 28. **D)** The predicted binding between miR-21 and RHOB based on data from miRTarBase. The mean expression level in each bicalutamide-treated group was normalised to the mean expression level of the vehicle-treated group, groups contained at least 4 mice. One-way t-tests were used to compare condition means to the control (hypothetical value 100) and p-values considered significant when *p<0.05, **p<0.01, ***p<0.001.

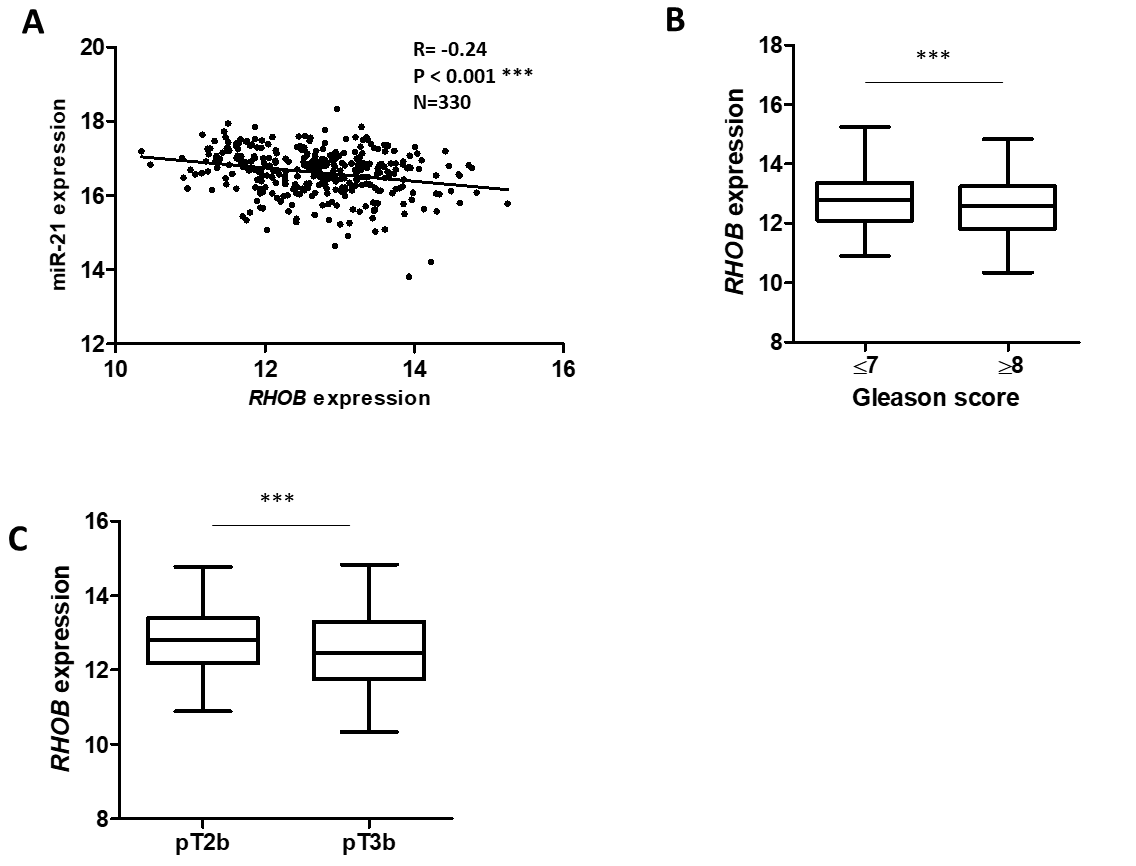

D

RHOB

CLINICAL FEATURE	No. of samples	Spearman's Correlation	p-value	Q-value
GLEASON SCORE	497	-0.1116	0.01275	0.0325
NUMBER OF LYMPH NODES	406	-0.0549	0.2697	0.47
PATHOLOGY T STAGE	490	-0.132	0.003417	0.0165
PSA VALUE	440	-0.0381	0.4259	0.629

Figure 12. *RHOB* expression in TCGA datasets. In the PRAD dataset, **A)** miR-21 and *RHOB* expression correlate inversely, **B)** *RHOB* expression is reduced in Gleason score ≥8 compared with score ≤7, and **C)** in pathological T stage pT3b compared with pT2b. **D)** In the Firebrowse dataset, *RHOB* expression significantly inversely correlated with Gleason score and number of PCa-positive lymph nodes.

4. 2. VII. Stratification of TCGA samples based on miR-21 and miR-210 expression improves the ability of Gleason score to predict PCa remission

Taken together, the above data indicates that like miR-210, miR-21 is probably a hypoxia-regulated miRNA with oncogenic properties. Therefore, levels of these miRNAs could have clinical value as markers of hypoxia and/or cancer progression. To determine if the levels of these "hypoxamiRs" together in combination with Gleason score for each individual patient, might predict their response to therapy, we performed a decision tree and random forest analysis (using code designed by colleague Christopher McNally). The TCGA data was mined using Regulome Explorer to collect the expression level of miR-21 and miR-210, as well as the Gleason score, and remission response (re-grouped as complete or incomplete) for each patient (n=330). Alone, neither miRNA was able to predict the patient's response, however, the combination of both miRNAs improved the ability of Gleason score to predict complete remission. An individual decision tree is illustrated in Figure 13A. The random forest model, which is based on 500 decision trees, was capable of predicting complete remission with over 90% accuracy, 100% specificity, and 50% sensitivity ($p<0.001$) (Figure 13B).

This model indicates that including quantification of miR-21 and miR-210 with Gleason grading at biopsy would be superior to Gleason score alone and therefore this model could have clinical value. Since my data suggest both of the miRNAs are hypoxamiRs in PCa, their levels may reflect tumour hypoxia and could be used to help distinguish a subset of tumours that are intrinsically more aggressive and/or more difficult to treat. However, in order to confirm the validity of this approach, the model should be tested on additional datasets.

A

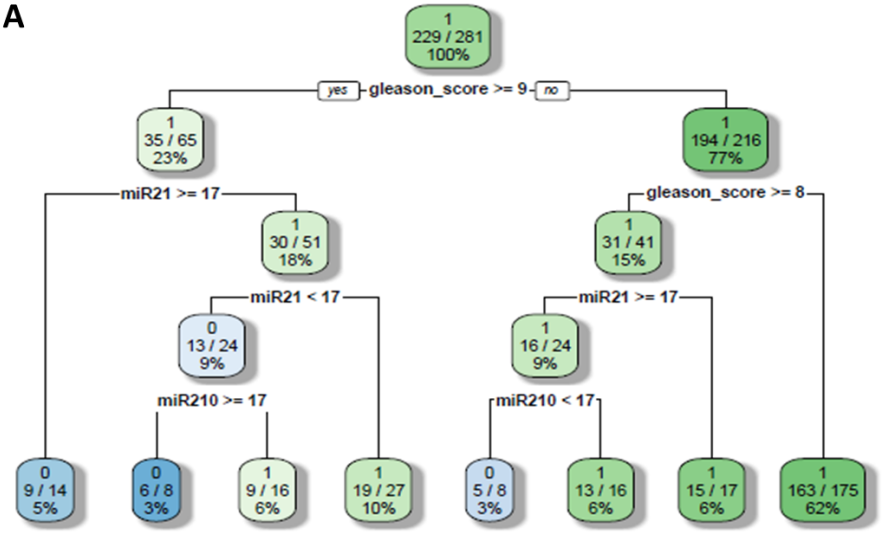

B

Accuracy	:	0.909700
95% CI	:	(0.8697, 0.9407)
No Information Rate	:	0.815900
P-Value [Acc>NIR]	:	0.000010
Kappa	:	0.629200
Mcnemars's test P-Value	:	0.000002
Sensitivity	:	0.509800
Specificity	:	1.000000
Pos Pred Value	:	1.000000
Neg Pred Value	:	0.900400
Prevalence	:	0.184120
Detection Rate	:	0.093860
Detection Prevalence	:	0.093860
Balanced Accuracy	:	0.754900

Figure 13. Combining miR-21 and miR-210 levels with recorded Gleason Score increases accurate prediction of complete remission response to therapy. A) Decision tree visualisation of the combination of miR-21 and miR-210 levels to Gleason Score and prediction of complete (1) or non-complete (0) remission response after therapy, with number of patients / total in this group and as the % of the total cohort. **B)** Random forest based on 500 decision trees showing the addition of the three variables produces a model with accuracy >90%, sensitivity >50%, specificity 100%, p<0.001.

4.3 Discussion

4. 3. I. Summary of findings

The literature is replete with studies attributing miR-21 diagnostic or prognostic potential in various cancer settings. A link between miR-21 and hypoxia is emerging although it has not been confirmed in PCa. The work in this chapter present novel data to show that miR-21 expression is upregulated by hypoxia in PCa. Furthermore, the biological effects of this up-regulation were assessed, to show how it could contribute to tumour progression by regulating cell migration and clonogenicity. Moreover, a simple statistical model, based on miR-210, miR-21 and Gleason score for each patient, was able to predict response to treatment with over 90% accuracy in the PRAD dataset. Increasingly, clinicians are making use of personalised medicine and bioinformatics-based approaches such as these in order to best diagnose, prognose, and treat each patient, and the efficacy of this model highlights the importance of *in vitro* identification of miRNAs involved in disease and the integration of *in vitro* findings with bioinformatics.

Intriguingly, miR-21 was upregulated in the sera of bicalutamide-treated mice, which suggests that it could additionally prove useful as a circulating marker of hypoxia. Circulating biomarkers are particularly valuable since they are less invasive, and can be used for longitudinal measurement during routine blood sampling and could be used to monitor disease progression or response to treatment, whereas biopsies provide only a snapshot at diagnosis. In fact, studies of other tissue types have reported that miR-21 was detected in exosomes, in correlation with the degree of stress including hypoxia (Eisman*n et al*., 2017)(Li *et al.*, 2019). Furthermore, transfer of the secreted fluid or exosomes to other cells (including immune cells) induced behaviours associated with cancer progression, such as proliferation and migration (Ren *et al.*, 2019)(Tejchman *et al.*, 2017). Similarly, hypoxic culture of glioblastoma cells stimulated the release of exosomes with a distinct miRNA expression profile (including increased levels of miR-21), which could modulate immune cell function when applied to them. Myeloid-derived suppressor cells, a regulatory immune cell type with a dampening effect on T cell activity, became enhanced and multiplied upon application of these exosomes that had been derived from hypoxic glioblastoma cells (Guo *et al.*, 2018). Taken together these findings indicate that miR-21 could be an important mediator of paracrine signalling during the hypoxic response in PCa as well as other cell types. However, the promiscuity of miR-21's activity in numerous signalling pathways bodes caution for its use as a marker of hypoxia. MiR-21 was involved in the pathogenesis of inflammatory diseases and autoimmune diseases including multiple sclerosis, systemic lupus erythematosus, and type 1 diabetes (Husakova, 2016; Sanders *et al.*, 2016; Sekar *et al.*, 2016; Zhao and Shao, 2016). It was also overexpressed during asthma, chronic obstructive pulmonary disease (COPD), fibrosis, and regulates infection by viruses such as herpesvirus and retrovirus (Kim *et al.*, 2017; Bernier and Sagan, 2018; Zeng *et al.*, 2018)(Wang *et al.*, 2018). Therefore, it may be useful as part of a hypoxic-signature panel but not specific enough for use alone.

The effect of miR-21 expression on PCa cell functionality has been disputed. Some studies reported that it exerted growth-promoting effects while others found it to have no effect. My experiments suggested that miR-21 increased migration and clonogenicity in RWPE-1 but did not affect cell proliferation, at least, not when overexpressed alone, in a cell line, and at these time points, although it cannot be ruled out that it could exert longer-term effects through the regulation of its targets. Furthermore, screening of potential mRNA targets identified Rho GTPase B (RhoB, also known as Ras homolog family member B), as downregulated by miR-21 overexpression. RhoB was one of a candidate list of targets that were chosen due to their reported tumour-suppressive functions in PCa and an involvement in the hypoxic response.

RHOB expression inversely correlated with tumour aggressiveness in the TCGA data, indicating that it has tumour-suppressive effects in PCa. As will now be discussed, RhoB has been attributed both oncogenic and tumour suppressive effects in different tumour types, although it has scarcely been explored in PCa. One study reported that RhoB increased migration and *MMP1* expression in DU145 (Yoneda *et al*., 2010), but otherwise it has not been investigated.

RhoB is a Rho GTPase, which are a family of signalling proteins. They are small guanine nucleotide binding proteins, which are inactive while bound to GDP and become active when bound to GTP. They have intrinsic (although inefficient) GTPase activity meaning that they are active until they have catalysed GTP hydrolysis to GDP. GTPases are activated by guanine exchange factors (GEFs) that convert the bound GDP to GTP, and inactivated by GTPase-activating proteins (GAPs) that stimulate their GTPase activity. Rho GTPases are mainly localised to the plasma membrane and participate in G protein receptor signalling. Activated Rho GTPases bind to a variety of downstream effectors and regulate cell migration, invasion, cell division, wound healing, and actin reorganisation, among other pathways and therefore they are important mediators of diverse processes. There are many forms of RhoGTPase although three are closely related: RhoA, RhoB, and RhoC. RhoB is a small protein (22KDa) encoded by a single exon; it is thought to have arisen by reverse copy integration of RhoA (Vega and Ridley, 2018). Interestingly, although they share over 87% sequence identity, the function of RhoB is distinct and in many ways elusive (Ju and Gilkes, 2018). All three proteins are regulated by posttranslational modifications (PTMs), mostly by the addition of a lipid group to the C-terminal domain such as a farnesyl and geranylgeranyl (RhoB can also be palmitolated) or phosphorylation, and the PRK family of kinases have higher affinity for RhoB than RhoA and RhoC. The PTMs regulate their cellular localisation and their interactions with the plasma membrane and with downstream effectors; the differences in PTMs likely underlies the distinct activities of RhoB. While RhoA and RhoC were only detected at the plasma membrane, RhoB was also found in endosomes, multivesicular bodies, and in the nucleus. Due to the differences in cell localisation, RhoB could be exposed to different downstream effectors as well as different GAPs and GEFs, and this could allow it to participate in different pathways (Ridley, 2013)(Vega and Ridley, 2018).

Due to their role in growth factor signalling, the Rho GTPases have been investigated as a potential cancer treatment targets. *RHOB* knockout is not embryonic lethal, indicating that its function is not essential for development (although its knockout was associated with neurological impairments); nevertheless it is considered important for healthy cell integrity and development, as indicated by the defects that are observed in RhoB expression levels in various cancers. Initial experiments reported that RhoB was an oncogene because it was upregulated in response to growth factors and cytokines. However, it has since been confirmed to have tumour-suppressive effects. In fact, oncogenes such as Ras, Akt, and EGFR all downregulate *RHOB* at both the transcriptional and mRNA level, and immunohistochemistry experiments demonstrated that RhoB protein levels are reduced in solid tumours. Furthermore, its knockout is associated with increased propensity for carcinogenesis (Huang and Prendergast, 2006; Vega and Ridley, 2018). Early research showed that RhoB was involved in mediating apoptosis and was important for stress responses (Prendergast, 2001). This is particularly important during the response to UV or DNA damage; for example, RhoB-deficient cells cannot perform homologous recombination following DNA damage, which was linked to an impaired de-phosphorylation of histone γH2AX by phosphatase PP2A. DNA damage also drives Akt and Chk1 signalling that downregulates *RhoB* expression (Wang *et al*., 2014a). It has long been known that farnesyltransferase inhibitors, a widely used chemotherapeutic agent, act by causing an accumulation of geranylgeranylated RhoB which inhibits proliferation (Mazière*s et al*., 2005). *RHOB* expression is epigenetically upregulated by histone acetylation and histone deacetylase-1 (HDAC1) suppresses *RHOB* expression to the extent that HDAC inhibitors effectively reduce tumours when used in combination with paclitaxel, by inducing *RHOB* expression (Marlow *et al.*, 2015). It is also important to note that the specific localisation of RhoB to endosomes permits it to regulate the trafficking and recycling of numerous proteins, such as the oncogenic intracellular kinases Src and Akt, and the oncogenic receptors EGFR and CXCR2, which have been co-localised with RhoB in endosomes of varying stages (Vega and Ridley, 2018). Therefore, insufficient levels of RhoB could result in the accumulation of these oncogenes. Since the continued proliferation and suppression of apoptosis in the presence of DNA damage is a hallmark of cancer cells, the downregulation of *RHOB* could be one means of facilitating cancer cell survival in this context.

Another reason that RhoB is interesting as a target of miR-21, is its involvement in hypoxia, inflammation and vasculogenesis. One study used *in vitro* and *in vivo* models to show that it regulated TNFα and nitric oxide secretion in macrophages, in response to lipopolysaccharide (Wan*g et al*., 2014b). RhoB may be important for macrophage morphology, function, and migration; it was reported to be involved in hypoxia-activated inflammation (Wang *et al*., 2013). As previously mentioned, miR-21 is a key player in inflammatory signalling and therefore its regulation of RhoB could also be relevant in this context. Perhaps, miR-21 secreted by hypoxic tumour cells helps to dampen macrophage activation by targeting *RHOB*. This suggests that the regulation of RhoB by miR-21 could have implications for both PCa cell function and the regulation of the tumour microenvironment as a whole.

4. 3. II. Future experiments

4. 3. II. a) Short term

To confirm RhoB as a target of miR-21 a Western blot analysis of its reduction at the protein level following miR-21 overexpression should be performed, followed by a luciferase reporter assay in a manner similar to that shown in Chapter 3 for miR-210 and *NCAM1*. This has been performed for miR-21 and *RHOB* in colorectal cancer cells (M. Liu *et al.*, 2011) although never in PCa. Alternatively, the cells could be transfected with oligonucleotides that bind the miR-21 binding site on *RHOB* which may prevent the miR-21 associated reduction in *RHOB* mRNA levels (miRNA zippers)(Meng *et al.*, 2017).

The effect of miR-21 on cell invasion could be investigated by coating the Boyden chamber dividing membrane with matrigel, which cells must break down in order to reach the serum-containing media. This would mimic the ECM and confirm that miR-21 upregulates the expression of enzymes that would allow it to extravasate, and has been used in lung cancer models (Kadera *et al.*, 2013).

It has been reported that in some tissue types, *RHOB* was induced by hypoxia, such as glioblastoma (Skuli *et al.*, 2009)(Skuli *et al.*, 2006), clear cell renal carcinoma (Turcotte, Desrosiers and Béliveau, 2003) and lung cancer (Huang *et al.*, 2016). In macrophages, RhoB was essential for their activation (Huang *et al.*, 2017). *RHOB* expression should be measured following hypoxia in PCa to explore whether it is similarly induced, in which case its regulation by miR-21 could provide an essential means of negative feedback.

As an alternative to transient transfection of the miRNA, lenti/retroviral methods of genomic transduction could be used. This have been suggested as a more realistic model of miRNA overexpression since the expressed levels will be lower and more physiological, and the classic miRNA biogenesis pathway will be used to produce them in the cell. This could be useful as there have been concerns that transient transfection of precursors induces too high levels of the molecule which a) is not physiological and b) can cause large RNA aggregates as observed by Northern blot experiments although this was most associated with a 100nM concentration whereas we use 25nM (Jin *et al.*, 2015). However, these genes are already in the genome but subject to regulation, and so I do not see a clear benefit of transduction methods. Use of a concentration lower than 25nM could be another option, although this concentration has been optimised previously by our laboratory for the purpose of exaggerating its effect in order to clearly observe the phenotype. Perhaps it would be useful to perform a titration of the miRNA precursor levels, and then perform the phenotypic assays again, to pinpoint a level that produces the effect. This could be useful to determine the optimal miRNA concentration to transfect while minimises off target effects. It could also highlight the effect of increasing miRNA expression as hypoxia would increase.

4. 3. II. b) Medium term

To complement the migration assay, some groups used antagomiRs (inhibitors) to show that the inhibition of miR-21 prevented cancer-associated behaviours such as colony formation or migration. However, miR-

21 expression was already reduced in the cancer cell lines compared to RWPE-1 and in the absence of a stimulus such as hypoxia, an inhibitor would be unlikely to exert an effect (Báez-Vega *et al*., 2016)(Li *et al.*, 2009b). However, use of inhibitors could complement the precursor studies, and would be expected to exert the opposite effects, such as increase in *RHOB* levels, although as previously mentioned in basal conditions they may exert no effect, comparable to the control pre-miR-neg. It could be informative to compare cell transfected with pre-miR-neg and miR-21 inhibitors following a stress condition such as hypoxia or lack of growth factors. If the inhibitor transfected cells were more sensitive to cell death following the stress condition, it would highlight a role for miR-21 in suppressing cell death. It is also worth noting that future therapies could involve using miR-21 inhibitors to reduce the deleterious effects of tumour hypoxia, and although no miRNA inhibitors have yet entered the clinic such use is imminent (Bardin *et al.*, 2018).

My cell proliferation assay could not isolate an effect of miR-21, although it may yet contribute to the regulation of proliferation but require the context of other miRNAs or genes. It would be interesting to perform co-transfection of miR-21 and miR-210 to examine if the two miRNAs could work together to regulate proliferation or suppress apoptosis.

In order to confirm that RhoB has tumour suppressive effects in PCa, it could be knocked down using an siRNA or shRNA based approach, and the phenotypic assays performed to isolate its function. This has successfully been used to study RhoB's function in the endothelial cell barrier (Marcos-Ramiro *et al.*, 2016).

Additionally, tissue sections from PCa specimens could be stained for RhoB which would indicate its abundant or localisation, and could potentially be correlated with Gleason grade or resistance to therapy. This has been used to correlate the protein NUP98 with response to treatment in breast cancer (Mullan *et al.*, 2019). However, unless extremely different the staining could be difficult to quantify accurately and so potentially quantification by mass spectrometry could be more effective.

Similarly, the exosomes of hypoxic PCa cells could be extracted by centrifugation and analysed for miR-21 levels, which would confirm that miR-21 is exported during hypoxia as a paracrine mediator. These could be applied normoxic macrophages or prostatic epithelial cells and levels of *RHOB* be measured, to indicate if secreted miR-21 could modulate immune cell activation. Numerous studies have screened for exosomal miRNAs and performed similar studies, as reviewed in (Zhang *et al.*, 2015).

Some groups have investigated the regulation of miR-21 expression by DNA methylation in other diseases; one group found miR-21 was hypomethylated in papillary thyroid cancer (Ortiz *et al.*, 2018) and it was upregulated by hypomethylating agent therapies for myelodysplastic syndromes (Kim *et al.*, 2014). Therefore, the regulation of miR-21 expression by DNA methylation of its promoter region could be relevant in PCa. This theme is explored in chapter 5.

Interestingly, putting the list of miR-21 targets that from the miRTarBase database into DAVID reveals functional enrichment of apoptosis associated pathways (Supplementary Table 1). The involvement of miR-21 in the regulation of apoptosis could be explored using flow cytometry (by dual staining with propidium iodide and Annexin V) or caspase 3/9 activity, as has been used by other researchers (Dong *et al*, 2018). Apoptosis could be measured following miR-21 overexpression or inhibition in healthy cells, and cells subjected to a stress such as hypoxia or chemotherapy, to determine if miR-21 can inhibit stress-induced apoptosis.

Supplementary Table 1. DAVID Gene Ontology Enrichment of the list of predicted targets of miR-21.

Functional annotation	No. of genes	p-value	Benjamini
Cellular protein modification process	247	5.90E-25	3.90E-21
Regulation of molecular function	193	1.90E-20	6.50E-17
Apoptosis process	128	1.70E-15	1.60E-12
Programmed cell death	133	1.90E-15	1.60E-12
Regulation of apoptosis process	110	1.90E-15	1.60E-12
Cell death	136	1.10E-14	5.80E-12

4. 3. II. c) Long term

As previously mentioned, failure to identify an effect of miR-21 on the proliferation of cell lines could reflect the cell line environment and its effect may only be evident within the context of the tumour. To explore this, nanoparticles could be used to transfect pre-miR-21 into tumours *in vivo*, and the tumour could be monitored for changes such as in growth, metastasis, and resistance to treatment, as has been utilised in the study of the miR-200 family (Pecot *et al.*, 2013).

Cell lines could be transfected with pre-miR-21 or pre-miR-neg, and then analysed by total RNA-sequencing, as has been performed using transfected kidney cancer cells (Lichawska-Cieslar *et al.*, 2018), and the differentially expressed genes analysed by pathway analysis (such as DAVID, or Ingenuity Pathway Analysis) as a top-down approach to identifying novel functions of miR-21.

Given the prominent function of miR-21 in the inflammatory response, it is tempting to speculate that RhoB mediates some of its effects, and thus the regulation of RhoB by miR-21 could be important in other disease settings such as inflammatory disorders or autoimmune diseases; regulation of RhoB could be tested in cell line models of these diseases to confirm this. It also invites the question of whether secreted miR-21 from cancer cells could modulate macrophage function *via* RhoB, to mediate immunosuppression during hypoxic conditions. This could be tested by applying the pre-miR-21 mimic to macrophages and monitoring their intracellular levels of RhoB to show that the cells import and/or respond to miR-21. This would confirm miR-21 as a key mediator of the tumour microenvironment.

Kaplan-Meier plots generated using the KM plotter tool (http://kmplot.com/analysis/) revealed that when expression of miR-21 was dichotomised into “high” and “low”, high expression was significantly associated with reduced survival time in other cancer types (Supplementary Figure 1)(data for PCa was not available). The role of miR-21 in these cancer types could be a worthwhile avenue for further research.

Finally, as we demonstrated in the simple example shown in Figure 13, bioinformatics can be used to combine genomic information with clinical parameters for precision medicine based approaches. As mentioned previously our model requires validation by testing on further datasets, and other models could be explored, such as the use of RHOB levels, or investigating the ability to identify additional parameters such as tumour hypoxia. Potentially the expression levels of miRNAs such as miR-21 and miR-210 could be added to Gleason grading or another clinical parameter to identify the most hypoxic tumours, which may benefit from specific therapies such as oxygen perfusion or a hypoxia-activated prodrug as reviewed in (Jordan and Sonveaux, 2012).

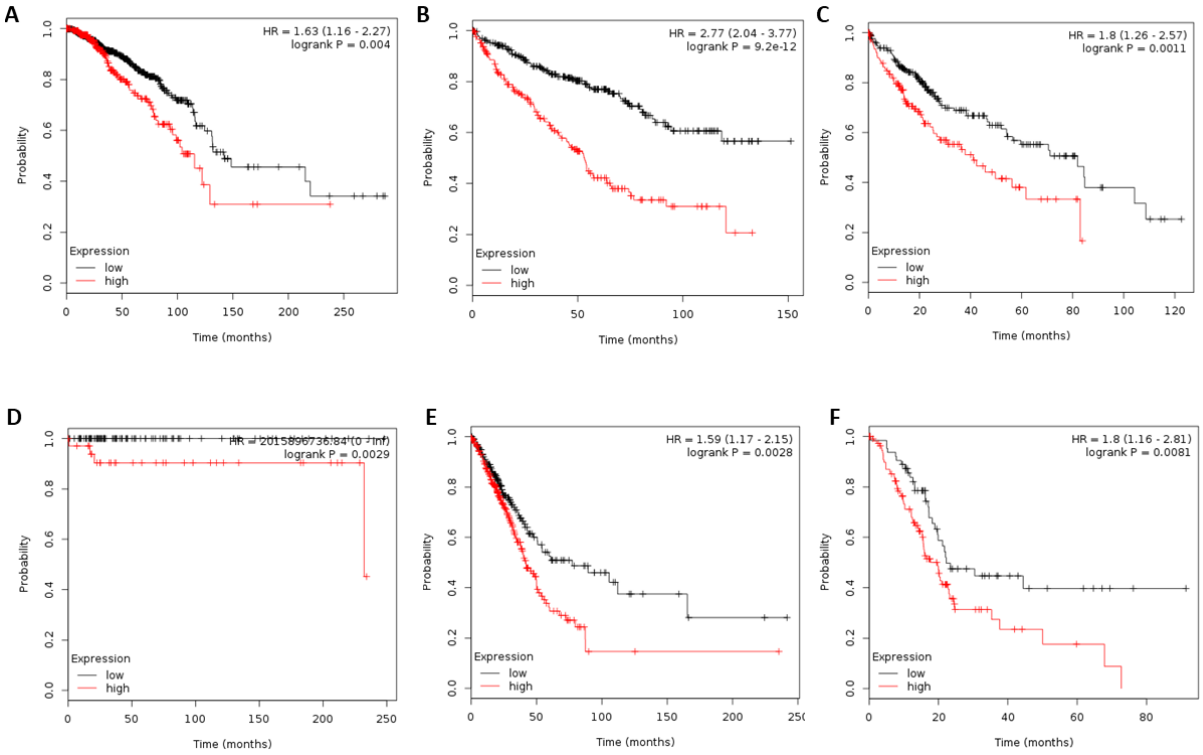

Supplementary Figure 1. High expression of miR-21 is significantly associated with reduced survival. In **A)** breast cancer, **B)** clear cell renal carcinoma, **C)** liver hepatocellular carcinoma, **D)** testicular germ cell tumour, **E)** lung adenocarcinoma, **F)** pancreatic ductal adenocarcinoma, and **G)** sarcoma.

4. 4. Bibliography

Anwar, S. L. *et al.* (2019) 'Upregulation of Circulating MiR-21 Expression as a Potential Biomarker for Therapeutic Monitoring and Clinical Outcome in Breast Cancer', *Asian Pacific Journal of Cancer Prevention*, 20(4), pp. 1223–1228. doi: 10.31557/APJCP.2019.20.4.1223.

Báez-Vega, P. M. *et al.* (2016) 'Targeting miR-21-3p inhibits proliferation and invasion of ovarian cancer cells', *Oncotarget*, 7(24), pp. 36321–36337. doi: 10.18632/oncotarget.9216.

Bahreyni, A. *et al.* (2019b) 'Diagnostic, prognostic, and therapeutic potency of microRNA 21 in the pathogenesis of colon cancer, current status and prospective', *Journal of Cellular Physiology*. John Wiley & Sons, Ltd, 234(6), pp. 8075–8081. doi: 10.1002/jcp.27580.

Bao, B. *et al.* (2012) 'Hypoxia Induced Aggressiveness of Prostate Cancer Cells Is Linked with Deregulated Expression of VEGF, IL-6 and miRNAs That Are Attenuated by CDF', *PLoS ONE*. Edited by S. K. Batra, 7(8), p. e43726. doi: 10.1371/journal.pone.0043726.

Bardin, P. *et al.* (2018) 'Emerging microRNA Therapeutic Approaches for Cystic Fibrosis', *Frontiers in Pharmacology*. Frontiers, 9, p. 1113. doi: 10.3389/fphar.2018.01113.

Bernier, A. and Sagan, S. M. (2018) 'The Diverse Roles of microRNAs at the Host–Virus Interface.', *Viruses*. Multidisciplinary Digital Publishing Institute (MDPI), 10(8). doi: 10.3390/v10080440.

Bica-Pop, C. *et al.* (2018) 'Overview upon miR-21 in lung cancer: focus on NSCLC', *Cellular and Molecular Life Sciences*, 75(19), pp. 3539–3551. doi: 10.1007/s00018-018-2877-x.

Bienertova-Vasku, J., Novak, J. and Vasku, A. (2015) 'MicroRNAs in pulmonary arterial hypertension: pathogenesis, diagnosis and treatment', *Journal of the American Society of Hypertension*, 9(3), pp. 221–234. doi: 10.1016/j.jash.2014.12.011.

Chen, R. *et al.* (2019) 'MicroRNA-21 attenuates oxygen and glucose deprivation induced apoptotic death in human neural stem cells with inhibition of JNK and p38 MAPK signaling', *Neuroscience Letters*, 690, pp. 11–16. doi: 10.1016/j.neulet.2018.09.060.

Chen, Z. *et al.* (2016) 'Tissue microRNA-21 expression predicted recurrence and poor survival in patients with colorectal cancer - a meta-analysis.', *OncoTargets and therapy*. Dove Press, 9, pp. 2615–24. doi: 10.2147/OTT.S103893.

Dong, C. *et al.* (2019) 'Hypoxic non-small-cell lung cancer cell-derived exosomal miR-21 promotes resistance of normoxic cell to cisplatin', *OncoTargets and Therapy*, Volume 12, pp. 1947–1956. doi: 10.2147/OTT.S186922.

Dong, P. *et al.* (2018) 'Anti-microRNA-132 causes sevoflurane-induced neuronal apoptosis via the PI3K/AKT/FOXO3a pathway.', *International journal of molecular medicine*. Spandidos Publications, 42(6), pp. 3238–3246. doi: 10.3892/ijmm.2018.3895.

Eismann, J. *et al.* (2017) 'Hypoxia- and acidosis-driven aberrations of secreted microRNAs in endometrial cancer in vitro', *Oncology Reports*, 38(2), pp. 993–1004. doi: 10.3892/or.2017.5717.

Feng, Y.-H. and Tsao, C.-J. (2016) 'Emerging role of microRNA-21 in cancer.', *Biomedical reports*. Spandidos Publications, 5(4), pp. 395–402. doi: 10.3892/br.2016.747.

Folini, M. *et al.* (2010) 'miR-21: an oncomir on strike in prostate cancer', *Molecular Cancer*, 9(1), p. 12. doi: 10.1186/1476-4598-9-12.

Gao, Y. *et al.* (2016) 'MicroRNA-21 as a potential diagnostic biomarker for breast cancer patients: a pooled analysis of individual studies.', *Oncotarget*. Impact Journals, LLC, 7(23), pp. 34498–506. doi: 10.18632/oncotarget.9142.

Guan, C. *et al.* (2019) 'Upregulation of MicroRNA-21 promotes tumorigenesis of prostate cancer cells by targeting KLF5', *Cancer Biology & Therapy*, 20(8), pp. 1149–1161. doi: 10.1080/15384047.2019.1599659.

Guo, X. *et al.* (2018) 'Immunosuppressive effects of hypoxia-induced glioma exosomes through myeloid-derived suppressor cells via the miR-10a/Rora and miR-21/Pten Pathways', *Oncogene*. Nature Publishing Group, 37(31), pp. 4239–4259. doi: 10.1038/s41388-018-0261-9.

Hu, G. *et al.* (2016) 'Prognostic value of microRNA-21 in pancreatic ductal adenocarcinoma: a meta-analysis', *World Journal of Surgical Oncology*, 14(1), p. 82. doi: 10.1186/s12957-016-0842-4.

Huang, G.-X. *et al.* (2016) 'The mechanisms and significance of up-regulation of RhoB expression by hypoxia and glucocorticoid in rat lung and A549 cells', *Journal of Cellular and Molecular Medicine*, 20(7), pp. 1276–1286. doi: 10.1111/jcmm.12809.

Huang, G. *et al.* (2017) 'RhoB regulates the function of macrophages in the hypoxia-induced inflammatory response', *Cellular & Molecular Immunology*, 14(3), pp. 265–275. doi: 10.1038/cmi.2015.78.

Huang, M. and Prendergast, G. C. (2006) 'RhoB in cancer progression', *Histology and Histopathology*, 21, pp. 213–218. doi: 10.14670/HH-21.213.

Husakova, M. (2016) 'MicroRNAs in the key events of systemic lupus erythematosus pathogenesis', *Biomedical Papers*, 160(3), pp. 327–342. doi: 10.5507/bp.2016.004.

JIANG, S. *et al.* (2016) 'MicroRNA-21 modulates radiation resistance through upregulation of hypoxia-inducible factor-1α-promoted glycolysis in non-small cell lung cancer cells', *Molecular Medicine Reports*, 13(5), pp. 4101–4107. doi: 10.3892/mmr.2016.5010.

Jin, H. Y. *et al.* (2015) 'Transfection of microRNA Mimics Should Be Used with Caution', *Frontiers in Genetics*. Frontiers Media SA, 6. doi: 10.3389/FGENE.2015.00340.

Jordan, B. F. and Sonveaux, P. (2012) 'Targeting tumor perfusion and oxygenation to improve the outcome of anticancer therapy.', *Frontiers in pharmacology*. Frontiers Media SA, 3, p. 94. doi: 10.3389/fphar.2012.00094.

Ju, J. A. and Gilkes, D. M. (2018) 'RhoB: Team Oncogene or Team Tumor Suppressor?', *Genes*. Multidisciplinary Digital Publishing Institute (MDPI), 9(2). doi: 10.3390/genes9020067.

Kadera, B. E. *et al.* (2013) 'MicroRNA-21 in pancreatic ductal adenocarcinoma tumor-associated fibroblasts promotes metastasis.', *PloS one*. Public Library of Science, 8(8), p. e71978. doi: 10.1371/journal.pone.0071978.

Kim, R. Y. *et al.* (2017) 'MicroRNA-21 drives severe, steroid-insensitive experimental asthma by amplifying phosphoinositide 3-kinase–mediated suppression of histone deacetylase 2', *Journal of Allergy and Clinical Immunology*, 139(2), pp. 519–532. doi: 10.1016/j.jaci.2016.04.038.

Kim, Y. *et al.* (2014) 'Serum microRNA-21 as a Potential Biomarker for Response to Hypomethylating Agents in Myelodysplastic Syndromes', *PLoS ONE*. Edited by D. T. Starczynowski, 9(2), p. e86933. doi: 10.1371/journal.pone.0086933.

Kulshreshtha, R. *et al.* (2007) 'A microRNA signature of hypoxia.', *Molecular and cellular biology*. American Society for Microbiology (ASM), 27(5), pp. 1859–67. doi: 10.1128/MCB.01395-06.

Kurul, N. O. *et al.* (2019) 'The association of let-7c, miR-21, miR-145, miR-182, and miR-221 with clinicopathologic parameters of prostate cancer in patients diagnosed with low-risk disease', *The Prostate*, p. pros.23825. doi: 10.1002/pros.23825.

Leite, K. R. M. *et al.* (2015) 'Controlling RECK miR21 Promotes Tumor Cell Invasion and Is Related to Biochemical Recurrence in Prostate Cancer', *Journal of Cancer*, 6(3), pp. 292–301. doi: 10.7150/jca.11038.

Li, L. *et al.* (2019) 'Microenvironmental oxygen pressure orchestrates an anti- and pro-tumoral γδ T cell equilibrium via tumor-derived exosomes', *Oncogene*, 38(15), pp. 2830–2843. doi: 10.1038/s41388-018-0627-z.

Li, T. *et al.* (2009a) 'MicroRNA-21 directly targets MARCKS and promotes apoptosis resistance and invasion in prostate cancer cells', *Biochemical and Biophysical Research Communications*, 383(3), pp. 280–285. doi: 10.1016/j.bbrc.2009.03.077.

Lichawska-Cieslar, A. *et al.* (2018) 'RNA sequencing reveals widespread transcriptome changes in a renal carcinoma cell line.', *Oncotarget*. Impact Journals, LLC, 9(9), pp. 8597–8613. doi: 10.18632/oncotarget.24269.

Liu, L.-Z. *et al.* (2011) 'MiR-21 Induced Angiogenesis through AKT and ERK Activation and HIF-1α Expression', *PLoS ONE*. Edited by A. Navarro, 6(4), p. e19139. doi: 10.1371/journal.pone.0019139.

Liu, M. *et al.* (2011) 'miR-21 targets the tumor suppressor RhoB and regulates proliferation, invasion and apoptosis in colorectal cancer cells.', *FEBS letters*, 585(19), pp. 2998–3005. doi: 10.1016/j.febslet.2011.08.014.

Lu, Z. *et al.* (2008) 'MicroRNA-21 promotes cell transformation by targeting the programmed cell death 4 gene', *Oncogene*, 27(31), pp. 4373–4379. doi: 10.1038/onc.2008.72.

Marcos-Ramiro, B. *et al.* (2016) 'RhoB controls endothelial barrier recovery by inhibiting Rac1 trafficking to the cell border.', *The Journal of cell biology*. Rockefeller University Press, 213(3), pp. 385–402. doi: 10.1083/jcb.201504038.

Marlow, L. A. *et al.* (2015) 'RhoB upregulation leads to either apoptosis or cytostasis through differential target selection', *Endocrine-related cancer*. NIH Public Access, 22(5), p. 777. doi: 10.1530/ERC-14-0302.

Mazières, J. *et al.* (2005) 'Geranylgeranylated, but not farnesylated, RhoB suppresses Ras transformation of NIH-3T3 cells', *Experimental Cell Research*, 304(2), pp. 354–364. doi: 10.1016/j.yexcr.2004.10.019.

Meng, L. *et al.* (2017) 'Small RNA zippers lock miRNA molecules and block miRNA function in mammalian cells.', *Nature communications*. Nature Publishing Group, 8, p. 13964. doi: 10.1038/ncomms13964.

Mishra, S *et al.* (2014) 'Androgen receptor and microRNA-21 axis downregulates transforming growth factor beta receptor II (TGFBR2) expression in prostate cancer', *Oncogene*, 33(31), pp. 4097–4106. doi: 10.1038/onc.2013.374.

Mishra, Sweta *et al.* (2014) 'MicroRNA-21 inhibits p57Kip2 expression in prostate cancer', *Molecular Cancer*, 13(1), p. 212. doi: 10.1186/1476-4598-13-212.

Mullan, P. B. *et al.* (2019) 'NUP98 – a novel predictor of response to anthracycline-based chemotherapy in triple negative breast cancer', *BMC Cancer*. BioMed Central, 19(1), p. 236. doi: 10.1186/s12885-019-5407-9.

Ortiz, I. M. D. P. *et al.* (2018) 'Loss of DNA methylation is related to increased expression of miR-21 and miR-146b in papillary thyroid carcinoma', *Clinical Epigenetics*, 10(1), p. 144. doi: 10.1186/s13148-018-0579-8.

Pecot, C. V. *et al.* (2013) 'Tumour angiogenesis regulation by the miR-200 family', *Nature communications*. NIH Public Access, 4, p. 2427. doi: 10.1038/NCOMMS3427.

Prendergast, G. C. (2001) 'Actin' up: RhoB in cancer and apoptosis', *Nature Reviews Cancer*, 1(2), pp. 162–168. doi: 10.1038/35101096.

Qin, W. *et al.* (2009) 'BMPRII is a direct target of miR-21', *Acta Biochimica et Biophysica Sinica*, 41(7), pp. 618–623. doi: 10.1093/abbs/gmp049.

Reis, S. T. *et al.* (2012) 'miR-21 may acts as an oncomir by targeting RECK, a matrix metalloproteinase regulator, in prostate cancer', *BMC Urology*, 12(1), p. 14. doi: 10.1186/1471-2490-12-14.

Ren, W. *et al.* (2019) 'Extracellular vesicles secreted by hypoxia pre-challenged mesenchymal stem cells promote non-small cell lung cancer cell growth and mobility as well as macrophage M2 polarization via miR-21-5p delivery', *Journal of Experimental & Clinical Cancer Research*, 38(1), p. 62. doi: 10.1186/s13046-019-1027-0.

Ribas, J. *et al.* (2009) 'miR-21: An Androgen Receptor-Regulated MicroRNA that Promotes Hormone-Dependent and Hormone-Independent Prostate Cancer Growth', *Cancer Research*, 69(18), pp. 7165–7169. doi: 10.1158/0008-5472.CAN-09-1448.

Ridley, A. J. (2013) 'RhoA, RhoB and RhoC have different roles in cancer cell migration', *Journal of Microscopy*. John Wiley & Sons, Ltd (10.1111), 251(3), pp. 242–249. doi: 10.1111/jmi.12025.

Sanders, K. A. *et al.* (2016) 'Next-generation sequencing reveals broad down-regulation of microRNAs in secondary progressive multiple sclerosis CD4+ T cells', *Clinical Epigenetics*. BioMed Central, 8(1), p. 87. doi: 10.1186/s13148-016-0253-y.

Sekar, D. *et al.* (2016) 'Role of microRNA 21 in diabetes and associated/related diseases', *Gene*, 582(1), pp. 14–18. doi: 10.1016/j.gene.2016.01.039.

Sha, M. *et al.* (2015) 'Celastrol induces cell cycle arrest by MicroRNA-21-mTOR-mediated inhibition p27 protein degradation in gastric cancer.', *Cancer cell international*. BioMed Central, 15, p. 101. doi: 10.1186/s12935-015-0256-3.

Shen, H. *et al.* (2019) 'miR-21 enhances the protective effect of loperamide on rat cardiomyocytes against hypoxia/reoxygenation, reactive oxygen species production and apoptosis via regulating Akap8 and Bard1 expression.', *Experimental and therapeutic medicine*. Spandidos Publications, 17(2), pp. 1312–1320. doi: 10.3892/etm.2018.7047.

Shi, G. *et al.* (2010) 'Involvement of microRNA-21 in mediating chemo-resistance to docetaxel in androgen-independent prostate cancer PC3 cells', *Acta Pharmacologica Sinica*, 31(7), pp. 867–873. doi: 10.1038/aps.2010.48.

Skuli, N. *et al.* (2006) 'Activation of RhoB by Hypoxia Controls Hypoxia-Inducible Factor-1α Stabilization through Glycogen Synthase Kinase-3 in U87 Glioblastoma Cells', *Cancer Research*, 66(1), pp. 482–489. doi: 10.1158/0008-5472.CAN-05-2299.

Skuli, N. *et al.* (2009) 'v 3/ v 5 Integrins-FAK-RhoB: A Novel Pathway for Hypoxia Regulation in Glioblastoma', *Cancer Research*, 69(8), pp. 3308–3316. doi: 10.1158/0008-5472.CAN-08-2158.

Tao, Y.-J. *et al.* (2015) 'Antisense oligonucleotides against microRNA-21 reduced the proliferation and migration of human colon carcinoma cells', *Cancer Cell International*. BioMed Central, 15. doi: 10.1186/S12935-015-0228-7.

Tejchman, A. *et al.* (2017) 'Tumor hypoxia modulates podoplanin/CCL21 interactions in CCR7+ NK cell recruitment and CCR7+ tumor cell mobilization', *Oncotarget*, 8(19), pp. 31876–31887. doi: 10.18632/oncotarget.16311.

Turcotte, S., Desrosiers, R. R. and Béliveau, R. (2003) 'HIF-1alpha mRNA and protein upregulation involves Rho GTPase expression during hypoxia in renal cell carcinoma', *Journal of Cell Science*, 116(11), pp. 2247–2260. doi: 10.1242/jcs.00427.

Vega, F. M. and Ridley, A. J. (2018) 'The RhoB small GTPase in physiology and disease.', *Small GTPases*. Taylor & Francis, 9(5), pp. 384–393. doi: 10.1080/21541248.2016.1253528.

Vila-Navarro, E. *et al.* (2019) 'Novel Circulating miRNA Signatures for Early Detection of Pancreatic Neoplasia', *Clinical and Translational Gastroenterology*, 10(4), p. e00029. doi: 10.14309/ctg.0000000000000029.

Wang, M. *et al.* (2014a) 'ATR/Chk1/Smurf1 pathway determines cell fate after DNA damage by controlling RhoB abundance', *Nature Communications*. Nature Publishing Group, 5(1), p. 4901. doi: 10.1038/ncomms5901.

Wang, M. *et al.* (2014b) 'ATR/Chk1/Smurf1 pathway determines cell fate after DNA damage by controlling RhoB abundance', *Nature Communications*, 5(1), p. 4901. doi: 10.1038/ncomms5901.

Wang, W. *et al.* (2018) 'Doxycycline attenuates chronic intermittent hypoxia-induced atrial fibrosis in rats', *Cardiovascular Therapeutics*, 36(3), p. e12321. doi: 10.1111/1755-5922.12321.

Wang, X. H. *et al.* (2013) 'RhoB is involved in lipopolysaccharide-induced inflammation in mouse in vivo and in vitro', *Journal of Physiology and Biochemistry*, 69(2), pp. 189–197. doi: 10.1007/s13105-012-0201-z.

Wu, Z.-H. *et al.* (2016) 'MiRNA-21 induces epithelial to mesenchymal transition and gemcitabine resistance via the PTEN/AKT pathway in breast cancer', *Tumor Biology*, 37(6), pp. 7245–7254. doi: 10.1007/s13277-015-4604-7.

Xing, Y. and Li, L. (2019) 'Gastrodin protects rat cardiomyocytes H9c2 from hypoxia-induced injury by up-regulation of microRNA-21', *The International Journal of Biochemistry & Cell Biology*, 109, pp. 8–16. doi: 10.1016/j.biocel.2019.01.013.

Xu, X. *et al.* (2014) 'miR-21 in ischemia/reperfusion injury: a double-edged sword?', *Physiological Genomics*, 46(21), pp. 789–797. doi: 10.1152/physiolgenomics.00020.2014.

Yan, J. *et al.* (2016) 'FZD6, targeted by miR-21, represses gastric cancer cell proliferation and migration via activating non-canonical wnt pathway', *American Journal of Translational Research*. e-Century Publishing Corporation, 8(5), p. 2354.

Yang, Y., Guo, J.-X. and Shao, Z.-Q. (2017) 'miR-21 targets and inhibits tumor suppressor gene PTEN to promote prostate cancer cell

proliferation and invasion: An experimental study', *Asian Pacific Journal of Tropical Medicine*. No longer published by Elsevier, 10(1), pp. 87–91. doi: 10.1016/J.APJTM.2016.09.011.

Yoneda, M. *et al.* (2010) 'RhoB enhances migration and MMP1 expression of prostate cancer DU145', *Experimental and Molecular Pathology*, 88(1), pp. 90–95. doi: 10.1016/j.yexmp.2009.09.010.

Zeng, Z. *et al.* (2018) 'MicroRNA-21 aggravates chronic obstructive pulmonary disease by promoting autophagy', *Experimental Lung Research*, 44(2), pp. 89–97. doi: 10.1080/01902148.2018.1439548.

Zhang, J. *et al.* (2015) 'Exosome and Exosomal MicroRNA: Trafficking, Sorting, and Function', *Genomics, Proteomics & Bioinformatics*. Elsevier, 13(1), pp. 17–24. doi: 10.1016/J.GPB.2015.02.001.

Zhao, X. and Shao, K. (2016) '[Roles of MicroRNA-21 in the Pathogenesis of Insulin Resistance and Diabetic Mellitus-induced Non-alcoholic Fatty Liver Disease].', *Zhongguo yi xue ke xue yuan xue bao. Acta Academiae Medicinae Sinicae*, 38(2), pp. 144–9. doi: 10.3881/j.issn.1000-503X.2016.02.004.

Zheng, W. *et al.* (2018) 'MicroRNA-21: A promising biomarker for the prognosis and diagnosis of non-small cell lung cancer.', *Oncology letters*. Spandidos Publications, 16(3), pp. 2777–2782. doi: 10.3892/ol.2018.8972.

Zhou, H. and Zhu, X. (2019) 'MicroRNA-21 and microRNA-30c as diagnostic biomarkers for prostate cancer: a meta-analysis', *Cancer Management and Research*, Volume 11, pp. 2039–2050. doi: 10.2147/CMAR.S189026.

Chapter 5. Identifying novel genes, pathways, and epigenetic changes in prostate cancer

5. 1. Introduction

5. 1. I. Omics data in cancer research

Cancer is a disease based on the accumulation of genetic abnormalities, contributed to by both germline mutations that predispose the individual, and somatic mutations that trigger and propel it. Our understanding of inherited variants and somatic occurrences that drive cancer have been vastly expanded by technological advances in next-generation sequencing (NGS) techniques, which have been used to characterise the genomics, epigenomics, and proteomics of diseased states (or predisposed individuals). Germline susceptibilities have been uncovered by genome-wide association studies across populations, and key somatic mutations in tumours have been characterised by whole-exome sequencing, whole-genome sequencing, RNA sequencing (RNA-seq), and probe-based arrays such as methylation arrays. Such "-omics" studies have thus been a key focus of cancer research for the last 20 years. Furthermore, massive international collaborative projects have facilitated the curation and organisation of omics data, such as The Cancer Genome Atlas (TCGA) database, which provide publicly available repositories of datasets that are hugely powerful in identifying critical genomic alterations. NGS discoveries have thus clarified the genetic basis of many cancers and have identified novel drug targets, and have also provided advances in stratifying patients, which has been used to improve diagnosis, prognosis, and to inform treatment strategies in many diseases. It is therefore an extremely important aspect of cancer research.

5. 1. II. Aims and hypothesis

The focus of this thesis is to characterise somatic events that drive PCa progression, namely, the dysregulation of miRNAs following hypoxia. The previous chapters have used prior knowledge of miRNAs that would make them likely to be involved in PCa hypoxia. This chapter includes genomic and epigenomic techniques to offer an unbiased approach to identify novel genetic abnormalities that are involved in hypoxia and tumour progression.

The chapter is split into three parts, which will be presented as mini-papers with Introduction, Results and Discussion sections. Part 1 utilises RNA-seq and miRNA-seq to analyse the prostatectomy samples and identify a novel hypoxia-regulated miRNA in PCa. Part 2 explores the effect of hypoxia on global DNA methylation; the R package "RnBeads" was employed to compare DNA methylation patterns in hypoxic tumours using a publicly available dataset from the NCBI Gene Expression Omnibus (GEO) database. Part 3 applies the *in vitro* method pyrosequencing to measure the methylation levels of DNA at individual miRNA loci in PCa cell lines, to investigate the regulation of their expression by DNA methylation. The overarching hypothesis of this chapter is that bioinformatics tools can identify novel differentially expressed and differentially methylated genomic loci, to direct wet-lab discoveries.

5. 2. Part 1: RNA-sequencing based approach to identifying a novel miRNA involved in PCa development

5. 2. I Introduction

To explore PCa-associated miRNAs, RNA-sequencing (mRNA-seq and miRNA-seq) was performed on the cohort of prostatectomy specimens obtained from Altnagelvin Area Hospital (n=19). The sequencing work was performed in collaboration with Biospyder Technologies (CA, USA). As outlined in Methods section *2.3.I*, RNA was extracted from formalin-fixed specimens followed by amplification and sequencing. The expression data was normalised using the DESeq2 method (Love, Huber and Anders, 2014), to identify differentially expressed mRNAs and miRNAs in the cancer specimens relative to paired non-cancer tissue. Next, the regulation of differentially expressed miRNAs by hypoxia was examined followed by *in vitro* functional studies of the effect of miRNA overexpression on behaviours associated with tumour progression, and potentially important downstream mRNA targets.

5. 2. II. Results

5. 2. II. a) Differentially expressed miRNAs in the prostatectomy cohort

For RNA-seq transcriptome data, the effect size is estimated by the log2 fold-change (log2FC) value (the logarithm in base 2 of the ratio between normalised counts in the test and control conditions). Figure 1 presents volcano plots of the data, which enable visualisation of each gene in terms of its effect size and statistical significance. Genes that are significantly differentially expressed (adjusted p-value < 0.1) are highlighted in red.

Of the screen performed, thirteen miRNAs and 175 mRNAs were differentially expressed (DE) in the tumour tissue compared to matched adjacent normal tissue (Table 1). Interestingly, among the 13 miRNAs identified were members of the miR-200 family, which our lab and others had previously shown to be important in PCa (Lynch *et al.*, 2016a)(Kumar, Nag and Mandal, 2015). In light of the results from chapters 3 and 4, it was interesting to note that miR-21 and miR-210 were not DE overall in this small set of samples, although miR-21 was upregulated with relatively high significance, whereas miR-210 was downregulated with relatively low statistical significance. Plotting the mean+SEM of the miRNA levels in tumour versus non-tumour samples showed increased expression of miR-210 and miR-21 in the tumour samples as measured by RNAseq, confirming the qPCR results from chapters 3 and 4. A two-tailed t-test indicated that that miR-21 levels were significantly upregulated in the tumour samples (Figure 2A-B), which contrasted with the statistical test performed by BioSpyder.

The most significantly DE was miR-23a, and moreover there was limited evidence that its expression positively correlated with tumour aggressiveness in the TCGA Regulome Explorer dataset (http://explorer.cancerregulome.org/). MiR-23a was increased in tumours of TNM stage T3b vs T4 (-

log10p=2, R=0.28, n=88), higher in patients whose lymph nodes were examined (-log10p=2.5, R= -0.16, n=326), and lower in T1c tumours compared to other stages (-log10p= 2.6, R=-0.19, n=256)

MiR-30a expression was significantly reduced in the tumour samples. This reflected the TCGA data, in which miR-30a negatively correlated with Gleason Score (R=-0.22, -log10p=4.2, n=330), higher in tumours which showed complete remission response (-log10p=3.9, n=237), lower in progressive disease (-log10p=3.8, n=246), and decreased in tumour pT2c vs pT3b (-log10p=4.5, n=194). This suggested that miR-30a may be a tumour suppressor in PCa.

Therefore, miR-30a and miR-23 were selected for further investigation as potential hypoxamiRs. Furthermore, since primers were available in our stocks for miR-146a and miR-196a, these were also analysed to explore their relationship with hypoxia in PCa.

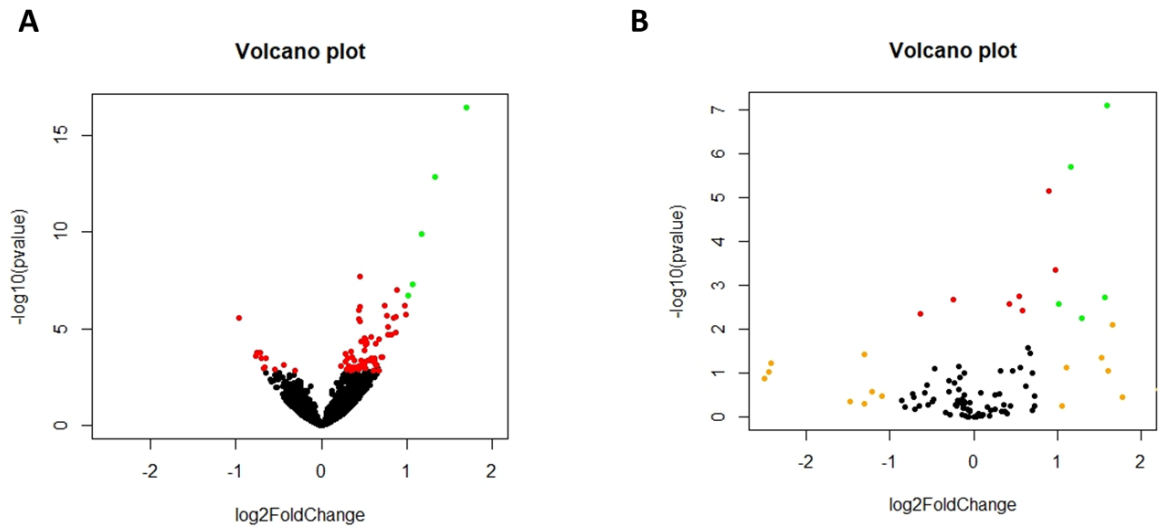

Figure 1. Volcano plots of RNA-seq and miRNA-seq data, generated using RStudio software (version 3.5). Volcano (scatter) plots of the **A)** genes and **B)** miRNAs, illustrating the significantly differentially expressed genes in red (adjusted p-value >0.1), with upregulated genes in orange, significantly so in green.

Table 1. Differentially expressed miRNAs after DESeq2 normalisation. Padj: adjusted p value.

Rank	***Gene name***	***log2FoldChange***	***pvalue***	***padj***
1	miR-23a	1.589327206	7.80E-08	7.72E-06
2	hsa-miR-146a-5p	1.160470593	2.03E-06	0.000101
3	hsa-miR-200c-3p	0.894925383	7.02E-06	0.000232
4	hsa-mir-664	0.969208828	0.00045	0.011141
5	hsa-miR-17-5p	2.328991692	0.001485	0.02563
6	hsa-miR-200a-3p	0.535626255	0.001807	0.02563
7	hsa-miR-30a-5p	-0.251709487	0.002071	0.02563
8	miR-4539	1.560949137	0.001862	0.02563
9	hsa-miR-200b-3p	0.419178352	0.002571	0.025827
10	miR-200c	1.008562632	0.002609	0.025827
11	hsa-let-7c-5p	0.585124726	0.003686	0.033175
12	hsa-miR-221-3p	-0.63918125	0.00432	0.035643
13	hsa-miR-196a-5p	1.284004995	0.005683	0.043275
	----------	----------	----------	----------
20	hsa-miR-21-5p	0.550821518	0.075228	0.334625
89	hsa-miR-210-3p	-0.279442101	0.860249	0.95818

5. 2. II. b) The effect of hypoxia on the differentially expressed miRNAs

In order to determine if the DE miRNAs were also involved in the hypoxic response, their expression level was measured in PCa cell lines following 24h hypoxic culture relative to normoxia, by RT-qPCR.

The melt curves were inspected to confirm robust expression in the cell lines, and at this point miR-23a was excluded from the investigations since multiple peaks were observed, indicating poor primer specificity for the sequence. However, miR-146a, miR-196a, and miR-30a were all detected in at least one cell line. MiR-30a, despite being expected to have tumour-suppressive functions based on the biopsy and TCGA data, was increased by hypoxia, and miR-146a was slightly induced by hypoxia at 24h but no further by 48h suggesting it was not regulated by hypoxia in a linear fashion (data not shown).

MiR-196a was upregulated by 24h hypoxia in PC3 and more so by 48h in 22Rv1 in a linear fashion. Moreover, PubMed searches revealed that miR-196a has never previously been implicated in PCa, yet gene ontology (GO) analysis of the predicted mRNA targets of miR-196a using the online tool DAVID v6.8 revealed significant functional enrichment of cancer-related pathways including prostate cancer (Figure 2). Therefore, miR-196a was considered a potentially novel hypoxamiR of interest in PCa, and was selected for functional studies using 22Rv1 and PC3.

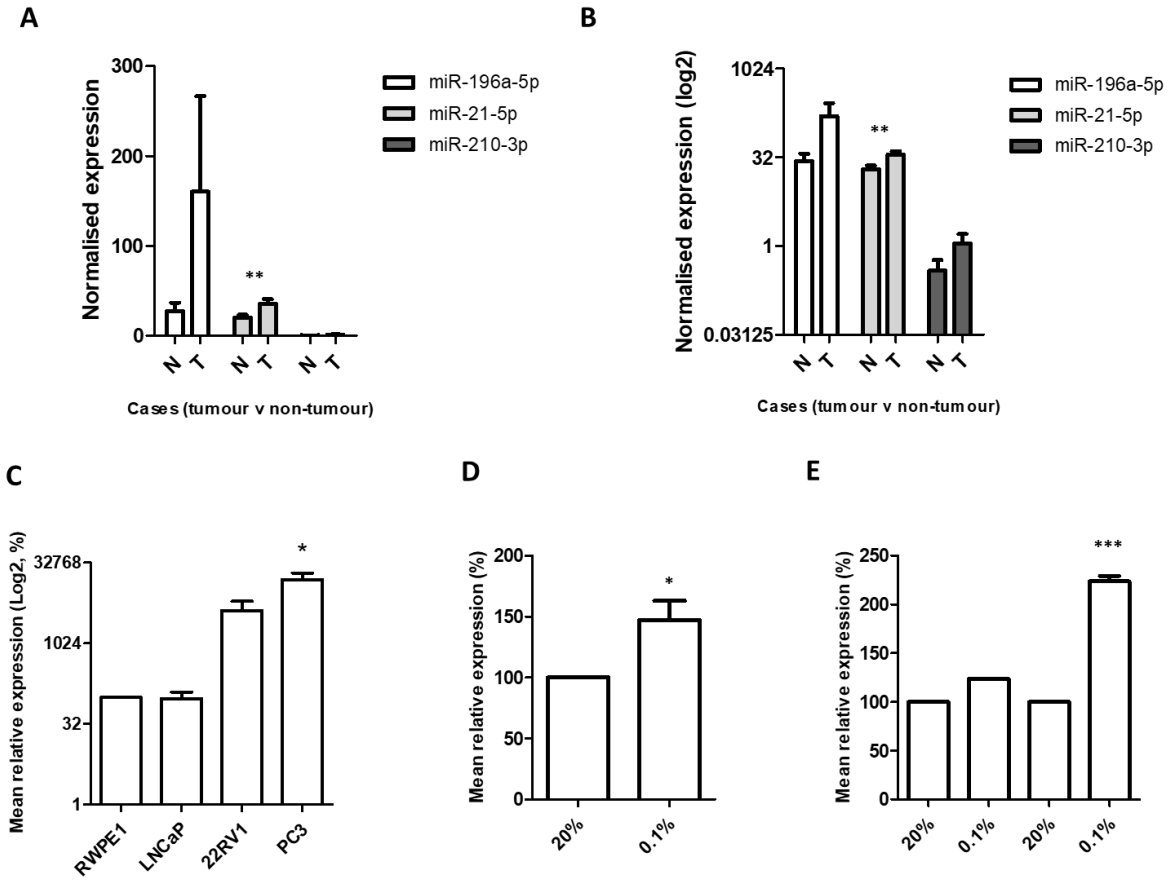

F

Term	Count	%	P-Value	Benjamini
Thyroid hormone signaling pathway	11	3.6	7.40E-05	1.60E-02
Prostate cancer	9	2.9	2.90E-04	3.00E-02
Transcriptional misregulation in cancer	12	3.9	3.90E-04	2.70E-02
Chronic myeloid leukemia	8	2.6	4.70E-04	2.40E-02
Cell cycle	9	2.9	2.80E-03	6.40E-02
MicroRNAs in cancer	14	4.6	3.70E-03	7.50E-02
FoxO signaling pathway	9	2.9	4.50E-03	8.30E-02
Small cell lung cancer	7	2.3	6.10E-03	1.00E-01
Glioma	6	2	8.40E-03	1.20E-01
Colorectal cancer	5	1.6	3.20E-02	3.10E-01
HIF-1 signaling pathway	6	2	3.90E-02	3.30E-01

Figure 2. MiR-196a implicated as a novel hypoxamiR with important functions in PCa. A) Comparison of normalised expression levels of miR-210, miR-21, and miR-196a in non-tumour and tumour samples. Results of two-way two-tailed t-tests comparing tumour with non-tumour samples' normalised expression level: miR-196a p=0.216, miR-21 p=0.004, miR-210 p=0.206. **B)** Log2 scaled version of the graph for greater clarity. **C**) RT-qPCR detection of miR-196a in prostate cell lines. **D)** MiR-196a upregulated by 24h hypoxia (0.1% O_2) relative to normoxia (20% O_2). **E)** MiR-196a upregulated by 24h hypoxia in 22Rv1 and significantly by 48h. **F)** DAVID gene ontology analysis of the list of predicted mRNA targets of miR-196a reveals enrichment of cancer-related functions. The mean + SEM is shown. One-way t-tests were used to compare condition means to the control (hypothetical value 100) and p-values considered significant when *p<0.05, **p<0.01, ***p<0.001.

5. 2. II. c) Functionality of miR-196a

To determine if hypoxia-induced miR-196a could contribute to PCa progression, cells were transfected with the pre-miR-196a molecule, using lipofectamine as described in Methods section *2.1.I.e*. Following overexpression, phenotypic assays were used to evaluate its effect on cell function (XTT assay, colony forming assay, and Boyden chamber migration assay, as described in Methods section *2.1.III*). However, the phenotypic assays revealed no consistent effect on cell proliferation, colony forming ability, or migration. Across the cell lines PC3, 22Rv1, and LNCaP, replicates were highly varied and the effects appeared to depend on the cell lines used, for instance miR-196a increased colony forming ability in 22Rv1 yet reduced it in PC3 and RWPE-1 (data not shown).

The DAVID analysis as well as Pubmed searching was used to identify a panel of specific genes considered to have tumour suppressive functions, or an involvement in hypoxic signalling. Three of these were detectable in the cell line 22Rv1 (*PRUNE2, FOXO1,* and *BACH1*) but none of these were significantly reduced at the mRNA level following transfection with pre-miR-196a based on three biological replicates (data not shown).

Therefore, the *in vitro* experiments suggested that miR-196a overexpression alone did not consistently increase proliferation, clonogenicity, nor migration in PCa cell lines. Furthermore, investigation of several proposed mRNA targets did not reveal targeting of known tumour suppressors. This could mean that miR-196a does not have a driving role in PCa disease progression. Instead, miR-196a could have been overexpressed in a "passenger" type effect (due to the activity of a more important upstream regulator) rather than a driver. Alternatively, miR-196a could have been upregulated in non-epithelial cell types in the tumours and contributing to their phenotypes which indirectly leads to tumour development, for instance, affecting the integrity of stromal or immune cells.

However, it is important to note the limitations of these assays in determining oncogenic effect, as they cover relatively few behaviours and it is possible that the miRNA exerts an oncogenic only when dysregulated in combination with other miRNAs, or dependent on another feature of the tumour microenvironment. Therefore, to investigate further the potential influence of miR-196a on the tumour samples, the RNA-seq and miRNA-seq data was probed further by pathway analysis.

5. 2. II. d) Ingenuity Pathway Analysis (IPA) analysis of the sequencing data

The program Ingenuity Pathway Analysis (IPA, Qiagen Bioinformatics) was used to explore potential networks related to miR-196a to attempt to identify novel pathways or regulators in PCa (https://www.qiagenbioinformatics.com/products/ingenuity-pathway-analysis/). Pathway analysis is an effective means of probing omics data to identify the biological causes of the observed changes in gene

expression. Furthermore, the mRNA-seq and miRNA-seq data was integrated to identify novel mRNA : miRNA pairs.

IPA is a highly sophisticated software that is suitable for most forms of omics data, and what sets it apart from tools like DAVID is that it takes into consideration the direction and magnitude of each gene's expression, as well as the statistical significance. IPA enables visualisation of the DE genes, and has extensive annotations such as localisation in the cell, type of molecule (i.e., enzyme, receptor, transcription factor), and biomarker applications. It has a rigorously curated functional database, including miRNA : mRNA sequence predictions and disease signalling annotations.

The network and upstream regulator analyses did not highlight any novel pathways, only already characterised regulators such as Myc signalling. However, the integrative analysis of the miRNA-seq and mRNA-seq data revealed that several predicted mRNA targets of miR-196a were significantly inversely correlated. A network was built containing miR-196a and its inversely DE targets, highlighting those previously implicated in PCa, and linked with Apoptosis signalling (Figure 9) and angiogenesis (since hypoxia was not an option) (Supplementary Figure 3). This analysis suggests that the targets such as *COL15A1* could be interesting future targets to analyse, it is involved with PCa, or TRAF6 which is involved in apoptosis signalling, or *IGFBP3*, which has been linked to both PCa and angiogenesis. None of these have previously been validated as targets of miR-196a in PCa. Therefore, the oncogenic effects of miR-196a could be linked with the regulation of one or more of these cancer-associated targets.

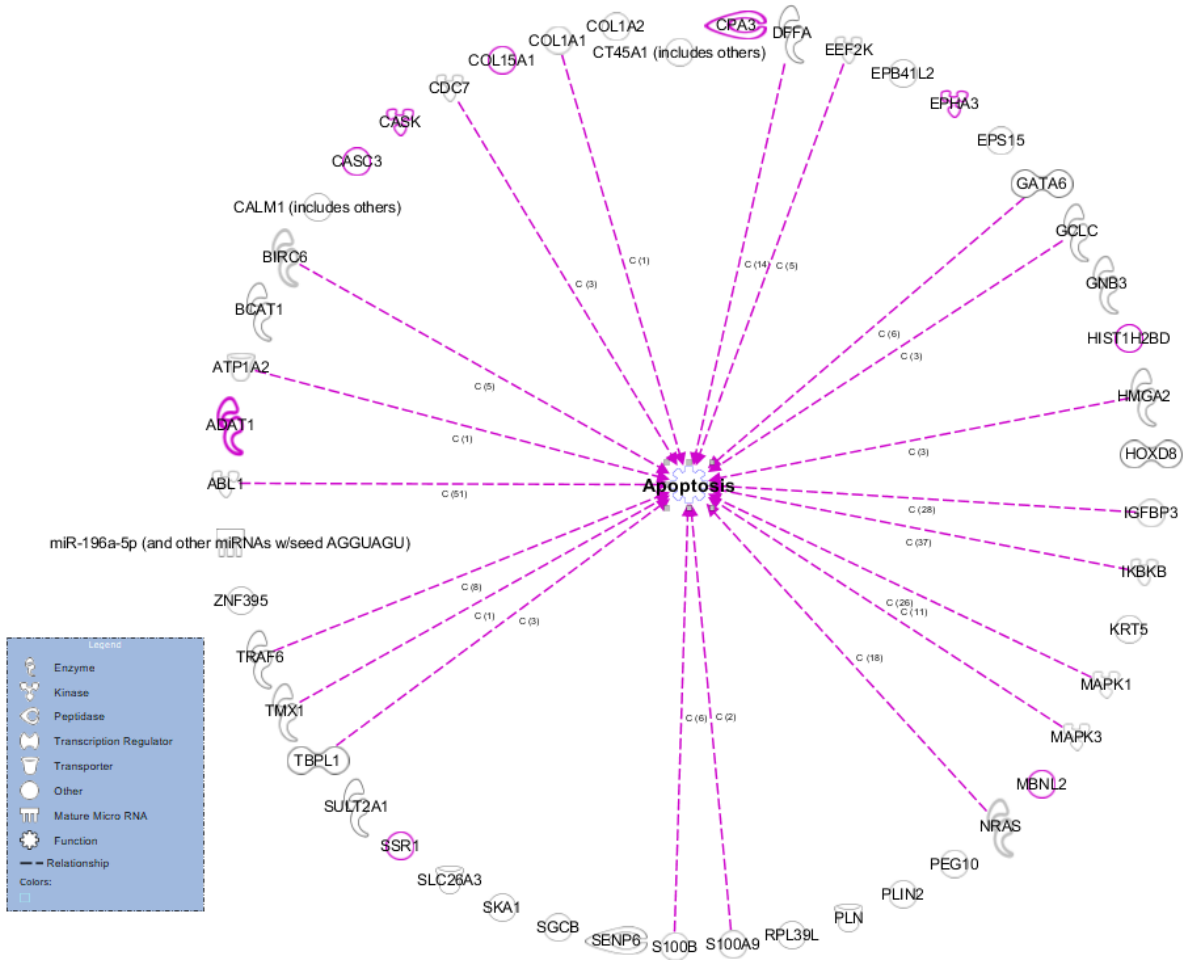

Figure 9. Integrative Analysis of mRNA-seq and miRNA-seq data using IPA reveals numerous predicted mRNA targets of miR-196a with significant inverse expression correlation. MiR-196a was significantly upregulated in the miRNA-seq dataset, the other proteins represent mRNAs with seed-binding complementarity that were significantly downregulated in the mRNA-seq data. Pathway overlay with "prostate carcinoma" disease used to highlight molecules previously implicated in PCa (molecules highlighted in purple). Pathway build with "Apoptosis" function used to illustrate the molecules known to be implicated in apoptosis (connected by purple arrows in the direction of regulation, dashed lines indicate indirect regulation, full lines indicate direct). The shape of each icon identifies the type of molecule, as coded in the legend.

5. 2. III. Discussion

5. 2. III. a) Summary

This study utilised an RNA-seq approach to characterise a cohort of prostate biopsy samples. The approach has several strengths, such as an unbiased identification of DE molecules. Furthermore, we utilised the DESeq2 method for normalisation, which is a Bayesian approach that improves on several problems caused by the standard log fold change analysis. These are: that small changes that are statistically highly significant but biologically unimportant are weighted too heavily, that the number of significantly differentially expressed genes that are identified is affected by the number of samples being compared, and that the ranking by fold change is sensitive to noise from low counting genes (based on the base mean) (Love, Huber and Anders, 2014). Therefore, because the DESeq2 method is highly stringent it produces a much shorter list of significant genes than standard methods, although these changes are more likely to be biologically relevant. Indeed, our results were similar to TCGA data, confirming its reliability.

5. 2. III. b) Future directions

The RNA-seq analysis highlighted miR-196a as one of several DE miRNAs, for the first time in PCa. Furthermore it was upregulated by hypoxia as has previously been reported in liver cancer (Hu *et al.*, 2018). Several of the targets of miR-196a are involved in the regulation of the cell cycle and other cancers, suggesting an effect on cancer progression. However, preliminary *in vitro* overexpression and functional studies failed to isolate a growth-promoting effect of miR-196a in PCa cell lines. Future investigations could perform these phenotypic assays using more replicates which may clarify an effect. However, these assays are limited in that they can only measure one aspect of cell behaviour, and a very drastic effect must be elicited for the cells to behave significantly differently. Additionally, the activity of miR-196a could depend on other miRNAs or genes that are modulated in the context of the tumour but absent from this model. Therefore, it may be best to focus on a different feature of carcinogenesis, such as regulation of apoptosis, to determine how miR-196a may contribute to PCa development. MiR-196a's involvement in apoptosis signalling could be investigated experimentally by methods similar to those suggested for miR-21 in chapter 4 section (*4.3.II*).

Another benefit of the RNA-seq approach was the large amount of data that was provided. I chose to investigate miR-196a, although there are numerous other miRNAs that were DE and may be interesting to focus on for further research. Pathway analysis using IPA was used to integrate the miRNA-seq and mRNA-seq data and highlighted inversely DE mRNA: miRNA target pairs, of which some mRNAs are known regulators of apoptosis or angiogenesis, but have never been validated experimentally as targets in PCa. These could be explored in the manner shown in chapter 3, using RT-qPCR and Western blot to initially monitor the effect on the target levels, followed by luciferase reporter assay. Alterantively, an unbiased approache to miRNA taret identification could be used, such as CLASH (crosslinking ligation and sequencing of hybrids), which involves crosslinking miRNAs to their targets *in vitro* or *in vivo*, followed by immunoprecipitation of the miRNA and sequencing, to identify novel targets (Helwak and Tollervey, 2014).

Another option for future research would be to obtain samples of benign prostatic hyperplasia (BPH) tissue, which as mentioned in General Introduction section *1.1. V.*, is non-cancerous but often mistaken for PCa during screening. Identifying DE miRNAs or mRNAs in the PCa samples relative to BPH could help identify the most important miRNAs contributing to PCa development, and could be useful additions to screening panels to distinguish the cancer cases.

Finally, it is important to acknowledge that this is a relatively small sample size, and a large number of samples would presumably be more powerful. The study could be replicated on a larger population, or perhaps including more aggressive, metastatic, or therapy-resistant tumours. However, this was useful as an exploratory pilot project, to illustrate the potential of the approach. Overall, the use of RNA-seq to elucidate the molecular profiles of these biopsy samples has opened extensive opportunities for further research.

5. 3. Part 2: The effect of hypoxia on global and regional methylation as measured by methylation array

5. 3. I. Introduction

As mentioned in the General Introduction section 1.1. VII., gene expression is regulated by epigenetic modifications, of which the most widely studied is DNA methylation on cytosine residues. Certain tumour-suppressors have been reported to be silenced in PCa due to hypermethylation of the promoter region, such as *GSTP1*, which has been thoroughly examined as a methylation-based biomarker for PCa in tissues and liquids and can be detected by methylation specific PCR (Martignano *et al.*, 2016). MiRNA expression is also governed by DNA methylation in PCa, for instance miR-200c and miR-141 (Lynch *et al.*, 2016b). However, to the best of my knowledge the regulation of miRNA expression by DNA methylation during hypoxia in PCa has never been investigated.

A previous project from our laboratory showed that in the prostatectomy cohort, the expression of miR-200c and miR-141 was regulated by DNA methylation, using the wet-lab technique pyrosequencing (Lynch *et al.*, 2016b). However, the use of this method proved laborious across the many samples. A powerful method of assessing genome-wide changes in DNA methylation is by methylation array, in which probes specific to the methylated and unmethylated forms of DNA at specific CpGs are used to quantify methylation. Several methylation arrays have been developed, such as the Illumina Infinium Human DNA Methylation 27k, 450k and 850k (EPIC) arrays, which contain approximately the respective number of probes covering the genome (Stirzaker *et al.*, 2014).

To explore the effect of hypoxia on genome-wide DNA methylation changes, the NCBI Gene Expression Omnibus (GEO) database (https://www.ncbi.nlm.nih.gov/geo/) was searched in order to obtain a publicly available dataset of hypoxic and normoxic cancer samples. Unfortunately, there were no methylation array datasets available including hypoxic PCa cell lines or tumours, which highlights that this is an understudied area.

However, a dataset was found containing the DNA methylation and hydroxymethylation profiles of non-small cell lung cancer (NSCLC) tumours, obtained using the Illumina Infinium 450k array from DNA extracted from fresh-frozen tumour samples (GEO identifier: GSE71403)(Thienpont *et al.*, 2016). The tumours had been classed as hypoxic or normoxic based on an established hypoxic gene signature (Buffa *et al.*, 2010). In the absence of a suitable PCa dataset, this data was selected to illustrate a proof-of-principle approach to the exploration of hypoxia-related genetic datasets.

Levels of DNA methylation (5mc) had been measured by BeadChip v1.2 Array and hydroxymethylation (5hmc, its oxidative product representing demethylated cytosine) by TAB-Chip array. The authors described a global reduction in 5hmc in the hypoxic tumour samples, and confirmed that it was due to reduced activity of the TET enzymes that catalyse DNA demethylation, indicating that they are oxygen-dependent

(which they subsequently validated by wet-lab methods). However, the authors had not reported the effects of hypoxia on 5mc levels in the manuscript.

5. 3. II. Results

5. 3. II. a) Download and preview of a publicly-available dataset

The dataset was downloaded from GEO using RStudio v3.5 and the TAB-chip data was removed from the BeadChip data using the 'remove samples' function. The data was visually inspected by box and whisker plot, which suggested that it may contain an outlier (sample 14, Figure 11, later removed). The β-value reports the ratio of intensities between methylated and unmethylated alleles, where a β=0 value means the sites were invariably unmethylated on all fragments assayed, and β=1 where the sites were fully methylated.

Next, the RnBeads package and Ghostscript interpreter software were downloaded for Exploratory and Differential analyses (Assenov *et al.*, 2014), which has previously been used successfully to characterise genome-wide methylation profiles (see Methods section *2. 4. III.*)(Mackin, O'Neill and Walsh, 2018a)(Irwin *et al.*, 2019). The Exploratory analysis enables visualisation of overall difference in methylation level between the conditions and by type of genomic region (such as at CpG islands, as described General Introduction section *1.1. VII*.). The Differential analysis quantifies the difference in methylation at each probe between the conditions, and maps the differentially methylated CpGs to specific genomic regions, providing lists of differentially methylated loci (coordinates, and associated genes and promoters).

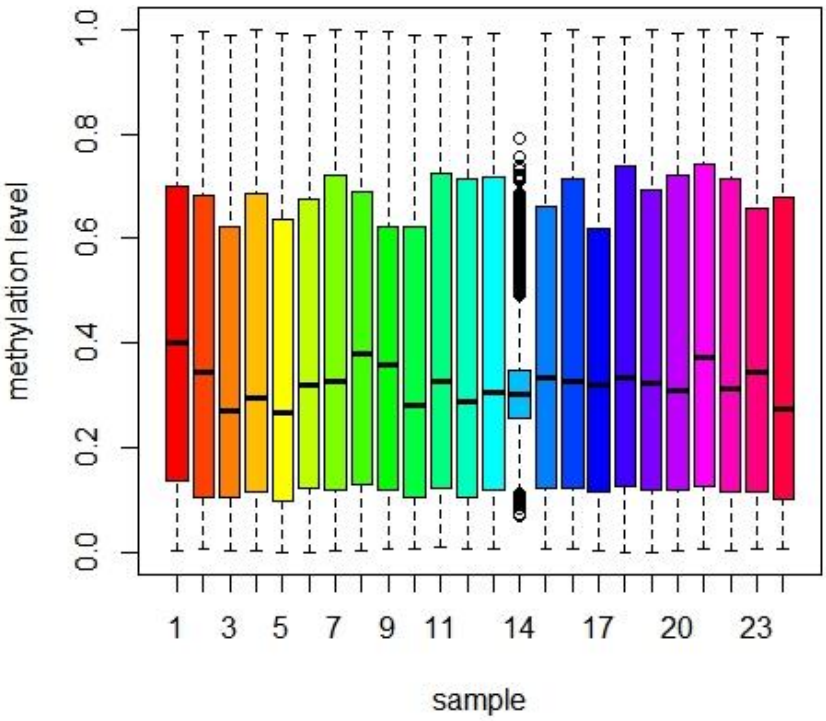

Figure 11. Box and whisker display of methylation distribution per sample in the NSCLC dataset (GEO identifier: GSE71403). Samples 1-12 represent the hypoxic tumours and 13-24 the normoxic tumours, as pre-determined by the authors using a hypoxia metagene score. The whiskers depicts the minimum and maximum methylation values in the sample and the box depicts the median with first and third quartile (interquartile range). The data was from the BeadChip 450k human methylation array, which measures 5mc (methylation) levels, provided as the β-level which reports ratio of intensities between unmethylated and methylated alleles, where 0 is unmethylated and 1 fully methylated. Y-axis: methylation β level, x-axis: patient sample. The graph reveals abnormal methylation levels in sample 14 which could be an outlier. Colours: rainbow pattern, not corresponding to any sample characteristic. Welch Two Sample t-test comparison of mean normoxic versus hypoxic samples p=0.9642.

5. 3. II. b) RnBeads Exploratory Analysis

5. 3. II. b) i) Multivariate analysis

First, multidimensional scaling (MDS) and principal component analysis (PCA) methods were used to inspect the dataset for clustering of the methylation profiles. These are methods of "dimension reduction" and involve mapping the data to a lower dimensional space which maximises (and allows visualisation of) the most evident source of variance between them (Li, 2010). PCA and MDS differ based on their input; the PCA input is the original vectors in n-dimensional space with the data projected in the direction with the most variance (*i.e.*, based on the angles between vectors), which roughly maintains the spread of data and is best for large datasets. The MDS input is the pairwise distances between points (*i.e*. based on distances between points) transformed into 2-dimensional space, which preserves the distance between points and thus better represents their multivariate dissimilarity (Lacher and O'donnell, 1988). Both of these approaches produced a faint clustering of the normoxic samples compared with hypoxic at the second PCA component, with the exception of one (hypoxic sample number 7) which clustered with the normoxic (Figure 12). This indicated that the normoxic and hypoxic samples had distinct relatedness based on their methylation profiles. At this point, the outlier sample 14 had been removed using RStudio (remove function), as it had indeed appeared to be skewing the data as evident by dimension reduction (Supplementary Figure 4).

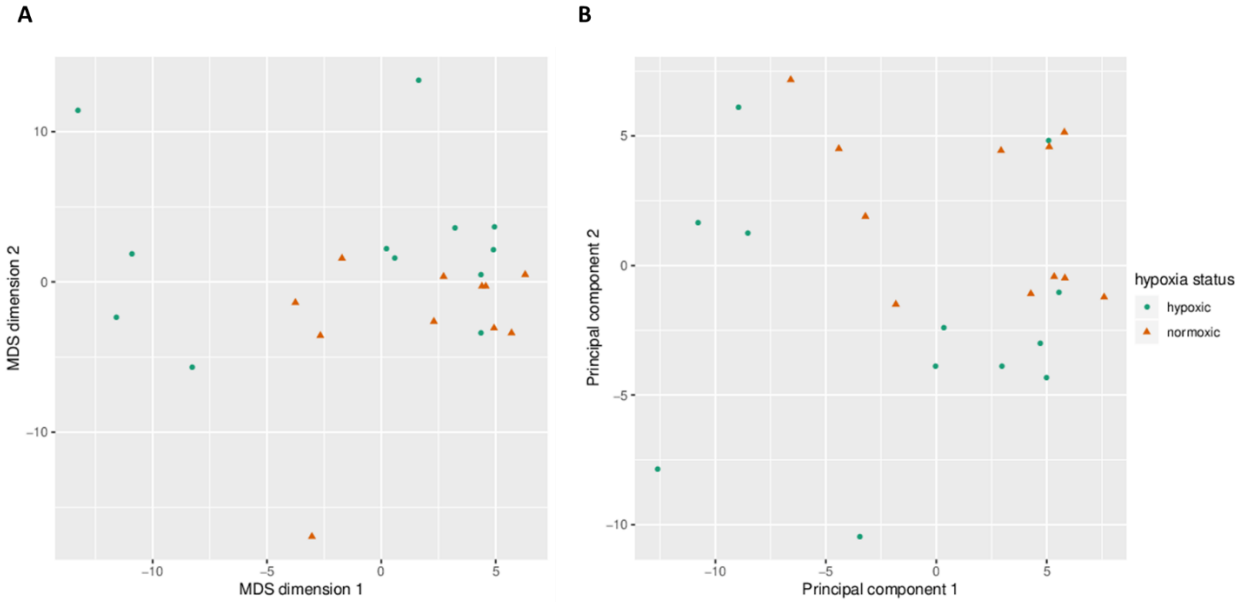

Figure 12. Principal component analysis (PCA) and multidimensional scaling (MDS) methods of dimension reduction. Sample 14 has been excluded. Euclidean distance used as a dissimilarity metric. Each point represents a sample, colour and shape distinguish hypoxic status where green circles are tumours classed as hypoxic and orange triangles normoxic. **A)** MDS applied to the dataset reveals clustering of the hypoxic samples with the exception of one (identifier: sample 7). **B)** PCA applied to the dataset similarly segregates hypoxic samples, with the exception of one sample (identifier: sample 7).

5. 3. II. b) ii) Methylation value distributions

The multivariate analysis indicated variance between the methylation profiles of the hypoxic and normoxic data. To compare their overall methylation levels, methylation density plots were used to quantify the densities of probes with high and low methylation values. The data was separated based on 4 types of genomic regions covered: promoter regions, genes, CpG islands, and tiling (units of approximately 5000 base pairs). Interestingly, the methylation density plots revealed global hypomethylation of the hypoxic data compared with normoxic data. Figure 13 illustrates the reduced density of highly methylated probes (indicating hypomethylation) across total probes, tiling regions, and promoter and gene regions in the hypoxic samples, whereas CpG islands were only slightly hypomethylated.

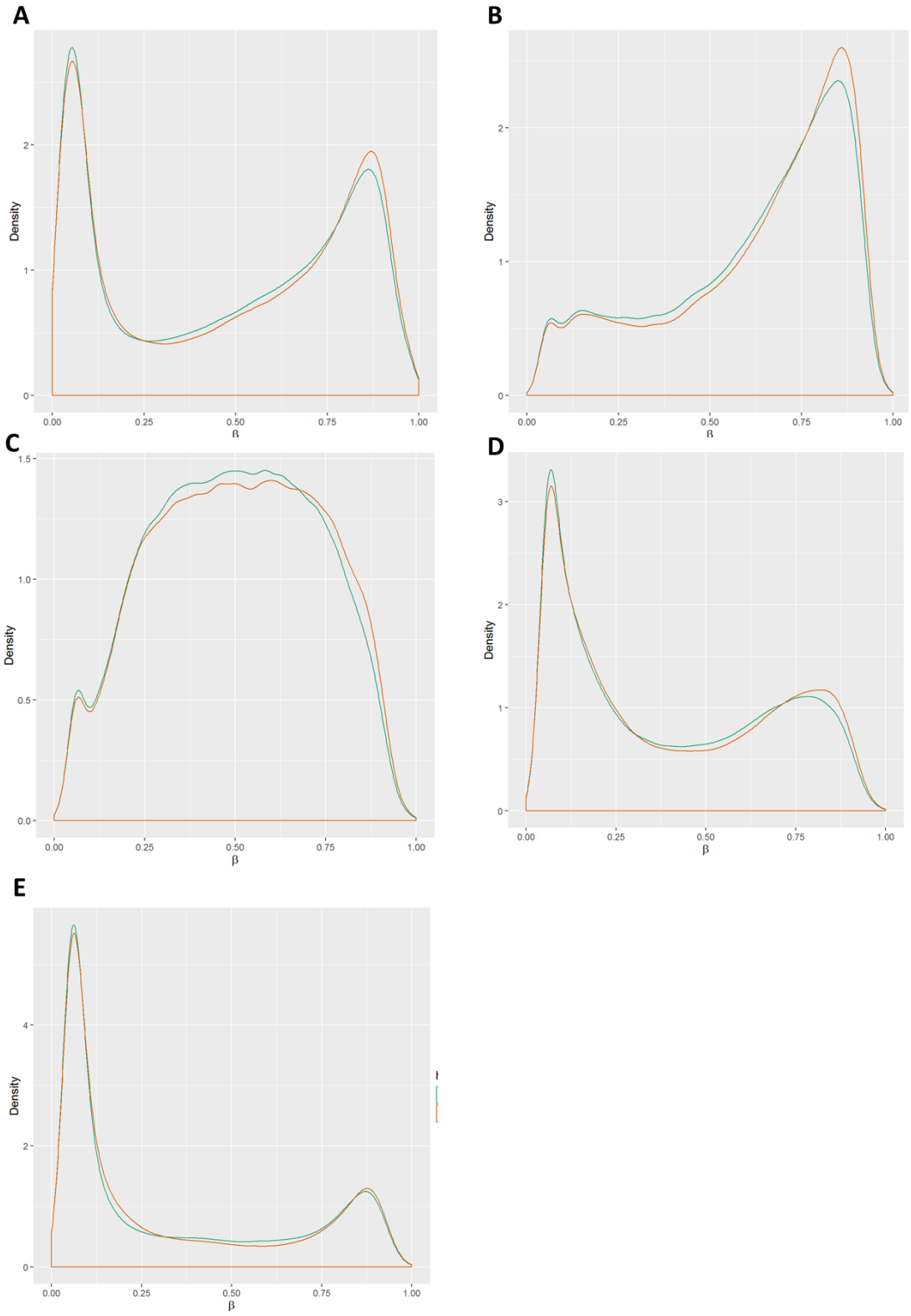

Figure 13. Methylation Value Densities by Hypoxic Status. Y-axis represents the density of probes detected corresponding to the degree of methylation status (x-axis). Hypoxic data is represented by the green lines, normoxic by the orange lines. **A)** Methylation densities across all probes, showing slightly higher densities of lowly methylated probes and a lower density of highly methylated probes in the hypoxic data, suggesting global hypomethylation due to hypoxia. **B)** Hypomethylation of tiling regions (genomic units) in hypoxic samples compared with normoxic. **C)** Hypomethylation of gene regions in hypoxic samples compared with normoxic. **D)** Hypomethylation of promoter regions in hypoxic samples compared with normoxic. **E)** Very slight hypomethylation of CpG islands in the hypoxic samples compared with normoxic samples.

5. 3. II. c) RnBeads Differential analysis

Next, a differential analysis was executed, to map DM probes to specific CpGs of the genome and estimate the differential methylation at each locus between the conditions (based on the absolute difference in methylation and the relative ratio β-value, and the statistical significance). RnBeads ranks differentially methylated CpGs across the genome where the first ranked sites are those with highest probability of differential methylation. The "combined rank" combines absolute and relative effect size with the p-value by statistical modelling to produce a single score.

Figure 14A depicts the differentially methylated sites across the genome, based on the combined rank, with the top 100 highlighted in red. This indicated that while the density of hypomethylated probes had been increased in the hypoxic samples, the top ranking DM sites in the hypoxic samples were gains in methylation. However, regarding promoter and gene regions, there was a mixture of gains and losses although the most significantly DM promoters were gains in methylation which could be associated with gene silencing. Figure 14B-C illustrates that at specifically promoters and gene regions (respectively) there was a comparable degree of gains and losses in methylation.

This highlighted that while there was broad losses in methylation across all the probes, the change in methylation was regionally specific and site specific, indicating that the regulation of the methylation of individual CpGs could be dependent on the type of locus, and thus represent altered activity of epigenetic regulators specifically governing those regions.

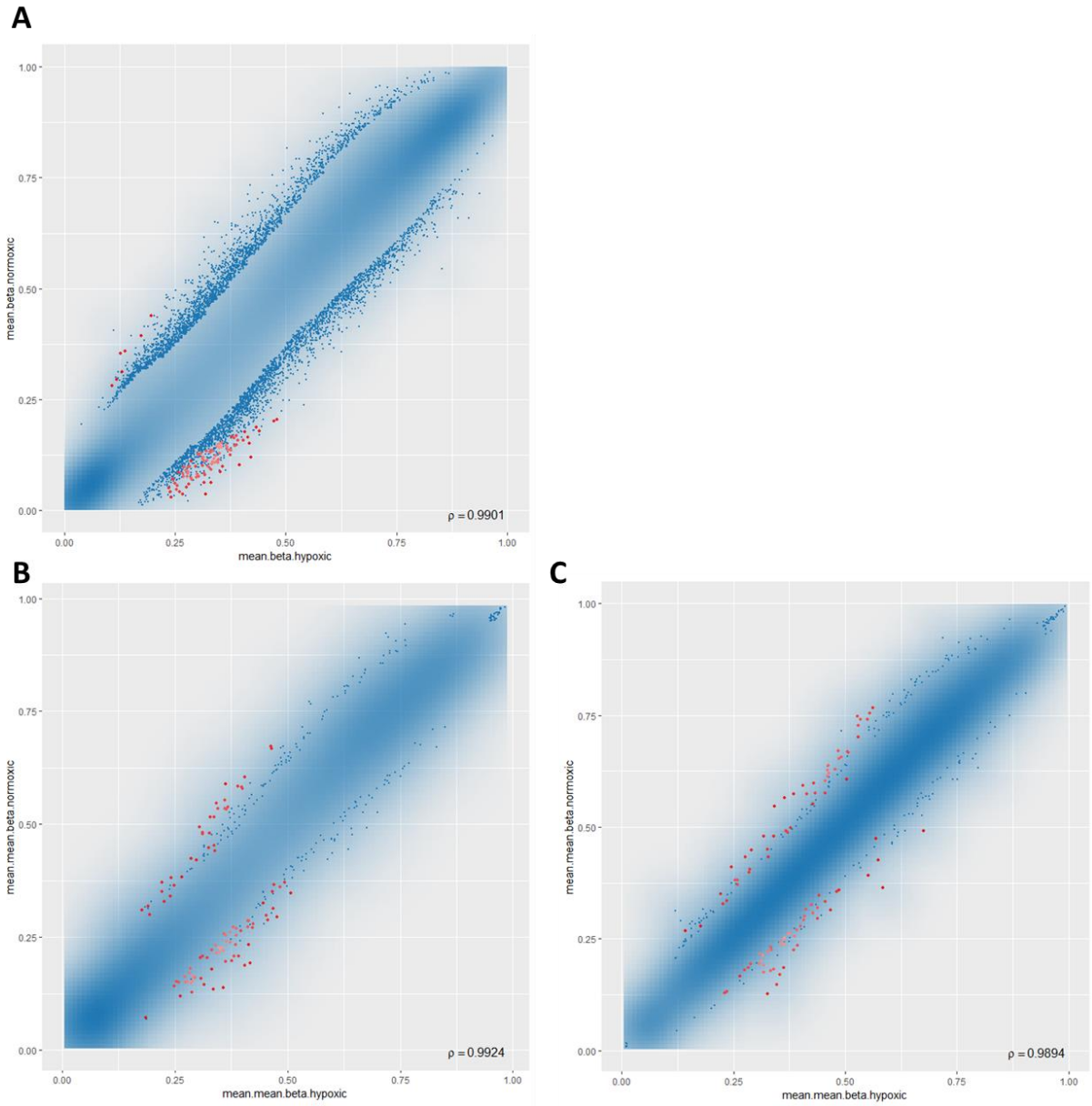

Figure 14. Differentially methylated sites in the hypoxic data relative to normoxic data. The difference in mean β value for hypoxic versus normoxic samples by CpG site, the top 100 differentially methylated sites highlighted in red according to rank. **A)** Top 100 combined rank sites (all probes) enriched for gains in methylation. **B)** Top 100 combined rank sites (promoters alone) containing a mixture of gains and losses with slight emphasis on gains, **C)** Top 100 combined rank sites (gene body regions alone) containing a mixture of gains and losses, with slight emphasis on losses.

5. 3. II. d) Functional analysis of the DM promoters and genes

Since there were different proportions of gains and losses depending on the type of genomic region, I wanted to investigate the functions of the most highly ranked DM sites.

The lists of DM genes and promoters were downloaded and functional annotation was performed using DAVID v6.8, analysing the top 100 ranking DM promoters and genes.

The top 100 ranking DM genes and promoters (after excluding probes not mapped to a known gene region) were split into those representing losses and gains in methylation and functional annotation used to identify subsets with similar functions (Tables 2-5). The full functional annotation charts containing significantly enriched gene ontologies for promoters and genes with losses and gains in methylation are available in Supplementary Tables 1-3.

Intriguingly, DAVID revealed that the promoters associated with losses in methylation were significantly enriched with GO functions "*Inflammatory response*", "*Signalling*", and "*Cell membrane*". These could potentially be upregulated if DNA methylation was a mechanism governing expression. Promoters with gains in methylation were enriched with the GO functions "*homeodomain*" and "*DNA-binding*". Likewise, it is possible that the gains in methylation could here pre-empt gene suppression.

Interestingly, there was a similar pattern regarding the gene regions, DM sites representing losses in methylation were enriched for the GO terms "*G-protein coupled receptor activity*", "*Inflammatory response*", and "*Membrane*"; while DM sites representing gains in methylation were enriched for "*Homeodomain/homeobox*", "*DNA-binding*", "*Positive regulation of transcription from RNA Pol II promoter*" and "*Negative regulation of transcription from RNA Pol II promoter*".

Finally, the miRNAs alone were analysed. The DM miRNAs from both the DM promoter and DM gene lists were extracted and ranked by combined rank, and then stratified by methylation status in hypoxia (hypo or hyper-methylated miRNAs). Interestingly, among the top 100 hypomethylated miRNAs was miR-210, and miR-205, miR-200c and miR-141, which have previously been shown by our group to be implemental in PCa (Lynch *et al.*, 2016b). According to the probes associated with both the miR-21 gene (n=2 sites analysed) and promoter (n=7 sites analysed), miR-21 was hypomethylated but was not in the top 100 combined rank positions. MiR-196a was hypermethylated based on data from both the promoter and gene lists.

The top 100 combined rank hypo- and hyper- DM miRNAs were analysed by DAVID, which highlighted that numerous were implicated in the pathway "MicroRNAs in Cancer" although no other pathways were enriched (Table 6).

Overall, the differential analysis and DAVID GO indicated that hypoxia could influence the expression of cancer-associated miRNAs *via* changes in DNA methylation, and affect the epigenetic regulation of genes

involved in inflammation, cell signalling, and transcription, and a number of miRNAs including those previously implicated in cancers.

Table 2. Functional Annotation of Promoters with losses in methylation in hypoxic samples relative to normoxic. From the top 100 combined rank promoters, n=44.

Inflammatory response	**Signalling**	**Cell membrane**
complement C3a receptor 1(C3AR1)	ADAM metallopeptidase domain 28(ADAM28)	ADAM metallopeptidase domain 28(ADAM28)
secreted phosphoprotein 1(SPP1)	calcitonin receptor like receptor(CALCRL)	GRB2 binding adaptor protein, transmembrane(GAPT)
toll like receptor 1(TLR1)	cystatin F(CST7)	calcitonin receptor like receptor(CALCRL)
toll like receptor 6(TLR6)	ecotropic viral integration site 2B(EVI2B)	complement C3a receptor 1(C3AR1)
	granzyme A(GZMA)	synaptotagmin like 1(SYTL1)
	secreted phosphoprotein 1(SPP1)	toll like receptor 1(TLR1)
	toll like receptor 1(TLR1)	toll like receptor 6(TLR6)
	toll like receptor 6(TLR6)	tumor protein p53 inducible protein 13(TP53I13)
	transcobalamin 1(TCN1)	
	tumor protein p53 inducible protein 13(TP53I13)	

Table 3. Functional Annotation of Promoters with gains in methylation in hypoxic data relative to normoxic. From the top 100 combined rank promoters, n=56.

Homeodomain	**DNA-binding**
NK1 homeobox 1(NKX1-1)	NK1 homeobox 1(NKX1-1)
NK2 homeobox 3(NKX2-3)	NK2 homeobox 3(NKX2-3)
homeobox A11(HOXA11)	T-box 1(TBX1)
homeobox A3(HOXA3)	T-box 20(TBX20)
homeobox B7(HOXB7)	T-box 4(TBX4)
homeobox D9(HOXD9)	T-box 5(TBX5)
iroquois homeobox 2(IRX2)	homeobox A11(HOXA11)
	homeobox A3(HOXA3)
	homeobox B7(HOXB7)
	homeobox D9(HOXD9)
	iroquois homeobox 2(IRX2)
	zinc finger protein 132(ZNF132)
	zinc finger protein 382(ZNF382)

Table 4. Functional Annotation of Genes with Losses in methylation in hypoxic data relative to normoxic. From the top 100 combined rank promoters, n=51.

G-protein coupled receptor activity	Inflammatory response	Membrane
olfactory receptor family 4 subfamily C member 12(OR4C12)	CD163 molecule(CD163)	CD163 molecule(CD163)
olfactory receptor family 4 subfamily C member 3(OR4C3)	S100 calcium binding protein A8(S100A8)	S100 calcium binding protein A8(S100A8)
olfactory receptor family 5 subfamily AN member 1(OR5AN1)	pyrin domain containing 2(PYDC2)	carcinoembryonic antigen related cell adhesion molecule 4(CEACAM4)
olfactory receptor family 51 subfamily A member 2(OR51A2)		epithelial mitogen(EPGN)
olfactory receptor family 8 subfamily B member 12(OR8B12)		glycophorin A (MNS blood group)(GYPA)
olfactory receptor family 8 subfamily H member 2(OR8H2)		myc target 1(MYCT1)
purinergic receptor P2Y10(P2RY10)		olfactory receptor family 4 subfamily C member 12(OR4C12)
taste 2 receptor member 1(TAS2R1)		olfactory receptor family 4 subfamily C member 3(OR4C3)
		olfactory receptor family 5 subfamily AN member 1(OR5AN1)
		olfactory receptor family 51 subfamily A member 2(OR51A2)
		olfactory receptor family 8 subfamily B member 12(OR8B12)
		olfactory receptor family 8 subfamily H member 2(OR8H2)
		purinergic receptor P2Y10(P2RY10)
		solute carrier family 9 member A7(SLC9A7)
		taste 2 receptor member 1(TAS2R1)
		transmembrane 4 L six family member 1(TM4SF1)

Table 5. Functional Annotation of Genes with Gains in methylation in hypoxic data relative to normoxic. From the top 100 combined rank promoters, n=49.

Homeodomain, homeobox	**DNA-binding**	**Positive regulation of transcription from RNA Pol II promoter**	**Negative regulation of transcription from RNA Pol II promoter**
ISL LIM homeobox 2(ISL2)	Fer3 like bHLH transcription factor(FERD3L)	NK2 homeobox 3(NKX2-3)	Fer3 like bHLH transcription factor(FERD3L)
NK1 homeobox 2(NKX1-2)	ISL LIM homeobox 2(ISL2)	achaete-scute family bHLH transcription factor 1(ASCL1)	SRY-box 14(SOX14)
NK2 homeobox 3(NKX2-3)	NK1 homeobox 2(NKX1-2)	homeobox D10(HOXD10)	achaete-scute family bHLH transcription factor 1(ASCL1)
T-cell leukemia homeobox 1(TLX1)	NK2 homeobox 3(NKX2-3)	homeobox D9(HOXD9)	homeobox D9(HOXD9)
homeobox B13(HOXB13)	SRY-box 14(SOX14)	orthodenticle homeobox 2(OTX2)	
homeobox D10(HOXD10)	T-cell leukemia homeobox 1(TLX1)	paired box 7(PAX7)	
homeobox D9(HOXD9)	achaete-scute family bHLH transcription factor 1(ASCL1)		
iroquois homeobox 1(IRX1)	homeobox B13(HOXB13)		
orthodenticle homeobox 2(OTX2)	homeobox D10(HOXD10)		
paired box 7(PAX7)	homeobox D9(HOXD9)		
	iroquois homeobox 1(IRX1)		
	oligodendrocyte transcription factor 1(OLIG1)		
	orthodenticle homeobox 2(OTX2)		
	paired box 7(PAX7)		
	zinc finger protein 132(ZNF132)		
	zinc finger protein 418(ZNF418)		
	zinc finger protein 542, pseudogene(ZNF542P)		

Table 6. Analysis of DM miRNAs only. From the list of DM genes and promoters, the miRNAs were extracted, and then the top 100 combined rank miRNAs were split by methylation status (hypermethylated (italicised) and hypomethylated). Those highlighted by DAVID as involved in the KEGG pathway "microRNAs in Cancer" are highlighted in bold.

Hypomethylated (from promoter list, n=82)	***Hypermethylated (from promoter list n=18)***	**Hypomethylated (from gene list n=70)**	***Hypermethylated (from gene list n=30)***
miR-4437	*miR-4646*	**miR-205hg**	*miR-184*
miR-4513	*miR-5691*	**miR-128-1**	*miR-145*
miR-2053	*miR-641*	miR-382	*miR-551a*
miR-4760	***miR-125b-1***	**miR-485**	*miR-1306*
miR-1298	*miR-99b-1*	miR-54812	*miR-130b*
miR-887	*miR-224*	miR-1298	*miR-1908*
miR-181b-1	*miR-452*	miR-181a-1	*miR-302a*
miR-181a-1	*miR-320c-1*	miR-214	*miR-663a*
miR-718	***miR-30d***	miR-489	***miR-let-7f-2***
miR-3714	***miR-126***	**miR-181b-1**	*miR-542*
miR-214	*miR-196a-2*	**miR-100**	*miR-503*
miR-770	*miR-629*	miR-543	*miR-503hg*
miR-320d-2	***miR-124-2***	miR-592	*miR-143hg*
miR-653	*miR-3170*	miR-379	*miR-346*
miR-4897	*miR-3185*	**miR-181a-1hg**	***miR-25***
miR-548f-2	*miR-3622a;mir3622b-8*	miR-139	*miR-193a*
miR-205hg	***miR-let-7a-1***	miR-595	*miR-3663*
miR-511-2	*miR-196a-1*	**miR-494**	*miR-1180*
miR-511-1		miR-514a-1	*miR-1289-2*
miR-128-1		miR-301a	*miR-196a-2*
miR-2117		miR-2117	*miR-1178*
miR-100		**miR-141**	*miR-148b*
miR-512-2		miR-758	***miR-126***
miR-5700		miR-495	***miR-199a-2***
miR-1179		miR-509-1	***miR-129-2***
miR-5010		miR-519a-2	***miR-30a***
miR-147a		miR-4664	*miR-4508*
miR-764		miR-140	*miR-34a*
miR-223		**miR-193b**	*miR-124-2*
miR-548a-1		miR-323a	*miR-196a-1*
miR-let-7a-2		miR-223	
miR-153-2		miR-4444-1;miR-4444-2	
miR-626		miR-154	
miR-1304		**miR-449a**	
miR-200c		miR-568	
miR-4439		miR-138-2	
miR-495		miR-647	
miR-550a-3		miR-598	
miR-549		**miR-143**	
miR-128-2		miR-1208	

Hypomethylated (from promoter list, n=82)	***Hypermethylated (from promoter list n=18)***	**Hypomethylated (from gene list n=70)**	***Hypermethylated (from gene list n=30)***
miR-3935		miR-659	
miR-3646		miR-585	
miR-592		miR-665	
miR-595		miR-31hg	
miR-141		miR-517a	
miR-490		miR-211	
miR-891b		**miR-133b**	
miR-1514a-1		miR-4297	
miR-1249		**miR-200c**	
miR-548i-2		miR-519b	
miR-550a-1		miR-425	
miR-1265		miR-381hg	
miR-889		miR-431	
miR-5684		miR-563	
miR-1251		miR-519c	
miR-154		miR-377	
miR-329-2		miR-1914	
miR-1912		miR-892a	
miR-1283-1		miR-487b	
miR-365a		miR-4323	
miR-1257		miR-299	
miR-4752		miR-4724	
miR-4425		miR-133bhg	
miR-4418		miR-1193	
miR-3166		miR-410	
miR-509-3		miR-409	
miR-570		miR-4444-1;miR-4444-2	
miR-649		**miR-17hg**	
miR-514a-3		miR-330	
miR-193b		**miR-210**	
miR-4444-1; miR-4444-2			
miR-7-2			
miR-567			
miR-541			
miR-4801			
miR-2113			
miR-3907			
miR-5708			
miR-122			
miR-4664			
miR-3917			
miR-5588			

5. 3. III. Discussion

5. 3. III. a) Summary

A link between hypoxia and DNA methylation has been emerging, as emphasised by a recent review on the effect of hypoxia on epigenetics, which can partly be attributed to the reduced activity of key enzymes such as the demethylating TETs, or reduced expression of enzymes such as DNMT1 due to HIF signalling (Camuzi *et al.*, 2019). Accordingly, my analysis indicates a profound effect of hypoxia on DNA methylation.

The initial exploratory analysis suggested that hypoxia was associated with global hypomethylation in this NSCLC dataset, with particular hypomethylation of promoters and gene regions while CpG islands were largely unaffected. However, this could reflect the natural hypomethylated state of CpG islands (with the exception of CpG islands that regulate imprinted regions) which endured little changes while suggesting that hypoxia was inducing hypomethylation specifically at regions that regulate somatic gene expression. This hypomethylation could be due to a reduction in levels of the methyl donor S-adenosylmethionine, as occurred during hypoxia in liver cells (Liu *et al.*, 2011).

The Differential Analysis was used to identify individual promoters and genes that were differentially methylated between the hypoxic and normoxic conditions. The gene ontology analysis revealed that hypoxia was associated with hypomethylation of promoters regulating "*Inflammatory response*", "*Signalling*", and "*Cell membrane*", and hypermethylation of promoters regulating "*homeodomain*" and "*DNA-binding*". Therefore, hypoxia may induce inflammatory signalling or morphological changes *via* hypomethylation, and suppress development-associated transcription *via* hypermethylation of Hox-genes and other transcription factors. The enrichment of inflammatory associated genes was particularly intriguing, since cancer cells are known to modulate inflammatory pathways following hypoxia (and indeed the two pathways often go hand-in-hand, as outlined in General Introduction section *1.2. II*), although very few studies have linked this to changes in DNA methylation. One similar report comes from a group studying systemic hypoxia and cardiovascular disease, who have recently showed that systemic hypoxia in antenatal mice was associated with hypomethylation of CGIs and CPG-island shores around the transcription start sites of genes involved in inflammatory signalling (Huang *et al*>, 2019). Taken together these findings suggest that hypoxia could regulate inflammation *via* DNA methylation, in a conserved mechanism that is not specific to the cancer state. Likewise, the hypermethylation of *HOX* gene promoters (and others involved in development) suggests that hypoxia may regulate the acquisition of a stem-like phenotype through modulation of DNA methylation, which has not been largely explored. One recent study showed that demethylation of the *CXCR4* promoter occurred following hypoxia in lung cancer cell lines and its resulting expression induced EMT (Kang *et al.*, 2019). Although the promoter of *CXCR4* was not significantly DM in this dataset, my results similarly point towards a regulation of de-differentiation and stemness by DNA methylation.

Interestingly, analysis of DM gene regions similarly indicated hypomethylation of gene regulating "*G-protein coupled receptor activity*", "*Inflammatory response*", and "*Membrane*" and hypermethylation of genes regulating "*Homeodomain/homeobox*", "*DNA-binding*", "*Positive regulation of transcription from RNA Pol II promoter*" and "*Negative regulation of transcription from RNA Pol II promoter*".

It must be noted that the DM promoter regions may provide a clearer picture than the DM genes, since DNA methylation at promoters is more consistently associated with transcriptional repression, whereas methylation of gene bodies can have activating or inhibitory effects on expression, depending on the CpG (as described in General Introduction section *1.1. VII*., gene body CpGs can be used to regulate splicing, elongation, or transcription factor recruitment). It nevertheless points towards epigenetic changes occurring at these types of genes, perhaps suggesting altered activity of transcriptional regulators that govern these subsets of genes. For instance, a chromatin modifying enzyme localised to these genes could be influencing higher-order structures that then affects the activity of DNA methyltransferases, or vice versa. Therefore, regardless of the effect on transcription, it seems clear that there are profound epigenetic alterations occurring at genes involved in development, transcription and inflammation, with a potential mixture of activating and silencing methylation patterns that suggests that these pathways are being epigenetically modulated and are involved in the hypoxic response. From these results we can conclude that there is an epigenetic regulator controlling DNA methylation at these subsets of genes, that is somehow responsive to hypoxia.

5. 3. III. b) Future directions

It would be important to investigate if the expression of these genes correlates with the changes in methylation, by integrating the methylation array data with an expression analysis such as RNA-seq or RT-qPCR. An another interesting future experiment could be to determine what the overall effect on pathway activation would be using IPA (which I unfortunately could not achieve since I had been using the free trial which has limited analyses). Perhaps the top 100 combined rank promoters and genes could be analysed (without considering the degree of hypo/hyper methylation) although on such a small number, the results may not be particularly powerful or informative. Alternatively, one could input the mean.diff (absolute difference in methylation between conditions) of the top 1000 combined rank. To do this, the mean.diff signs (*i.e.* positive and negative for hyper and hypomethylation respectively) should be reversed so that a positive mean.diff could be used to approximate reduced expression. This would be based on the assumption that hyper and hypo-methylation associate with down and up-regulation of expression. It could nevertheless be useful for network and pathway analysis.

To explore whether hypomethylation is important for inflammatory gene activation, inflammation signalling could be activated by treating the cells with stimulants such as lipopolysaccharide or IFN-γ, to upregulate inflammation signalling as has previously been published (Kämpfer *et al.*, 2017). If this is also

associated with hypomethylation, it could support the regulation of inflammation by DNA methylation and indicate how hypoxia helps subvert immune surveillance.

To monitor the activity of these pathways, methylation could be monitored across a time course. Since in this dataset, the key genes affected were *HOX*/inflammatory, these could be specifically investigated on a smaller scale than whole-genome array, by wet-lab techniques such as methylation specific PCR, COBRA, or Pyrosequencing. To monitor methylation changes with increasing hypoxia or increasing time spent in hypoxia, a hypoxic chamber could be used and DNA extracted over short time points to measure the methylation of specific genes over time, combined with expression analysis.

To explore potential epigenetic regulators, a list of HIF-1a response genes could be compiled, and those involved in chromatin regulation be assessed. Then, ChIP or ChIP-seq could be used to discover if they localise to the DM sites.

There were no methylation array datasets from hypoxic PCa cell lines or tumours available on the GEO database, reflecting the lack of study in the area, and so a similar experiment could be performed to create a PCa dataset.

Finally, the key DM genes such as the *HOX* genes or inflammatory genes could be explored in hypoxia across a number of different cancer types, using the previously mentioned wet-lab techniques. An illustration of how the methylation of specific sites can be validated *in vitro* is exemplified in Part 3.

5. 4. Part 3: Regulation of miRNA expression by DNA methylation in prostate cancer

5. 4. I. Introduction

In vitro methylation analysis has been an essential tool for investigating the methylation status of individual loci, as it is quicker and more cost-effective than whole-genome array. It has been successfully used to analyse imprinted regions (Thakur *et al.*, 2016), monitor changes in methylation status during processes such as adipogenesis (Flores *et al.*, 2019), and been used to demonstrate cancer-associated changes in methylation (Lynch *et al.*, 2016a).

Part 2 demonstrated how hypoxia exerted profound effects on the DNA methylation of the genome in NSCLC. Interestingly, the miR-210 gene locus was identified as hypomethylated in the hypoxic samples, and one of the more statistically significant. MiR-21 was also hypomethylated although not significantly, inviting the question of whether hypomethylation of these regions could be a means of inducing their expression during hypoxia. However, miR-196a was hypermethylated following hypoxia, which was not in keeping with its observed expression level. Interestingly, analysis of the TCGA Regulome Explorer dataset revealed that a CpG site in the gene body of the pri-miR-21 gene was significantly inversely correlated with its expression (Figure 15). Moreover, as mentioned in chapter 4 discussion section *4.3.II b)*, DNA methylation has been suggested to regulate miR-21 (in thyroid cancer, and myelodysplastic syndromes) and miR-210 expression (in schwannoma, gastric cancer, and neural progenitor cells) (Ortiz *et al.*, 2018)(Kim et al., 2014)(Wang *et al.*, 2017)(Kiga *et al.*, 2014)(Xiong *et al.*, 2012).

For this reason, Part 3 investigates whether miR-210 and miR-21 expression could be regulated by DNA methylation in PCa cell lines.

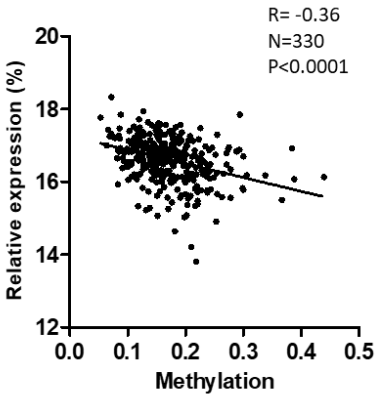

Figure 15. Association between methylation and expression of miR-21 in TCGA data. In the Regulome Explorer dataset (n=330), methylation of probe cg15759721 in the gene body of pri-miR-21 was significantly inversely correlated with miR-21 expression.

A series of pyrosequencing experiments were designed to investigate the transcriptional regulation of miR-21 and miR-210 expression by DNA methylation. Pyrosequencing is a quantitative *in vitro* method of assessing DNA methylation at specific CpGs (cytosines next to guanines), based on the use of sodium bisulfite (hereafter referred to as bisulfite). Bisulfite is a chemical that deaminates unmethylated cytosines to uracils by hydrolysis, thus providing a means of distinguishing between methylated and unmethylated cytosines (Delaney, Garg and Yung, 2015). Pyrosequencing has been shown to be the most reproducible method of DNA methylation quantification (Bock *et al.*, 2016). The Method is outlined in section *2.1.IV*.

5. 4. II. Results

5. 4. II. a) Assay design

Two CpG islands cover the pri-miR-210 gene (CpG islands 149 and 179). As expected, the region was littered with CpGs which made primer design difficult since there were very few regions without CpGs for over 15 nucleotides (the minimal length of a primer) that would also be suitable as primers due to their sequence (size of the amplicon, specificity, CG content, C/G ends, etc). However, 1 pair of primers were successfully obtained that amplified a non-CpG island region including 14 CpGs (Figure 16) of which 10 were successfully sequenced.

Fewer CpGs were present around the pri-miR-21 gene, so two regions were assayed each containing 3 CpGs (assay 1 and assay 2); assay 1 was upstream of the pri-miR-21 gene and assay 2 downstream. Figure 17 contains the UCSC depiction of the pri-miR-210 and pri-miR-21 genes, highlighting the regions assayed, and including tracks annotating nearby CpG islands and CpG probe identifiers from NGS arrays such as the Illumina 450K and EPIC (850k) arrays.

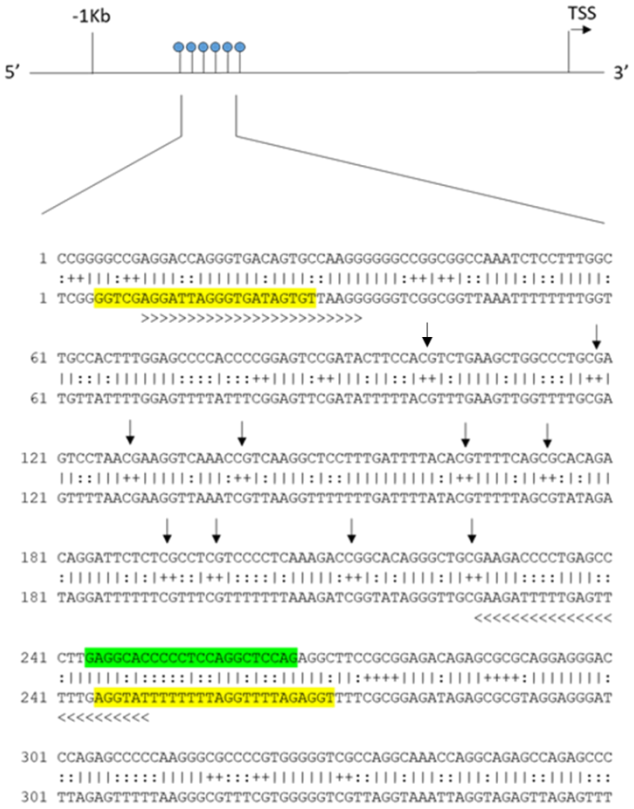

Figure 16. MiR-210 pyrosequencing assay. DNA depicted with CpGs covered by the assay highlighted in relation to transcription start site (TSS) of the gene encoding pri-miR-210. The sequence paired against its bisulfite-converted form (above and below, respectively) is shown as predicted by MethPrimer software, assuming that all CpGs are unmethylated and all cytosines converted to thymine. PCR primers suggested by methprimer are depicted as greater than/ less than symbols and the primers that were finally selected using PyroMark software are highlighted (yellow as forward and reverse PCR primers and green as sequencing primer). The forward primer was biotinylated as the sequencing primer binds the reverse strand. Black arrows indicate CpG sites of potential methylation that were successfully assayed by the sequencing reaction.

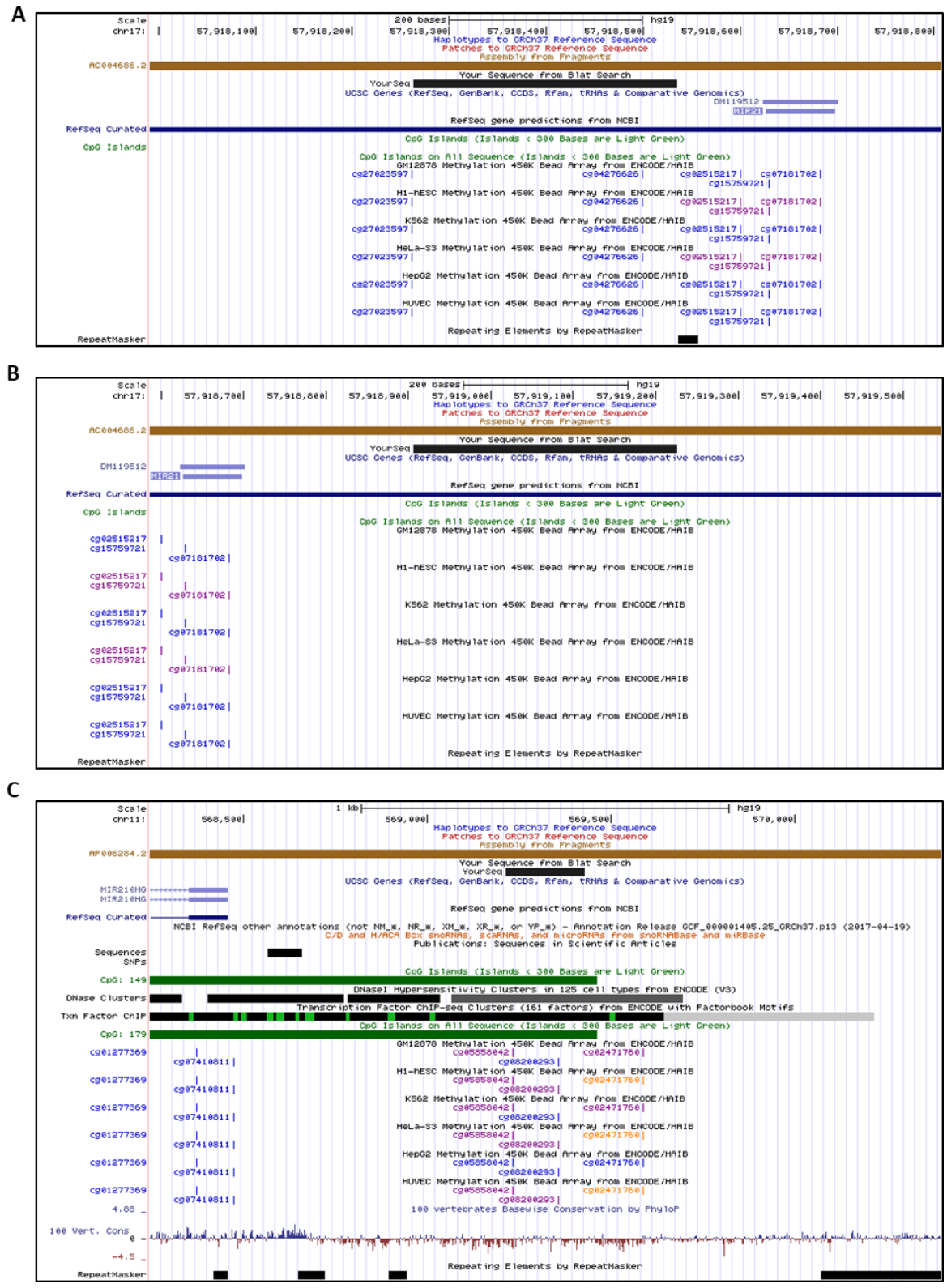

Figure 17. Genomic location of regions assayed relative to gene, neighbouring CpG islands, and CpG array probes. Sequencing was performed on regions amplified from bisulfite-treated DNA. Primers were designed that would amplify the regions (illustrated on UCSC) relative to the gene (regions illustrated by black boxes labelled "YourSeq"). Nearby CpGs with probes covered by various arrays shown on the cg tracks. **A)** First primer set for miR-21 designed to amplify region upstream, covers three CpGs (Assay 1). **B)** Second primer set for miR-21 designed to amplify region downstream, covers three CpGs (Assay 2). **C)** Primer set for miR-210 designed to amplify region upstream of the gene (miR-210 is on the reverse strand so region is to the right of the gene).

5. 4. II. b) DNA methylation at miR-210 and miR-21 loci and the relationship with gene expression

First, the methylation levels of the assayed CpGs was measured in untreated cells, to examine the basal level of methylation, and this was compared with basal expression level (Figure 18 and 19). Interestingly, this revealed consistent patterns of methylation in multiple cell lines, which could indicate a conserved function, such as increased methylation at the 7th CpG in the miR-210 assay compared to the 6th (Figure 18). Moreover, the methylation levels of the regions inversely correlated with the expression levels of the miRNA transcripts, suggesting that DNA methylation may regulate gene expression. Another striking feature was the increased methylation of CpGs in the cancer cell lines compared with RWPE-1, in all three assays.

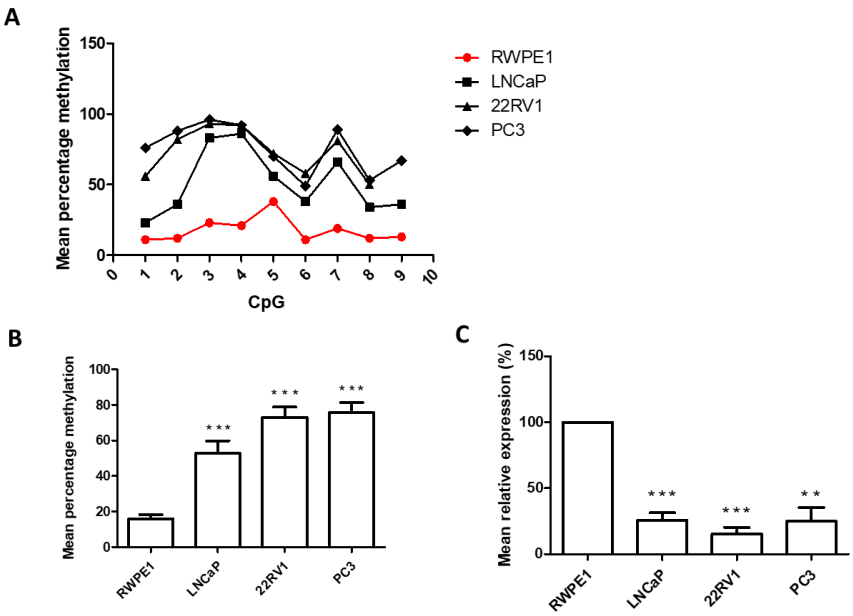

Figure 18. Methylation of CpGs in the promoter region of miR-210 inversely correlates with its expression level. A) Pyrosequencing demonstrates conserved pattern of methylation across the region assayed, cancer cell lines LNCaP, 22Rv1 and PC3 displaying increased methylation per CpG site compared to RWPE-1, and **B)** significantly increased mean methylation across the region. **C)** Accordingly**,** RT-qPCR reveals significantly lower expression of miR-210 in PCa cell lines compared to RWPE-1. One-way t-tests were used to compare condition means to the control (hypothetical value 100) and p-values considered significant when *p<0.05, **p<0.01, ***p<0.001.

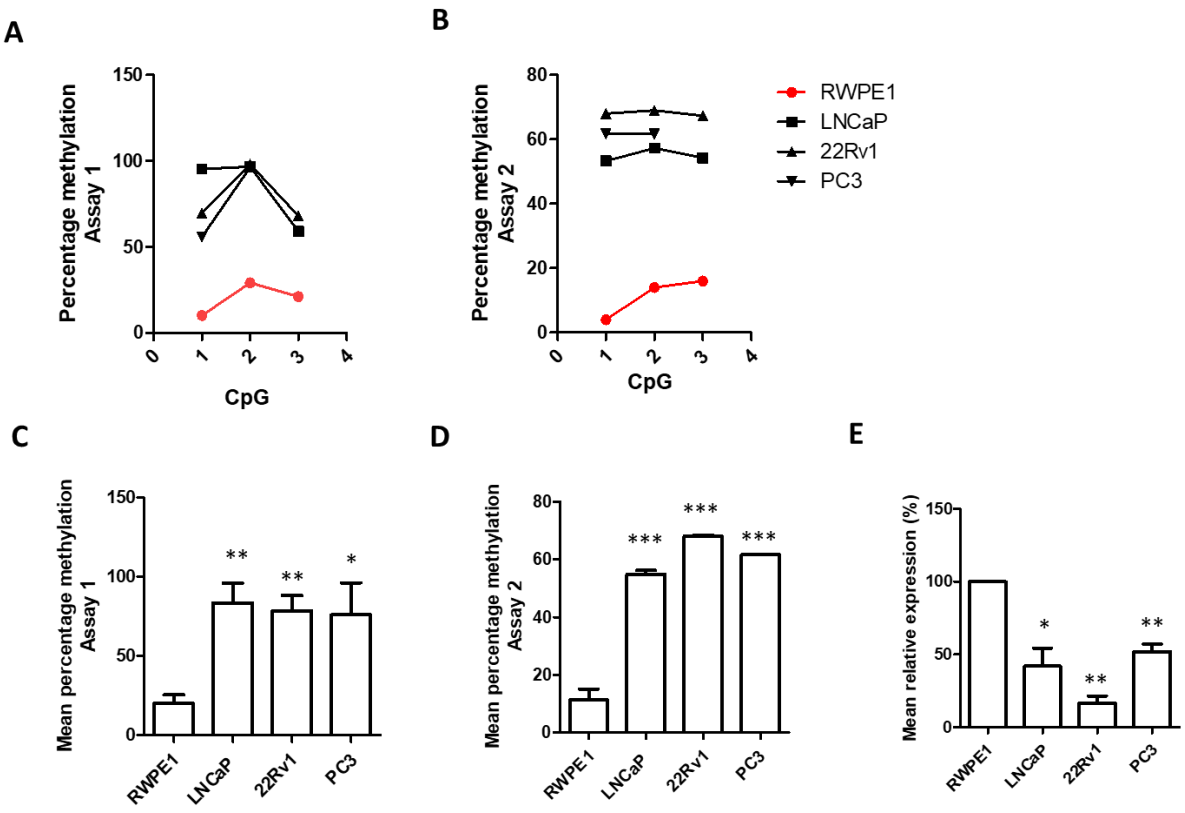

Figure 19. Methylation of the promoter region of miR-21 inversely correlates with its expression level. A) Pyrosequencing demonstrates increased methylation of individual CpGs in the PCa cell lines compared to RWPE-1, in Assay 1 and **B)** Assay 2. **C)** Mean percentage methylation across the region is increased in PCa cell lines compared with RWPE-1 in Assay 1 and **D)**, Assay 2. **E**) Accordingly, RT-qPCR reveals reduced expression of miR-21 in PCa cell lines relative to RWPE-1. One-way t-tests were used to compare condition means to the control (hypothetical value 100) and p-values considered significant when *p<0.05, **p<0.01, ***p<0.001.

5. 4. II. c) The effect of Aza-dc treatment on DNA methylation and gene expression

However, to prove that DNA methylation was regulating the miRNAs expression, the increased methylation the cancer cell lines should be reduced (with a demethylating agent) and the effect on expression level be reversed accordingly. Therefore, LNCaP, 22Rv1 and PC3 were treated with a pharmacological inhibitor of DNA methyltransferase (DNMT), 5-Aza-2'-deoxycytidine (hereafter referred to as Aza-dc). Aza-dc is a cytosine analogue with a nitrogen replacing the fifth carbon, which is incorporated into DNA in place of endogenous cytosine. DNMT binds Aza-dc but cannot catalyse its methylation, and so remains bound and is eventually degraded due to activation of a DNA-damage response pathway, which is particularly evident in the case of the maintenance methylation enzyme DNMT1 but also true for the *de novo* methylation enzymes DNMT3A/B (Palii *et al.*, 2008).

The cells were either untreated or treated with 5µM Aza-dc for 72h, as has been shown effective in these cell lines by another research group *(Li et al*, 2015). After 72h, PC3 were almost confluent and were harvested, while 22Rv1 and LNCaP were left to grow an additional 24h to maximise cell number. During harvesting, cells were split into two pellets for RNA and DNA extraction of the same population. The efficacy of the dose on the cell lines was confirmed by upregulation of the genes *SYPC3* and *DAZL* by RT-qPCR (Figure 20), which are germline genes known to be regulated by DNA methylation (Maatouk *et al.*, 2006). Of note, the cell line 22Rv1 appeared to be most sensitive to Aza-dc as shown by the vast upregulation of these markers and that by 72h of treatment the cells had acquired a senescent phenotype (wide and squashed looking, with faint membranes).

Encouragingly, Aza-dc treatment increased the levels of miR-21 and miR-210 in some cell lines (miR-21 in PC3 and 22Rv1, and miR-210 in 22Rv1 and LNCaP), suggesting that their expression may be regulated by DNA methylation (Figure 21).

Next, the methylation status of the Aza-dc treated cells was measured by Pyrosequencing, with the view to correlate the methylation status of each sample with the expression level of the miRNAs. Curiously however, Aza-dc treatment did not demethylate the DNA at the miR-210 and miR-21 assayed regions, and in fact the miR-21 assay 1 results show increased methylation in Aza-dc treated 22Rv1 and LNCaP (Figure 7). The miR-210 assay showed reduced methylation in all cell lines after Aza-dc treatment at one specific CpG (depicted as CpG number 4, Figure 7C). Furthermore, the mean methylation of the whole miR-210 assay region was slightly lower in Aza-dc treated cells (Figure 8). Although small, this could potentially be biologically relevant, particularly if it produced a cumulative effect across a large region. However, miR-210 expression was not upregulated by Aza-dc in PC3 and so the degree of demethylation did not correlate with degree of expression across the cell lines, and the effect of DNA methylation on transcription could not be determined.

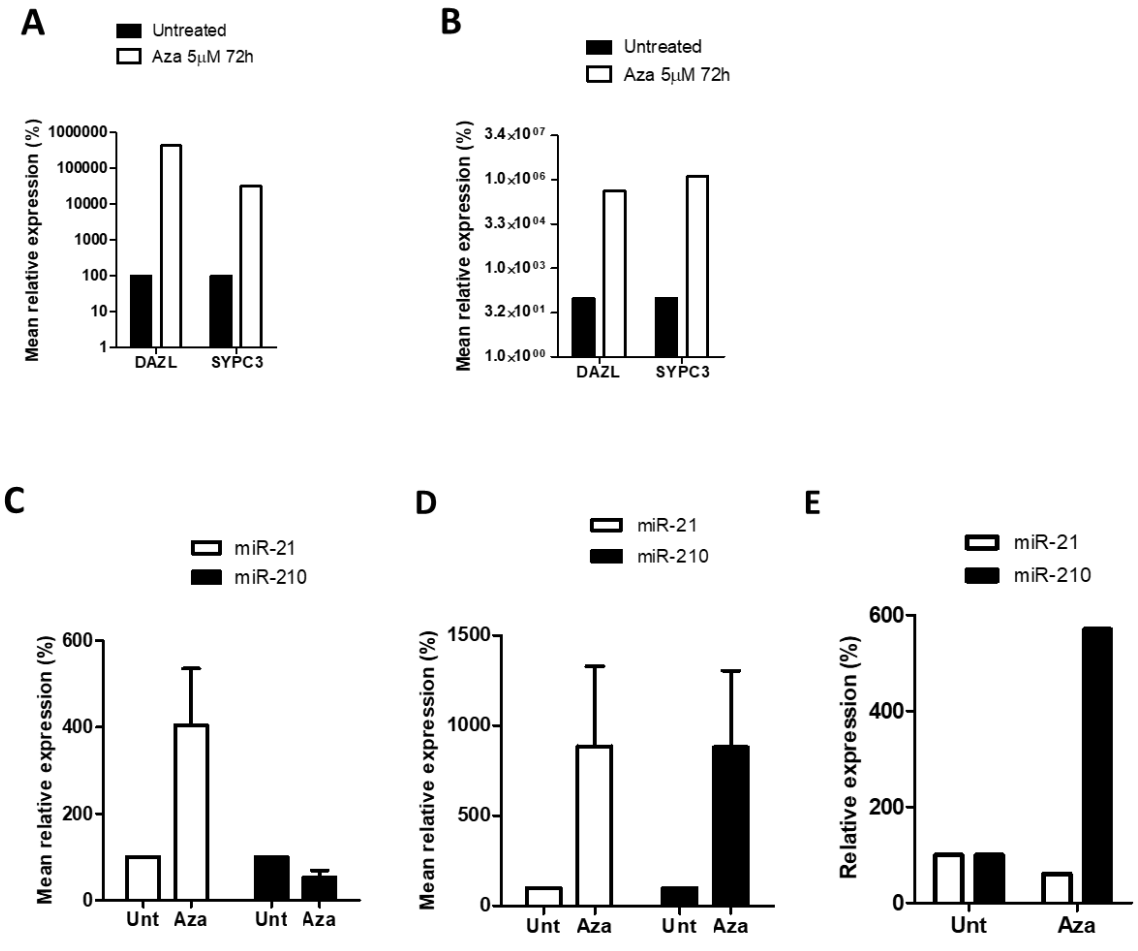

Figure 20. Confirmation of the efficacy of 5μM Aza-dc for 72h on PCa cell lines, and measurement of miRNA expression in Aza-dc treated cells. Upregulation of germline genes SYPC3 and DAZL following aza-dc treatment of **A)** PC3 and **B)** 22Rv1. **C)** MiRNA RT-qPCR results showing upregulated miR-21 expression in Aza-dc treated PC3. **D)** Upregulated miR-21 and miR-210 expression in Aza-dc treated 22Rv1. **E)** Upregulated miR-210 expression in Aza-dc treated LNCaP. Mean + SEM of two biological replicates shown with the exception of LNCaP due to RNA degradation of one Aza-dc treated sample. One-way t-tests were used to compare condition means to the control (hypothetical value 100) and p-values considered significant when *p<0.05, **p<0.01, ***p<0.001.

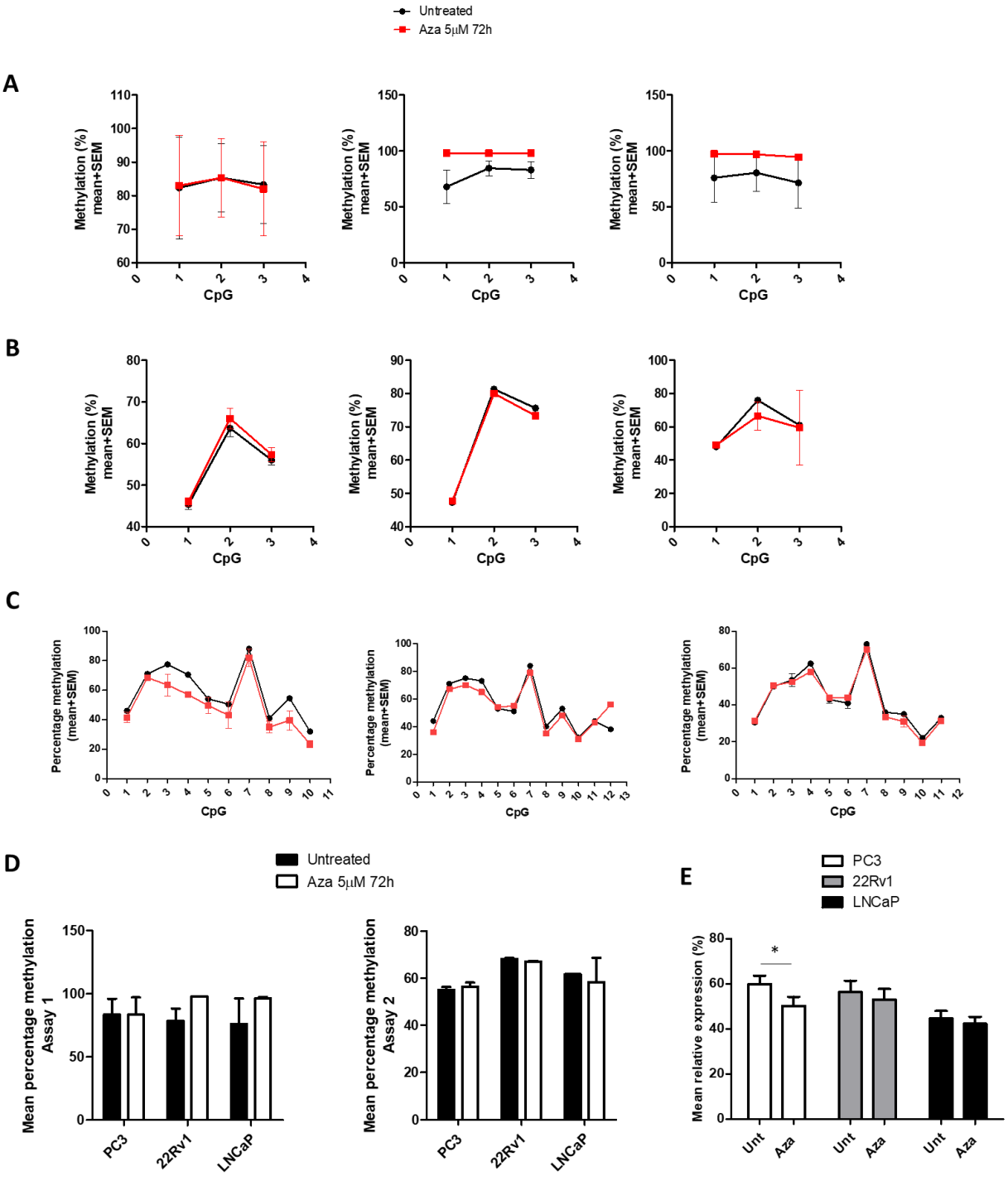

Figure 21. Pyrosequencing results showing the effect of Aza-dc treatment on DNA methylation of the promoter regions of miR-21 and miR-210, in PCa cells either untreated (black lines) or treated with 5μM Aza-dc treatment (red lines) for 72h. From left to right, graphs depict PC3, 22Rv1 and LNCaP. **A)** Assay 1 (miR-21). **B)** Assay 2 (miR-21) **C)** miR-210 assay. **D)** Analysis of the mean percentage methylation across the whole assayed regions of miR-21 gene, showing increase in percentage methylation in Aza-dc treated cells (white bars) compared to untreated cells (black bars). **E)** Mean percentage methylation of the miR-210 assay showing slight reduction in mean methylation in all cell lines. Mean + SEM of two biological replicates shown. Two-way t-tests (one-tailed, homoscedastic) were used to compare each set of means and p-values considered significant when *p<0.05, **p<0.01, ***p<0.001. No error bars where identical values were obtained for both replicates.

5. 4. II. d) Hypoxia and DNA methylation of LINE1 and pri-miR-21 and pri-miR-210

Part 2 indicated that hypoxia had influenced the methylation of DNA at promoters and gene regions in NSCLC. I wanted to explore the effect of hypoxia on DNA methylation in PCa, overall and specifically at the miR-210 and miR-21 loci, to determine if perhaps hypoxia would affect these regions.

The methylation status of *long interspersed nuclear element 1* (*LINE1*) is considered representative of global methylation (Ehrlich, 2002), so this was used as a measure of the global methylation associated with hypoxia.

One biological replicate was conducted culturing LNCaP in hypoxia (0.1% O_2 relative to 20% O_2) which produced no change in methylation of *LINE1* at the CpGs assayed, potentially suggesting that hypoxia did not affect DNA methylation across the genome. Likewise, analysis of the pri-miR-21 and pri-miR-210 genes did not demonstrate a consistent effect of hypoxia on the assayed CpGs, although at some CpGs at the miR-210 region, methylation was reduced in the hypoxic versus normoxic conditions (Figure 22). However, this would require further replicates.

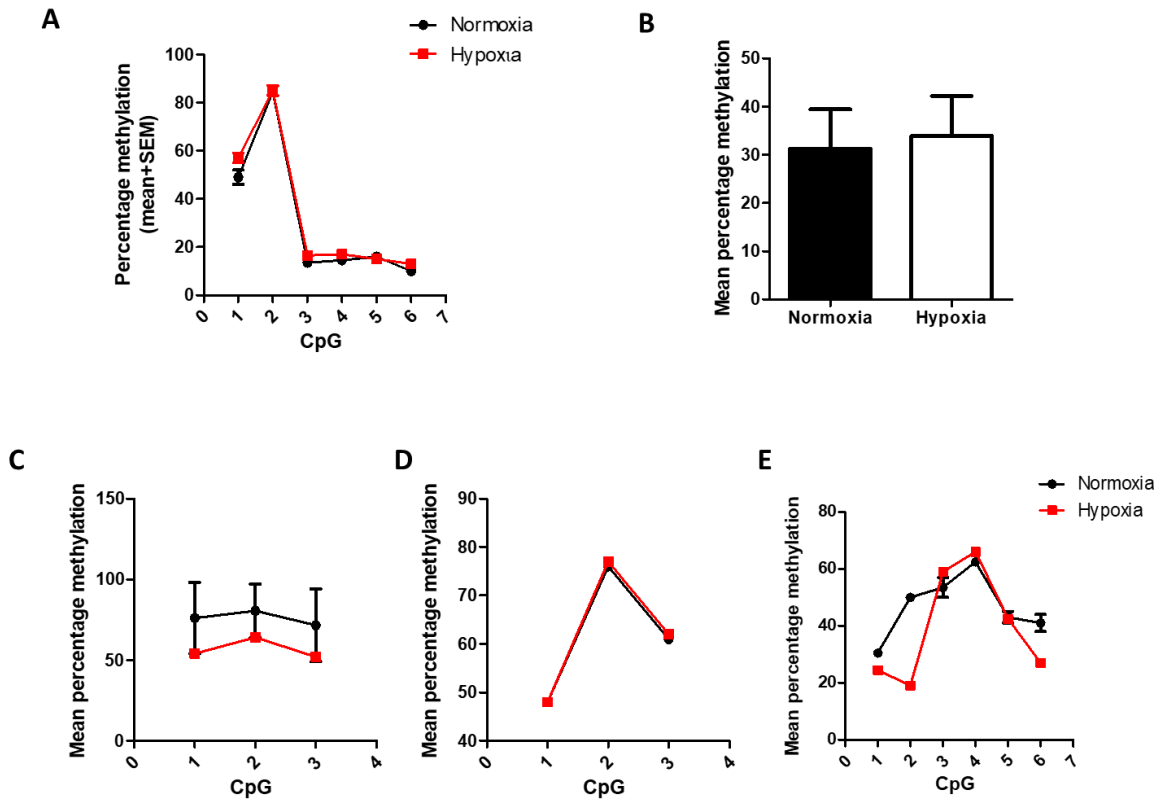

Figure 22. The effect of hypoxia on the DNA methylation of *long interspersed nuclear element 1* (*LINE1*) and miR-21 and miR-210 in LNCaP as measured by Pyrosequencing. Hypoxic culture was 0.1% O_2 relative to normoxia 20% O_2 for 48h. One biological replicate (hypoxia) and two technical replicates (independent PCR amplifications) shown (mean + SEM). **A)** No effect of hypoxia on the percentage methylation of most CpGs in a *LINE1* element assay, which is representative of global methylation status. **B)** Mean percentage methylation of the whole assayed region showing no change mean percentage methylation of the *LINE1* assay region in hypoxic cells. Two-way t-test (two-tailed, homoscedastic) were used to compare each set of means and p-values considered significant when *p<0.05, **p<0.01, ***p<0.001. **C)** No effect of hypoxia on the DNA methylation of regions proximal to pri-miR-21 assay 1, nor **D)** pri-miR-21 assay 2. **E)** Slight difference in the methylation pattern of CpGs at the pri-miR-210 region in hypoxic versus normoxic conditions.

5. 4. III. Discussion

5. 4. III. a) Summary

The initial experiments demonstrated that the DNA methylation levels of the miR-21 and miR-210 genes was increased in the cancer cell lines compared with RWPE-1, and this inversely correlated with their expression level, suggesting that these miRNAs could be regulated by DNA methylation. Indeed, in some cell lines, Aza-dc treatment upregulated their expression. However, Aza-dc did not significantly reduce the methylation of the assayed regions. The fact that the percentage methylation at the individual CpGs was conserved across the three cell lines could indicate an essential function of the methylation of these sites, but from my data I cannot conclude that it is to regulate gene expression, since I could not remove the methylation and correlate that with an increase in expression.

Potentially, the concentration of Aza-dc was insufficient, although this is perhaps unlikely, since *DAZL* and *SYPC3* were induced and 22Rv1 (which was most sensitive to Aza-dc) was not more demethylated that the other cell lines. However, potentially the 24h of extra growth time after the end of the Aza-dc treatment could have facilitated some re-methylation, and in fact PC3 were harvested immediately after 72h of Aza-dc treatment (as they had been almost confluent) and this cell line had slightly lower methylation levels. This suggests that cells should always be harvested at the end of the treatment.

It is also important to note that methylation patterns are highly abnormal in cancer, and the increased methylation of miR-21 and miR-210 could simply reflect abnormal establishment of methylation patterns and be unrelated to expression regulation. Furthermore, if methylation were governing these miRNAs expression, one might expect them to be hypomethylated in the cancer state rather than hypermethylated, considering their oncogenic properties. A more interesting question is whether the abnormal methylation at these genes somehow primes them to respond differently to hypoxia. A preliminary experiment in LNCaP showed that hypoxia did not affect the methylation of these promoter regions. However, in these samples hypoxic culture did not significantly affect *LINE1* methylation. This was surprising, as it was in contrast to the NSCLC dataset in which hypoxia associated with global hypomethylation. Hypomethylation of repetitive elements (such as *LINE1*) is associated with increased chromosomal instability and rearrangements and is common in cancers (Imperatori *et al*., 2017) (Baba *et al*., 2010), so it would have made more sense if hypoxia had reduced methylation at this element. However, more replicates would obviously be needed. Furthermore, the conditions are immensely different. Firstly the NSCLC dataset analysed DNA extracted from 24 different tumour specimens whereas this is a single cell line replicate. Secondly, the tumours were classified based on a hypoxia metagene score, whereas the LNCaP replicate was cultured for 24h at 0.1% O_2. It could be that the degree of hypoxic was too intense (*i.e*. oxygen levels too low) for cell replication and so changes in methylation-mediating enzymes (*e.g*. DNMT1) cannot be observed. Perhaps, culturing at 1% or 5% O_2 would permit replication and differences in methylation would become clear. Finally, since the tumour samples were heterogeneous cell populations and it is not possible to confirm that the changes

occurred in the carcinoma cells themselves, but could be partly due to changes in infiltrating immune cells or stromal cells.

There was an unexpectedly small demethylating effect of Aza-dc. Perhaps, a difference of just 5% could have biological effects if it was a critical CpG or had an additive effect across many CpGs in the region. Indeed, in PC3 the Aza-dc induced hypomethylation was significant across the miR-210 assayed region (9 CpGs). Bizarrely, there was no demethylating effect of Aza-dc at the miR-21 regions (in fact there was an occasional increase in methylation at some CpGs). This may suggest that some regions more readily incorporate Aza-dc rather than endogenous cytosine, or it could simply be chance. In fact, a lack of demethylation at certain genes following Aza-dc treatment has been previously reported in a study by the Walsh lab, comparing methylation changes in Aza-dc treated and siRNA DNMT1 treated cells. The authors demonstrated that Aza-dc caused hypermethylation at the promoter regions of certain genes, which DAVID analysis revealed was enriched for genes encoding G-protein coupled receptors and particularly olfactory receptors (Mackin, O'Neill and Walsh, 2018b). Potentially, DNA-associated proteins at these regions somehow inhibit the incorporation of Aza-dc into DNA, although it is difficult to imagine how. Alternatively, *de novo* methylation (by DNMT3A and DNMT3B enzymes) could be particularly important at these regions and the maintenance methylation enzyme DNMT1 less important, and thus its inhibition does not affect methylation. However, in the study comparing Aza-dc with siRNA DNMT1, gains in methylation were only observed in the Aza-dc treated cells. It could be that in these cells, DNMT3A/B were affected by off-target gene silencing.

5. 4. III. b) Future directions

To address the issue of lack of demethylation due to Aza-dc, a future experiment could involve measuring the methylation levels using the miR-21 and miR-210 assays, in cells treated with siRNA DNMT1 to have a better chance of observing demethylation. Alternatively, a CRISPR/Cas9 system could be used to guide DNMT1 to these regions for it to dememthylate them, as a CRISPR/Cas9/DNMT1 system has recently been published (Lu *et al.*, 2019).

There was a discrepancy between the Aza-dc demethylation and Aza-dc induced expression (*e.g*. demethylation of the miR-210 region in PC3 was not associated with upregulation of miR-210). This could suggest that the gene is not governed by DNA methylation at the region assayed. However, this is an oversimplification since it may be almost impossible to ever fully isolate the effect of DNA methylation on cancer-associated gene expression using Aza-dc. This is firstly because there is interplay between many epigenetic mechanisms, and perhaps artificial demethylation by Aza-dc is insufficient alone, and also requires modification of histones (such as histone deacetylase inhibition) or chromatin. Furthermore, Aza-dc induces a DNA damage response (DDR) pathway that could confound its effects. That is, the activated DDR could have knock-on effects on genes like miR-21 and miR-210 since they have pleiotropic, homeostatic functions. Similarly, we also have to be conscious that Aza-dc has potent anti-cancer effects,

and it could be that the changes in miRNA expression that were observed following Aza-dc treatment were in fact a result of cell death pathway activation. Based on this, and since methylation patterns are abnormal in cancer cells, future experiments analysing this mechanism could use a different cell line to unpick the regulation of the gene regions by methylation, such as a normosomic, nontransformed fibroblast cell line as has been successfully utilised by other researchers (Rutledge *et al*., 2014).

Interestingly, a number of miRNAs have been shown to be regulated by DNA methylation and in turn, many regulate epigenetic processes; these "epi-miRNAs" – regulate the translation of enzymes including DNMT, polycomb repressive complex 1/2 (PRC1/2), retinoblastoma like protein 2 (RBL2), histone deacetylase (HDAC), heterochromatic protein-1 (HP1). This produces feedback loops that finely tune epigenetic regulation (Ramassone *et al.*, 2018). Therefore, a mutation in one of the miRNA processing machinery can affect global epigenetics and *vice versa*, a mutation in an epigenetic regulator can affect global miRNA function. Interestingly, miRNAs have also been detected bound to DNA, recruiting epigenetic and transcription factors (Ramassone *et al.*, 2018). It could be interesting in the future to examine if either miR-21 or miR-210 target epigenetic regulators, which could elucidate a hypoxia-dependent epigenetic signature.

5. 5. IV. Overall discussion and future perspectives

5. 5. IV. a) Summary

This chapter has applied omics methods to study genomic and epigenomic profiles. The RNA-seq characterisation of the prostatectomy cohort successfully informed the discovery of miR-196a as a hypoxia-regulated miRNA in PCa, and pathway analysis was used to suggest how it may operate within a network of its targets and may drive tumour progression. Next, the methylation profiles of hypoxic and normoxic NSCLC tumours were analysed using the R package "RnBeads", which revealed global and regional hypomethylation associated with hypoxia and changes in the methylation patterns of promoters and genes governing inflammation, cell signalling, and development. Finally, the regulation of miR-21 and miR-210 by DNA methylation was examined using a bisulfite conversion and sequencing approach. Therefore, this chapter has demonstrated how different types of molecular data can contribute to understanding the biology of diseases or conditions. The NGS and array approaches were especially powerful since they produced quantitative data for many transcripts/genomic loci in parallel, with a significance score based on the effect size across multiple samples. In contrast, the *in vitro* analysis of miR-21 and miR-210 methylation was more laborious and eventually rather inconclusive.

5. 5. IV. b) Applications for personalised medicine

In the future, personalised medicine approaches will probably consist of a mixture of these types of approache (multi-omics). For example, as sequencing becomes more affordable for clinical labs, specimens may be sequenced and analysed for specific patterns or panels, to characterise a tumour or serum. Methylation profiling could be used to indicate hypoxia, or other cell features, for patient stratification. For example, methylation profiling could predict if lung cancer patients would respond to demethylating agents, which have been used to treat myelodysplastic syndromes for decades (Santini, 2019). Several studies in the literature have reported growth inhibiting effects of either 5-azacytidine or 5-aza-2'deoxyazacytidine on NSCLC cell lines and concluded that it could be a treatment option for patients in the future (Lai *et al.*, 2018)(Desjobert *et al.*, 2019)(Yang *et al.*, 2017). This data would suggest that hypoxic tumours already display hypomethylation and if this was shown to contribute to tumour development then these agents may do more harm than good.

5. 5. IV. c) Benefits and challenges of omics data in cancer research

When the human euchromatic genome was published in 2004, the bottleneck in omics data was the limitations of the available technologies for generating data. Since then, high-throughput technologies have advanced and become increasingly efficient and affordable, and the bottleneck has now shifted from data generation to data processing and interpretation. As this chapter has exemplified, despite ready access to omics data it remains difficult to untangle the complex molecular mechanisms that underlie a disease. This is because the dynamics of the cell are intricate and complex, plus the type of data that comes from biological samples is noisy due to cellular heterogeneity, and there are limitations

of the applied statistics such as false positives (Alyass, Turcotte and Meyre, 2015). On top of that, the data represents a snapshot in time. Transcription and decay are dynamic and stochastic, and genes can be expressed briefly to influence numerous downstream effects before being rapidly degraded, although methylation profiling may be less susceptible to fluctuations, as global changes in methylation may require multiple cell divisions to become evident whereas proteins and RNAs can be rapidly turned over. Overall, detecting legitimate interactions and networks remains very challenging. However, many sophisticated programs are available that can be used to characterise gene expression patterns to uncover biological processes (and are helpfully based on pre-designed workflows that are suitable for the inexperienced bioinformatician). Using the programs IPA and DAVID, specific pathways were indicated as being enriched (such as apoptosis signalling in the prostatectomy cohort and inflammatory genes in the hypoxic lung tumours). Another issue in omics analysis is the difficulty in integrating multiple types of data. Indeed, the miRNA-seq and mRNA-seq pathway analyses indicated rather different pathway profiles, and even when integrated the results were no clearer. It is also important to note the caveat of such functional annotation and network analyses is they are based on curated data, and the networks are extrapolated based on information generated from many different cell types. Overall this highlights that pathway analysis must be interpreted with caution, although it was very useful for revealing inversely correlated miRNA : mRNA pairs. There is also the caveat of tumour analysis that the cell type of origin cannot be proven. Indeed, the difficulty in finding a miRNA that was expressed robustly in the PCa cells lines, may reflect the heterogenous sample and highlights the need for validation *in vitro*.

In summary, omics data is immensely powerful in identifying novel genes, pathways, and epigenetic features in cancers. The global transition to personalised medicine depends on omics approaches to direct new research avenues and for patient stratification. Multiple types of omics data, such as RNA-seq and methylation array, will be involved. However, the effective integration of different types of omics data is an important bottleneck to consider.

5. 5. IV. d) Future directions

It would be interesting to examine the proteomics of the hypoxic tumour samples or the prostatectomy cohort, to explore if the results reflected the epigenomic or transcriptomic profiles respectively. The proteomic profiles could be investigated by quantitative mass spectrometry, which has recently been used to characterise protein biomarkers in colon cancer (Atak *et al.*, 2018).

Alternatively, to address the issue of cellular heterogeneity, the tumours could be separated into single cells by flow cytometry activated cell sorting (FACS) and single cell RNA sequencing or single cell methylation analysis could be performed. This would provide a high resolution picture of the differences across cells in the microenvironment, and help decipher the behaviour and contribution of individual cells.

There was unexpected discordance between the mRNA-seq and miRNA-seq data. Apparently, integrative analyses of transcriptomic and proteomic data often reveals low level of correlation between the two, which has been attributed to regulation at the post-transcriptional and post-translational levels. If a proteomic analysis was used, the pathway analysis of the integrated data could be improved by accounting for regulating factors, by including in the model a network analysis of protein-protein and DNA-protein interactions, such as by Bayesian network models, although this would require statistical modelling expertise (Alyass, Turcotte and Meyre, 2015).

Throughout this chapter I have referred to the use of miRNA or methylation based biomarkers of disease, however, these would need to be obtained by biopsy. Prostate biopsies are not ideal since they are invasive and only provide data from a snapshot in time. It would be better to characterise biomarkers taken from a liquid, perhaps a future experiment could involve extracting circulating RNA or DNA and repeating the analyses. Serum is a commonly used liquid for biomarkers, although urine may be more appropriate for PCa, and has already been investigated and some cohorts of PCa patients have been shown to have specific urine miRNA profiles and DNA methylation patterns such as *GSTP1* methylation (Fredsøe *et al.*, 2018)(Bakavicius *et al.*, 2019).

5. 6. Bibliography

Alyass, A., Turcotte, M. and Meyre, D. (2015) 'From big data analysis to personalized medicine for all: challenges and opportunities.', *BMC medical genomics*. BioMed Central, 8, p. 33. doi: 10.1186/s12920-015-0108-y.

Assenov, Y. *et al.* (2014) 'Comprehensive analysis of DNA methylation data with RnBeads', *Nature Methods*, 11(11), pp. 1138–1140. doi: 10.1038/nmeth.3115.

Atak, A. *et al.* (2018) 'Quantitative mass spectrometry analysis reveals a panel of nine proteins as diagnostic markers for colon adenocarcinomas.', *Oncotarget*. Impact Journals, LLC, 9(17), pp. 13530–13544. doi: 10.18632/oncotarget.24418.

Bakavicius, A. *et al.* (2019) 'Urinary DNA methylation biomarkers for prediction of prostate cancer upgrading and upstaging', *Clinical Epigenetics*, 11(1), p. 115. doi: 10.1186/s13148-019-0716-z.

Bock, C. *et al.* (2016) 'Quantitative comparison of DNA methylation assays for biomarker development and clinical applications', *Nature Biotechnology*. Nature Publishing Group, 34(7), pp. 726–737. doi: 10.1038/nbt.3605.

Buffa, F. M. *et al.* (2010) 'Large meta-analysis of multiple cancers reveals a common, compact and highly prognostic hypoxia metagene', *British Journal of Cancer*, 102(2), pp. 428–435. doi: 10.1038/sj.bjc.6605450.

Camuzi, D. *et al.* (2019) 'Regulation Is in the Air: The Relationship between Hypoxia and Epigenetics in Cancer', *Cells*, 8(4), p. 300. doi: 10.3390/cells8040300.

Delaney, C., Garg, S. K. and Yung, R. (2015) 'Analysis of DNA Methylation by Pyrosequencing.', *Methods in molecular biology (Clifton, N.J.)*. NIH Public Access, 1343, pp. 249–64. doi: 10.1007/978-1-4939-2963-4_19.

Desjobert, C. *et al.* (2019) 'Demethylation by low-dose 5-aza-2'-deoxycytidine impairs 3D melanoma invasion partially through miR-199a-3p expression revealing the role of this miR in melanoma', *Clinical Epigenetics*, 11(1), p. 9. doi: 10.1186/s13148-018-0600-2.

Ehrlich, M. (2002) 'DNA methylation in cancer: too much, but also too little', *Oncogene*. Nature Publishing Group, 21(35), pp. 5400–5413. doi: 10.1038/sj.onc.1205651.

Flores, E. M. *et al.* (2019) '*Thy1* (CD90) expression is regulated by DNA methylation during adipogenesis', *The FASEB Journal*, 33(3), pp. 3353–3363. doi: 10.1096/fj.201801481R.

Fredsøe, J. *et al.* (2018) 'Diagnostic and Prognostic MicroRNA Biomarkers for Prostate Cancer in Cell-free Urine', *European Urology Focus*, 4(6), pp. 825–833. doi: 10.1016/j.euf.2017.02.018.

Helwak, A. and Tollervey, D. (2014) 'Mapping the miRNA interactome by crosslinking ligation and sequencing of hybrids (CLASH)', *Nature protocols*. Europe PMC Funders, 9(3), p. 711. doi: 10.1038/NPROT.2014.043.

Hu, B. *et al.* (2018) 'Differentially expressed miRNAs in hepatocellular carcinoma cells under hypoxic conditions are associated with transcription and phosphorylation.', *Oncology letters*. Spandidos Publications, 15(1), pp. 467–474. doi: 10.3892/ol.2017.7349.

Huang, L. *et al.* (2019) 'Foetal hypoxia impacts methylome and transcriptome in developmental programming of heart disease', *Cardiovascular Research*, 115(8), pp. 1306–1319. doi: 10.1093/cvr/cvy277.

Irwin, R. E. *et al.* (2019) 'A randomized controlled trial of folic acid intervention in pregnancy highlights a putative methylation-regulated control element at ZFP57', *Clinical Epigenetics*, 11(1), p. 31. doi: 10.1186/s13148-019-0618-0.

Kämpfer, A. A. M. *et al.* (2017) 'Development of an in vitro co-culture model to mimic the human intestine in healthy and diseased state.', *Toxicology in vitro : an international journal published in association with BIBRA*. Elsevier, 45(Pt 1), pp. 31–43. doi: 10.1016/j.tiv.2017.08.011.

Kang, N. *et al.* (2019) 'Hypoxia-induced cancer stemness acquisition is associated with CXCR4 activation by its aberrant promoter demethylation', *BMC Cancer*, 19(1), p. 148. doi: 10.1186/s12885-019-5360-7.

Kiga, K. *et al.* (2014) 'Epigenetic silencing of miR-210 increases the proliferation of gastric epithelium during chronic Helicobacter pylori infection', *Nature Communications*, 5(1), p. 4497. doi: 10.1038/ncomms5497.

Kim, Y. *et al.* (2014) 'Serum microRNA-21 as a Potential Biomarker for Response to Hypomethylating Agents in Myelodysplastic Syndromes', *PLoS ONE*. Edited by D. T. Starczynowski, 9(2), p. e86933. doi: 10.1371/journal.pone.0086933.

Kumar, S., Nag, A. and Mandal, C. C. (2015) 'A Comprehensive Review on miR-200c, A Promising Cancer Biomarker with Therapeutic Potential.', *Current drug targets*, 16(12), pp. 1381–403.

Lacher, D. A. and O'donnell, E. D. (1988) *Comparison of Multidimensional Scaling and Principal Component Analysis of Interspecific Variation in Bacteria**, *ANNALS OF CLINICAL AND LABORATORY SCIENCE*.

Lai, Q. *et al.* (2018) 'Decitibine improve the efficiency of anti-PD-1 therapy via activating the response to IFN/PD-L1 signal of lung cancer cells', *Oncogene*, 37(17), pp. 2302–2312. doi: 10.1038/s41388-018-0125-3.

Li, L. (2010) 'Dimension Reduction for High-Dimensional Data', in *Methods in molecular biology (Clifton, N.J.)*, pp. 417–434. doi: 10.1007/978-1-60761-580-4_14.

Li, S. *et al.* (2015) 'Downregulation of EphA5 by promoter methylation in human prostate cancer', *BMC Cancer*. BioMed Central, 15(1), p. 18. doi: 10.1186/s12885-015-1025-3.

Liu, Q. *et al.* (2011) 'Hypoxia Induces Genomic DNA Demethylation through the Activation of HIF-1 and Transcriptional Upregulation of MAT2A in Hepatoma Cells', *Molecular Cancer Therapeutics*, 10(6), pp. 1113–1123. doi: 10.1158/1535-7163.MCT-10-1010.

Love, M. I., Huber, W. and Anders, S. (2014) 'Moderated estimation of fold change and dispersion for RNA-seq data with DESeq2', *Genome Biology*. BioMed Central, 15(12), p. 550. doi: 10.1186/s13059-014-0550-8.

Lu, A. *et al.* (2019) 'Reprogrammable CRISPR/dCas9-based recruitment of DNMT1 for site-specific DNA demethylation and gene regulation', *Cell Discovery*. Nature Publishing Group, 5(1), p. 22. doi: 10.1038/s41421-019-0090-1.

Lynch, S. M. *et al.* (2016a) 'Regulation of miR-200c and miR-141 by Methylation in Prostate Cancer', *The Prostate*, 76(13), pp. 1146–1159. doi: 10.1002/pros.23201.

Lynch, S. M. *et al.* (2016b) 'Regulation of miR-200c and miR-141 by Methylation in Prostate Cancer', *The Prostate*, 76(13), pp. 1146–1159. doi: 10.1002/pros.23201.

Maatouk, D. M. *et al.* (2006) 'DNA methylation is a primary mechanism for silencing postmigratory primordial germ cell genes in both germ cell and somatic cell lineages', *Development*, 133(17), pp. 3411–3418. doi: 10.1242/dev.02500.

Mackin, S.-J., O'Neill, K. M. and Walsh, C. P. (2018b) 'Comparison of DNMT1 inhibitors by methylome profiling identifies unique signature of 5-aza-2′deoxycytidine', *Epigenomics*. Future Medicine Ltd London, UK , 10(8), pp. 1085–1101. doi: 10.2217/epi-2017-0171.

Martignano, F. *et al.* (2016) 'GSTP1 Methylation and Protein Expression in Prostate Cancer: Diagnostic Implications.', *Disease markers*. Hindawi Limited, 2016, p. 4358292. doi: 10.1155/2016/4358292.

Ortiz, I. M. D. P. *et al.* (2018) 'Loss of DNA methylation is related to increased expression of miR-21 and miR-146b in papillary thyroid carcinoma', *Clinical Epigenetics*, 10(1), p. 144. doi: 10.1186/s13148-018-0579-8.

Palii, S. S. *et al.* (2008) 'DNA Methylation Inhibitor 5-Aza-2′-Deoxycytidine Induces Reversible Genome-Wide DNA Damage That Is Distinctly Influenced by DNA Methyltransferases 1 and 3B', *Molecular and Cellular Biology*. American Society for Microbiology Journals, 28(2), pp. 752–771. doi: 10.1128/MCB.01799-07.

Ramassone, A. *et al.* (2018) 'Epigenetics and MicroRNAs in Cancer', *International Journal of Molecular Sciences*, 19(2), p. 459. doi: 10.3390/ijms19020459.

Santini, V. (2019) 'How I treat MDS after hypomethylating agent failure.', *Blood*. American Society of Hematology, 133(6), pp. 521–529. doi: 10.1182/blood-2018-03-785915.

Stirzaker, C. *et al.* (2014) 'Mining cancer methylomes: prospects and challenges', *Trends in Genetics*, 30(2), pp. 75–84. doi: 10.1016/j.tig.2013.11.004.

Thakur, A. *et al.* (2016) 'Widespread recovery of methylation at gametic imprints in hypomethylated mouse stem cells following rescue with DNMT3A2', *Epigenetics & Chromatin*, 9(1), p. 53. doi: 10.1186/s13072-016-0104-2.

Thienpont, B. *et al.* (2016) 'Tumour hypoxia causes DNA hypermethylation by reducing TET activity', *Nature*. Nature Publishing Group, 537(7618), pp. 63–68. doi: 10.1038/nature19081.

Wang, Z. *et al.* (2017) 'Hypoxia-induced miR-210 promoter demethylation enhances proliferation, autophagy and angiogenesis of schwannoma cells', *Oncology Reports*, 37(5), pp. 3010–3018. doi: 10.3892/or.2017.5511.

Xiong, L. *et al.* (2012) 'DNA demethylation regulates the expression of miR-210 in neural progenitor cells subjected to hypoxia', *FEBS Journal*, 279(23), pp. 4318–4326. doi: 10.1111/febs.12021.

Yang, Y. *et al.* (2017) 'Combination of azacitidine and trichostatin A decreased the tumorigenic potential of lung cancer cells', *OncoTargets and Therapy*, Volume 10, pp. 2993–2999. doi: 10.2147/OTT.S136218.

5. 7. Supplementary figures

Supplementary Figure 1. Analyses of mRNAseq data. Normalised by DESeq2 method.

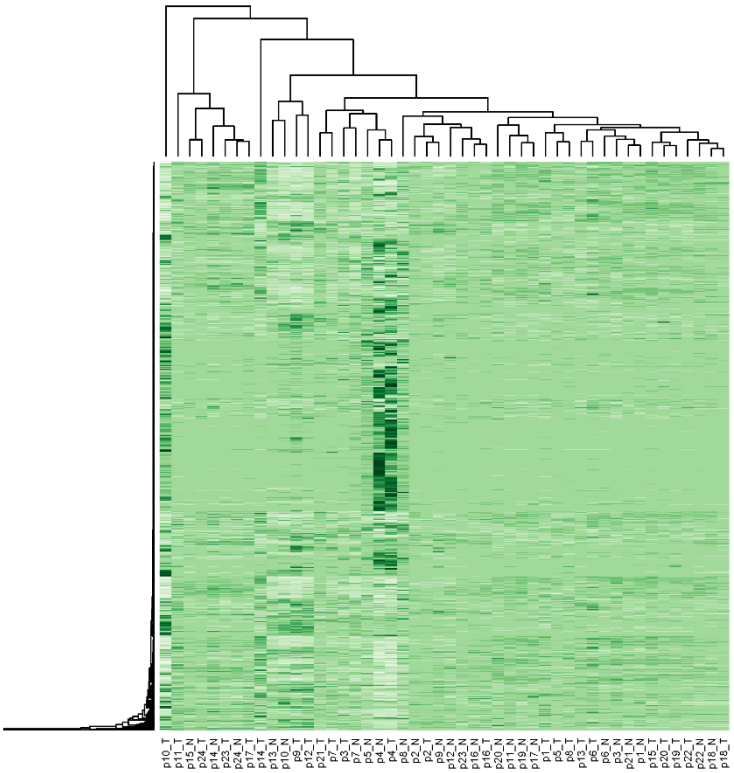

Figure 1A. Unsupervised clustering of all samples based on DESeq2 normalised mRNAseq data. Produced with the base function heatmap() using DESeq2 normalised data.

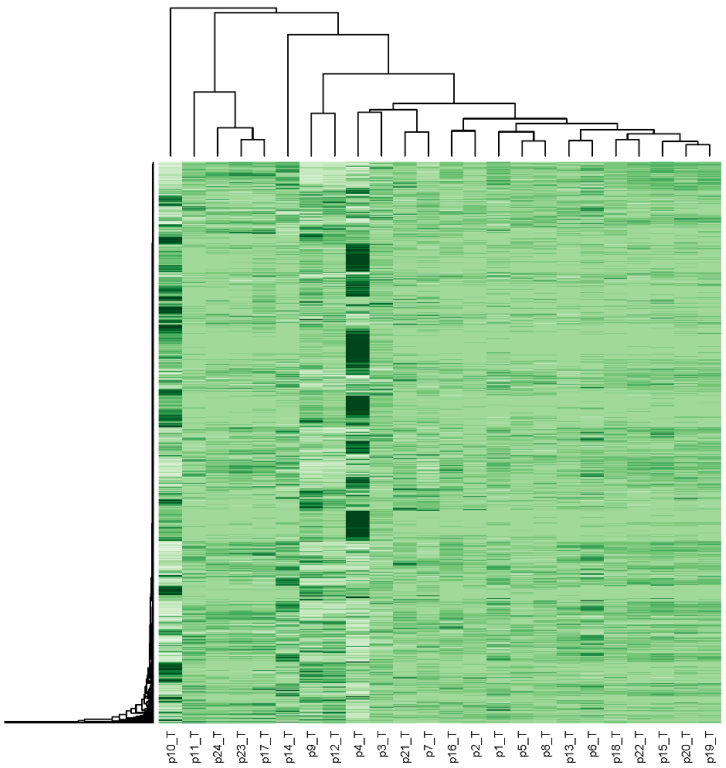

Figure 1B. Unsupervised clustering of tumour samples based on DESeq2 normalised mRNAseq data. Produced with the base function heatmap() using DESeq2 normalised data.

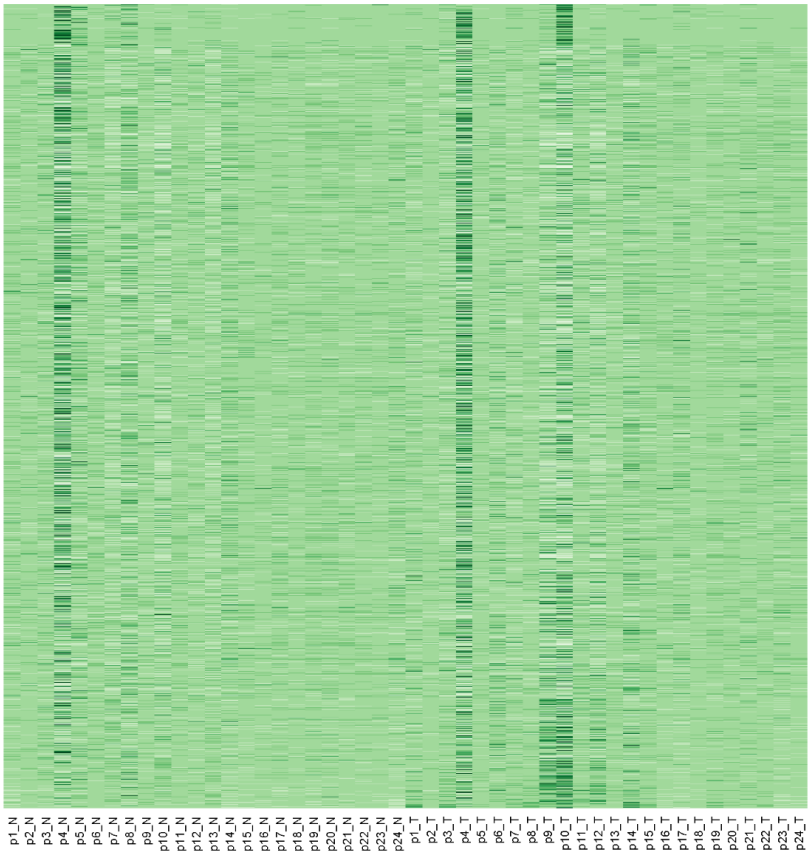

Figure 1C. Supervised clustering of all samples, comparing tumour with non-tumour status, based on DESeq2 normalised mRNAseq data. Produced with the base function heatmap() using DESeq2 normalised data.

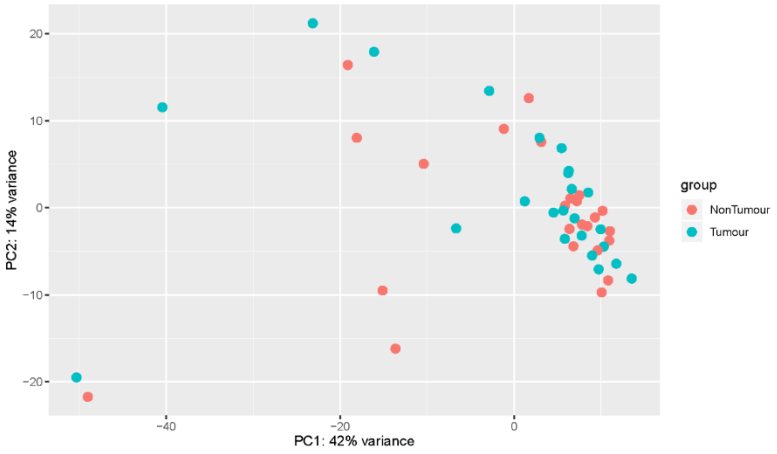

Figure 1D. PCA analysis comparing tumour with non-tumour status, based on DESeq2 normalised mRNAseq data with log2 transformed data by the variance stabilising transformation method. Produced using pretty heatmap (pheatmap) package in RStudio v3.5.1.

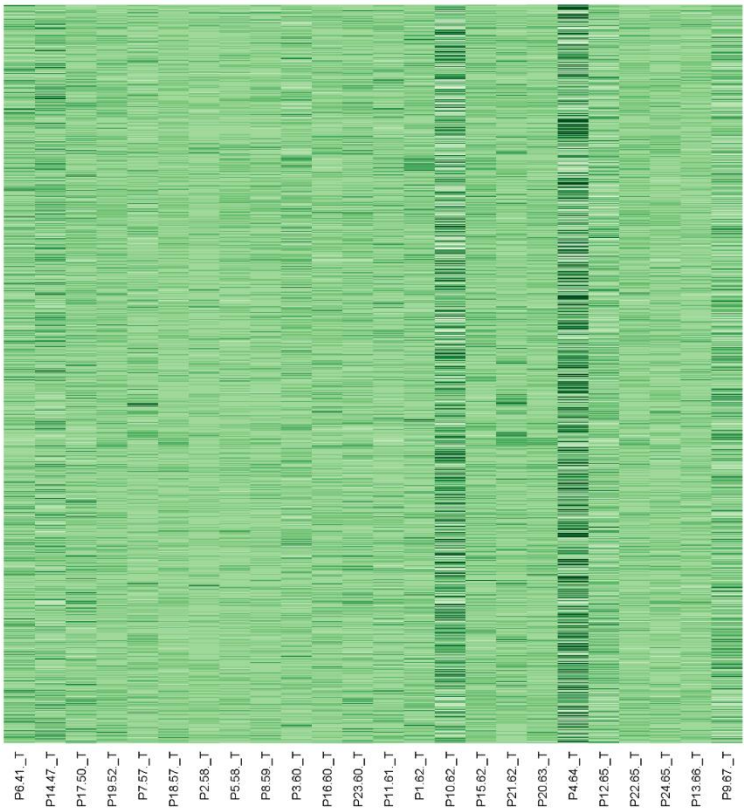

Figure 1E. Supervised clustering of tumour samples by patient age shows distinctness between older and younger patients (age shown after patient number on x-axis), based on DESeq2 normalised mRNAseq data. Produced with the base function heatmap() using DESeq2 normalised data.

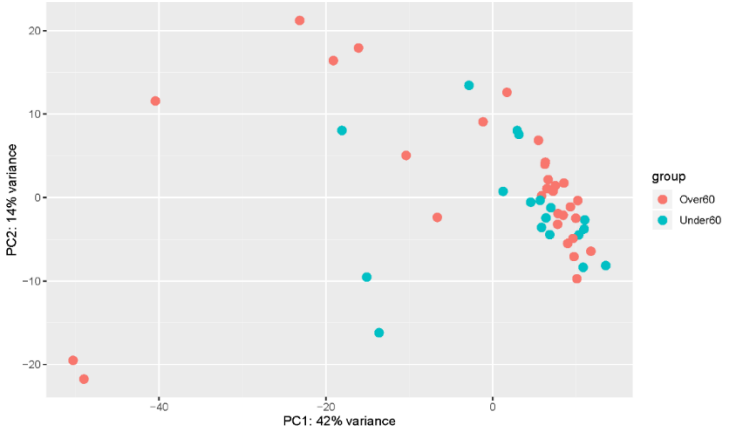

Figure 1F. PCA analysis of tumour samples, modelling patients over 60 years versus under 60 years, based on DESeq2 normalised mRNAseq data with log2 transformed data by the variance stabilising transformation method. Produced using pretty heatmap (pheatmap) package in RStudio v3.5.1.

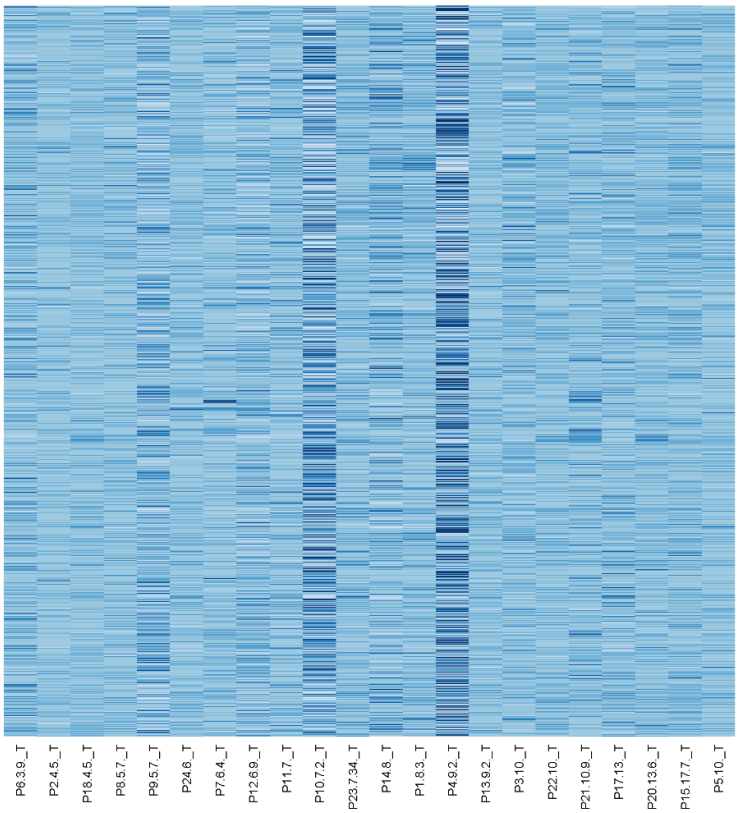

Figure X. Heatmap using supervised clustering of tumour samples by PSA level (shown in ng/µL following patient number on x-axis) based on DESeq2 normalised mRNAseq data. Produced with the base function heatmap() using DESeq2 normalised data.

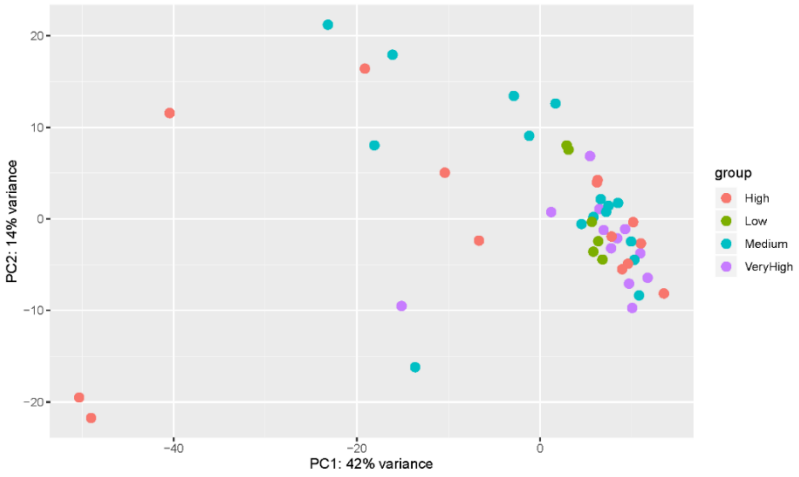

Figure 1G. PCA analysis of tumour samples by PSA level group (Low: ≤5ng/µL, Medium: 5-7ng/µL, High 7-10ng/µL, Very High: ≥10ng/µL), based on DESeq2 normalised mRNAseq data with log2 transformed data by the variance stabilising transformation method. Produced using pretty heatmap (pheatmap) package in RStudio v3.5.1.

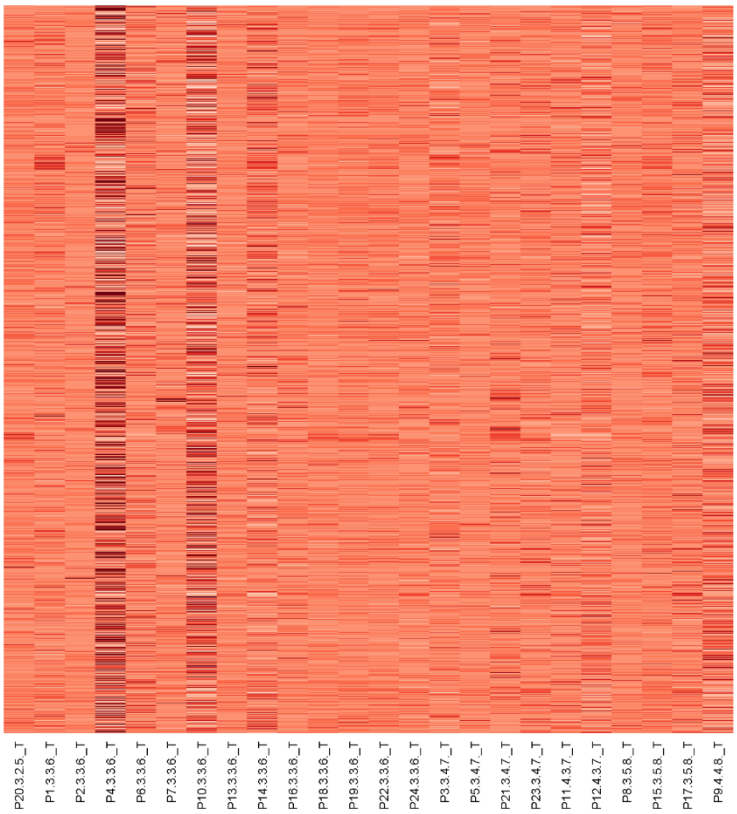

Figure 1H. Heatmap showing supervised clustering of tumour samples by Gleason score (shown following patient number on the x-axis) based on DESeq2 normalised mRNAseq data. Produced with the base function heatmap() using DESeq2 normalised data.

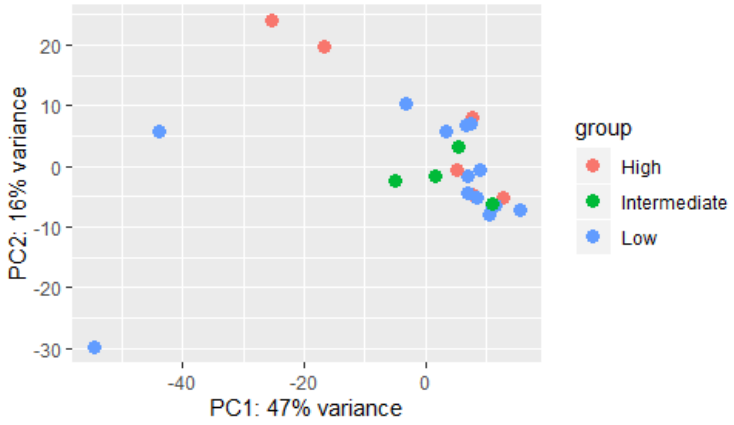

Figure 1I. PCA analysis of tumour samples by Gleason score groups (Low: 6, Intermediate: 3 + 4 =7, High ≥4 + 3 = 7). Produced using pretty heatmap (pheatmap) package in RStudio v3.5.1.

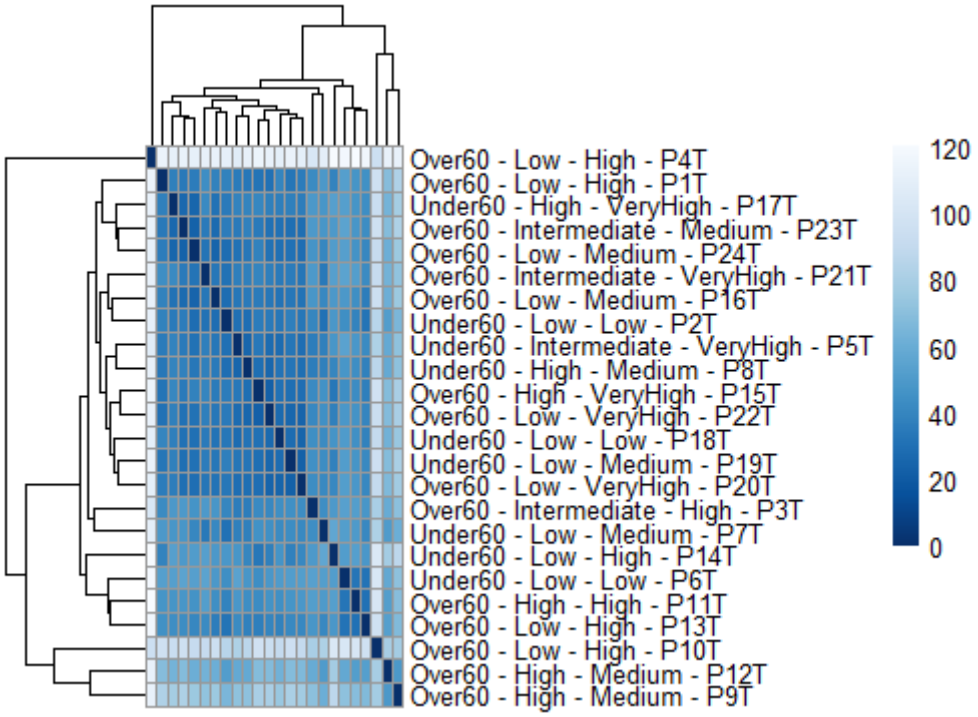

Figure 1J. Distances matrix by patient similarity, including patient characteristics. Produced using pretty heatmap (pheatmap) package in RStudio v3.5.1.

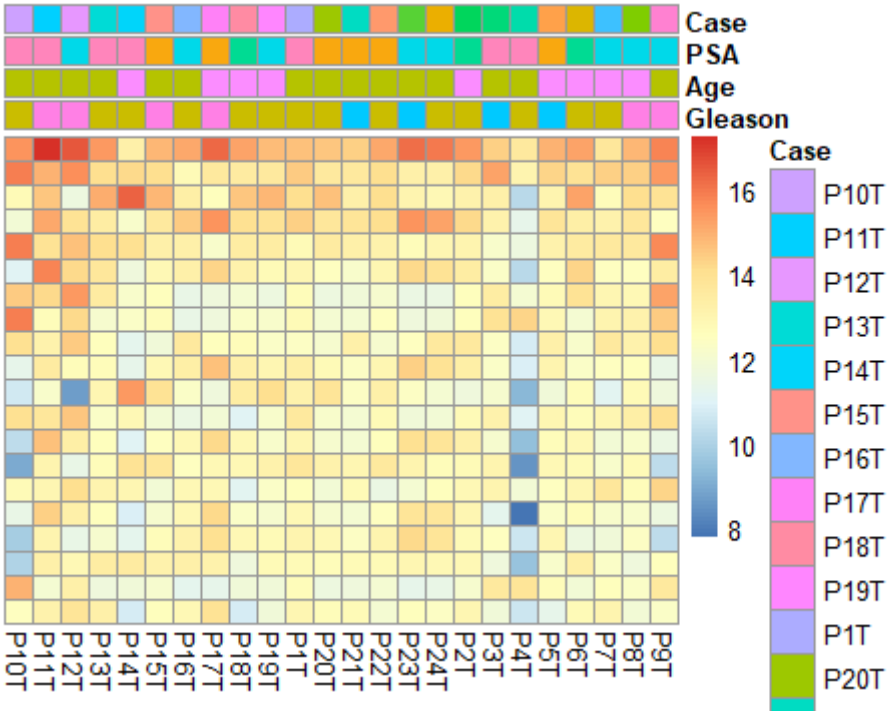

Figure 1K. Heatmap including all patient characteristics. Produced using pretty heatmap (pheatmap) package in RStudio v3.5.1.

Supplementary Figure 2. Analyses of mRNAseq data. Normalised by DESeq2 method.

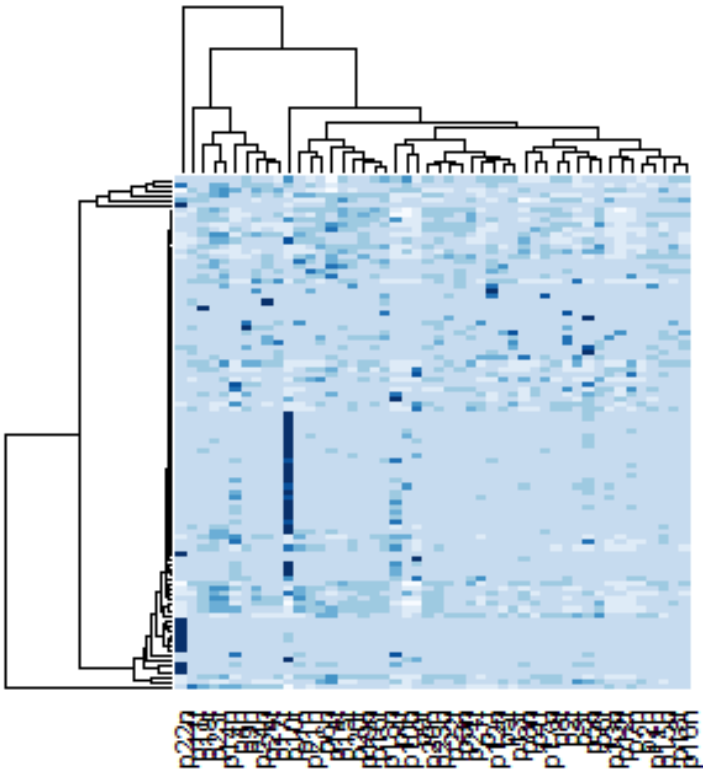

Figure 2A. Unsupervised clustering of all samples. Produced with the base function heatmap() using DESeq2 normalised data. Produced with the base function heatmap() using DESeq2 normalised data.

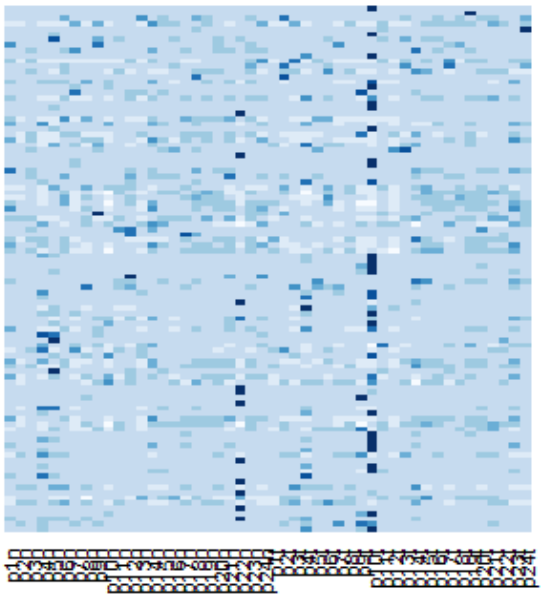

Figure 2B. Supervised clustering of all samples by tumour versus non-tumour status. Produced with the base function heatmap() using DESeq2 normalised data. Produced with the base function heatmap() using DESeq2 normalised data.

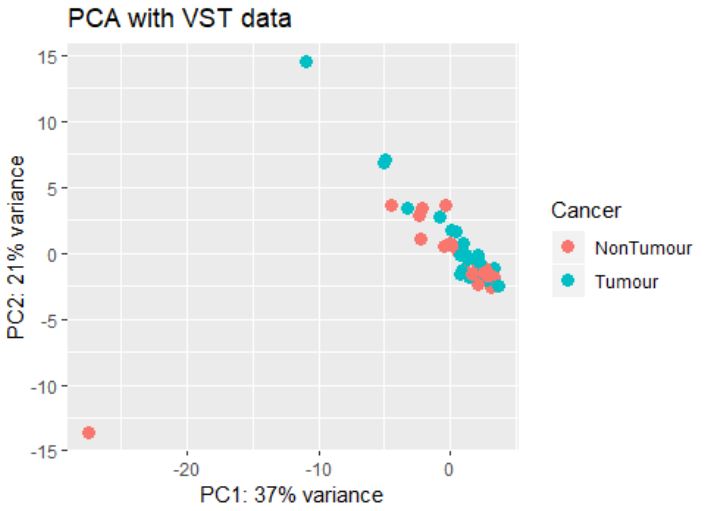

Figure 2C. PCA analysis comparing tumour versus non-tumour samples. Produced using pretty heatmap (pheatmap) package in RStudio v3.5.1.

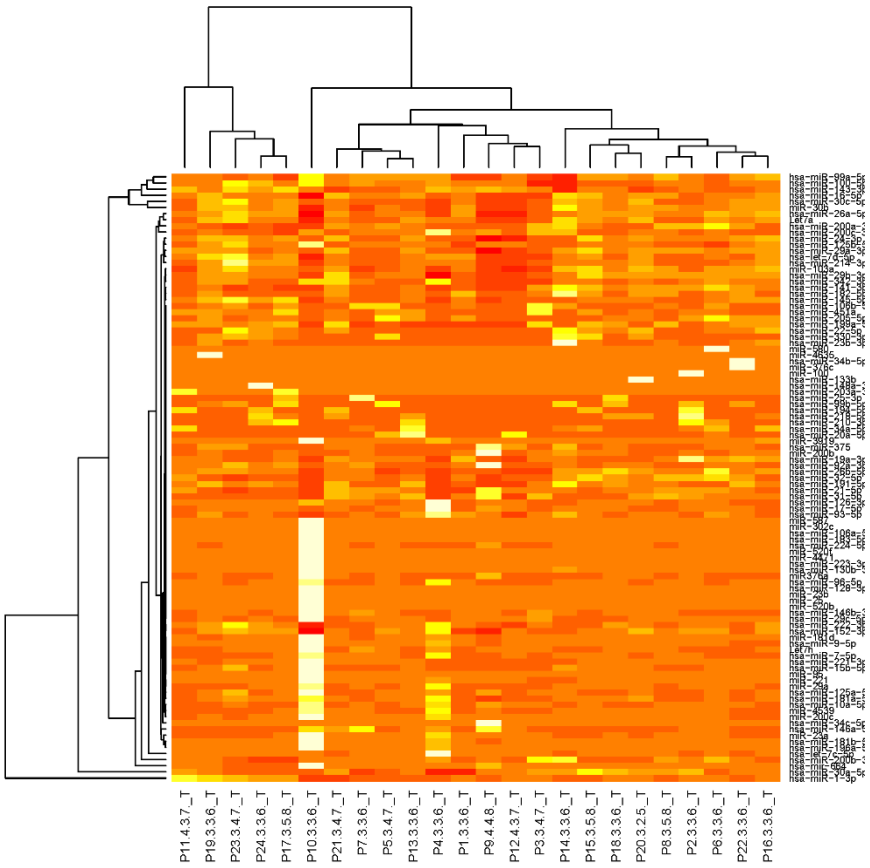

Figure 2D. Heatmap showing unsupervised clustering of tumour samples. Produced with the base function heatmap() using DESeq2 normalised data.

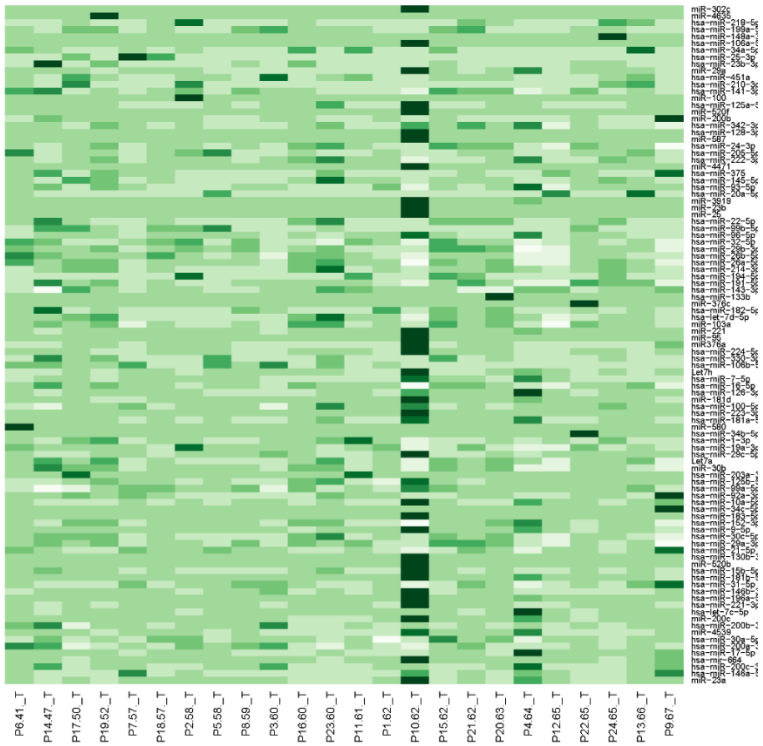

Figure 2. Heatmap showing supervised clustering of tumour samples by patient age. Produced with the base function heatmap() using DESeq2 normalised data.

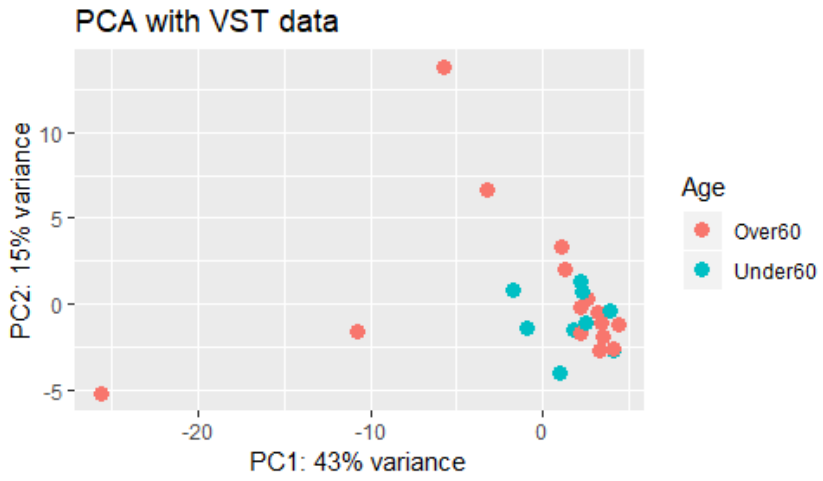

Figure 2F. PCA analysis of tumour samples by patient age. Produced using pretty heatmap (pheatmap) package in RStudio v3.5.1.

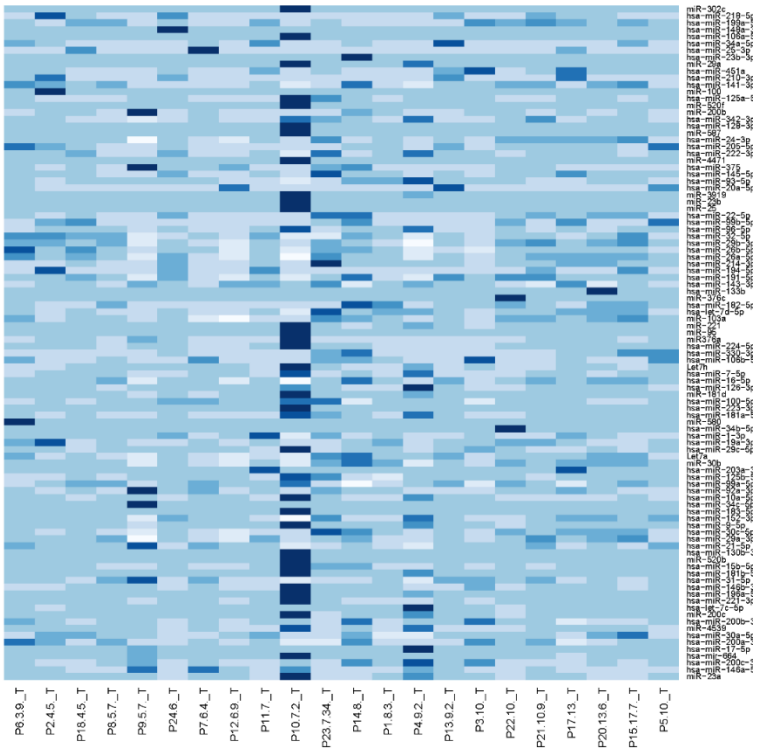

Figure 2G. Heatmap showing supervised clustering of tumour samples by patient PSA level (ng/µL, shown after the patient number on x-axis). Produced with the base function heatmap() using DESeq2 normalised data.

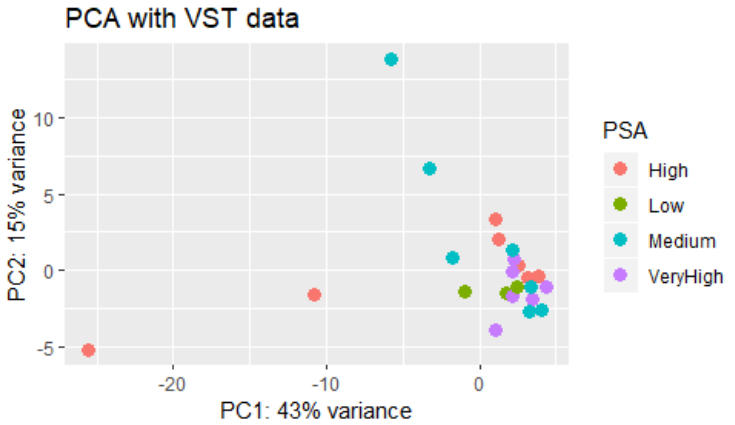

Figure 2H. PCA analysis of tumour samples by patient PSA level in ng/µL (Low: ≤5ng/µL, Medium: 5-7ng/µL, High 7-10ng/µL, Very High: ≥10ng/µL). Produced using pretty heatmap (pheatmap) package in RStudio v3.5.1.

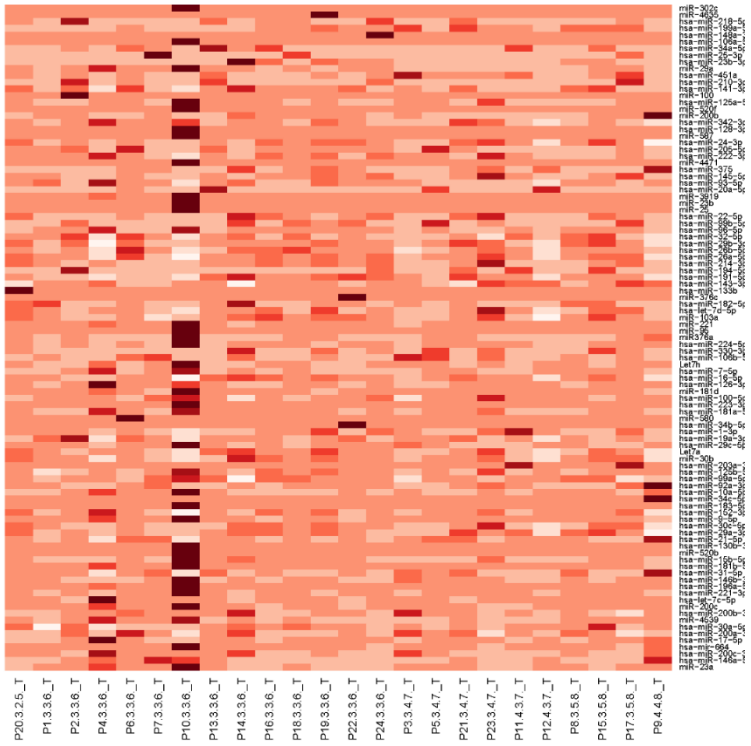

Figure 2I. Heatmap showing supervised clustering of tumour samples by patient Gleason score (shown after the patient number on x-axis). Produced with the base function heatmap() using DESeq2 normalised data.

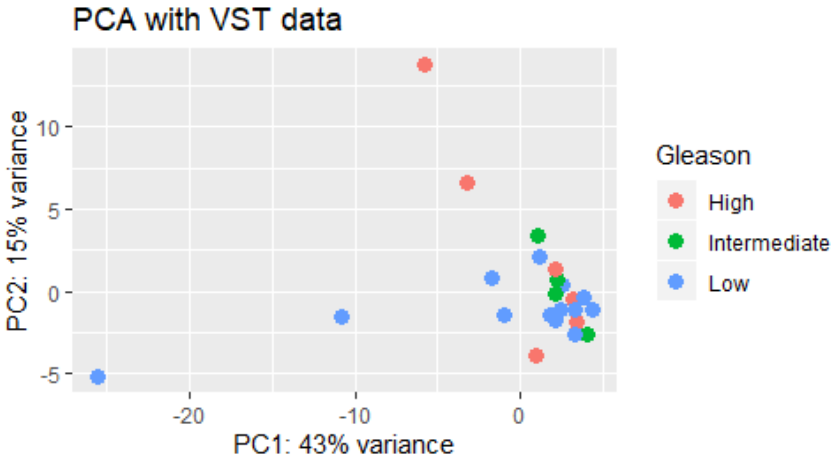

Figure 2J. PCA analysis of tumour samples by Gleason score groups (Low: 6, Intermediate: 3 + 4 =7, High ≥4 + 3 = 7). Produced using pretty heatmap (pheatmap) package in RStudio v3.5.1.

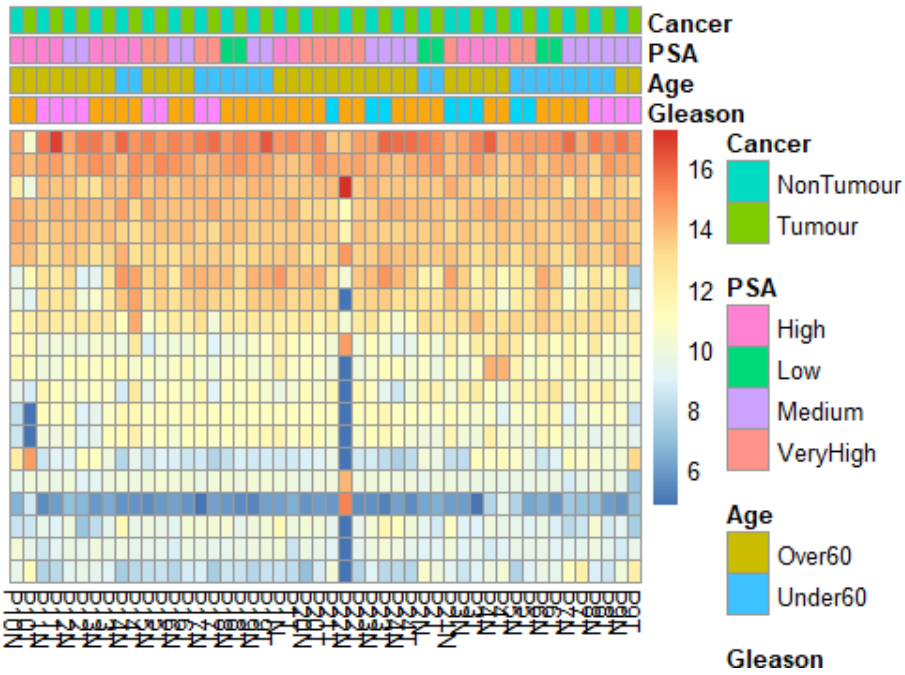

Figure 2K. Heatmap of all samples, including all patient characteristics. Produced using pretty heatmap (pheatmap) package in RStudio v3.5.1.

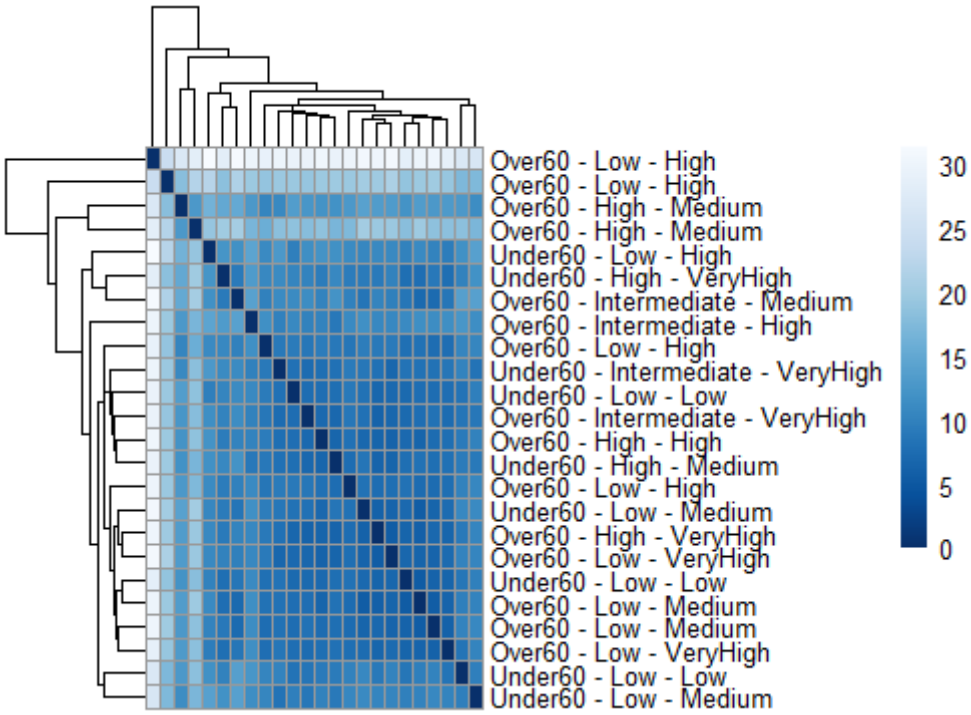

Figure 2L. Distances matrix of all tumour samples by patient similarity, including patient characteristics. Produced using pretty heatmap (pheatmap) package in RStudio v3.5.1.

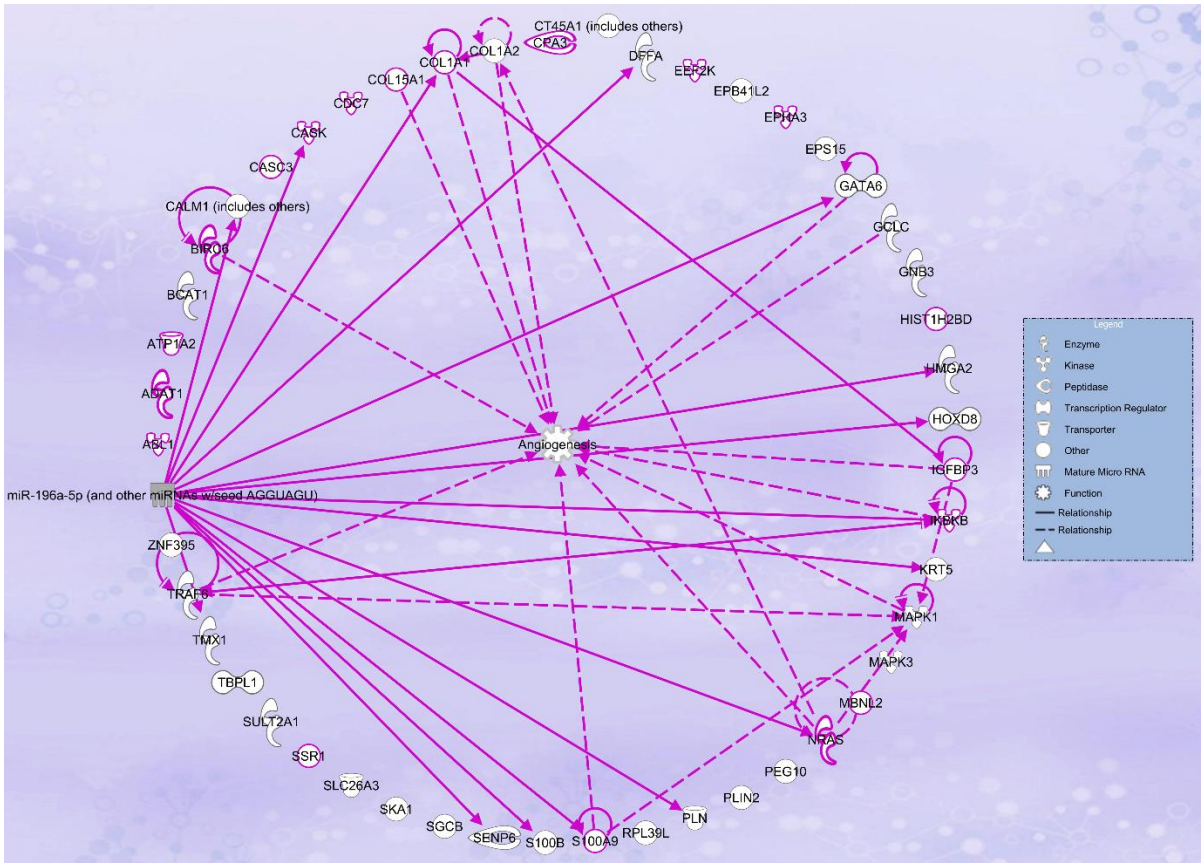

Supplementary Figure 3. Integrative Analysis of mRNA-seq and miRNA-seq data using IPA reveals numerous predicted mRNA targets of miR-196a with significant inverse expression correlation. MiR-196a (left-hand side, coloured grey) was significantly upregulated in the miRNA-seq dataset, the other proteins represent mRNAs with seed-binding complementarity that were significantly downregulated in the mRNA-seq data. Those which have been validated as mRNA targets (among all other cell types) are connected with arrows. Pathway overlay with “prostate carcinoma” disease used to highlight molecules previously implicated in PCa (molecules highlighted in purple). Pathway build with “angiogenesis” pathways used to illustrate the molecules previously implicated in this process, which may have relevance for hypoxia (connected by purple arrows in the direction of regulation, dashed lines indicate indirect regulation, full lines indicate direct). The shape of each icon identifies the type of molecule, as coded in the legend.

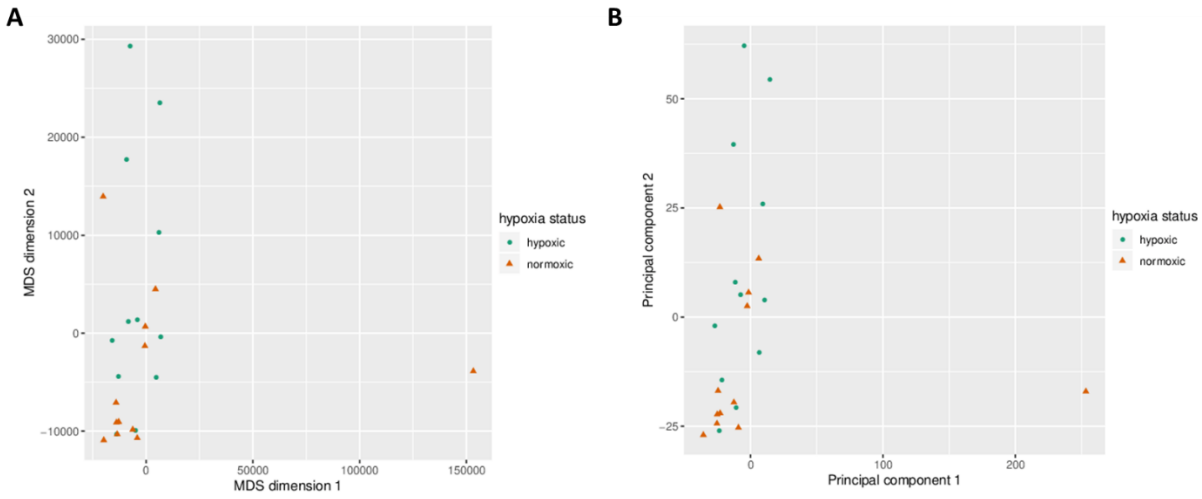

Supplementary Figure 4. Principal component analysis (PCA) and multidimensional scaling (MDS) methods of dimension reduction, including sample 14. Each point represents a sample, colour and shape represents hypoxic status. **A)** MDS applied to the dataset reveals some clustering of the normoxic samples. **B)** PCA applied to the dataset does not cluster by hypoxic status.

Supplementary Table 1. Functional Annotation Chart of the Promoters with Losses in methylation. From the top 100 combined rank promoters, promoters analysed n=44.

Category	Term	Count	%	P-Value	Benjamini
GOTERM_MF_DIRECT	Toll-like receptor 2 binding	2	6.1	3.20E-03	1.60E-01
INTERPRO	Toll-like receptor	2	6.1	4.30E-03	2.40E-01
PIR_SUPERFAMILY	toll-like receptor, 1/2/4/6/10 types [Parent=PIRSF800008]	2	6.1	4.70E-03	9.40E-03
KEGG_PATHWAY	Toll-like receptor signaling pathway	3	9.1	6.20E-03	1.40E-01
GOTERM_BP_DIRECT	inflammatory response	4	12.1	8.40E-03	8.00E-01
GOTERM_MF_DIRECT	lipopeptide binding	2	6.1	8.50E-03	2.10E-01
UP_SEQ_FEATURE	signal peptide	10	30.3	8.60E-03	5.40E-01
GOTERM_BP_DIRECT	positive regulation of interleukin-6 biosynthetic process	2	6.1	9.00E-03	5.80E-01
UP_SEQ_FEATURE	site:Reactive site	2	6.1	1.00E-02	3.70E-01
GOTERM_BP_DIRECT	immune response	4	12.1	1.10E-02	5.20E-01
GOTERM_BP_DIRECT	regulation of cytokine secretion	2	6.1	1.20E-02	4.50E-01
UP_SEQ_FEATURE	short sequence motif:Secondary area of contact	2	6.1	1.40E-02	3.40E-01
GOTERM_BP_DIRECT	megakaryocyte development	2	6.1	1.80E-02	5.00E-01
INTERPRO	Proteinase inhibitor I25, cystatin	2	6.1	1.90E-02	4.60E-01
GOTERM_BP_DIRECT	platelet formation	2	6.1	2.10E-02	5.00E-01
SMART	CY	2	6.1	2.20E-02	3.70E-01
INTERPRO	Toll/interleukin-1 receptor homology (TIR) domain	2	6.1	2.80E-02	4.50E-01
UP_SEQ_FEATURE	domain:TIR	2	6.1	2.80E-02	4.70E-01

UP_KEYWORDS	Thiol protease inhibitor	2	6.1	2.90E-02	8.90E-01
SMART	TIR	2	6.1	2.90E-02	2.60E-01
UP_KEYWORDS	Signal	10	30.3	2.90E-02	6.70E-01
GOTERM_BP_DIRECT	toll-like receptor signaling pathway	2	6.1	3.00E-02	5.70E-01
GOTERM_MF_DIRECT	cysteine-type endopeptidase inhibitor activity	2	6.1	3.60E-02	4.90E-01
GOTERM_BP_DIRECT	MyD88-dependent toll-like receptor signaling pathway	2	6.1	3.70E-02	5.90E-01
UP_SEQ_FEATURE	glycosylation site:N-linked (GlcNAc...)	10	30.3	3.80E-02	4.90E-01
KEGG_PATHWAY	Neuroactive ligand-receptor interaction	3	9.1	3.90E-02	3.80E-01
UP_KEYWORDS	Glycoprotein	10	30.3	4.90E-02	7.20E-01
UP_KEYWORDS	Cell membrane	8	24.2	5.30E-02	6.40E-01
GOTERM_CC_DIRECT	phagocytic vesicle membrane	2	6.1	6.90E-02	9.50E-01
UP_KEYWORDS	Disulfide bond	8	24.2	7.50E-02	7.00E-01
INTERPRO	Cysteine-rich flanking region, C-terminal	2	6.1	8.60E-02	7.60E-01
GOTERM_CC_DIRECT	integral component of plasma membrane	5	15.2	8.60E-02	8.40E-01
UP_SEQ_FEATURE	topological domain:Extracellular	7	21.2	8.90E-02	7.50E-01

Supplementary Table 7. Functional Annotation Chart of the Promoters with Gains in methylation. From the top 100 combined rank promoters, promoters analysed n=56.

Category	**Term**	**Count**	**%**	**P-Value**	**Benjamini**
INTERPRO	Homeodomain, metazoa	6	13.6	6.70E-07	6.60E-05
INTERPRO	Homeobox, conserved site	7	15.9	1.10E-06	5.60E-05
GOTERM_MF_DIRECT	sequence-specific DNA binding	9	20.5	2.40E-06	1.50E-04
UP_SEQ_FEATURE	DNA-binding region:T-box	4	9.1	3.20E-06	4.00E-04
INTERPRO	Transcription factor, T-box, conserved site	4	9.1	3.80E-06	1.20E-04
INTERPRO	Transcription factor, T-box	4	9.1	3.80E-06	1.20E-04
INTERPRO	Homeodomain	7	15.9	6.30E-06	1.60E-04
UP_KEYWORDS	Homeobox	7	15.9	9.20E-06	6.70E-04
SMART	TBOX	4	9.1	1.00E-05	2.40E-04
GOTERM_BP_DIRECT	anterior/posterior pattern specification	5	11.4	1.40E-05	4.10E-03
UP_SEQ_FEATURE	DNA-binding region:Homeobox	6	13.6	2.50E-05	1.60E-03
INTERPRO	Homeodomain-like	7	15.9	3.00E-05	5.80E-04
SMART	HOX	7	15.9	3.40E-05	4.00E-04
INTERPRO	p53-like transcription factor, DNA-binding	4	9.1	7.10E-05	1.20E-03
GOTERM_MF_DIRECT	transcription factor activity, sequence-specific DNA binding	9	20.5	2.00E-04	6.50E-03
UP_KEYWORDS	DNA-binding	13	29.5	2.80E-04	1.00E-02
UP_KEYWORDS	Developmental protein	9	20.5	3.40E-04	8.30E-03
GOTERM_BP_DIRECT	regulation of transcription, DNA-templated	10	22.7	1.20E-03	1.70E-01

GOTERM_BP_DIRECT	embryonic forelimb morphogenesis	3	6.8	1.60E-03	1.50E-01
GOTERM_CC_DIRECT	nucleus	20	45.5	2.00E-03	8.00E-02
GOTERM_BP_DIRECT	embryonic skeletal system morphogenesis	3	6.8	2.30E-03	1.60E-01
GOTERM_BP_DIRECT	embryonic limb morphogenesis	3	6.8	2.50E-03	1.40E-01
UP_KEYWORDS	Transcription regulation	12	27.3	3.20E-03	5.60E-02
UP_KEYWORDS	Transcription	12	27.3	3.90E-03	5.60E-02
GOTERM_BP_DIRECT	transcription, DNA-templated	10	22.7	7.10E-03	3.10E-01
GOTERM_BP_DIRECT	angiogenesis	4	9.1	7.90E-03	2.90E-01
GOTERM_BP_DIRECT	positive regulation of transcription from RNA polymerase II promoter	7	15.9	8.20E-03	2.70E-01
UP_KEYWORDS	Cardiomyopathy	3	6.8	1.00E-02	1.20E-01
GOTERM_BP_DIRECT	parathyroid gland development	2	4.5	1.30E-02	3.50E-01
INTERPRO	Beta tubulin	2	4.5	1.60E-02	2.10E-01
INTERPRO	Beta tubulin, autoregulation binding site	2	4.5	1.60E-02	2.10E-01
GOTERM_BP_DIRECT	atrial septum morphogenesis	2	4.5	2.40E-02	5.20E-01
GOTERM_BP_DIRECT	morphogenesis of an epithelium	2	4.5	2.60E-02	5.10E-01
UP_KEYWORDS	Atrial fibrillation	2	4.5	2.60E-02	2.40E-01
GOTERM_BP_DIRECT	endocardial cushion morphogenesis	2	4.5	2.90E-02	5.30E-01
GOTERM_BP_DIRECT	cellular response to cadmium ion	2	4.5	3.10E-02	5.20E-01
GOTERM_BP_DIRECT	positive regulation of chondrocyte differentiation	2	4.5	3.50E-02	5.30E-01
INTERPRO	Homeobox protein, antennapedia type, conserved site	2	4.5	3.60E-02	3.60E-01
INTERPRO	Tubulin/FtsZ, 2-layer sandwich domain	2	4.5	4.00E-02	3.60E-01
GOTERM_BP_DIRECT	positive regulation of cardiac muscle cell proliferation	2	4.5	4.00E-02	5.60E-01
INTERPRO	Tubulin, C-terminal	2	4.5	4.10E-02	3.40E-01
INTERPRO	Tubulin, conserved site	2	4.5	4.10E-02	3.40E-01
INTERPRO	Tubulin/FtsZ, C-terminal	2	4.5	4.10E-02	3.40E-01
UP_SEQ_FEATURE	short sequence motif:Antp-type hexapeptide	2	4.5	4.20E-02	8.30E-01
GOTERM_BP_DIRECT	outflow tract septum morphogenesis	2	4.5	4.20E-02	5.60E-01
INTERPRO	Tubulin	2	4.5	4.30E-02	3.30E-01
GOTERM_BP_DIRECT	proximal/distal pattern formation	2	4.5	4.30E-02	5.50E-01
INTERPRO	Tubulin/FtsZ, GTPase domain	2	4.5	4.50E-02	3.20E-01
GOTERM_BP_DIRECT	thyroid gland development	2	4.5	4.50E-02	5.40E-01
GOTERM_BP_DIRECT	pattern specification process	2	4.5	5.00E-02	5.60E-01
UP_KEYWORDS	Nucleus	16	36.4	5.10E-02	3.80E-01
GOTERM_MF_DIRECT	RNA polymerase II regulatory region sequence-specific DNA binding	3	6.8	5.20E-02	6.80E-01
GOTERM_BP_DIRECT	cellular response to fibroblast growth factor stimulus	2	4.5	5.40E-02	5.70E-01

SMART	SM00865	2	4.5	5.50E-02	3.70E-01
GOTERM_BP_DIRECT	blood vessel remodeling	2	4.5	5.70E-02	5.80E-01
GOTERM_BP_DIRECT	dorsal/ventral pattern formation	2	4.5	5.70E-02	5.80E-01
SMART	SM00864	2	4.5	6.00E-02	3.10E-01
GOTERM_BP_DIRECT	microtubule-based process	2	4.5	6.40E-02	6.00E-01
KEGG_PATHWAY	Pathogenic Escherichia coli infection	2	4.5	6.50E-02	6.80E-01
GOTERM_BP_DIRECT	positive regulation of transcription, DNA-templated	4	9.1	6.80E-02	6.10E-01
GOTERM_BP_DIRECT	multicellular organism development	4	9.1	7.00E-02	6.00E-01
GOTERM_BP_DIRECT	thymus development	2	4.5	7.60E-02	6.20E-01
GOTERM_BP_DIRECT	blood circulation	2	4.5	8.00E-02	6.20E-01
GOTERM_BP_DIRECT	cellular response to transforming growth factor beta stimulus	2	4.5	8.70E-02	6.40E-01
GOTERM_BP_DIRECT	odontogenesis of dentin-containing tooth	2	4.5	9.70E-02	6.70E-01

Supplementary Table 2. Functional Annotation Chart of the Genes with Losses in methylation. From the top 100 combined rank promoters, promoters analysed n=51.

Category	Term	Count	%	P-Value	Benjamini
GOTERM_MF_DIRECT	G-protein coupled receptor activity	8	22.2	1.60E-05	6.10E-04
UP_KEYWORDS	Glycoprotein	17	47.2	3.30E-05	2.50E-03
UP_SEQ_FEATURE	glycosylation site:N-linked (GlcNAc...)	16	44.4	5.00E-05	4.60E-03
UP_SEQ_FEATURE	topological domain:Extracellular	13	36.1	7.30E-05	3.40E-03
UP_KEYWORDS	G-protein coupled receptor	8	22.2	8.10E-05	3.00E-03
UP_KEYWORDS	Sensory transduction	7	19.4	1.10E-04	2.80E-03
UP_KEYWORDS	Transducer	8	22.2	1.20E-04	2.30E-03
GOTERM_MF_DIRECT	olfactory receptor activity	6	16.7	1.50E-04	3.00E-03
GOTERM_BP_DIRECT	detection of chemical stimulus involved in sensory perception of smell	6	16.7	1.90E-04	2.00E-02
INTERPRO	Olfactory receptor	6	16.7	1.90E-04	9.80E-03
INTERPRO	G protein-coupled receptor, rhodopsin-like	7	19.4	2.40E-04	6.20E-03
UP_KEYWORDS	Olfaction	6	16.7	2.50E-04	3.70E-03
INTERPRO	GPCR, rhodopsin-like, 7TM	7	19.4	2.80E-04	4.70E-03
KEGG_PATHWAY	Olfactory transduction	6	16.7	5.60E-04	9.50E-03
UP_SEQ_FEATURE	disulfide bond	12	33.3	5.60E-04	1.70E-02
UP_SEQ_FEATURE	topological domain:Cytoplasmic	13	36.1	5.90E-04	1.30E-02
UP_KEYWORDS	Disulfide bond	13	36.1	6.70E-04	8.30E-03
GOTERM_BP_DIRECT	G-protein coupled receptor signaling pathway	7	19.4	8.20E-04	4.40E-02
UP_KEYWORDS	Receptor	9	25	9.30E-04	9.90E-03
GOTERM_CC_DIRECT	integral component of membrane	15	41.7	3.40E-03	8.70E-02
UP_SEQ_FEATURE	transmembrane region	14	38.9	5.60E-03	9.80E-02

GOTERM_MF_DIRECT	odorant binding	3	8.3	5.80E-03	7.20E-02
UP_KEYWORDS	Transmembrane helix	15	41.7	6.00E-03	5.50E-02
UP_KEYWORDS	Transmembrane	15	41.7	6.20E-03	5.00E-02
UP_KEYWORDS	Antimicrobial	3	8.3	8.80E-03	6.40E-02
GOTERM_CC_DIRECT	plasma membrane	12	33.3	1.40E-02	1.80E-01
UP_KEYWORDS	Cell membrane	10	27.8	1.60E-02	1.10E-01
UP_KEYWORDS	Inflammatory response	3	8.3	1.70E-02	1.00E-01
UP_KEYWORDS	Sialic acid	2	5.6	2.60E-02	1.40E-01
UP_KEYWORDS	Signal	11	30.6	3.20E-02	1.60E-01
UP_KEYWORDS	Membrane	16	44.4	3.30E-02	1.50E-01
UP_KEYWORDS	Secreted	7	19.4	3.90E-02	1.70E-01
UP_KEYWORDS	Innate immunity	3	8.3	4.60E-02	1.90E-01
GOTERM_BP_DIRECT	antibacterial humoral response	2	5.6	5.60E-02	8.80E-01
GOTERM_BP_DIRECT	inflammatory response	3	8.3	8.70E-02	9.20E-01

Supplementary Table 3. Functional Annotation Chart of the Genes with Gains in methylation. From the top 100 combined rank promoters, promoters analysed n=49.

Category	**Term**	**Count**	**%**	**P-Value**	**Benjamini**
INTERPRO	Homeobox, conserved site	10	25.6	1.80E-12	9.60E-11
INTERPRO	Homeodomain	10	25.6	2.60E-11	7.00E-10
UP_KEYWORDS	Homeobox	10	25.6	8.70E-11	5.60E-09
INTERPRO	Homeodomain-like	10	25.6	3.00E-10	5.30E-09
UP_SEQ_FEATURE	DNA-binding region:Homeobox	9	23.1	3.80E-10	3.40E-08
SMART	HOX	10	25.6	4.20E-10	5.00E-09
UP_KEYWORDS	DNA-binding	17	43.6	3.30E-09	1.10E-07
GOTERM_MF_DIRECT	sequence-specific DNA binding	10	25.6	3.00E-08	1.10E-06
UP_KEYWORDS	Developmental protein	12	30.8	4.60E-08	1.00E-06
INTERPRO	Homeodomain, metazoa	5	12.8	6.60E-06	8.80E-05
GOTERM_BP_DIRECT	regulation of transcription, DNA-templated	11	28.2	4.50E-05	1.00E-02
GOTERM_BP_DIRECT	transcription, DNA-templated	12	30.8	7.50E-05	8.50E-03
GOTERM_BP_DIRECT	peripheral nervous system neuron development	3	7.7	1.00E-04	7.80E-03
UP_KEYWORDS	Transcription regulation	12	30.8	2.70E-04	4.40E-03
UP_KEYWORDS	Nucleus	18	46.2	2.70E-04	3.50E-03
UP_KEYWORDS	Transcription	12	30.8	3.50E-04	3.70E-03
GOTERM_CC_DIRECT	nucleus	17	43.6	2.30E-03	7.60E-02
GOTERM_MF_DIRECT	transcription factor activity, sequence-specific DNA binding	7	17.9	2.30E-03	4.20E-02

INTERPRO	Myc-type, basic helix-loop-helix (bHLH) domain	3	7.7	1.10E-02	1.10E-01
GOTERM_BP_DIRECT	spinal cord motor neuron cell fate specification	2	5.1	1.10E-02	4.60E-01
GOTERM_BP_DIRECT	hindlimb morphogenesis	2	5.1	1.20E-02	4.30E-01
UP_SEQ_FEATURE	domain:Helix-loop-helix motif	3	7.7	1.40E-02	4.60E-01
GOTERM_BP_DIRECT	positive regulation of transcription from RNA polymerase II promoter	6	15.4	1.60E-02	4.50E-01
GOTERM_BP_DIRECT	spinal cord association neuron differentiation	2	5.1	2.00E-02	4.80E-01
SMART	HLH	3	7.7	2.10E-02	1.20E-01
GOTERM_BP_DIRECT	neuromuscular process	2	5.1	2.30E-02	4.80E-01
UP_SEQ_FEATURE	compositionally biased region:Poly-Gln	3	7.7	2.40E-02	5.20E-01
GOTERM_BP_DIRECT	neuron fate commitment	2	5.1	2.60E-02	4.90E-01
GOTERM_BP_DIRECT	proximal/distal pattern formation	2	5.1	3.70E-02	5.70E-01
GOTERM_MF_DIRECT	RNA polymerase II regulatory region sequence-specific DNA binding	3	7.7	3.80E-02	3.80E-01
GOTERM_BP_DIRECT	negative regulation of transcription, DNA-templated	4	10.3	4.10E-02	5.80E-01
GOTERM_BP_DIRECT	multicellular organism development	4	10.3	4.60E-02	5.90E-01
GOTERM_BP_DIRECT	response to nicotine	2	5.1	5.60E-02	6.30E-01
GOTERM_BP_DIRECT	embryonic skeletal system morphogenesis	2	5.1	5.90E-02	6.30E-01
UP_SEQ_FEATURE	compositionally biased region:Poly-Gly	3	7.7	7.40E-02	8.20E-01
GOTERM_BP_DIRECT	skeletal muscle tissue development	2	5.1	7.60E-02	7.00E-01
GOTERM_BP_DIRECT	adult locomotory behavior	2	5.1	7.80E-02	6.80E-01
GOTERM_BP_DIRECT	odontogenesis of dentin-containing tooth	2	5.1	8.20E-02	6.80E-01
GOTERM_BP_DIRECT	negative regulation of neuron differentiation	2	5.1	8.30E-02	6.70E-01
GOTERM_MF_DIRECT	transcriptional repressor activity, RNA polymerase II transcription regulatory region sequence-specific binding	2	5.1	8.40E-02	5.60E-01
GOTERM_BP_DIRECT	single fertilization	2	5.1	8.80E-02	6.70E-01
GOTERM_MF_DIRECT	DNA binding	6	15.4	9.50E-02	5.20E-01
GOTERM_MF_DIRECT	RNA polymerase II core promoter proximal region sequence-specific DNA binding	3	7.7	9.60E-02	4.60E-01
UP_SEQ_FEATURE	domain:KRAB	3	7.7	9.80E-02	8.40E-01
GOTERM_BP_DIRECT	negative regulation of transcription from RNA polymerase II promoter	4	10.3	9.80E-02	6.90E-01

Chapter 7 – Investigation of the Role of Androgen Receptor Variants in Prostate Cancer.

7. 1. Introduction

7.1. I. Collaboration with the Institute of Genetics and Molecular and Cellular Biology, University of Strasbourg.

This chapter is a report of my collaboration with researchers at the University of Strasbourg, on a study investigating the effect of the expression of pathological AR variants in PCa.

In December 2017, I was awarded a scholarship provided by Ulster University's Department for Research and Impact. The scheme was called "Global Research Opportunities for Ulster Postgraduate Researchers: Internationalising your Networks (GRO-Ur-Networks)" and comprised a £2,000 grant to fund a 1-3 week research stay at a foreign institution with the objective of acquiring new skills and connections.

My host was Dr Jocelyn Céraline from the *Institut de Génétique et de Biologie Moléculaire et Cellulaire* (IGBMC) in Ilkirch, France, which is affiliated with the nearby University of Strasbourg. I had approached three different PIs working on PCa research and in the end chose to write the grant with Dr Céraline because he had an upcoming project involving RNA-seq analysis, which I was keen to develop skills in.

Dr Céraline's research focuses on the pathological androgen receptor (AR) variants. As discussed in the General Introduction Section 1.1. *VII* b), one way in which PCa cells evade AR inhibitors is by upregulating AR mutants, such as splice variants that lack the entire or vast parts of the C-terminal (ligand-binding) domain, which when unbound auto-inhibits AR's transcription factor activity. The mutants are thus constitutively active transcription factors regardless of circulating androgen levels or the presence of AR antagonists like bicalutamide or enzalutamide that bind this domain. AR variant 7 (AR-V7) is the most prevalent AR splice variant, and has a specific C-terminus encoded by the cryptic (alternatively spliced) exon 3 that contains a stop codon at the hinge region thus truncating further expression (Hu *et al.*, 2009). This project investigated this variant as well as another one, AR variant Q641X (formerly AR-Q641X), which contains a nonsense mutation that produces a premature stop codon instead of the glutamine at position 641 resulting in a similar truncation (Céraline *et al.*, 2004).

A previous study published by Dr Céraline's group reported that the gene encoding N-cadherin (*CHD2*) was upregulated by the AR variant AR-V7, demonstrating one mechanism through which PCa cells expressing this mutant may gain mesenchymal features to acquire increased malignancy. This study involved lentiviral transduction of LNCaP cells with plasmids encoding the wild-type AR (AR-WT) and AR-V7, and then sequencing total RNA (mRNA-seq and miRNA-seq) (Cottard *et al.*, 2017). When reading this paper I noticed in their paper that one of the genes upregulated significantly by AR-V7 was miR-210-3p, further supporting a distorted link between hypoxia and AR signalling in CRPC. It was this link with miR-210 as well as a keen interest in his research, that lead me to approached Dr Céraline in the first place. Initially, the project had planned to include more miRNA-related analysis although the focus later shifted to concentrate primarily

on AR variants. Nevertheless, as discussed below, there is a link between hypoxia and AR variants that is worthy of investigation, and it was an excellent opportunity to gain experience in RNA-seq analysis.

The project that I collaborated on builds on their previous study; again, they overexpressed AR-WT and AR-V7 in LNCaP, this time including AR-Q641X and using a doxycycline-inducible vector plasmid, meaning that they could capture the immediate response to AR variant expression. The cells were transfected and then treated with doxycycline to induce expression of the variants, and then sequenced to explore the transcriptional effects of the variants' expression. My role in the project would be to shadow and possibly perform some of the analysis of the sequencing data and to contribute to writing the publication.

Author Contributions:

- **Pauline Ould Madi Berthelemy**: Performed laboratory work, performed all bioinformatics analysis, contributed to study design, wrote the manuscript.
- **Jocelyn Ceraline**: Contributed to study design.
- **C. Zoe Angel**: Shadowed bioinformatics analysis and performed a small portion to repeat and validate Pauline's analysis, performed one of the IPA analyses, carried out a literature review on one of the groups of significantly differentially expressed genes, contributed to writing the manuscript.

7. 1. II. Project Overview

The plasmids had been generated by cloning AR variant genes (AR-WT, AR-V7 or AR-Q641X) into the vector (known as C3) downstream of a doxycycline-inducible promoter, and then transfected into LNCaP by a lentiviral method. The vector also contained enhanced GFP (eGFP) to confirm transfection efficiency.

The cells were treated for 24 hours with 20ng/ml of doxycycline to induce the promoter. It is important to note that LNCaP cells express an endogenous AR that is full-length (AR-FL) but distinct from the wild-type version as it is mutated at T878A (Veldschol*te et al*>, 1990). The cells were therefore also treated with 10nM of DHT to activate AR (FL and/or WT) or vehicle alone (ethanol, EtOH). The eGFP-expressing cells were selected by FACS and sequenced at the IGBMC bioinformatics core. Table 1 recaps the treatments.

Relative to the negative control eGFP+dox+vehicle, the log2(fold change) was calculated in the following conditions: eGFP+dox+DHT, AR-WT+dox+DHT, AR-Q641X+dox+vehicle, and AR-V7+dox+vehicle. These ratios indicated the impact of endogenous AR-FL, AR-WT, AR-Q641X and AR-V7, respectively. To compare the transcriptional effects of the pathological AR variants, the genes differentially expressed in the AR-WT condition were compared with those differentially expressed (DE) in the AR-Q641X and AR-V7 conditions (Figure 1). Pathways analysis was performed using Ingenuity Pathway Analysis (IPA) software on the lists of genes deregulated by each AR condition.

Table 1. LNCaP conditions used in the study. All received 20ng/ml doxycycline (Dox) to induce the promoter. DHT at 10nM for 24 hours or vehicle alone (ethanol). The log2(fold change) of gene expression between conditions 1 and 2-6 were calculated.

Condition	Plasmid	Doxycycline	Treatment (24h)	Represents
1	eGFP	+ Dox	+ Vehicle	Effect of the plasmid
2	eGFP	+ Dox	+ DHT	Endogenous AR-FL (T8784)
3	eGFP-AR-WT	+ Dox	+ DHT	AR-WT + endogenous AR-FL
4	eGFP-AR-Q641X	+ Dox	+ Vehicle	AR-Q641X
5	eGFP-AR-V7	+ Dox	+ Vehicle	AR-V7

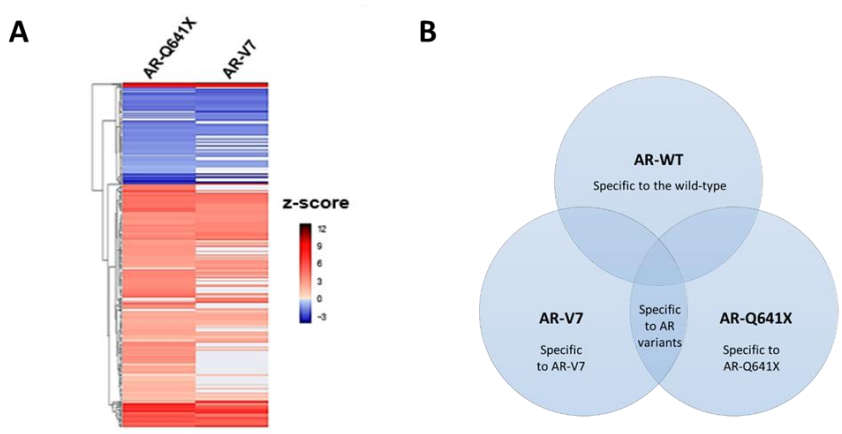

Figure 1. Results of the ARV sequencing. **A)** Heatmap showing significantly different gene expression pattern for the AR-Q641X and AR-V7 conditions. **B)** Significantly up- or down-regulated genes in the AR variant conditions were identified, relative to expression level in the AR-WT condition.

7. 2. Tasks

In the end, I contributed three tasks during my internship. After being trained in the program Jupyter and being given the datasets, I produced a list of DE genes in the AR-Q641X condition relative to AR-WT (to repeat and validate Pauline's earlier analysis). I also performed the IPA analysis on this gene list. Since returning, I also performed some preliminary analysis of publically-available chromatin immunoprecipitation sequencing (ChIP-seq) data, to see if I could validate any of the genes, although this part was for my own interest and not a part of the collaboration. These four tasks are outlined below.

7. 2. I. RNA-seq analysis

Jupyter Notebook (a python-based command line environment) was used to produce tables containing genes significantly deregulated in the AR variant conditions but not in the AR-WT condition, and then to compare them with each other to identify genes deregulated by each variant and those deregulated by both.

Below is an excerpt of code that I wrote for the analysis, using the Jupyter Notebook software with the packages: pandas, numpty and matplotlib.pyplot. Most of the functions were previously designed by members of the Céraline group and are stored on a network folder, where they can be re-used and refined for different applications. I designed an analysis and put some of the functions together and did some troubleshooting when functions hadn't worked. This analysis produced a list of genes that were significantly DE in the AR-Q641X (+EtOH) condition but not in the AR-WT (+DHT) condition, and this list was later compared with the AR-V7 specifically DE genes.

Table 2. Identification of commonly deregulated genes by AR-Q641X expression but not AT-WT expression. Code written in Jupyter Notebook using the packages pandas, numpty and matplotlib.pyplot. Lines beginning with hash symbols are annotations for the reader (ignored by the program). Gene list tables depict the first few genes only.

Identification of genes deregulated by AR-Q641X compared to AR-WT

```
# Import the required packages, specify the path (directing Jupyter to the correct folder)
import pandas as pd
import numpy as np
import matplotlib.pyplot as plt
%matplotlib notebook
path = "./"

# Choose the desired files and import the data to Jupyter kernel in the form of tables
fname1 = "Q641X_EtOH_WT_EtOH.xlsx"
fname2 = "WT_DHT_WT_EtOH.xlsx"
t1=pd.read_excel(path+fname1,index_col="Ensembl gene id")
t2=pd.read_excel(path+fname2,index_col="Ensembl gene id")

# Change column names to something readable
t1.columns = ["Gene_name","log2","pvalue"]
t2.columns = ["Gene_name","log2","pvalue"]

# Filter significant fold changes
t105 = t1[t1["pvalue"] < 0.05]
t205 = t2[t2["pvalue"] < 0.05]

# Make tables containing the up and down regulated genes
gene1_up = t105[t105["log2"]>1.]
gene1_down = t105[t105["log2"]<-1.]
gene2_up = t205[t205["log2"]>1.]
gene2_down = t205[t205["log2"]<-1.]

# Have a look at genes upregulated in AR-WT
print (gene2_up)
```

Ensembl gene id	Gene_name	log2_WT	pvalue_WT
ENSG00000134216	CHIA	4.046172	2.648248e-09
ENSG00000175040	CHST2	2.370637	1.709631e-04
ENSG00000229314	ORM1	3.355856	2.257708e-10

```
# make tables of all deregulated using the Append function
gene1_all = gene1_up.append(gene1_down)
gene2_all = gene2_up.append(gene2_down)

# Find genes deregulated in both datasets AR-WT and AR-Q641X using the merge function
gene_common = gene1_all.merge(gene2_all,left_index=True, right_index=True, how='inner')

# Drop the column for "gene name" that appears twice
gene_common = gene_common.drop("Gene_name_y",1)
```

```
# Rename columns
gene_common.columns = ["Gene_name","log2_Q641X","pvalue_Q641X", "log2_WT", "pvalue_WT"]

# Have a look at the common genes in a table format
gene_common
```

Ensembl gene id	Gene_name	log2_Q641X	pvalue_Q641X	log2_WT	pvalue_WT
ENSG00000134216	CHIA	2.680970	7.787479e-04	4.046172	2.648248e-09
ENSG00000229314	ORM1	3.785498	1.377485e-13	3.355856	2.257708e-10
ENSG00000258926	RP11-47I22.1	3.481220	1.516913e-07	3.199291	2.412471e-06

```
# Find genes upregulated in both AR-WT and AR-Q641X
gene_up = gene1_up.merge(gene2_up,left_index=True, right_index=True, how='inner')
gene_up = gene_up.drop("Gene_name_y",1)
gene_up.columns = ["Gene_name","log2_Q641X","pvalue_Q641X", "log2_WT", "pvalue_WT"]

# Find genes downregulated in both AR-WT and AR-Q641X
gene_down = gene1_down.merge(gene2_down,left_index=True, right_index=True, how='inner')
gene_down = gene_down.drop("Gene_name_y",1)
gene_down.columns = ["Gene_name","log2_Q641X","pvalue_Q641X", "log2_WT", "pvalue_WT"]

# Find genes deregulated in Q641X but not in AR-WT
gene_Q641X = gene1_all.merge(gene2_all,left_index=True, right_index=True, how='left',indicator=True)
gene_Q641X = gene_Q641X[gene_Q641X["_merge"] == "left_only"]

# Drop columns
gene_Q641X = gene_Q641X.drop(["Gene_name_y","pvalue_y","log2_y","_merge"],1)

# Rename columns
gene_Q641X.columns = ["Gene_name","log2_Q641X","pvalue_Q641X"]

gene_Q641X
```

Ensembl gene id	Gene_name	log2_Q641X	pvalue_Q641X
ENSG00000142319	SLC6A3	3.916246	3.451926e-16
ENSG00000166828	SCNN1G	2.068318	1.062004e-03
ENSG00000136867	SLC31A2	1.520619	1.118436e-06
ENSG00000070182	SPTB	2.253254	2.868471e-04

```
# Save this table as an Excel sheet
from pandas import ExcelWriter
writer = ExcelWriter('deregQ641X.xlsx')
gene_Q641X.to_excel(writer,'Sheet1')
writer.save()
```

7. 2. II. Ingenuity Pathway Analysis

After obtaining a list of deregulated genes from each AR variant, we used Ingenuity Pathway Analysis (IPA) software to identify known signalling pathways enriched in each condition. There were 59 genes deregulated by both the variants compared with AR-WT, and these were also analysed. The IGBMC institute has an annual subscription to IPA and it was there that I was trained in this program, which as shown in chapter 5 I have since applied to my own project.

The below figures contain some of my IPA analyses, exploring the lists of genes specifically DE in the AR variant conditions (*NB:* since there are a limited number of images that can be downloaded on IPA, screenshots were used instead). First, I showed using a heat map that specific pathways and functions were enriched by AR-WT, but not by either of the AR variants (such as "*Invasion of Cells"*, and "*Transport of Molecule"*). Surprisingly, AR-V7 was most dissimilar to the others in terms of the types of genes that were deregulated. For instance, while AR-WT and AR-Q641X had strongest upregulation of "*Cell movement*" and "*Synthesis of Lipid*", AR-V7 did not (Figure 2). This seemed peculiar since AR-V7 and AR-Q641X have similar protein structures due to the truncated CTD. Next, I compared the IPA core analysis profiles of the AR-V7 and AR-Q641X conditions, which were indeed strikingly different. The AR-Q641X condition was associated with several growth-promoting pathways such as *STAT3 signalling*, *VEGF signalling*, and interestingly, *HIF-mediated glucocorticoid regulation* which could point towards a link between hypoxic signalling (Figure 3). The AR-V7 gene list was enriched for metabolic pathways: *Thyroid hormone metabolism, Nicotine degradation, NAD salvage pathway, Serotonin degradation,* and *Coagulation system*. Finally, there were some interesting networks highlighted by IPA based on the AR-Q641X list, revealing that the subsequent effect of AR-Q641X expression could include Erk, Akt, and NF-κβ, which could suggest how these variants are associated with increased malignancy (Figure 4).

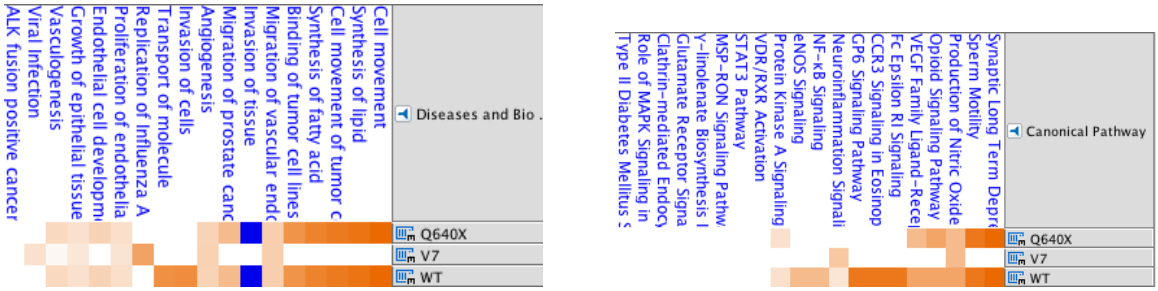

Figure 2. IPA heatmaps of diseases and biological functions, and pathways enriched in each condition. AR-V7 data appears to be dissimilar to the other conditions.

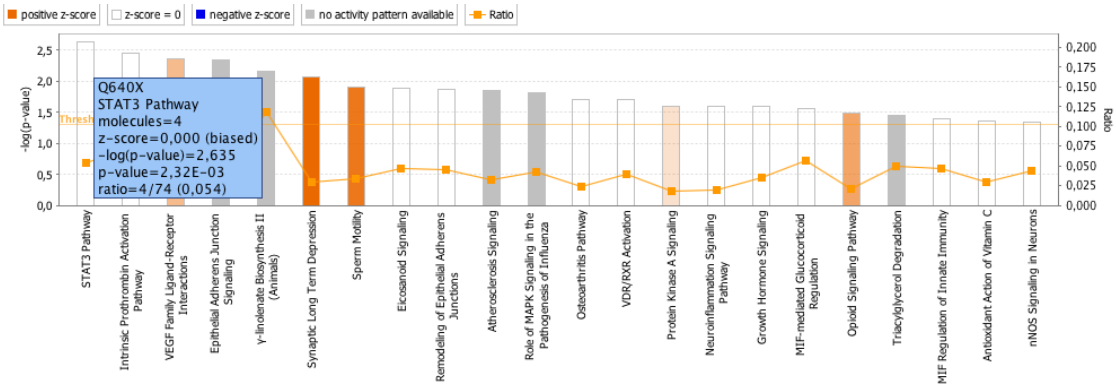

Figure 3. Canonical pathways enrichment chart. Pathways enriched by Q641X expression relative based on the ratio between the number of genes from that pathway that are significantly deregulated, out of the total number of genes known to be involved in the pathway. Top enriched pathway is STAT3 signalling; 4 genes were significantly deregulated in this dataset out of a total of 74 genes known to be involved in STAT3 signalling (hence the small ratio) although it is highly significant. Also of interest are VEGF signalling, metabolic, growth, and HIF-mediated glucocorticoid regulation.

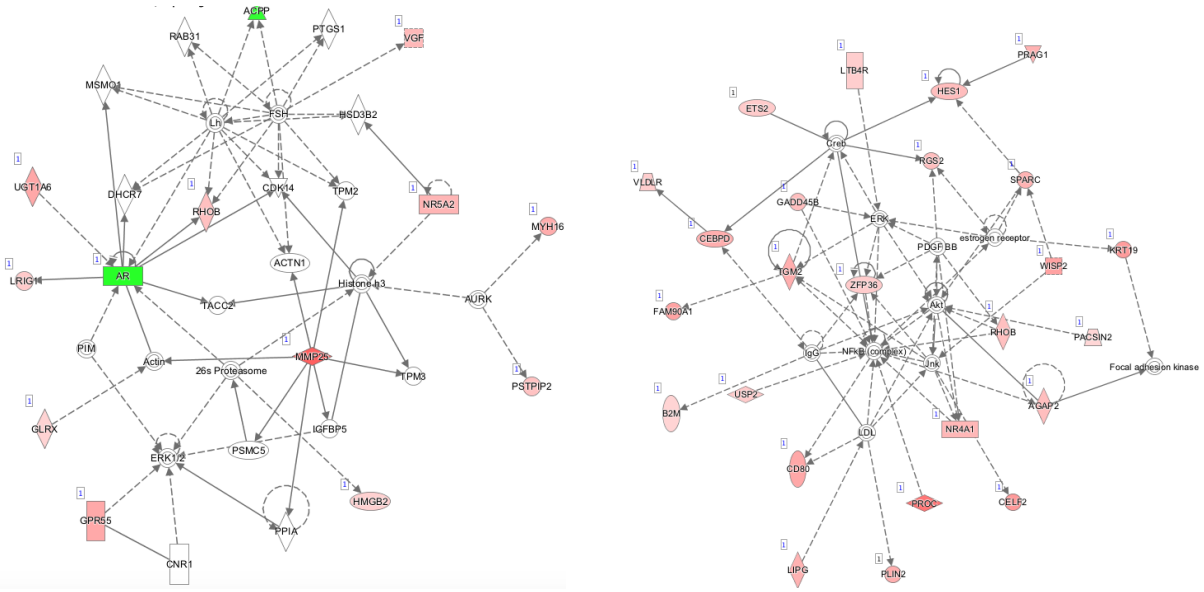

Figure 4. Two networks highlighted by IPA, based on the significantly DE genes specific to the AR-Q641X conditions. Right-hand network suggests that ERK1/2 could be activated as a result of these genes, while left-hand network indicates that NF-κβ and Akt could be activated.

7. 2. III. Literature review

The IPA analysis provided some hints as to how the AR variants could promote cancer progression, although we wanted to understand better the long term effects of their expression. This experiment had produced much shorter lists of specific DE genes for each condition than their previous study, perhaps because of the new dox-inducible system (previously they had harvested the cells 72h after transfection, this time 24h after dox treatment). One of my tasks was to take half of the DE genes and perform a literature review on them, and I proposed that many were transcription factors that could shape the long-term response. We therefore highlighted all of the transcription factors from the gene lists and produced a table, which has been included in the manuscript. There were 24 transcription factors upregulated by AR-Q641X and 12 by AR-V7 but not by the endogenous AR-FL of eGFP condition nor the AR-WT, and 10 of these were upregulated by both AR variants (Table 3). Some of them have already been characterised in relation to cancer, such as the orphan nuclear receptor nuclear receptor subfamily 5 group A member 2 (*NR5A2),* CCAAT/enhancer-binding protein delta *(CEBPD),* Hes family BHLH transcription factor 1 (*HES1*), the nucleoside diphosphate kinase 2 (*NME2*), and ETS proto-oncogene 2 (*ETS2*). However, this is the first time that they have been implicated in the response to AR variant activation.

Table 3. Transcription factors upregulated in each condition. Blue: transcription factors upregulated by both variants, AR-WT, and AR-FL. Red: those upregulated by just the AR variants.

	eGFP	AR-WT	AR-Q641X	AR-V7
Up-regulated	SNAI2, WWTR1, TBX15, BRIP1, BRCA1, E2F8BRCA2, HOPX, RUNX2, E2F2, E2F1, RAD51, TCF19, MCM4, NKX3-1, RAD54B, WDHD1, CENPK, MCM2, KNTC1, AFF3, MCM6, CHAF1A, ZNF695, MCM8, MED30, ANKRD22, MCM3, TRIP13, HMGB2	TBX15, RUNX1, SNAI2, CSRP2, RFX6, CUX2, WWTR1, FHL2, HOPX, NKX3-1, MAF, ANKRD22, EGR1, RUNX2, FOXD4, TNFAIP3, BRIP1, RAD54B, KLF5, ELL2, BRCA1, RAD51, SEC14L2, TCF19, AFF3, ZDHHC9, E2F8, HMGXB3, MCM4, CREB3L4, ATF3	HOPX, FOXD4, PER1, KLF15, ASB9, TBX15, NR4A1, CEBPD, RFX6, ZBTB16, ELL2, BHLHA15, E4F1, IRF7, CAPN15, HDAC10, MAFK, EGR1, NME2, FOXD4L1, CBX4, HES1, SOX9, PDLIM1, NR5A2, RP11-2C24, CEBPB, RUNX2, HMGXB3, NFKIA	HOPX, FOXD4, KLF15, PER1, RFX6, TBX15, NR4A1, ZBTB16, ELL2, NR5A2, EGR1, CEBPD, NME2, SNAI2, ASB9, FOXD4L1, HES1, ETS2
Down-regulated	HOXC13, ETV5, CALCOCO1, PBX1, TOX3, LHX4, BHLHE41, SSBP2, PGR, DMRT1, HDAC9	ZBTB43, ZNF117, HOXA10, NR3C2, LEF1, TSHZ3, ARNT2, IRX5, PAX1, YB, HOXC13, PBX1, IRX3, EBF2, HOXC9, SALL2, ZIC2, SMARCD3, TRPS1, LHX4, TOX3, DLX3, SSBP2, LHX9, BHLHE41, EOMES, DMRT1, KCNIP3, NFATC4, NR4A2, PGR, NR2F1, HDAC9	PBX1, ZNF624, PGR, ZNF679	PBX1, ZNF624, HDAC9, PGR

7. 2. IV. ChIP-seq analysis

I was invited to be part of the group discussions regarding the manuscript and in one of the last meetings that I attended; a paper that had just been published was discussed and had a similar study design. The authors had also overexpressed AR-WT and AR-V7 using plasmid vectors in 22Rv1 yet they had also included a ChIP-seq analysis to examine precisely which genes the AR variants were regulating (He *et al.*, 2018). When I returned home I uploaded this dataset from GEO using Integrative Genomics Viewer (IGV, https://software.broadinstitute.org/software/igv/) to explore if the DE genes from my list were indeed shown to be enriched in the ChIP-seq data. However, I did not observe any enrichment for the genes that I searched. As an example, I compared the *chitinase acidic* (*CHIA*) locus in the 22Rv1 AR-WT and AR-V7 datasets, since this was the most significantly upregulated gene in the LNCaP AR-WT dataset but was not induced by the variants, although there was no different (Figure 5). However, this was a different cell line and when I uploaded two other ChIP-seq datasets using AR-WT in LNCaP, there were peaks at the CHIA promoter so it could be unique to LNCaP (Figure 6) (Ramos-Montoya *et al.*, 2014)(McNair *et al.*, 2017).

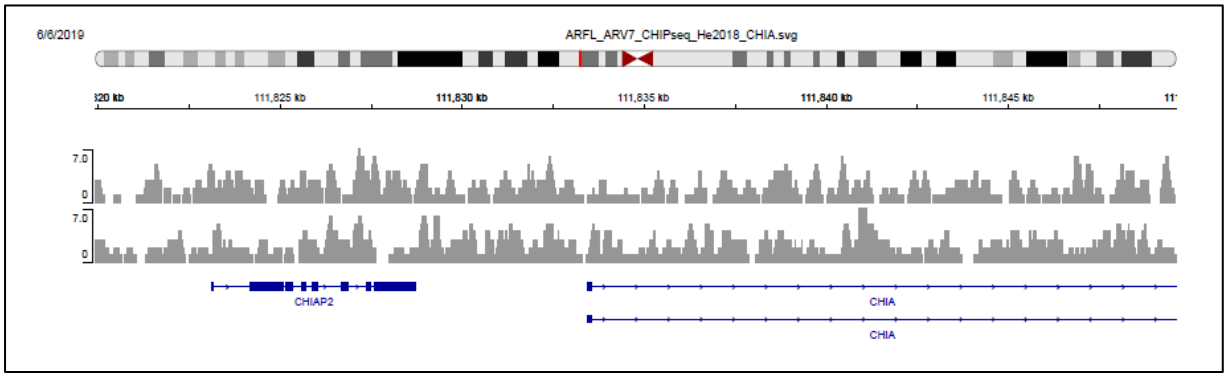

Figure 5. ChIP-seq analysis of the *CHIA* locus. No difference between the peaks at *CHIA* locus in the AR-WT and AR-V7 pull downs in another ChIP-seq analysis using 22RV1.

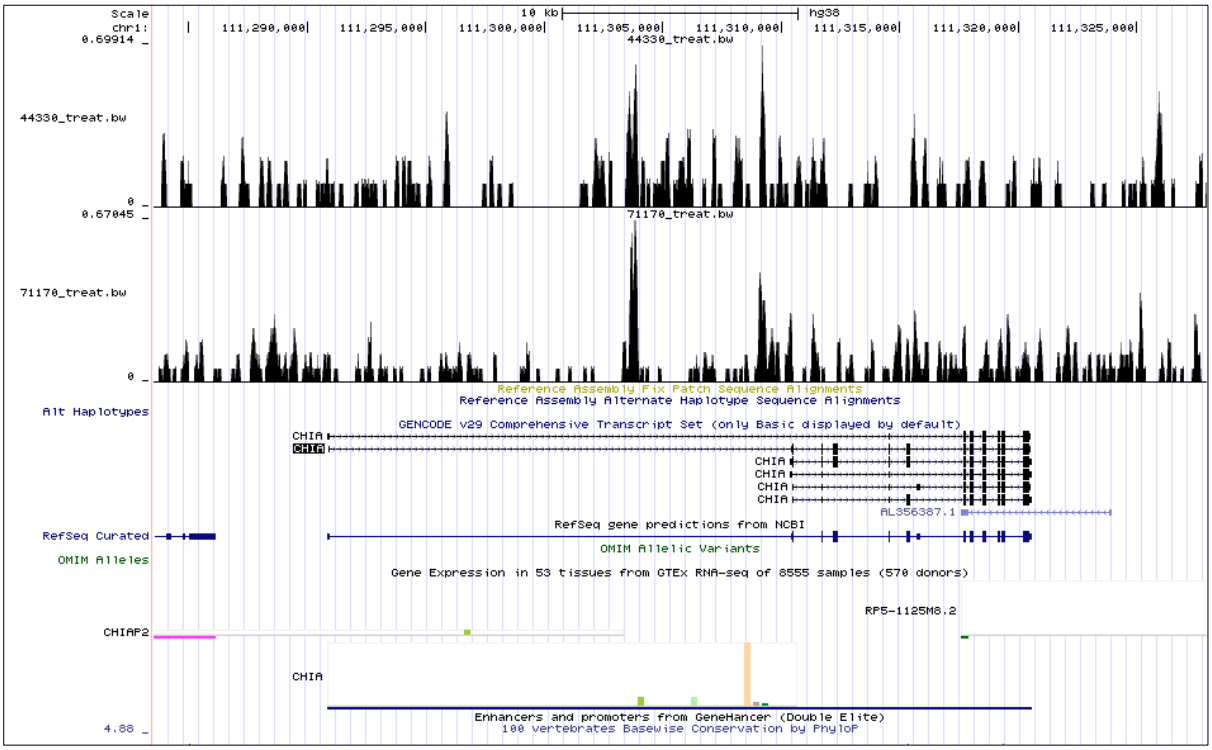

Figure 6. **Binding of AR-WT to the CHIA promoter**. Based on data from two independent ChIP-seq studies, peaks observed at the CHIA promoter locus, suggesting CHIA may be a direct target of AR in LNCaP that is not expressed by the AR variants.

7. 3. Discussion

7. 3. I. Summary of findings

This study confirms that the AR variants have distinct transcriptional activity compared to the wild-type. There were many genes, and even entire signalling pathways, that were activated by the AR variants that were not activated by wild-type nor endogenous full-length AR. Furthermore, we reported a number of transcriptional factors induced that may shape an increasingly malignant cell state. The variants lack the LBD meaning that they are constitutively active, however, this study also highlights that it changes AR's transcription factor activity; there were fewer pathways activated by the AR variants than AR-WT and AR-FL, suggesting they have decreased transcriptional activity. However, we highlighted some known oncogenes that were overexpressed exclusively by the variants, which could contribute to the increased aggressiveness that is associated with their expression. The different transcriptional activity could reflect different binding partners or transcriptional co-regulators, due to the change in the structure of the AR protein.

7. 3. II. Strengths and limitations of the study

This study reports some interesting findings and the study design was novel. Most published studies have used a cell line like 22Rv1 or PC3 that have a deleted or mutated AR. Here, LNCaP was chosen because it has an active endogenous AR-FL and is sensitive to AR signalling and so this is the first study of its kind in LNCaP. This was designed to be a more accurate representation of the situation in a prostate tumour in which AR-WT is expressed and at the same time, the variants are upregulated, resulting in a mixture of wild-type and mutant AR in the cell. Furthermore, LNCaP does not have endogenous expression of most of the AR variants, unlike 22Rv1 (Wadosky and Koochekpour, 2017). The effect of AR-WT was distinguished from AR-FL by comparing the transcriptome of cells expressing only eGFP and treated with DHT, which has not been shown previously. Furthermore, the study included AR-Q641X which is a relatively unstudied variant, and utilised a novel dox-inducible system. However, in my opinion one limitation is that the AR-V7 condition should have been excluded from the analysis since it has a suspiciously different expression profile from AR-Q641X when the proteins are structurally highly similar, and including AR-V7 could have biased the list of commonly deregulated genes. I noticed when performing the literature review of the deregulated genes, that some of the most significantly deregulated were pseudogenes, which have no known function. This highlighted the inherent limitation of all RNA-seq based studies in that we may mistakenly attribute a change in RNA levels to be biologically relevant because the p-value happens to be significant. As with all cell line studies, this experiment is limited in that the overexpression of the variants was out of the context of a tumour. However, it was a valuable model to dissect the pathway in a homogenous population to improve reproducibility and without the noise of other cell types. Finally, IPA was used for pathway analysis, which has a wealth of information on gene ontology and it incorporated the effect size and significance. However, the graphs such as the network analysis must be interpreted

cautiously since the information is based on published discoveries from numerous cell types and the interactions and functions that it attributed here may not exist or be relevant in a PCa setting.

7. 3. III. Future directions

To confirm their differential expression in the AR variant conditions, the key deregulated genes could be validated by another technology such as RT-qPCR, and their oncogenic effects could be confirmed by phenotypic assays. For instance, the IPA analysis suggested that proliferation may be reduced in the variant conditions, due to the downregulation of E2F targets, G2M checkpoint and PI3K/AKT/mTOR signalling. This could be confirmed by growth curves or MTT assay. To confirm that the IPA predicted interactions between co-expressed genes occur in this system, these could be confirmed by co-immunoprecipitation.

An RT-qPCR or Western blot for the AR-WT, AR-V7 and AR-Q641X in the cells could be used to confirm the integrity of the plasmid and gene. This could additionally give an indication of the expression level produced by the dox-inducible system, to ensure it is effective but not too high. We observed far fewer genes induced after 24h of dox treatment than they previously observed; in future, collecting cells over a time-course could to map the progressive effects of AR variant expression. Immunoprecipitation-based studies could examine the non-genomic functions of AR, such as its scaffolding functions as loss of the CTD would change its interacting partners, which could underlie the differing transcriptional effects. If a critical structural difference between the AR variants and AR-WT is identified, such as a binding site for another protein, it could inform the development of an agent to inhibit the variants. Binding partners could be predicted by the database POSSUM and validated by co-immunoprecipitation and mass spectrometry, or *de novo* using BioID (an IP-based assay for identifying interacting proteins) (Roux, Kim and Burke, 2013). It would also be valuable to determine whether the variants are heterodimerising with endogenous AR-FL or each other (since active AR is a homodimer), which would have implications for its transcription factor activity. Similar to the 22Rv1 study by He *et al*., integrating the RNA-seq data with ChIP-seq data could determine which genes are direct transcriptional targets of AR and the variants (He *et al.*, 2018).

The previous study highlighted miR-210 as induced by AR-V7, a ChIP experiment could confirm this and if so the effect of the variants on other mediators of the hypoxic response could be explored. Alternatively, perhaps overexpression of the variants confers increased resistance or different transcriptional effects during hypoxia. Then, miRNA-seq could be performed on the variant expressing cells, to examine their effect on miRNA profiles during normoxia and hypoxia. This could reveal critical miRNAs that mediate increased malignancy following expression of the variants, either in the basal state or during hypoxia. Androgen receptor variant behaviour in hypoxia and the effect of miRNAs remains unexplored and could have significance in understanding the response to therapy and how resistance develops.

7. 3. IV. Concluding remarks

In conclusion, this internship was extremely interesting and useful, as I gained insight into another field of PCa research and gained understanding and skills in analysis of omics data, which I have been able to apply to my own project.

7.4. Bibliography

Céraline, J. *et al.* (2004) 'Constitutive activation of the androgen receptor by a point mutation in the hinge region: A new mechanism for androgen-independent growth in prostate cancer', *International Journal of Cancer*. John Wiley & Sons, Ltd, 108(1), pp. 152–157. doi: 10.1002/ijc.11404.

Cottard, F. *et al.* (2017) 'Dual effects of constitutively active androgen receptor and full-length androgen receptor for N-cadherin regulation in prostate cancer.', *Oncotarget*. Impact Journals, LLC, 8(42), pp. 72008–72020. doi: 10.18632/oncotarget.18270.

He, Y. *et al.* (2018) 'Androgen receptor splice variants bind to constitutively open chromatin and promote abiraterone-resistant growth of prostate cancer.', *Nucleic acids research*. Oxford University Press, 46(4), pp. 1895–1911. doi: 10.1093/nar/gkx1306.

Hu, R. *et al.* (2009) 'Ligand-independent androgen receptor variants derived from splicing of cryptic exons signify hormone-refractory prostate cancer.', *Cancer research*. NIH Public Access, 69(1), pp. 16–22. doi: 10.1158/0008-5472.CAN-08-2764.

McNair, C. *et al.* (2017) 'Cell cycle-coupled expansion of AR activity promotes cancer progression', *Oncogene*, 36(12), pp. 1655–1668. doi: 10.1038/onc.2016.334.

Ramos-Montoya, A. *et al.* (2014) 'HES6 drives a critical AR transcriptional programme to induce castration-resistant prostate cancer through activation of an E2F1-mediated cell cycle network.', *EMBO molecular medicine*. Wiley-Blackwell, 6(5), pp. 651–61. doi: 10.1002/emmm.201303581.

Roux, K. J., Kim, D. I. and Burke, B. (2013) 'BioID: A Screen for Protein-Protein Interactions', in *Current Protocols in Protein Science*. Hoboken, NJ, USA: John Wiley & Sons, Inc., pp. 19.23.1-19.23.14. doi: 10.1002/0471140864.ps1923s74.

Veldscholte, J. *et al.* (1990) 'A mutation in the ligand binding domain of the androgen receptor of human LNCaP cells affects steroid binding characteristics and response to anti-androgens', *Biochemical and Biophysical Research Communications*, 173(2), pp. 534–540. doi: 10.1016/S0006-291X(05)80067-1.

Wadosky, K. M. and Koochekpour, S. (2017) 'Androgen receptor splice variants and prostate cancer: From bench to bedside.', *Oncotarget*. Impact Journals, LLC, 8(11), pp. 18550–18576. doi: 10.18632/oncotarget.14537.

Chapter 8. Systematic Review and Exploratory Meta-Analysis: the Appetite-Regulating Hormones – Leptin, Adiponectin and Ghrelin – and the Development of Prostate Cancer.

7. 1. Foreword

This chapter consists of a systematic review that I lead authored, which broadly addresses the relationship between obesity and prostate cancer development. It was written because the opportunity arose for me to collaborate with the WHO International Agency for Research in Cancer (IARC), based in Lyon in France, as a follow-on from an internship that I completed there before starting my PhD. Although this was not strictly aligned with the scope of my PhD, it was still in the field of PCa and was an excellent chance for international collaboration, so it was worked into the overall PhD schedule.

My review was a collaboration between the Nutritional Epidemiology and the Screening groups, as the two PIs were scientists from those groups. The PIs were Inge Huybrechts PhD who is an expert in nutrition and epidemiology, and Vitaly Smelov MD PhD who is a practicing urologist and PCa researcher. I was given primary responsibility for designing and executing a systematic review and meta-analysis related to both nutrition and cancer screening. Since my PhD investigates PCa, and I was collaborating with a Nutrition group, I chose the timely topic of obesity-related hormones in PCa, with the specific title "Appetite-Regulating Hormones – Leptin, Adiponectin and Ghrelin – and the Development of Prostate Cancer: A Systematic Review and Exploratory Meta-Analysis".

The scope of the review was to combine the results of observation studies that have compared the levels of these hormones in PCa patients and controls, to determine if the hormone levels associated with disease incidence or progression to an advanced stage. Many such studies have been published over the last 30 years although the conclusions have been mixed. The aim of the review was to elucidate the relationship between obesity and PCa, and to assess their reliability as biomarkers for diagnosis or prognosis.

The review was accepted for publication in the Nature Publishing Group journal *Prostate Cancer and Prostatic Diseases* (PCAN) in April 2019. The completed published version of the manuscript follows this Foreword, supplemented by an extra Afterword to discuss the relevance to my overall thesis.

Author Contributions:

- Ms Zoe Angel (PhD student at Ulster University).
    - Prepared topics and performed preliminary searches, performed the systematic searching for the review, screening, data extraction, meta-analysis, reviewing, designed and made the figure, wrote the first draft of the manuscript, wrote final draft after receiving the co-authors comments, submitted the manuscript, performed reviewers corrections, wrote the rebuttal, re-submitted manuscript.
- Dr Isabel Iguacel (Research intern at IARC)
    - Advised on meta-analysis statistics, reviewed the final manuscript.
- Dr Amy Mullee (Postdoctoral fellow at IARC)
    - Advised on systematic reviewing, reviewed the first draft and final manuscript.
- Dr Neela Guha (Scientist, IARC)
    - Advised on the meta-analysis statistics, reviewed the draft and final manuscript.
- Ms Rachel Wasson (Undergraduate placement student at IARC)
    - Acted as the second screening reviewer for the systematic search results.
- Dr Declan McKenna (Primary supervisor at Ulster University)
    - Reviewed the first draft, assisted with the rebuttal for the PCAN reviewers.
- Dr Marc Gunter (Head of the Section at IARC)
    - Reviewed the final manuscript, approved the topic for review.
- Dr Vitaly Smelov and Dr Inge Huybrechts (co-supervisors)
    - Provided guidance throughout, reviewed the first draft and final manuscript.

7. 2. Afterword

7. 2. I. Summary

As outlined in the review, leptin levels were not associated with PCa incidence or advancement. However, I concluded that adiponectin levels may be inversely associated with advanced stage disease. Too little evidence was available on ghrelin levels for an association to be determined.

This type of epidemiological research evidences association only and cannot be used to evidence causation, and so a tumour suppressive effect of adiponectin cannot be confirmed. However, as cited in the paper, some *in vitro* functional studies have reported growth-inhibiting effects of adiponectin on PCa cell lines. Therefore, the review supports other evidence that obesity may create systemic effects which prostate tumours may be sensitive to, in this case, low levels of adiponectin. This suggests that the prostate tumour is a dynamic entity that is responsive to the systemic as well as the local environment (*e.g.* hypoxia), and that a holistic approach to PCa research is important, considering the influence of lifestyle risk factors as well as inherited and sporadic genomic abnormalities and the tumour microenvironoment.

Overall, I found this experience extremely valuable as I gained experience in reading and reviewing published research, in epidemiology statistics, and scientific writing, as well as collaborating within a multi-disciplinary team. The review has also helped me to structure my literature searches when preparing my general introduction and chapters.

7. 2. II. Future directions

The systematic review approach described here could easily be expanded to the topics of miRNAs in PCa and/or obesity. Indeed, as the number of publications in this area increases, a structured meta-analysis/review would be very timely and useful. There are currently many reports of miRNAs being dysregulated during obesity, either in metabolic tissues or in circulation (the PubMed search: miRNA AND obesity NOT review, reveals over 800 research articles). For many of the implicated miRNAs, a functional role has been determined, for example regulating adipogenesis, insulin resistance, or glucose uptake (Xie, Sun and Lodish, 2009)(del Carmen Martínez-Jiménez, Méndez-Mancilla and Portales-Pérez, 2018). It would therefore be interesting to focus on obesity-related miRNAs that influence PCa development. A couple of publications are available that have addressed this issue, although too few for review and mainly implicating inflammation mediating miRNAs which are likely dysregulated due to the systemic subclinical inflammation that is associated with obesity. It therefore appears that this area requires further investigation. To explore this, perhaps the serum or PCa tissue of men with differing BMIs could be analysed for miRNA expression by miRNA-seq (matching the case and control groups for tumour stage and patient age and family history).

Interestingly, this review highlighted the difficulties in assessing the use of serum hormone biomarkers. The study designs were highly heterogeneous, for example the different types of protein quantification

assays (such as ELISA, or RIA). Indeed, unexpected variation was observed in the absolute hormone levels across the different cohorts, perhaps reflecting assays of different sensitivities. It would be simpler to use a biomarker such as a small RNA, which are reliably detected by PCR methods, using smaller amounts of starting material, and may be less varied due to the type of assay used. An important next stage of this research would be to perform a similar systematic review investigating the association between obesity-related miRNAs and PCa, however, as mentioned above this will not be possible until more literature is available (that is, more observation studies have been carried out, measuring miRNA levels in PCa patients). Alternatively, a list of miRNAs that regulate leptin or adiponectin could be compiled and measured in PCa patients as these could be more consistent as biomarkers.

Finally, one implication of this research is that body size and potentially diet, have the ability to influence cancer incidence. This could be further dissected at the molecular level, for instance by investigating the effect of diet on epigenetics or miRNA expression. As mentioned in the General Introduction section *1.1. III.*, PCa incidence varies widely between populations which could partially be due to their varying diets. As an example, Asian men have a relatively low incidence compared with European and North American men which could be linked with their higher consumption of soy products (Perabo *et al.*, 2008). It has been shown that genistein (a soy-derived isoflavone and phytoestrogen) influences PCa cell behaviour; it inhibited migration and invasion *in vitro* (Pavese, Krishna and Bergan, 2014). Similar observational and *in vitro* studies have linked polyphenols and other antioxidants with a tumour suppressive effects in PCa (Patel, 2014). Previous work in our laboratory demonstrated that treatment of PCa cells with genistein caused demethylation of the promoter CpG sites closest to the miR-200c loci, resulting in increased miR-200c expression (Lynch et al, 2016), and suggesting a potentially important relationship between diet and epigenetic regulation of miRNAs. With this in mind, it could be interesting to use an observation study to correlate dietary or exercise habits with miRNA expression or DNA methylation patterns in PCa, for instance by comparing the transcriptome or epigenome of PCa patients of different BMI groups, types of diet, or exercise patterns. Then, GO functional enrichment or network analysis would be used to characterise the differences, as demonstrated in chapter 5. Intriguingly, one study found that genistein modulated epigenetic profiles when given as a supplement to PCa patients (30mg daily); it was associated with differential DNA methylation of genes regulating development, proliferation, transcription, and stem cell markers, with enrichment analysis indicating overall reduction in Myc and increased PTEN activity (Bilir *et al.*, 2017). Similarly, an intervention study could be used, giving PCa patients a supplement such as antioxidants or polyphenols, and then performing methylation array or miRNA-seq to explore differences in methylation or miRNA expression patterns.

In summary, properly conducted systematic reviews are important tools for effectively appraising and evaluating the evidence that is rapidly accumulating in relation to the complex causative factors of PCa

development and progression. Such reviews and meta-analyses can help prioritise the areas to focus on, in order to maximise improvements in the management of this disease.

7. 3. Bibliography

Bilir, B. *et al.* (2017) 'Effects of genistein supplementation on genome- wide DNA methylation and gene expression in patients with localized prostate cancer.', *International journal of oncology*. Spandidos Publications, 51(1), pp. 223–234. doi: 10.3892/ijo.2017.4017.

del Carmen Martínez-Jiménez, V., Méndez-Mancilla, A. and Portales-Pérez, D. (2018) 'miRNAs in nutrition, obesity, and cancer: The biology of miRNAs in metabolic disorders and its relationship with cancer development', *Molecular Nutrition & Food Research*. John Wiley & Sons, Ltd, 62(1), p. 1600994. doi: 10.1002/mnfr.201600994.

Patel, V. H. (2014) 'Nutrition and prostate cancer: an overview', *Expert Review of Anticancer Therapy*, 14(11), pp. 1295–1304. doi: 10.1586/14737140.2014.972946.

Pavese, J. M., Krishna, S. N. and Bergan, R. C. (2014) 'Genistein inhibits human prostate cancer cell detachment, invasion, and metastasis.', *The American journal of clinical nutrition*. American Society for Nutrition, 100 Suppl 1(1), pp. 431S–6S. doi: 10.3945/ajcn.113.071290.

Perabo, F. G. E. *et al.* (2008) 'Soy isoflavone genistein in prevention and treatment of prostate cancer', *Prostate Cancer and Prostatic Diseases*, 11(1), pp. 6–12. doi: 10.1038/sj.pcan.4501000.

Xie, H., Sun, L. and Lodish, H. F. (2009) 'Targeting microRNAs in obesity.', *Expert opinion on therapeutic targets*. NIH Public Access, 13(10), pp. 1227–38. doi: 10.1517/14728220903190707.

Chapter 8. General Discussion

8. 1. Overall summary of findings

This thesis has focused on characterising the expression and function of miRNAs during hypoxia in PCa, while touching on other important influences such as gene regulation by DNA methylation, expression of pathological splice variants, and the interaction between obesity-related hormones and PCa outcome. Taken together, these chapters illustrate the complexity of the disease and highlight the utility of personalised medicine approaches, such as monitoring hypoxia or other patient-specific variables.

8. 2. HypoxamiRs in prostate cancer

Hypoxia is common in prostate tumours and is a known driver of tumour progression, so it is therefore important to understand its effects at the cellular level. Furthermore, hypoxia can be exacerbated by chemotherapies such as bicalutamide, as demonstrated in chapter 3. Hypoxic stress exerts widespread effects, through the activation of the master transcription factor HIF, plus the reduced activity of oxygen dependent enzymes. At the transcriptional level, hypoxia responsive miRNAs ("hypoxamiRs") may play a critical role in the hypoxic adaptation of cancer cells and subsequently increase malignancy. Numerous *in vitro* and NGS studies have previously shown that acute or chronic hypoxia affected the expression of swathes of miRNAs, and for many of them a functional role was confirmed. This thesis provides new data to evidence how hypoxia can contribute to tumour progression through its impact on miRNAs. Chapters 3, 4 and 5 have demonstrated that miR-210, miR-21, and miR-196a were induced by hypoxia in PCa models. In some cases we presented how it may contribute to PCa progression. For instance, *in vitro* phenotypic assays highlighted an ability of miR-21 overexpression alone to increase the cells' clonogenicity and migration, and miR-210 was shown to regulate the neural cell adhesion molecule. Therefore, our findings are in accordance with previous research on these miRNAs while adding novel data.

8. 3. MicroRNA biomarkers in prostate cancer

In addition to elucidating the aetiology of PCa, miRNAs such as these could be clinically valuable as biomarkers. Biomarkers are an essential component of personalised medicine as they can reveal the nature of the patient's disease and allow the clinician to estimate to which treatment they will best respond. They can also be used to monitor specific biochemical outcomes such as tumour reduction, hypoxia, imminent relapse, remission, or metastasis (Hayes, Peruzzi and Lawler, 2014). Potentially, in the future levels of miR-210 and/or miR-21 could be used to indicate PCa hypoxia, which would suggest that additional hypoxia-targeting treatment is necessary, such as addition of a hypoxia-activated prodrug or oxygen perfusion, or direct the clinician to choose surgery over radiotherapy alone. Chapter 4 reported that miR-21 was also upregulated in the serum of mice, suggesting that it may be a useful addition to liquid biopsy panels to monitor tumour hypoxia. Fluid based or circulating miRNAs can make diagnosis less invasive for the patient, and can easily provide longitudinal measurements across a period of "watchful waiting" or treatment. Moreover, in TCGA Regulome Explorer cohort of 333 patients, miR-21 tumour levels (in addition to miR-210 levels) improved the ability of Gleason scoring (a clinical parameter) to predict a patient's response to

therapy. It is important to note that miRNAs are particularly appropriate molecules for biomarker use as they are abundant and stable due to their short size, and their position within the RNAi machinery or within exosomes. Exosomal miRNAs from blood were found to be stable even after several freeze/thaw cycles and long periods at room temperature where longer RNA transcripts or proteins would have been degraded, emphasising their unique capacity as biomarkers (Mitchell *et al.*, 2008). However, although the potential of miRNA profiling seems great, more research is required to identify the best miRNAs, or combinations of miRNAs, that should be profiled for PCa and other diseases.

8. 4. MicroRNAs in prostate cancer therapeutics

Naturally, the use of miRNAs in therapeutics has been slower to emerge than in diagnostics, as an extra dimension of research is required to evaluate off-target effects and optimise effective delivery and stability of the molecule in its tissue. Nevertheless, RNAi based therapies are already entering the clinic (Bouchie, 2013). The major bottleneck has been efficient delivery of the molecule (*i.e*., foreign RNA) into living cells without it being destroyed, but new improved conjugates that mask them from the cell's innate response are being finalised (Springer and Dowdy, 2018). Another limitation to miRNA-based therapies is off target effects, since miRNAs operate within intricate networks. This reflects the inherent limitation of miRNA functional studies, as the majority involve a simplified model in which the targeting of a specific mRNA is validated *in vitro*, as reported in chapters 3 and 4. These studies are essential to confirm the biological function of the miRNA as a regulator of the mRNA in question. However in complex organisms, mRNAs are regulated by the simultaneous and coordinated action of numerous miRNAs operating within a network of interactions. Likewise, miRNAs are promiscuous and may regulate many other mRNAs, which may positively or negatively regulate each other (or act differentially on multiple nodes of the same pathway), and thus the net effect of a miRNA's overexpression can be difficult to ascertain (Figure 1). This was illustrated in chapter 3, in which in several replicates, miR-210 did not significantly reduce the mRNA level of *NCAM* although the luciferase reporter assay confirmed the targeting. In this way, miRNA promiscuity poses an issue in terms of therapeutics, as for example, using a miRNA inhibitor (antagomiR) could have unanticipated effects on diverse secondary targets. An alternative for miRNA inhibitors are "target protectors" (morpholinos), a similar molecule that binds to the mRNA target at its miRNA binding site (with 14-15 nucleotides in specificity) blocking miRNA-binding yet permitting translation (Ho *et al.*, 2012). This approach would be suitable if a miRNA had a single deleterious effect of suppressing a key target. For instance if a key target of miR-196a was identified (*e.g*. an apoptosis inducer) then a morpholino could be appropriate to singularly disrupt this interaction, whereas considering the many tumour-suppressors targeted by miR-21, an antagomiR inhibitor molecule would be more useful. Another issue with miRNA based therapies is resistance, although combinatorial miRNA modulation has been suggested to overcome this (Hayes, Peruzzi and Lawler, 2014). As an example, dual inhibition of miR-21 and miR-210 could be a viable strategy to suppress the deleterious effects of hypoxia. Similarly, resistance has been observed to

occur due to the redundancy between numerous miRNAs, or through different family members, although sequences can be designed that target the whole family. A benefit of miR-21 and miR-210 would be that they do not have known family members.

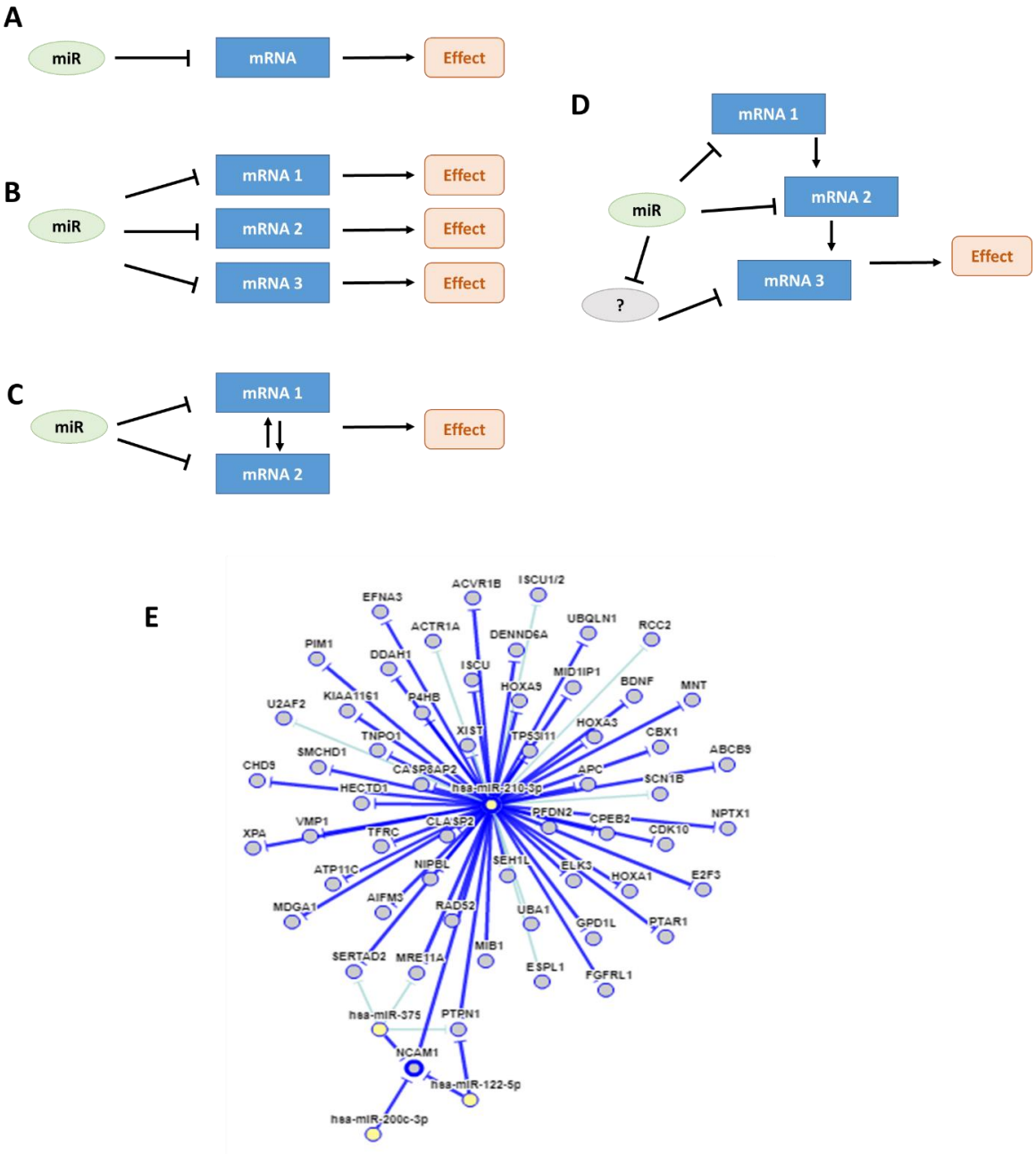

Figure 1. MiRNAs operate in networks with varying degrees of complexity. Networks based on a similar figure from (Hayes, Peruzzi and Lawler, 2014). **A)** The basic sequence of a single miRNA targeting a single mRNA, modulating an effect. **B)** MiRNA promiscuity, one miRNA has multiple mRNA targets thus modulating multiple effects, the sum of which may determine a phenotype. **C)** A miRNA may regulate multiple targets that are functionally related and thus interact with each other to produce a phenotype. **D)** A miRNA (or related miRNAs such as from a cluster) target multiple nodes in a pathway, potentially via other molecules (miRNAs or mRNAs). E) The potential structural complexity is amplified, considering the number of potential targets of each miRNA. Network of validated targets of miR-210 (in all cell types) from miRTarBase (http://mirtarbase.mbc.nctu.edu.tw/php/index.php), highlighting *NCAM* as a target among many other targets, which additionally has other known regulators.

8. 5. Multi-omics approaches in prostate cancer research and healthcare

This thesis has focused mainly on *in vitro* and *in vivo* methods, but I had the opportunity to work with some NGS datasets through collaborations with the BioSpyder company in California and a research group in Strasbourg. Furthermore, I replicated an RnBeads methylation analysis workflow process using a publicly-available methylation array dataset, which is a method that has been described by the Colum Walsh group at Ulster University. These collaborations allowed me to explore the immense utility of large datasets, and develop some introductory skills in bioinformatics. Multi-omics approaches are important in research and healthcare, and can involve screening for differentially expressed molecules, differentially methylated genomic regions, the pathological AR variants, or obesity-related signalling. However, to supplement omics analysis, wet-lab investigations remain essential to prove the functional roles of genes and this is particularly important for translating biomarkers into therapeutic targets. For functional analysis, phenotypic screens are useful, although as reported in chapter 5 they assess a limited number of cell behaviours, and may miss key interactions that take place in the context of the tumour.

8. 6. The value of miRNAs in personalised medicine

Investigating hypoxia-associated transcriptional or epigenetic changes is particularly impactful because it can be applied to many cancer settings, and perhaps beyond to diseases that similarly involve deregulated hypoxic signalling such as cardiovascular disease or stroke. Furthermore, miRNA or DNA based biomarkers are more stable and may be more cost-effective to analyse than protein markers since primers are generally cheaper than antibodies. While the extensive use of omics data for personalised medicine approaches has been hailed for patient stratification, it has also received criticism for failing to consider cost-effectiveness. A seminal meta-review highlighted that most studies that have investigated personalised medicine tests, had not included an economic assessment during the evaluation of their utility; they concluded that while many tests did prove to be cost-effective, remarkably few were cost-saving (Phillips *et al.*, 2014). As outlined in the chapter 5 discussion, personalised medicine will comprise a medley of approaches, although it is crucial that impact and applicability be considered to ensure that the eventual test or product will be viable. Already, only 12% of global health spending occurs in low and middle-income countries, despite containing 84% of the world's people, and the transition to personalised medicine (*i.e*. increasingly complicated and specific tests) will compound the widening gap (Gottret and Schieber, 2006). PCR based methods of detection are cheap, simple and reliable, which increases the chances that they can be utilised across the world, compared with other diagnostic tools such as multiplex assays for protein biomarker detection. So, as a final comment it is important to emphasise approaches such as simple PCRs or genomic arrays (for miRNAs, or methylation specific PCR) compared with proteomics or whole-genome NGS analyses. Figure 2 illustrates a multi-omics integrated approach to personalised medicine, including the use of miRNAs as a simple and robust measurement at each stage.

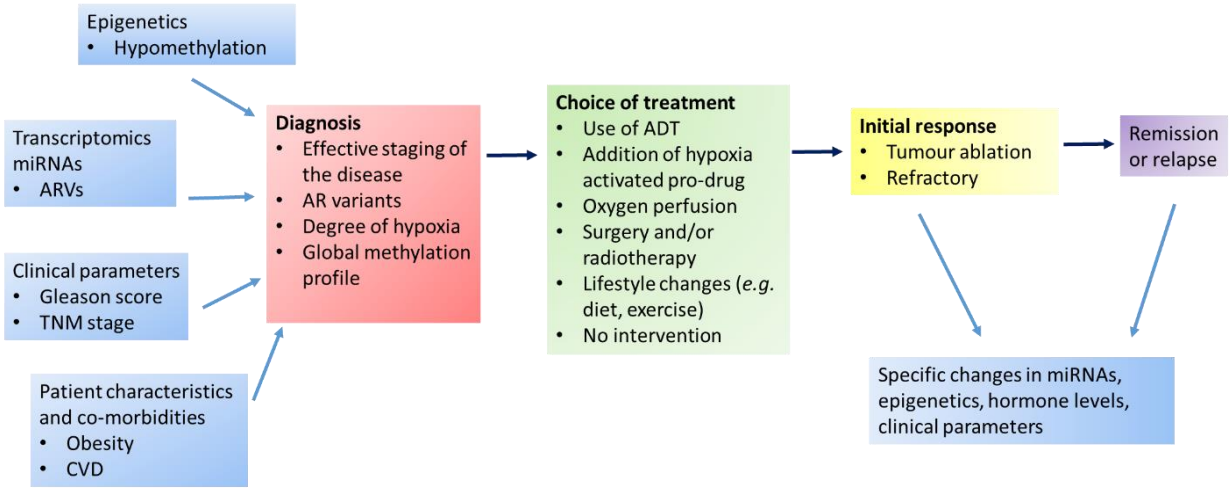

Figure 2. Towards a personalised medicine approach to prostate cancer diagnosis and management. A combination of genomics, clinicopathological, and patient specific characteristics will be used to accurately inform PCa diagnosis and determination of tumour characteristics such as hypoxia or AR variant status. This will thus inform the choice of treatment; co-morbidities such as cardiovascular disease (CVD) would suggest surgery is not suitable for the patient, AR variant expression could indicate androgen inhibiting chemotherapy is unsuitable, and hypoxia may indicate that radiotherapy is unsuitable or indicate the need for hypoxia targeting treatments like a hypoxia-activate prodrug or oxygen perfusion. The patient's response to treatment, and subsequent biochemical outcomes, will also be monitored by standard clinicopathological measurements (i.e. biopsy or PSA levels) supplemented by specific markers such as miRNAs, circulating DNA or epigenetic changes, or hormone levels.

8. 7. Future directions:

There are many broad areas for future investigation that could be pursued to build upon the data and ideas presented in this thesis, in addition to the focused suggestions already outlined in the discussion of each chapter. The study design could also be improved in several ways.

8. 7. I) Study design improvements

The RT-qPCR approach used throughout this thesis could have benefited from complete adherence to the "MIQE" guidelines (the Minimum Information for Publication of Quantitative Real-Time PCR Experiments) (Bustin et al., 2009). These aim to improve the reliability and reproducibility of RT-qPCR results across laboratories, and include a checklist of the essential features of an RT-qPCR experiment. One guideline which I did not adhere to was to computationally determine which housekeeping gene was most stable and thus best for each experiment, for which there are several algorithms available such as Bestkeeper (Pfaffl et al., 2004) and geNorm (Vandesompele et al., 2002)(Mestdagh et al., 2009).

Additionally, I used luciferase reporter assay to explore the regulation of NCAM by miR-210, which is frequently described as the "gold standard" in validating miRNA : mRNA interactions (Lewis et al., 2003). However, a newer approach such as CLIP-seq would be best as it will highlight novel interactors in an unbiased way. CLIP-seq involves immunoprecipitating miRNAs after crosslinking them to mRNA targets, and sequencing the targets (Chi et al., 2009).

It is vital to note that this thesis has made use of cell line models to explore the aetiology and progression of cancer, models in which there are profound limitations of cell lines. These cell lines provided a limited model of *in vivo* cancer as they are homogenous populations of epithelial cells, which were purified from tumours years (often decades) previously and have been subject to *in vitro* culture and freeze/thaw cycles since. Especially in the case of cancer as a disease, cell lines may be inappropriate since their genomes are unstable and they thus have increased propensity to mutate, adapt and evolve and at the point of laboratory measurement they may be incomparable to the original genotype. Moreover, since they were isolated from a small population of cells from a patients (highly heterogeneous) tumour they may not represent the cancer as it manifests across different patients. A more reliable way to identify gene expression in cancers would be to use tumours from a cohort of patients, sort the cells by FACS, and perform scRNAseq. However, the caveat of this approach would be that a vast number of patients would be required to obtain significant (*i.e.*, non patient-specific) results and it would be enormously expensive. Furthermore, cell lines are most useful for pathway analysis since they are homogenous and provide a smaller system to model changes without interference from other cell types.

Finally, this work made use of transient overexpression of hypoxia-associated miRNAs to explore their effect on cell behaviour. However, it would be more useful to have used antogomir molecules to block the

effects of the miRNA during hypoxia, to observe the lack of its effect. A loss of function during hypoxia study would have been more valuable than gain of function during normoxia.

8. 7. I) Future research

As mentioned, monitoring or targeting hypoxia could have uses in many tumour types. As an illustration, a panel of standard hypoxamiRs could be designed that effectively characterise the hypoxic tumour cell, perhaps including the addition of PCa-specific markers such as the long non-coding RNA PCA3 (see General Introduction section *1.1. V*.) or AR. Ideally, a serum profile would be developed but it must be able to distinguish between tumour hypoxia and cardiovascular disease or an inflammatory disorder.

The principles of profiling miRNA expression by PCR could also be extended to other non-coding RNAs, such as long non-coding RNAs (lncRNAs). Many researchers investigate lncRNAs as biomarkers, and several have been identified as biomarkers of PCa (such as PCA3) (Misawa, Takayama and Inoue, 2017). In general I believe miRNAs may be more valuable since their short size increases their physical stability which makes them more robust and suitable for simpler protocols, and thus more accessible to research groups. However, if reliable lncRNA biomarkers could be identified, a large panel may be useful. A number of lncRNAs have been identified that are expressed in response to hypoxia, in cancers such as breast, gastric and pancreatic cancers (Chang *et al.*, 2016). One study has shown that a lncRNAs was hypoxia-responsive and *in vitro* studies showed it could increase the proliferation of PCa cell lines and was associated with PCa patient prognosis (Zhao *et al.*, 2017). Therefore, this area could be further investigated.

Another option could be to look for circular RNAs (circRNA), which are currently the focus of intense investigation since they sponge miRNAs and are incredibly stable and thus ideal as biomarkers (Rong *et al.*, 2017)(Li *et al.*, 2015). CircRNAs are produced through a specific biogenesis pathway, or result from slicing events (Ashwal-Fluss *et al.*, 2014). Considering that a key problem in PCa is pathological AR splice variants, perhaps the missing segments could produce circular fragments and could be detected as markers of aberrant splicing.

As mentioned in chapter 5, DNA methylation at gene bodies is involved in the regulation of splicing, so it could also be interesting to investigate if methylation patterns of the AR gene body associate with expression of the AR variants, and perhaps if hypoxia could modulate it. Indeed, further investigation into the relationship between hypoxia, DNA methylation, and miRNAs would be interesting. The NSCLC study by Thienpont *et al*., demonstrated that the demethylating TET enzymes are oxygen dependent (Thienpont *et al.*, 2016) as are many other epigenetic regulators such as histone deacetylases (HDAC) and sirtuins (Camuzi *et al.*, 2019). The methyl donor S-adenosylmethionine is reduced during hypoxia in liver cells (Liu *et al.*, 2011) and the expression of *DNMT1* and *DNMT3a*/b have each been shown to be affected by hypoxia in different cell contexts (Camuzi *et al.*, 2019). These highlight how epigenetics will be immediately susceptible to hypoxia. They suggest that epigenetic based therapies such as HDAC inhibitor may not be

effective when tumours become hypoxic; future studies of such therapies should monitor and control for the effect of hypoxia and patients should be stratified accordingly.

Interestingly, miRNA biogenesis is regulated by hypoxia (via epigenetics) which could be important for the hypoxic response. It was reported that miRNA biogenesis is suppressed during hypoxia, as the H3K27me3 demethylases 6A and 6B (KDM6A/B), which are required for activation of the Dicer promoter, are oxygen-dependent (van den Beucken *et al.*, 2014). As discussed in the General Introduction section *1.3. VII*., miRNAs are essential for rapid stress responses and adaptation. However, whether this influenced the overall activity of miRNAs has not been shown. To explore this, point mutations in Ago could be performed, such as mutating the region that binds the 5' phosphate of the miRNA/siRNA. This knock-in could be achieved using a CRISPR/Cas9 or a cre-lox recombination system (Hagan *et al.*, 2019)(Balligand *et al.*, 2019). Then, the ability of the mutant cells to survive hypoxia could be measured.

This thesis has touched on how androgen deprivation therapy (ADT) such as bicalutamide can influence hypoxia, with the view to elucidate the link between ADT and tumour progression and/or relapse. To further these investigations, it would be interesting to explore the effect of hypoxia-responsive miRNAs on the AR signalling pathway, which could modulate the pathway and mediate AR independence. A list of AR targets could be compiled including miRNAs that regulate them. If any of these miRNAs are hypoxia-responsive, it could suggest a mechanism through which hypoxia facilitates AR independence.

The effects of ADT could also be investigated by single cell RNA-seq (scRNA-seq). As mentioned in chapter 5, scRNA-seq can be extremely powerful in characterising heterogeneous cell populations and has been used to discover rare and small cell populations. Here, scRNA-seq could be suitable to analyse tumours following ADT, using a model similar to the one presented in chapter 3. With increasing ADT treatment and hypoxia, tumours could be extracted and analysed by scRNA-seq. This may highlight the population of cells that facilitate relapse, which may have cancer stem cell like features and favour a hypoxic environment.

To conclude, it is clear from the work presented here that hypoxia in PCa does impact upon miRNA signalling. This is a complex interaction that overlaps with other hypoxic response axes within the cell, but there is great opportunity to use this information to help improve the management of PCa. This thesis has added valuable, novel data to the overall global research effort to combat PCa, with impact for researchers, clinicians and patients alike.

8. 8. Bibliography

Ashwal-Fluss, R. *et al.* (2014) 'circRNA Biogenesis Competes with Pre-mRNA Splicing', *Molecular Cell*. Cell Press, 56(1), pp. 55–66. doi: 10.1016/J.MOLCEL.2014.08.019.

Balligand, T. *et al.* (2019) 'Knock-in of murine Calr del52 induces essential thrombocythemia with slow-rising dominance in mice and reveals key role of Calr exon 9 in cardiac development', *Leukemia*. doi: 10.1038/s41375-019-0538-1.

van den Beucken, T. *et al.* (2014) 'Hypoxia promotes stem cell phenotypes and poor prognosis through epigenetic regulation of DICER', *Nature Communications*. Nature Publishing Group, 5(1), p. 5203. doi: 10.1038/ncomms6203.

Bouchie, A. (2013) 'First microRNA mimic enters clinic', *Nature Biotechnology*. Nature Research, 31(7), pp. 577–577. doi: 10.1038/nbt0713-577.

Camuzi, D. *et al.* (2019) 'Regulation Is in the Air: The Relationship between Hypoxia and Epigenetics in Cancer', *Cells*, 8(4), p. 300. doi: 10.3390/cells8040300.

Chang, Y.-N. *et al.* (2016) 'Hypoxia-regulated lncRNAs in cancer', *Gene*. Elsevier, 575(1), pp. 1–8. doi: 10.1016/J.GENE.2015.08.049.

Chi S. W. al (2009). Ago HITS-CLIP decodes miRNA-mRNA interaction maps. *Nature*; 460(7254):479–86.

Gottret, P. and Schieber, G. (2006) 'Health transitions, disease burdens, and health expenditure patterns. Health Financing Revisited: A Practitioner's Guide: The International Bank for Reconstruction and Development.', pp. 23–39. doi: 10.1596/978-0-8213-6585-4.

Hagan, A. S. *et al.* (2019) 'Generation and validation of novel conditional flox and inducible Cre alleles targeting fibroblast growth factor 18 (*Fgf18*)', *Developmental Dynamics*, 248(9), pp. 882–893. doi: 10.1002/dvdy.85.

Hayes, J., Peruzzi, P. P. and Lawler, S. (2014) 'MicroRNAs in cancer: biomarkers, functions and therapy', *Trends in Molecular Medicine*, 20(8), pp. 460–469. doi: 10.1016/j.molmed.2014.06.005.

Ho, J. J. D. *et al.* (2012) 'Functional Importance of Dicer Protein in the Adaptive Cellular Response to Hypoxia', *Journal of Biological Chemistry*, 287(34), pp. 29003–29020. doi: 10.1074/jbc.M112.373365.

Lewis B.,P., et al. (2003). Prediction of mammalian microRNA targets. *Cell*. Dec 26;115(7):787–798.

Li, Y. *et al.* (2015) 'Circular RNA is enriched and stable in exosomes: a promising biomarker for cancer diagnosis', *Cell Research*. Nature Publishing Group, 25(8), pp. 981–984. doi: 10.1038/cr.2015.82.

Liu, Q. *et al.* (2011) 'Hypoxia Induces Genomic DNA Demethylation through the Activation of HIF-1 and Transcriptional Upregulation of MAT2A in Hepatoma Cells', *Molecular Cancer Therapeutics*, 10(6), pp. 1113–1123. doi: 10.1158/1535-7163.MCT-10-1010.

Mestdagh, P., *et al.* (2009) A novel and universal method for microRNA RT-qPCR data normalization. *Genome Biology* 10, R64 doi:10.1186/gb-2009-10-6-r64

Misawa, A., Takayama, K. and Inoue, S. (2017) 'Long non-coding RNAs and prostate cancer', *Cancer Science*, 108(11), pp. 2107–2114. doi: 10.1111/cas.13352.

Mitchell, P. S. *et al.* (2008) 'Circulating microRNAs as stable blood-based markers for cancer detection', *Proceedings of the National Academy of Sciences*, 105(30), pp. 10513–10518. doi: 10.1073/pnas.0804549105.

Phillips, K. A. *et al.* (2014) 'The economic value of personalized medicine tests: what we know and what we need to know.', *Genetics in medicine : official journal of the American College of Medical Genetics*. NIH Public Access, 16(3), pp. 251–7. doi: 10.1038/gim.2013.122.

Pfaffl, M. W., et al. (2004) Determination of stable housekeeping genes, differentially regulated target genes and sample integrity: *BestKeeper* – Excel-based tool using pair-wise correlations. *Biotechnology Letters* 26: 509-515.

Rong, D. *et al.* (2017) 'An emerging function of circRNA-miRNAs-mRNA axis in human diseases', *Oncotarget*, 8(42), pp. 73271–73281. doi: 10.18632/oncotarget.19154.

Springer, A. D. and Dowdy, S. F. (2018) 'GalNAc-siRNA Conjugates: Leading the Way for Delivery of RNAi Therapeutics', *Nucleic Acid Therapeutics*, 28(3), pp. 109–118. doi: 10.1089/nat.2018.0736.

Thienpont, B. *et al.* (2016) 'Tumour hypoxia causes DNA hypermethylation by reducing TET activity', *Nature*. Nature Publishing Group, 537(7618), pp. 63–68. doi: 10.1038/nature19081.

Vandesompele, J., *et al.* (2002) Accurate normalization of real-time quantitative RT-PCR data by geometric averaging of multiple internal control genes. *Genome Biol* **3,** research0034.1 doi:10.1186/gb-2002-3-7-research0034

Zhao, R. *et al.* (2017) 'Upregulation of the long non-coding RNA FALEC promotes proliferation and migration of prostate cancer cell lines and predicts prognosis of PCa patients', *The Prostate*, 77(10), pp. 1107–1117. doi: 10.1002/pros.23367.

Extracurricular Activities, Funding Obtained, and Research Outputs

Teaching

- Lab supervision and training of undergraduate students
- Postgraduate Demonstrator Learning and Teaching Certification (Oct 2016). Demonstrated on the modules: Haematology and Blood Transfusion Sciences (BSc Biomedical Sciences), Applied Genetics (BSc Biomedical Sciences), Physician's Associate (MSc).
- Assessment responsibilities: marked coursework, class tests, and worksheets.
- STEM ambassador activities (supervision of school students, assisting at open days and events).

Leadership Roles and Society Memberships

- Early Career Representative, The Biochemical Society's Policy Advisory Panel (Jan 2019-Jan 2022).
- Elected Chairperson of the Biomedical Sciences Postgraduate Society (Sept 2017 - Sept 2018).
- Organised and obtained funding for a Postgraduate conference "All Ireland Biomedical Sciences Postgraduate Conference" with over 40 delegates from Universities across Ireland (Jun 2018).
- Organised and obtained funding for a "Careers Workshop" with talks from four Biomedical Science PhD graduates (working in Regulatory Affairs, Pharmaceuticals, Legal Services, and Business & Commerce) (June 2018).
- Organised and obtained funding for "Introduction to Statistical Programming with R" course (Sept 2017).
- Ulster University "3-minute thesis" finalist (Jun 2018).
- STEM ambassador (Jun 2017-present).
- Chaired women's focus group and submitted report that contributed to Ulster University's successful application for the Athena Swan Bronze Award (Nov 2017).
- International Leadership & Management Level 5 Award (Dec 2018).
- Member of the Royal Society of Biology (AMRSB Sep 2016 – Jan 2018, MRSB Jan 2018 - present).
- Member of the Genetics Society (Sep 2016 – present).
- Member of the Biochemical Society (Jun 2017 – present).
- European Association of Cancer Research (Feb 2018 – present).

Funding Awarded

- Successfully applied for a £2,000 scholarship (GRO-UR-Networks) from Ulster University for 3-week research stay with Dr Jocelyn Céraline, Institute of Molecular and Cellular Biology (Strasbourg, Mar 2018).
- Obtained £500 from Ulster University Doctoral College to fund the All Ireland Biomedical Sciences Postgraduate Conference.
- Collected £1,800 funding to attend Keystone Symposium on Small Regulatory RNAs (£550 Travel Award - The Biochemical Society; £750 Conference Grant - The Genetics Society, £500 Travel Grant - The Royal Society of Biology).
- Secured £1,000 from the Biomedical Sciences Research Institute to run social and academic events for the Biomedical Sciences Postgraduate Society (Sep 2017).
- Successfully requested £1,000 from the Ulster University Research and Impact department, to organise and run a workshop for PhD researchers: 'Introduction to Statistical Programming with R' (Jun 2017).
- Successfully applied for a £250 grant from Santander to run "Postgraduate Careers Workshop" (Sept 2017).
- Awarded £500 Training grant from The Genetics Society to attend 'Introduction to RNAseq' course (London, Nov 2017).
- Awarded £60 scholarship from the School of Biomedical Sciences to attend All Ireland Biomedical Sciences Postgraduate Conference (Sligo, Jun 2017)

Publications

Published

"Appetite-Regulating Hormones - Leptin, Adiponectin and Ghrelin - and the Development of Prostate Cancer: A Systematic Review and Meta-Analysis".
C. Zoe Angel, Isabel Iguacel, Amy Mullee, Neela Guha, Rachel Wasson, Declan J. McKenna, Marc J. Gunter, Vitaly Smelov & Inge Huybrechts. April 2019 *Prostate Cancer and Prostatic Diseases*.

"Serum levels of miR-199a-5p correlates with blood pressure in premature cardiovascular disease patients homozygous for the MTHFR 677C > T polymorphism"
Seodhna M. Lynch, Mary Ward, Helene McNulty, **C. Zoe Angel**, Geraldine Horigan, J.J. Strain, John Purvis, Mike Tackett, Declan J. McKenna. In press, *Genomics*.

"miR-210 is Induced by Hypoxia and Regulates Neural Cell Adhesion Molecule in Prostate Cells" **C. Zoe Angel**, Seodhna M. Lynch, Colum P. Walsh & Declan J. McKenna. Journal of Cellular Physiology Accepted Jan 2020

Submitted

"Transcriptional Landscapes of Constitutive Androgen Receptor Variants in Prostate Cancer"
Pauline Ould Madi - Berthélémy, Eva Erdmann, Edwige Schreyer, Mathieu Jung, **C. Zoe Angel**, Bruno Kieffer & Jocelyn Céraline. Submitted for publication to *Oncotarget*.

Conference presentations

Oral presentations:

The All Ireland Biomedical Sciences Postgraduate Conference (Sligo, 14th -15th Jun 2017) "**Regulation of miR-210 by hypoxia in prostate cancer**". **C. Zoe Angel**, Seodhna M. Lynch, Heather Nesbitt, Colum P. Walsh, Declan J. McKenna.

Ulster University PhD Festival of Research (9th Apr 2019). "**Investigating the role of miRNAs in the hypoxic response in prostate cancer**". **C. Zoe Angel**, Christopher J. McNally, Colum P. Walsh, Declan J. McKenna.

Poster presentations:

European Congress of Personalised Medicine, (Belfast, 27th – 30th Nov 2017) "**MicroRNAs in Prostate Cancer: Implications for Personalised Medicine**". **C. Zoe Angel**, Seodhna M. Lynch, Colum P. Walsh, Declan J. McKenna.

Irish Association for Cancer Research (Dublin, 22nd Feb 2018) "**miR-210 is regulated by hypoxia and contributes to malignant progression in prostate cancer**." **C. Zoe Angel**, Seodhna M. Lynch, Heather Nesbitt, Declan J. McKenna.

Androgens Meeting (Edinburgh, 3rd – 5th Sept 2018). "**The Androgen Receptor Variants ARV7 and ARVQ641X have distinct Transcriptional Activities in Prostate Cancer Cells**." Pauline Ould Madi - Berthélémy, Eva Erdmann, Edwige Schreyer, Mathieu Jung, **C Zoe Angel**, Bruno Kieffer & Jocelyn Céraline.

World Cancer Congress (Kuala Lampur, Malaysia, 1-4 Oct 2018) E-poster "**The Appetite-Regulating Hormones - Leptin, Adiponectin and Ghrelin - and the Development of Prostate Cancer: A Systematic Review and Meta-Analysis**" (presented by Dr I. Huybrechts) **C. Zoe Angel**, Isabel Iguacel, Amy Mullee, Neela Guha, Rachel Wasson, Declan McKenna, Marc Gunter, Vitaly Smelov & Inge Huybrechts.

Irish Association for Cancer Research (Dublin, 22nd Feb 2019) "**miR-21 is induced by hypoxia in prostate cancer and targets the tumour suppressor *Rho-related GTP-binding protein* (*RHOB*)". C. Zoe Angel**, Seodhna M. Lynch, Colum P. Walsh, Declan J. McKenna.

Keystone Symposium – D7 Small Regulatory RNAs (Daejeon, South Korea, 16th – 18th Apr 2019). "**Investigating the role of miRNAs in the hypoxic response in prostate cancer**". **C. Zoe Angel**, Christopher J. McNally, Colum P. Walsh, Declan J. McKenna.